Conference Proceedings International Conference on Applied Sciences and Engineering: ICASE 2025

1 October to 3 October 2025,İstanbul,Türkiye

Edited by:
GEBRAİL BEKDAŞ
SİNAN MELİH NİĞDELİ
ÜMİT IŞIKDAĞ

ISBN:978-625-00-6963-9

International Conference on Applied Sciences and Engineering: ICASE 2025

October 1–3, 2025

Istanbul, Türkiye

Organized by:

Advanced Computational Techniques Research Group

ISBN: 978-625-00-6963-9

Organizing Committee

Prof. Dr. Gebrail Bekdaş (Chair) – Istanbul University-Cerrahpaşa, Türkiye

Prof. Dr. Sinan Melih Nigdeli (Chair) – Istanbul University-Cerrahpaşa, Türkiye

Prof. Dr. Ümit Işıkdağ (Chair) – Mimar Sinan Fine Arts University, Türkiye

Ayla Ocak – Istanbul University-Cerrahpaşa, Türkiye

Yaren Aydın – Istanbul University-Cerrahpaşa, Türkiye

Editors

Prof. Dr. Gebrail Bekdaş (Chair) – Istanbul University-Cerrahpaşa, Türkiye

Prof. Dr. Sinan Melih Nigdeli (Chair) – Istanbul University-Cerrahpaşa, Türkiye

Prof. Dr. Ümit Işıkdağ (Chair) – Mimar Sinan Fine Arts University, Türkiye

Scientific Committee

Abdul Samed Kazi – VTT Technical Research Centre, Finland

Anupam Yadav – National Institute of Technology Jalandhar, India

Ali Cemal Benim – Duesseldorf University, Germany

Alias Abdul Rahman – Universiti Teknologi Malaysia, Malaysia

Aylin Ece Kayabekir – İstanbul Gelişim University, Türkiye

Camila Martins Saporetti – Rio de Janeiro State University, Brazil

Celal Cakiroglu – Eastern Michigan University, USA

Dario De Domenico – The University of Messina, Italy

David Arditi – Illinois Institute of Technology, USA

Farzad Rahimian – Teesside University, UK

Javier Fernando Jiménez Alonso – University of Seville, Spain

Marzia Bolpagni – Northumbria University and UCL, UK

Maziar Farzam – University of Maragheh, Iran

Melda Yücel – İstanbul Aydın University, Türkiye

Moacir Kripka – The University of Passo Fundo, Brazil

Mohamed Ghrici – Hassiba Benbouali University of Chlef, Algeria

Mohammed Rashad Baker – University of Kirkuk, Iraq

Nassim Djedoui – Biskra University, Algeria

Salah Djerouni – University Mohamed Khider Biskra, Algeria

Paul Coates – University of Salford, UK

Said Elias Rahimi – Leibniz University Hannover, Germany

Salman Azhar – Auburn University, USA

Sanghun Kim – Temple University, USA

Serdar Ulusoy – Turkish-German University, Türkiye

Xin-She Yang – Middlesex University, UK

Yasser E. Ibrahim – Prince Sultan University, Saudi Arabia

Zong Woo Geem – Gachon University, Korea

Zuzana Dimitrovová – Nova University of Lisbon, Portugal

Preface

It is our great pleasure to present the proceedings of the International Conference on Applied Sciences and Engineering (ICASE 2025), which is organized by Advanced Computational Techniques Research Group. The conference was held in Istanbul, Türkiye, on October 1-3, 2025.

ICASE 2025 provided an open and interdisciplinary platform for researchers, academicians, and industry professionals to exchange knowledge, present their latest findings, and discuss emerging trends and challenges in applied sciences and engineering. In the spirit of advancing science for the benefit of humanity, the conference was held freely and inclusively, allowing participation from around the world without financial barriers.

This year, ICASE 2025 attracted contributions from over 12 countries, reflecting a truly global collaboration. After a rigorous peer-review process, 28 high-quality papers were selected for presentation and inclusion in these proceedings.

We would like to express our sincere gratitude to the members of the Scientific Committee and Organizing Committee for their invaluable efforts, as well as to all the authors and participants for making ICASE 2025 a successful and fruitful event.

We hope that the research presented in these proceedings will inspire new collaborations, innovation, and further advancements in applied sciences and engineering.

Chairs of ICASE 2025
Prof. Dr. Gebrail Bekdaş
Prof. Dr. Sinan Melih Nigdeli
Prof. Dr. Ümit Işıkdağ

Keynote Speakers

Xin-She Yang is Reader in Modelling and Simulation as well as Optimization at Middlesex University London, with more than 25 years' experience in teaching and research. After receiving his DPhil in Applied Mathematics from Mathematical Institute, University of Oxford in 1998, he then worked at Cambridge University Engineering Department and later as a Senior Research Scientist at Mathematics and Scientific Computing Division of UK's National Physical Laboratory (Ranked #3 Lab in the world). He is also an elected Fellow of the Institute of Mathematics and its Applications, Fellow of Asian Computational Intelligence Society and Fellow of Soft Computing Research Society. He is the co-Editor for Springer's book series: Springer Tracts in Nature-Inspired Computing and has been on editorial boards of multiple international journals. He is also among the top 2% scientists and has won the Leader Awards in Computer Science. He was the IEEE Computational Intelligence Society (CIS) chair for the Task Force on Business Intelligence and Knowledge Management (2015 to 2020). He has authored/edited more than 50 books and has published more than 400 peer-reviewed research papers with more than 99,000 citations. He has been on the prestigious list of most influential researchers or highly-cited researchers (i.e., top 0.1% Scientists, Web of Science) for nine consecutive years (2016-2024).

Zong Woo Geem works for the Department of Smart City at Gachon University in South Korea. He has obtained B.Eng. from Chung-Ang University, M.Eng. and Ph.D. from Korea University, and M.Sc. from Johns Hopkins University, and researched at Virginia Tech, University of Maryland - College Park, and Johns Hopkins University. He invented a music-inspired optimization algorithm, Harmony Search (HS), which has been applied to various scientific and engineering problems as well as social and cultural problems. His research interest includes theoretical background (e.g. novel human-experience-based derivative of HS rather than existing analytic-calculus-based derivative) and problem-specific development (e.g. problem-specific operator of HS) of phenomenon-mimicking algorithm and its applications to sustainability & culture issues.

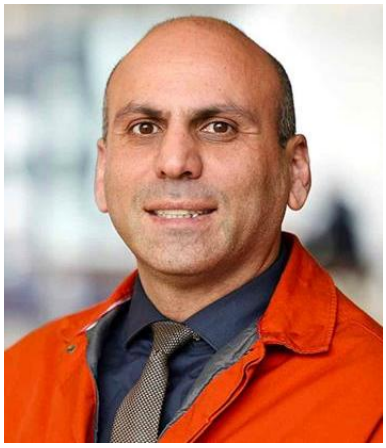

Farzad Rahimian is a Professor of Digital Engineering at the School of Computing, Engineering and Digital Technologies, Teesside University, UK. He is the leader of the Centre for Sustainable Engineering and Open Research and Output Quality Lead, SCEDT, Teesside University. He is Editor in Chief: Smart and Sustainable Built Environment (SCI/JCR IF=3.6, CiteScore Tracker: 9.1) and Associate Editor: AUTOMATION IN CONSTRUCTION (SCI/JCR IF=10.3, Citescore: 16.7). Farzad has a robust research track record delivering more than 200 quality publications and more than 3800 citations. Farzad's research covers various aspects of Construction 5.0, with a strong emphasis on adopting cutting-edge technologies to serve the NetZero and sustainability agenda, including XR for H&S training, AI and deep-learning for sustainable infrastructures and logistics, smart construction, circular construction, energy policies, data-driven digital twins, demand response optimisation, smart energies, DLT and blockchain technologies, and social innovation. Farzad has successfully led several high-profile research projects – from H2021, InnovateUK through to the Arts and Humanities Research Council (AHRC), European Regional Development Funds (ERDF), Construction Scotland Innovation Centre (CSIC), Scottish Funding Council (SFC), Data Lab, and Advanced Forming Research Centre (AFRC). Farzad secured research and innovation income of over £2.5m. This expertise and standing are also recognised through several high-profile bodies, including the International Council for Building (CIB) and buildingSMART International. He graduated with 10 PhD students in the topics across the fields above, and some of them are already senior academics at reputable institutions such as the University of Cambridge, the University of Edinburgh, and the University of Salford, and some hold leadership positions in the industry.

Marzia Bolpagni works as Head of BIM International at Mace where she develops and implements digital construction solutions for public and private international clients. She holds a PhD in ICT and Smart Construction and she is passionate in filling the gap between industry and academia. She is Honorary Assistant Professor at UCL The Bartlett School of Sustainable Construction and Visiting Professor at Northumbria University School of Engineering. She is the co-author of the 4th Edition of the BIM Handbook and co-editor of Industry 4.0 for the Built Environment book. She is co-Editor of the Springer Book Series Digital Innovations in Architecture, Engineering and Construction. She is Member of editorial committes for the Journal of Information Technology in Construction (ITcon), Construction Innovation by Emerald Publishing and Frontiers in Built Environment-Construction Management. She is Project Lead at the European Committee for Standardisation (CEN) TC 442 and ISO/TC 59/SC 13 where she chairs a Work Group on information requirements standardisation (Level of Information Need), an evolution from the concept of "LOD". She is lead author of the Level of Information Need standard ISO 7817-1. She is glad to be a member of the BIMExcellence Initiative, Assistant Editor of the BIM Dictionary and Ambassador of Nima, PastChair of EC3 Modelling and Standards Committee, . She is also founder of Italians in Digital Transformation Uk, she loves sharing her knowledge with students

and she is often invited as keynote speaker at academic and industrial events. She received 30+ awards for her activities including Young Engineer of the Year by the Royal Academy of Engineering, Emerging Professional of the Year, Woman of the Future in 2021, InspiringFifty Uk 2021 and Europe 2022, EC3 2023 Scherer Award and 2023 Design and Build UK Rising Star.

Table of Contents

AI-Driven Intelligent System Detection of Invalid Signatures for Identifying Malicious Nodes in VANETs

Thuvva Anjali[1] [0000-0003-3620-1624], Dr.Rajeev Goyal[2] [0000-0001-8126-8583], Dr. G.N. Balaji[3] [0000-0002-5346-0989]

[1, 2] Amity School of Engineering and Technology, Amity University, Gwalior, Madhya Pradesh, India
[3] Vellore Institute of Technology, Vellore, India
anjalithuvva.phd@gmail.com[1], goyal.rajeev@gmail.com[2], balaji.gnb@gmail.com[3]

Abstract. The security and dependability of VANETs are critical to the successful implementation of intelligent transportation systems. Automobiles to increase efficiency and safety are a key component of Intelligent Transportation Systems (ITS). Because of their scattered architecture, hostile nodes can use faked signatures, duplicate data, or miss messages to disrupt network connections. This work proposes an AI-driven approach that searches for incorrect signatures sent by attackers to detect rogue nodes in VANETs. Technology uses machine learning models to analyze network data and find anomalous activity linked to failed attempts to validate signatures. By fusing real-time node behavior monitoring with cryptographic techniques for signature verification, the proposed system ensures the isolation and detection of rogue nodes. By focusing on the selection of optimal nodes for the process of verification, an AI-augmented detection methodology significantly reduces computational overhead while simultaneously enhancing detection precision. To guarantee reliable communication within VANETs, the proposed methodology provides a scalable, efficient, and secure framework, thereby contributing to the enhancement of safety within transportation networks. Given that AI-driven approaches present robust instruments for the assessment and mitigation of threats, they play an essential role in ensuring the security of vehicular networks. Automotive networks are susceptible to many attacks, such as DoS, spoofing, and Sybil assaults, because of their decentralized governance, unpredictable network topology, and inadequate physical protection. To efficiently assess and detect these possible risks, Modern AI techniques like Supervised and deep learning can examine structured data gathered from sensors integrated into automotive systems.

Keywords: Ad Hoc Network Security, Intrusion Detection, Intelligent Transportation Systems, Attack Detection, Invalid Signature Detection.

1 Introduction

Vehicles are dynamic nodes that communicate with roadside units (RSUs) and other infrastructure components as part of the class of mobile ad hoc networks (MANETs)

known as VANETs. It facilitates smooth statement between automobiles and infrastructure to progress traffic control, road safety, and provide infotainment services. To reduce the incidence of accidents, optimize traffic flow, and elevate the overall driver experience, the real-time exchange of data among vehicles within Intelligent Transportation Systems (ITS) is significantly facilitated by VANETs. Today's technology allows for faster and easier completion of daily tasks. Vehicle ad hoc networks (VANETs), a type of MANET, could enhance smart transportation in the future. Without a strong base, these systems rely on motors to meet community demands. VANETs differ from traditional MANETs due to mobility restrictions, driving force behaviour, and excessive mobility. VANETs are wireless multihop communities with highly mobile nodes, resulting in fast topology changes. With more vehicles equipped with computer technology and Wi-Fi, inter-vehicular information is becoming a potential subject for study, standardization, and development. VANETs provide a wide variety of practical applications, such as real-time monitoring of site visitor situations, safety, blind crossing, and dynamic routing. Giving vehicle nodes to internet connectivity is additional essential software for VANETs. The idea of intelligent transportation systems (ITS) was presented in 1994 to address various transportation problems, including traffic congestion, weather reporting, vehicle monitoring, and road accidents/rescue.

The WHO has observed that road traffic accidents continue to be the primary cause of death globally, particularly in low- and middle-income nations. According to WHO reports, road accidents account for around 1.3 million deaths each year, making traffic-related injuries the eighth leading cause of mortality worldwide until 2024. 50 million injuries in addition to the estimated 50 million people killed in automobile accidents, a large percentage of these injuries result in permanent impairments. Young people affected: Traffic-related injuries are the leading cause of bereavement for individuals between the ages of 5 and 29. Human mistake is the cause of 94% of incidents: The main causes of traffic accidents are driver-related factors, such as excessive speed, careless driving, distractions. Human error is the cause of 94% of accidents. The primary causes of traffic accidents are driver-related problems such speeding, irresponsible driving, driving under the influence, or distracted driving. global campaign for safer roads: By emphasizing the value of technology, better road infrastructure, and safer cars, the World Health Organization (WHO) has launched a uncommon road safety projects and expects to reduce fatalities in half by 2030.

Detecting nodes in Vehicular Ad Hoc Networks (VANETs) using incorrect signature identification requires many important stages. This method protects the integrity and security of network communications by recognizing and isolating nodes that seek to inject erroneous or fabricated data. Distribute cryptographic keys to all legitimate nodes (vehicles and infrastructure) in the network. This can be handled by a trustworthy Certificate Authority (CA). When a node (vehicle or RSU) sends a message, it generates a digital signature using its private key. The message and signature are then sent to other nodes. Nodes that receive the message first extract the signature and public key of the sender from the received data. Receiving nodes use the sender's public key to validate the digital signature attached to the message. This verifies that the communication has not been tampered with and comes from a legitimate source. Continuous monitoring

and adaptation, as well as joint detection systems, are critical for ensuring the security and integrity of vehicle networks. [2][3].

1.1 Malicious nodes in vanet's

Technology has advanced to the point where it can now be used more readily and with less time and effort for a variety of daily tasks.
Vehicular Ad hoc Networks (VANETs), which enable communication between vehicles and infrastructure, enhance Intelligent Transportation Systems (ITS). Wireless communication allows cars to share information. However, there are still a number of ways to target this communication, particularly when it comes to Vehicle-to-Vehicle (V2V) scenarios [4][5].

Controlling unexpected changes in the topology of VANETs is problematic. The motors' high relative velocities generate rapid changes in the community structure. Despite substantial research on Manet's connection characteristics, few papers address this. VANET's connectivity is based on the existing condition. VANETs are not required for emergency protection messages when the community is not connected or there are no security concerns. Malicious nodes can impersonate other nodes, divert packets to the wrong path, retransmit packets, propagate false location information, and propagate misleading traffic statistics. Finding these nodes is therefore crucial to preserving network functionality [6][7].

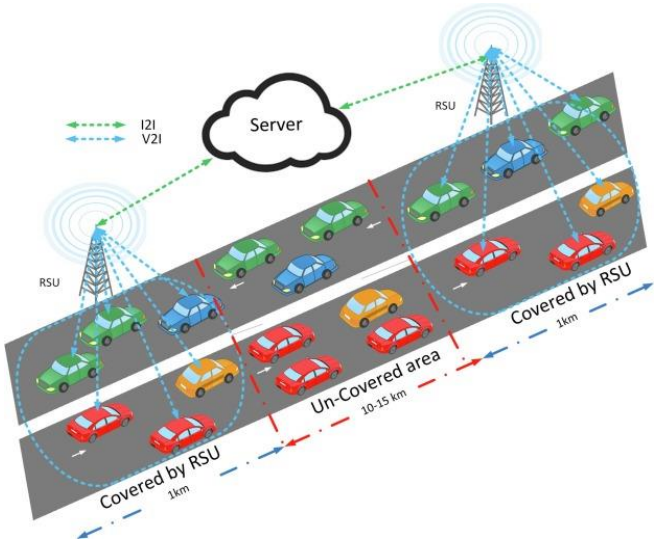

Fig. 1. VANET Communication covered and uncovered area [2]

2 Literature Survey

Vehicular Ad-hoc Networks typically use wireless technology such as Dedicated Short Range Communications (DSRC), a subset of Wi-Fi. Cellular and satellite networks are

also options for communication. Ad hoc vehicle networks are one possible component of Intelligent Transportation Systems (ITS). Ad hoc vehicle networks facilitate communication among moving vehicles in both scenarios. V2V communication provides for rapid two-way communication between moving vehicles. Future traffic is expected to be dominated by driverless autonomous vehicles, and VANET is a promising technology that makes it easier for these vehicles to communicate with conventional driver-controlled vehicles. VANET apps fall into two categories: traffic management apps and traffic safety apps. Route planning applications are among the traffic management applications. Examples of applications pertaining to safety include applications for road conditions and accident information systems [8].

Vehicular Ad Hoc Networks (VANETs) are an important component of intelligent transportation systems that improve road safety and traffic efficiency. However, their dynamic and open nature exposes them to a variety of security concerns, including the injection of incorrect signatures by hostile nodes. An IDS can successfully solve these security concerns by utilizing data analysis and pattern recognition techniques [8]. This section examines the concept, methodology, and efficacy of machine learning-based IDS for VANET security. Machine Learning-Based Intrusion Detection Systems analyse network traffic, detect anomalies, and identify malicious nodes. These systems are trained on datasets that include both normal and harmful behaviour, allowing them to discriminate between legal and fraudulent activity [9].

As Tesla's self-driving carriages arrived at the VANET market, the Vehicular Communication System (VCS) expanded over time. The processing and communication power of these vehicles increases over time, and malicious efforts to tamper with the data these devices generate also get more intense. Conferring to the data, about 33% of people in the industrialized world have a driver's license. The open architecture of VANET allows attackers to conduct attacks because its cars are outfitted with wireless technology, including 5G. The prevention just apprehensions the incoming information containers, which also provides these attackers with a way to catch and recruit them for propagation [10] [11].

3 Detection and Mitigation Method for DDoS

Current methods are ineffective in high-traffic environments and fail if the attacker sends false information. Inside attackers can use false emergency communications to report false events, such as traffic accidents. A fake message recognition technique is proposed. First, traffic flow theory is applied to assess vehicle behaviour in the context of a traffic accident. It describes a "bottleneck" situation, which occurs when road capacity is decreased due to closed lanes at an accident site. Security issues like invalid signature sent by the attacker will affect communication connectivity- Wireless standards that enable interactive communication among vehicles and effective communication in VANET. Security concerns include confidentiality, authenticity, integrity, availability, and non-repudiation, with the goal of ensuring communication between vehicles and infrastructure (V2I) [13][14].

3.1 VANET Environment

1. Presents the improved gated sway recurrent units, which are used to anticipate wormhole and sybil attacks in VANET environments.
2. Suggests the use of Chaotic Henon maps based on High-End Cryptography to fake attacks.
3. It has undergone extensive testing, and its effectiveness has been compared to other state-of-the-art learning models.

Pre-processing includes data labeling and normalization. Labeling the dataset is one of the most crucial data preprocessing stages.

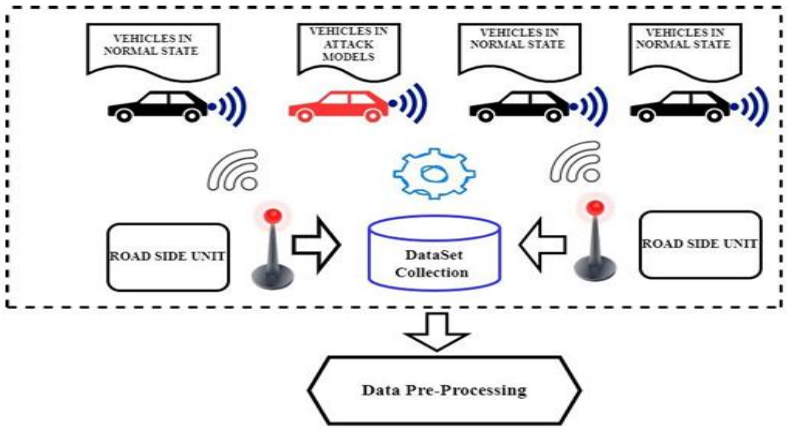

Fig. 1. Data Pre Processing in VANET communication [3]

4 Integrated Detection and Mitigation

Step 1: Gathering information and keeping update on traffic: Every interaction between vehicles (V2V) and infrastructure (V2I) is continuously monitored. Unusual traffic patterns are recognized by merging machine learning models with anomaly detection approaches.

Step 2: Filtering Based on Trust Ratings are assigned based on node traffic patterns. Suspicious nodes—such as those that surpass rate limits or exhibit peculiar traffic patterns—are assigned to lower trust scores.

Step 3: Immediate Mitigation via Inaccessibility and Rate Limiting: Rate limiting prevents malicious nodes from sending excessive amounts of packets.

Step 4: Dynamic Adaptation: The technology constantly modifies network traffic routing to steer clear of crowded or attacked areas.

The purpose of this research is to detect abnormalities and build mitigation techniques for VANETs. Today, security can be a big concern in a variety of VANET applications where indecent communication has a direct or indirect impact on human lives. The major purpose of this research is to improve the security and reliability of Vehicular Ad Hoc Networks (VANETs) by creating and testing methods for detecting incorrect signatures that may indicate hostile activity. Identify and categorize the numerous security threats to VANETs, with a focus on signature-based attacks. Understand how these attacks affect network performance and safety. Develop and implement a method for identifying incorrect signatures in VANET communications. Make sure the detection process is efficient and appropriate for the resource-constrained context of VANETs. Create a real-time IDS that includes a detection tool for incorrect signatures. Ensure that the IDS can operate efficiently in a high-mobility, dynamic network environment like VANETs. [10] The study's goal is to help design more secure and dependable VANETs that can withstand various cyber-attacks while also assuring safe and efficient vehicular communication. Let's consider a simple example where a decision tree is used to classify messages in VANETs based on two features: the validity of the signature and the message frequency [15].

Table 1. Sample Analysis of Training Data.

Message ID	**Signature Validity**	**Message Frequency**	**Label**
101	Valid	Low	Normal
102	Invalid	High	Malicious
103	Valid	High	Normal
104	Invalid	Low	Malicious

5 Conclusion

The study on the identification of incorrect signatures in Vehicular Ad Hoc Networks (VANETs) emphasized the vital necessity for strong security procedures to enable safe and reliable communication among vehicles. The study showed that by integrating modern cryptographic approaches and lightweight authentication protocols, VANETs may be secured against signature-based attacks effectively. The study of various machine learning algorithms for intrusion detection revealed that these techniques can considerably enhance the accuracy and efficiency of detecting harmful activity. Suitable possibilities for real-time anomaly detection in VANETs include decision trees, support vector machines, and neural networks. The development of a real-time IDS that incorporates machine learning for invalid signature detection offers a viable approach for improving VANET security. The system's capacity to promptly identify and respond to security threats ensures that network operations are minimally disrupted.

References

1. T. Anjali, R. Goyal and B. G. N, "Advanced Strategies for Mitigating Anomalies in Vehicular Ad-Hoc Networks (VANETs)," 2025 10th International Conference on Signal Processing and Communication (ICSC), Noida, India, 2025, pp. 212-217, doi: 10.1109/ICSC64553.2025.10968260.
2. Hossain, Mohammad Asif & Md. Noor, Rafidah & Yau, Kok-Lim & Razalli, Saaidal & Zraba, Muhammad & Ahmedy, Ismail. (2020). Comprehensive Survey of Machine Learning Approaches in Cognitive Radio-Based Vehicular Ad Hoc Networks. IEEE Access. 8. 78054-78108. 10.1109/ACCESS.2020.2989870.
3. Anjali, T., Goyal, R., Balaji, G.N. (2025). Enhanced gated sway network and hybrid Henon encryption for secured VANET communication. International Journal of Safety andSecurityEngineering,Vol.15,No.3,pp.543-553.https://doi.org/10.18280/ijsse.15031
4. Bangui, Hind & Ge, Mouzhi & Buhnova, Barbora. (2022). A hybrid machine learning model for intrusion detection in VANET. Computing. 104. 10.1007/s00607-021-01001-0.
5. Ahmed, M., Iqbal, M., & Khan, S. (2022). Efficient and Secure Signature Scheme for VANETs Using Elliptic Curve Cryptography. IEEE Transactions on Intelligent Transportation Systems.
6. Zhang, Y., Wang, L., & Li, H. (2022). Machine Learning-Based Intrusion Detection System for Securing VANETs. IEEE Access.
7. Kim, D., Lee, S., & Park, J. (2022). Lightweight Authentication and Privacy-Preserving Scheme for VANETs. IEEE Communications Letters.
8. Haydari, A., & Yilmaz, Y. (2022). RSU-Based Online Intrusion Detection and Mitigation for VANET. *Sensors (Basel, Switzerland)*, *22*(19), 7612. https://doi.org/10.3390/s22197612
9. Mannoni V., Berg V., Sesia S., Perraud E. A comparison of the V2X communication systems: ITS-G5 and C-V2X; Proceedings of the 2019 IEEE 89th Vehicular Technology Conference (VTC2019-Spring); Kuala Lumpur, Malaysia. 28 April–1 May 2019; pp. 1–5.
10. T. Anjali, R. Goyal and B. G.N, "Prevention of Attacks in Vehicular Adhoc Networks," 2024 IEEE International Students' Conference on Electrical, Electronics and Computer Science (SCEECS), Bhopal, India, 2024, pp. 1-8, doi: 10.1109/SCEECS61402.2024.10482267.
11. Faraj, K. M., Faeq, D. K., Abdulla, D. F., Ali, B. J., & Sadq, Z. M. (2021). Total Quality Management and Hotel Employee Creative Performance: The Mediation Role of Job Embeddedment. Journal of Contemporary Issues in Business and Government.
12. Bali, Rasmeet & Kumar, Neeraj & Rodrigues, Joel. (2014). Clustering in vehicular ad hoc networks: Taxonomy, challenges and solutions. Vehicular Communications. 1. 10.1016/j.vehcom.2014.05.004.
13. H. Ye, L. Liang, G. Y. Li, J. Kim, L. Lu, and M. Wu, "Machine Learning for Vehicular Networks: Recent Advances and Application Examples," IEEE Vehicular Technology Magazine, vol. 13, no. 2, pp. 94-101, 2019.
14. Internet of Vehicle Ad Hoc Networks (VANETs): Anomaly Detection Algorithms AnjaliThuvva,RajeevGoyalandG.N.Balajihttps://www.taylorfrancis.com/books/edit/10.1201/9781032665535/disruptive technologies-computing-communication-systems-suresh-babu-venkata-murali-mohan
15. Wang, T., & Zhou, X. (2022). A Reputation-Based Trust Management System for Secure VANETs. IEEE Transactions on Vehicular Technology.

Predicting the Swelling Potential of Soils Using Random Forest and XGBoost

Yaren Aydın[1], Gebrail Bekdaş[1], Sinan Melih Nigdeli[1] and Ümit Işıkdağ[2]

[1]Department of Civil Engineering, Istanbul University-Cerrahpaşa,
34320 Avcılar/Istanbul/Turkey
yaren.aydin@iuc.edu.tr, bekdas@iuc.edu.tr, melihnig@iuc.edu.tr
[2] Department of Architecture, Mimar Sinan Fine Arts University, 34427 Istanbul, Turkey
umit.isikdag@msgsu.edu.tr

Abstract. Fine-grained soils, especially those rich in clay, have high swelling potential. Determining swelling characteristics is critical for the safe design and cost-effectiveness of foundations. In recent years, machine learning (ML) -based prediction models have been increasingly preferred for the rapid and reliable forecasting of inflation potential. In this study, Random Forest and eXtreme Gradient Boosting (XGBoost) were used to predict the swelling potential of soil. An open-source dataset was used in the study. The performance metrics used are Coefficient of Determination (R^2), Root Mean Squared Error (RMSE) and Mean Absolute Error (MAE). In addition, visualization of model outputs and cross-validation analyses enabled a detailed comparison of the performance of both algorithms. Random Forest and XGBoost algorithms have demonstrated high prediction accuracy. While Random Forest explains 95.6% of the data, XGBoost has made more precise predictions with lower RMSE and MAE values. Overall, Random Forest offers strong explanatory power, while XGBoost delivers reliable performance with lower error rates. In conclusion, the findings demonstrate the effectiveness of machine learning models in predicting swelling potential in fine-grained soils rich in clay.

Keywords: Swelling Potential, Machine Learning, Regression.

1 Introduction

Expansive soils swell when they absorb moisture and shrink when they lose it; this depends on their particle structure and mineral content. The increase in volume of fine-grained soils when exposed to water can lead to serious problems such as soil heaving and settlement in engineering structures [1]. Therefore, it is crucial to determine the swelling properties of the soil units on which building foundations will settle and to design structures accordingly. The high swelling potential of clay soils can cause damage to structures [2]. In geotechnical applications, the accurate determination of swelling properties is critical for the safe design of structures such as foundations and retaining structures. Accurate predictions not only reduce costs but also help minimize

negative impacts [3]. The swelling pressure and swelling percentage of soils are significantly affected by geotechnical properties such as the plasticity index (PI), cation exchange capacity, water content (w), and clay content [4].

In recent years, machine learning methods have been increasingly used in this field and offer alternatives to classical approaches. The continuation of Section 1 compiles studies in this field. This literature review compiles existing studies that use machine learning to predict ground swelling potential. This compilation provides a general framework on the subject, enabling a comparison of different approaches in the field. Stell et al. [5] used machine learning to predict the spatial distribution and swelling potential of swelling soils in the state of Colorado. In this study, which employed regression trees and random forest models, the random forest model was able to explain over 80% of the spatial variability in soil swelling, and the model's prediction performance was validated using 10-fold cross-validation. Amin Benbouras and Petrisor [6] reduced the input variables using Principal Component Analysis, Gamma test, and forward selection on 875 Oedometer test data, then predicted the swelling index from geotechnical physical parameters using Overfitting Machine, Deep Neural Network, Support Vector Regression, Random Forest, LASSO, and other advanced machine learning methods. Among these models, the highest prediction performance for training/validation was achieved by (MAE ($5.6 \times 10{-}3/10.6 \times 10{-}3$), RMSE (0.007/0.013), IOS (0.165/0.298), NSE (0.75/0.13), R (0.94/0.71), and IOA (0.95/0.82)). Nguyen et al. [7] predicted the swelling potential of the soil using Gaussian Process (GP), Multi-Layer Perceptron (MLP), and Bagging-MLP models. The results showed that the Bagging-MLP model provided the most accurate prediction ($R^2 = 0.9$, MAE = 0.544, RMSE = 0.784). Habib et al. [8] predicted the one-dimensional free swelling potential of 210 soil samples using ensemble machine learning models based on parameters such as moisture content, unit weight, plasticity, and clay content. As a result, extremely randomized trees (ERT) and gradient boosting (GB) showed the highest success (R^2=0.97). Alnmr et al. [9] conducted loaded swelling pressure tests to examine the effects of factors such as sand content, initial dry unit weight, and degree of saturation. They used machine learning models such as decision tree regression (DTR), random forest regression (RFR), gradient boosting regression (GBR), extreme gradient boosting (XGBoost), support vector regression (SVR), and artificial neural networks (ANN) to predict and reduce soil swelling. The results show that XGBoost and ANN demonstrated high accuracy, with ANN in particular exhibiting superior consistency in the training and testing phases, achieving the highest R^2 (0.9917 and 0.9954) and lowest RMSE (7.92 and 0.086), and MAE (5.872 and 0.0488) values. Mohammed et al. [10] classified the swelling behavior of soils using easily measurable soil properties and predicted the free swell index (FSI) on 100 soil samples. For FSI prediction, they used random forest, gradient boosting, categorical boosting, artificial neural network (ANN), and preloaded multiple linear regression models. Among these models, the ANN model showed the highest success in FSI prediction (R^2=0.82, RMSE=6.13, and IOA=0.934). These findings clearly demonstrate the effectiveness of data-driven approaches in predicting soil swelling potential. Data-driven approaches not only provide higher accuracy but also offer significant advantages in terms of model flexibility and adaptability

to different conditions. This indicates that machine learning-based methods can be used as a reliable tool for predicting soil swelling potential.

In this study, Swelling potential of soil was predicted using Specific gravity (G_s), Initial moisture content (w), Void ratio (e), Dry unit weight (γ_d), Liquid limit (LL), Plastic limit (PL), Activity, Clay content (CC), Silt content (Sc), Optimum moisture content (OMC), Maximum dry density (MDD), Swelling potential. Random Forest and eXtreme Gradient Boosting (XGBoost) were used during this process.

2 Materials and Methods

2.1 Dataset Description

The dataset was obtained from the source of the Onyekp [11] study. The dataset is global in scale and has been compiled from different countries across Asia, Africa, and Europe [11]. The dataset contains swelling measurements and related soil properties. The data it contains covers both soil samples obtained under natural conditions and those obtained in a laboratory environment. The dataset consists of 78 rows and there is no missing data. In this study, not all data from the source where the dataset was obtained was used; only a specific portion was selected. Additionally, during the data preprocessing step, it has been removed from the surcharge load dataset.

Table 1 shows the basic descriptive statistics of the inputs and outputs in the dataset used in the study. The table provides the mean, standard deviation, minimum, maximum, and quartile values of these variables. The table shows that Specific gravity is distributed quite homogeneously compared to other variables.

Table 1. Descriptive statistics of inputs and outputs in the dataset

Variable	mean	std	min	25%	50%	75%	max
Inputs							
Specific gravity	2.8333	0.0474	2.8	2.8	2.8	2.9	2.9
Initial moisture content	24.6153	7.8859	15	20	25	30	40
Void ratio	1.2166	0.3059	0.7	1	1.2	1.4	1.8
Dry unit weight	13.8076	1.7268	11.5	13	14	15	17
Liquid limit	71.3333	3.8835	66	66	73	75	75
Plastic limit	25	2.9629	21	21	26	28	28
Activity	0.8833	0.1103	0.73	0.73	0.94	0.98	0.98
Clay content	52.3333	2.0681	50	50	52	55	55
Silt content	43.3333	3.7956	38	38	46	46	46
Optimum Moisture content	24.3333	1.8978	23	23	23	27	27
Maximum dry density	15.7666	0.4053	15.2	15.2	16	16.1	16.1
Output							
Swelling potential	11.3641	5.3420	0.5	9	12.05	14.8	22.1

Fig. 1 shows the correlation matrix for the variables in the dataset. Correlation coefficients indicate the direction and strength of the relationship between variables. Values close to 1 indicate strong positive correlation, while values close to -1 indicate strong negative correlation. Among the prominent relationships in the matrix in Figure 1, there are very high negative correlations (-0.98) between liquid limit and specific gravity. This indicates that these two variables are inversely proportional to each other. Very high positive correlations (0.99) were observed between maximum dry density and liquid limit. This coefficient indicates that these two variables are highly dependent on each other.

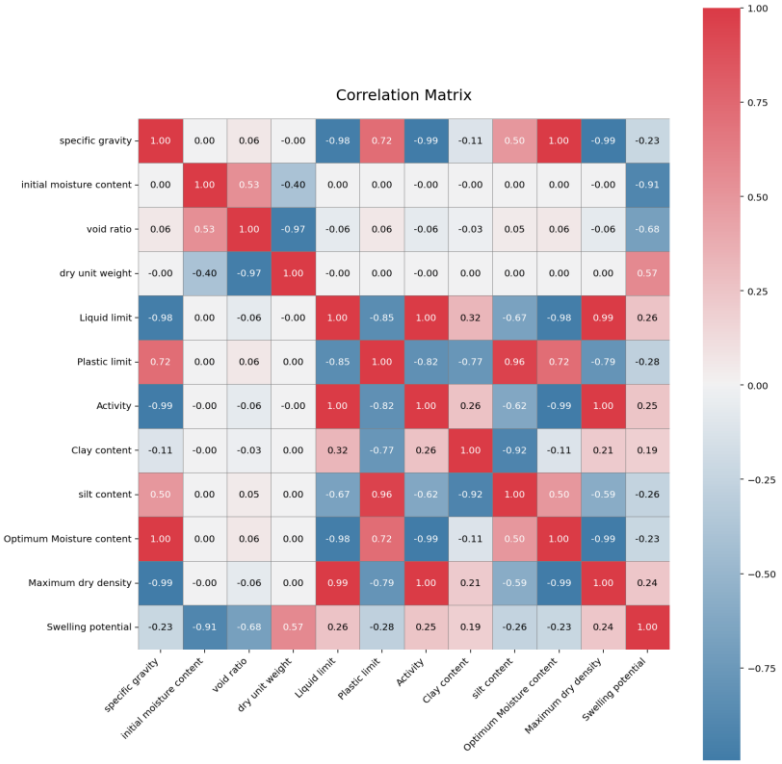

Fig. 1. Correlation matrix of the dataset.

2.2 Machine Learning (ML)

Machine Learning (ML), a subfield of Artificial Intelligence (AI), is a set of methods that uses mathematical and statistical techniques to draw conclusions from data and predict the unknown. ML methods learn from data and improve their performance without human intervention [12]. ML consists of four different types of learning. One of these, supervised learning, is divided into two categories: classification and regression.

In this study, regression algorithms were used to predict swelling potential. These are Random Forest and eXtreme Gradient Boosting (XGBoost).

Random Forest algorithm is a supervised ML algorithm consisting of multiple decision trees. Each tree is created using a random subset of the training data, and while the internal nodes split the data based on attributes, the leaf nodes predict the continuous target values of the examples. Randomly selected attributes are evaluated at each node, and the attribute that provides the best split is selected. The predicted value of an example is determined by averaging the outputs of all trees [13].

XGBoost is a powerful regression algorithm based on gradient boosting. It is fundamentally based on the boosting method that uses decision trees and improves accuracy by adding new trees that predict model errors in each iteration. It provides high speed and accuracy on large datasets. It first builds a strong model from weak learners and attempts to minimize the loss function at each iteration. New trees are combined with previous trees to correct the errors of the current model [14].

The performance metrics used are Coefficient of Determination (R^2), Root Mean Squared Error (RMSE) and Mean Absolute Error (MAE). R^2 shows how much of the total variance of the dependent variable is explained by the independent variables. RMSE is the square root of the average of the squares of the differences between the predicted values and the actual values. MAE is the average of the absolute values of the differences between the predicted values and the actual values [15]. In the study, 10-fold cross validation was performed to prevent overfitting.

3 Results

In this section, the performance metrics of Random Forest and XGBoost models are compared, and visual results for these algorithms are provided. Table 1 gives performance comparison of Random Forest and XGBoost models.

Table 2. Performance comparison of Random Forest and XGBoost models

Model	Average R^2	Average RMSE	Average MAE
Random Forest	0.9564	0.8807	0.7412
XGBoost	0.9488	0.7390	0.5732

Random Forest explains approximately 95.6% of the data. XGBoost explains approximately 94.9% of the data. In other words, both models explain the data quite well. Table 1 shows that the R^2 value of the Random Forest model is higher than that of XGBoost. However, the error values are also higher than those of XGBoost. This indicates that XGBoost exhibits more stable and reliable performance in terms of prediction accuracy. Random Forest explains the data very well, but it may not predict as accurately as XGBoost in some points.

Figure 2 shows four different graphs summarizing the results of the Random Forest model. The bar chart in the upper left shows the importance of the properties. It can be seen that initial moisture content and void ratio are the most decisive properties. The graph in the upper right shows that the predictions are mostly accurate, but the model

can deviate slightly at extreme values. The graph at the bottom left shows that the distribution of errors is mostly small, indicating the overall reliability of the model.

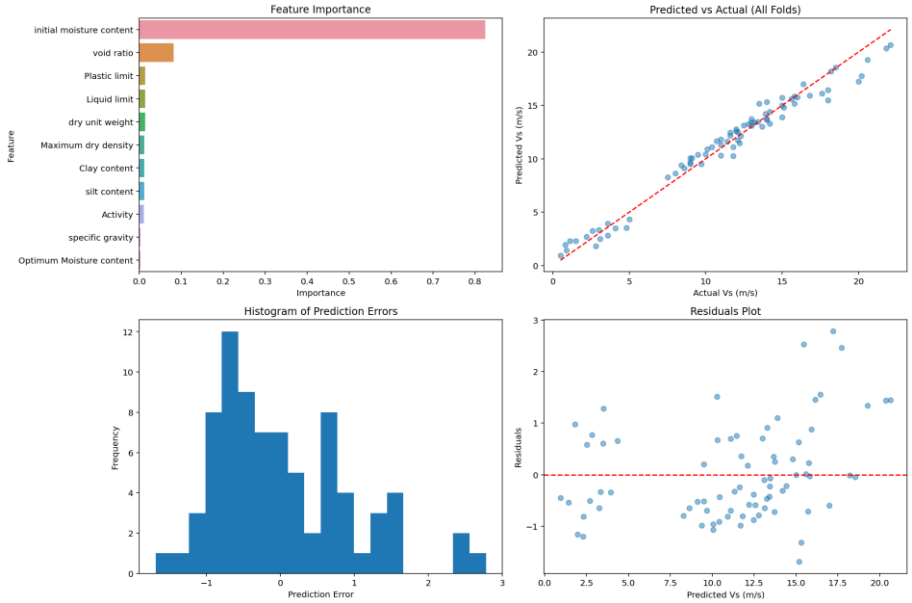

Fig. 2. Model prediction results and error analyses for Random Forest.

Fig 3. shows four different graphs summarizing the results of the XGBoost model. The bar chart in the upper left shows the importance of the properties. It can be seen that initial moisture content and liquid limit are the most decisive properties. The graph in the upper right shows that the predictions are mostly accurate, but the model can deviate slightly at extreme values. The graph at the bottom left shows that the distribution of errors is mostly small, indicating the overall reliability of the model.

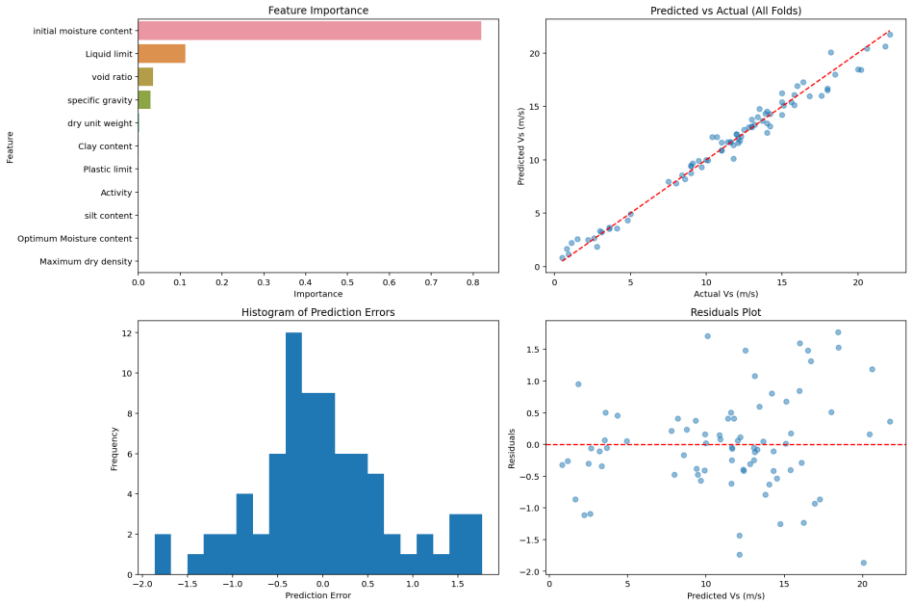

Fig. 3. Model prediction results and error analyses for XGBoost.

4 Conclusions

In this study, the Random Forest algorithm and eXtreme Gradient Boosting (XGBoost) were used to estimate the swelling potential of the soil, and the performance of these methods was compared. Performance metrics Coefficient of Determination (R^2), Root Mean Squared Error (RMSE) and Mean Absolute Error (MAE). were used for the comparison. According to the results obtained, both models demonstrated high accuracy. The Random Forest model showed strong explanatory power, explaining 95.6% of the data variance with its R^2 value. On the other hand, the XGBoost model showed lower errors in terms of RMSE and MAE values (0.7390 and 0.5732, respectively), indicating that the predictions were more accurate.

Overall, while both models performed very similarly, Random Forest explained the data better, while XGBoost offered more reliable performance with lower prediction errors. These results show that both algorithms have advantages depending on the dataset and model.

References

[1] M. Ismeik, A. M. Ashteyat, and K. Z. Ramadan, “Stabilisation of fine-grained soils with saline water,” *European Journal of Environmental and Civil Engineering*, vol. 17, no. 1, pp. 32–45, Jan. 2013, doi: 10.1080/19648189.2012.720399.

8

[2] V. H. R. Barbosa, M. E. S. Marques, and A. C. R. Guimarães, "Predicting Soil Swelling Potential Using Soil Classification Properties," *Geotechnical and Geological Engineering*, vol. 41, no. 8, pp. 4445–4457, Nov. 2023, doi: 10.1007/s10706-023-02525-2.

[3] P. Jamsawang, B. Adulyamet, P. Voottipruex, P. Jongpradist, S. Likitlersuang, and K. Tantayopin, "The free swell potential of expansive clays stabilized with the shallow bottom ash mixing method," *Eng Geol*, vol. 315, p. 107027, Mar. 2023, doi: 10.1016/j.enggeo.2023.107027.

[4] J. C. Parker, D. F. Amos, and D. L. Kaster, "An Evaluation of Several Methods of Estimating Soil Volume Change," *Soil Science Society of America Journal*, vol. 41, no. 6, pp. 1059–1064, Nov. 1977, doi: 10.2136/sssaj1977.03615995004100060008x.

[5] E. Stell, M. Guevara, and R. Vargas, "Soil swelling potential across Colorado: A digital soil mapping assessment," *Landsc Urban Plan*, vol. 190, p. 103599, Oct. 2019, doi: 10.1016/j.landurbplan.2019.103599.

[6] M. Amin Benbouras and A.-I. Petrisor, "Prediction of Swelling Index Using Advanced Machine Learning Techniques for Cohesive Soils," *Applied Sciences*, vol. 11, no. 2, p. 536, Jan. 2021, doi: 10.3390/app11020536.

[7] D. Dam Nguyen *et al.*, "Bagging and Multilayer Perceptron Hybrid Intelligence Models Predicting the Swelling Potential of Soil," *Transportation Geotechnics*, vol. 36, p. 100797, Sep. 2022, doi: 10.1016/j.trgeo.2022.100797.

[8] M. Habib, A. Habib, and B. Alibrahim, "Prediction and parametric assessment of soil one-dimensional vertical free swelling potential using ensemble machine learning models," *Adv Model Simul Eng Sci*, vol. 11, no. 1, p. 26, Dec. 2024, doi: 10.1186/s40323-024-00277-z.

[9] A. Alnmr, R. Ray, and M. O. Alzawi, "A Novel Approach to Swell Mitigation: Machine-Learning-Powered Optimal Unit Weight and Stress Prediction in Expansive Soils," *Applied Sciences*, vol. 14, no. 4, p. 1411, Feb. 2024, doi: 10.3390/app14041411.

[10] Z. Mohammed, G. Gouveia, A. Ramkissoon, and R. Clarke, "Prediction of soil swelling using machine learning techniques," *Model Earth Syst Environ*, vol. 11, no. 6, p. 392, Dec. 2025, doi: 10.1007/s40808-025-02576-9.

[11] E. E. U and U. Onyekpe, "Data on one-dimensional vertical free swelling potential of soils and related soil properties," *Data Brief*, vol. 39, p. 107608, Dec. 2021, doi: 10.1016/j.dib.2021.107608.

[12] M. Wazid, A. K. Das, V. Chamola, and Y. Park, "Uniting cyber security and machine learning: Advantages, challenges and future research," *ICT Express*, vol. 8, no. 3, pp. 313–321, Sep. 2022, doi: 10.1016/j.icte.2022.04.007.

[13] L. Breiman, "Random Forests," *Mach Learn*, vol. 45, no. 1, pp. 5–32, 2001, doi: 10.1023/A:1010933404324.

[14] T. Chen and C. Guestrin, "XGBoost," in *Proceedings of the 22nd ACM SIGKDD International Conference on Knowledge Discovery and Data Mining*, New York, NY, USA: ACM, Aug. 2016, pp. 785–794. doi: 10.1145/2939672.2939785.

[15] J. Singh Kushwah, A. Kumar, S. Patel, R. Soni, A. Gawande, and S. Gupta, "Comparative study of regressor and classifier with decision tree using modern tools," *Mater Today Proc*, vol. 56, pp. 3571–3576, 2022, doi: 10.1016/j.matpr.2021.11.635.

Optimizing Point-to-Point Wireless Bridge Networks for Performance and Cost: A Case Study on Improving Network Access in Eulogio "Amang" Rodriguez Institute of Science and Technology

Jesus S. Paguigan[1] , Larry T. Rutaquio Jr.[2] and, Rogelio T. Mamaradlo.[3]

[123] Eulogio "Amang" Rodriguez Institute of Science and Technology, Manila, Philippines

Abstract. The Eulogio "Amang" Rodriguez Institute of Science and Technology (EARIST) is encountering problems in making their academic and administrative systems' reliable and high-speed network connectivity operate smoothly whenever they like. The researcher assesses and applies point-to-point wireless bridge networks as they are the most productive and budget-friendly alternative. By specifically employing directional line-of-sight antennas in the processes, the technology contributes to better data transmission. It therefore reduces signal loss and infrastructure costs, which are greater when conventional wired solutions are eliminated. The research focused on designing an optimized network infrastructure using a star topology for permeability, reliability, and security. Important factors encompass site selection and line-of-sight optimization for higher single-pairing antennas and traffic power equipment. In addition to the pertinent issues, Data Center Bridging protocols are united to make the system more reliable, and fewer frames are lost. The budget report is rather detailed about the benefits of a wireless bridge network at EARIST in terms of its lifetime. Findings suggest that a point-to-point wireless bridge network for performance and cost utilization can enhance network reliability, speed, and security, and reduce costs associated with operations. The network layout, which was suggested, guarantees a regular internet connection from building to building on the campus and acts as a catalyst for improved digital learning environments. The wireless bridging technologies utilized as the means of network infrastructure optimization in EARIST bring accessibility to an intelligent pedagogical climate with a new operational model.

Keywords: Bridge network, Network, Performance, Point-to-Point, Optimization

1 Introduction

1.1 Background of Study

The Eulogio "Amang" Rodriguez Institute of Science and Technology (EARIST) is an emerging educational institution strong in diverse instructional, research, and extension programs, active student-faculty communities, and enlivened by the permeation of

digital pedagogies and the ever-heightening role of online resources in instruction, research, extension, and administration. Owing to a global move towards technological advancement and increased reliance on the internet to meet the world's educational needs, there is a growing need for reliable and fast access at institutions of learning to the World Wide Web. This study explores the challenges of network access at Eulogio "Amang" Rodriguez Institute of Science and Technology (EARIST). The widespread use and familiarity of Ethernet have driven growing interest in Ethernet-based convergence technologies. However, for certain applications to transition to an Ethernet network, enhancements are required through a data center bridge (DCB). A DCB comprises both point-to-point and end-to-end protocols, which must undergo testing to ensure interoperability among different vendors' products in a heterogeneous environment and to prevent frame loss during congestion. This article examines each of the four protocols individually, as well as in combination, to analyze how DCB interacts with various applications [1]. Priority-based Flow Control (PFC) and Enhanced Transmission Selection (ETS) can be adapted for wireless networks. Discuss their roles in managing traffic, ensuring quality of service (quality of service), and maintaining system reliability by preventing packet loss and managing bandwidth allocation. Wireless technologies, particularly point-to-point wireless bridge networks, have emerged as viable solutions for institutions facing challenges like EARIST. Point-to-point wireless bridging uses directional line-of-sight antennas, focusing on the signal for efficient data transmission. By nature, it reduces data loss and signal-to-noise issues, ensuring optimal performance. They offer the flexibility of quick deployment, reduced physical infrastructure, and the ability to span large areas that might be difficult or expensive to cover with wired solutions.

2 Infrastructure Design

2.1 Site Survey and Proposed Study

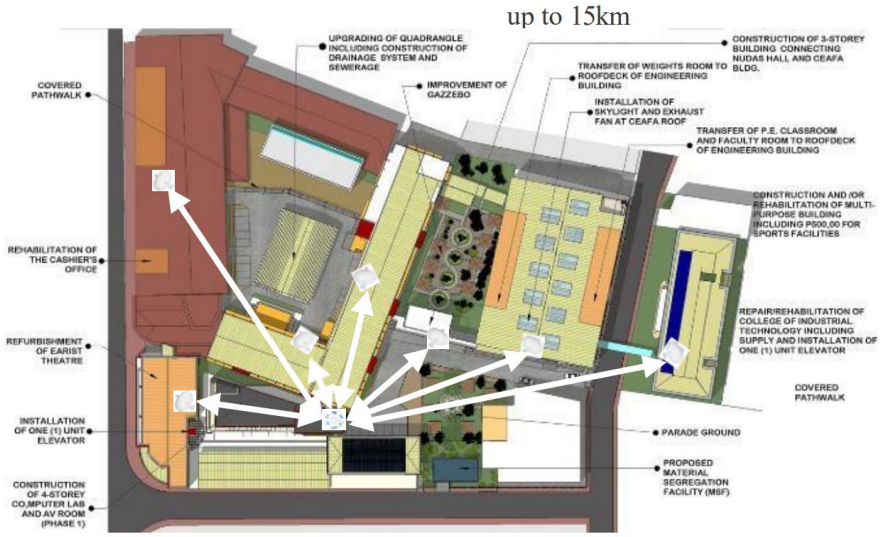

Fig.1. The Institute Vicinity Map for the Proposed Study

In Figure 1, the researcher follows key considerations for selecting the site survey location to optimize point-to-point wireless bridge networks at EARIST. The researcher uses the star topology in the case study, Optimization of Point-to-Point Wireless Bridge Networks for Performance and Cost to Improve Network Access for Eulogio “Amang” Rodriquez Institute of Science and Technology, to connect the wireless bridges to the university's network infrastructure. The researcher could also configure the switch to use power-saving features to reduce the network's energy consumption. This would help to reduce the cost of operating the network. The design goals emphasize centralized control, easier troubleshooting, and the ability to add or remove devices without affecting the entire network. Star topology is a good choice for point-to-point wireless bridge networks because it offers several advantages, including scalability, reliability, and security. Roof of the Main Building: This location would provide a good line of sight to most other campus buildings. It is essential to consider the height of the building and the surrounding buildings when selecting this location, as tall buildings can block the signal. The institute's nearby building could be a good location for a wireless bridge.

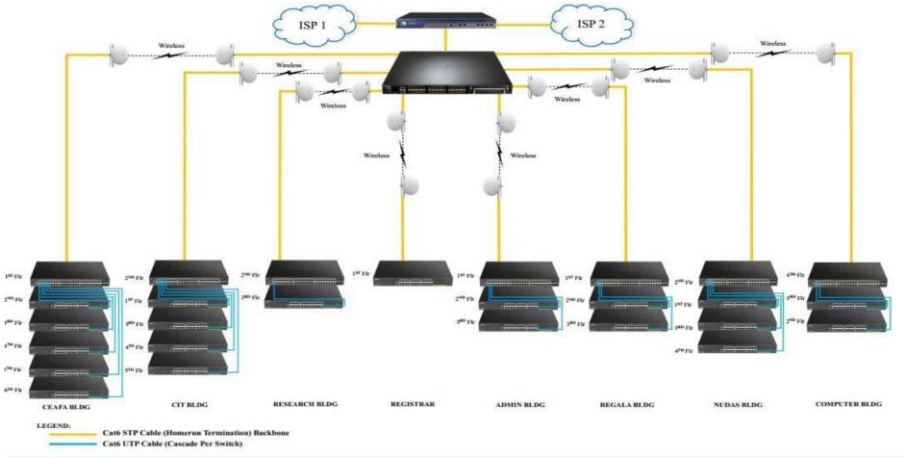

Fig. 2. Proposed Case Study: Optimization of Point-to-Point Wireless Bridge Networks for Performance and Cost to Improve Network Access

Figure 2 shows the optimization of a point-to-point wireless bridge network, which is well thought out for enhancing network access. The diagram effectively interconnects the different buildings through an effective combination of wired and wireless connections, hence raising the potential for improvement in performance and cost-effectiveness in the long run. The two ISPs and multiple wireless access points show that the network design is robust and redundant, meant to minimize downtime and enhance bandwidth availability to the greatest possible extent. A clear visualization of the network architecture is depicted by the color-coded lines indicating the UTP cables or Cat5e for backbone and cascade connections. Such visual clarity helps to perceive the data flow instantly, along with potential bottlenecks over the network. Overall, the setting is strong; this is a pragmatic and impactful case study that could significantly improve network access through strategic optimization of wireless bridge networks. An antenna is also needed at each end of the point-to-point link for data transmission from one point to another. The wireless LAN bridge solution focuses on achieving an efficient and well-structured interconnection. It incorporates key features such as effective traffic isolation, controlled access management, and necessary address translation, all while maintaining compatibility with the interests of internet service providers. This approach is particularly suitable for campus dormitory ISP internetworking scenarios, where establishing wired connections between campus and dorm networks is often impractical due to cost and environmental limitations [4]. With a powerful booster, the design is an intense wave that may be delivered quickly and effectively over a larger area in remote areas where cable networks fail. This technology makes it simple to connect to distant locations and is very practical for the institute, especially in the teaching modality. Wireless communication using microwaves, e.g., Wi-Fi, is increasingly important. Performance is a fundamental issue, resulting in more reliable and efficient communication. Laboratory measurements are made about several performance aspects of Wi-Fi (IEEE 802.11b, g) WEP point-to-point links using available access points from Enterasys Networks (RBTR2). Through OSI levels 4 and 7, detailed results from TCP, UDP, and FTP experiments, namely: TCP throughput, jitter, and percentage datagram loss, are presented and discussed.

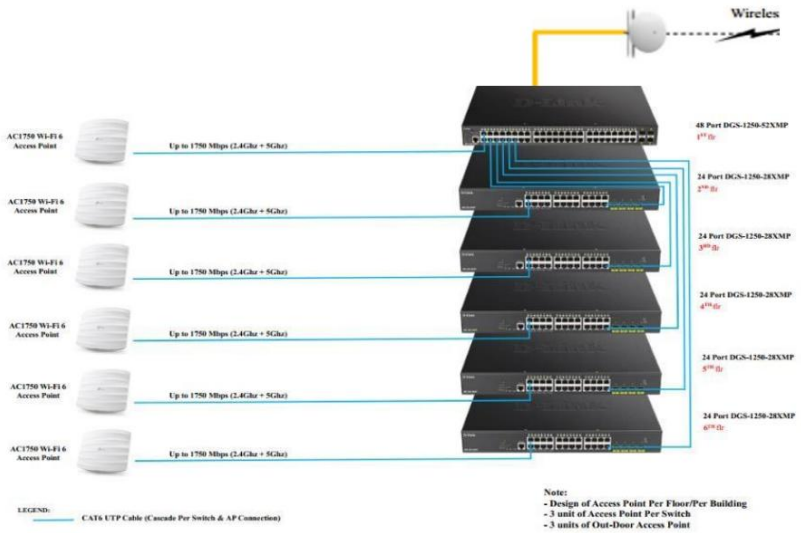

Fig.3. Network Structure per building floor

Figure 3 shows the overview of a properly structured network architecture for a typical building floor, relating to wired and wireless connectivity reciprocally. The design hierarchy with an Intermediate Distribution Frame harmoniously relates to wireless access points and wired Ethernet connections for user service on that floor. Actual model numbers for the access points and switches add practical details and imply a real implementation. The design considerations are the strategic distribution of access points per floor and the use of outdoor access points, reflecting thoughtfulness in coverage and capacity planning. The network architecture is visualized by the color-coded lines indicating the UTP cables (Cat5e) for backbone and cascade connections. It presents a well-designed and implemented network structure that effectively supports user access and connectivity within the building. The addition of aspect tends to dramatize the diagram.

2.2 Technology Research

The researcher considered the following for the design and implementation case study: optimization of point-to-point wireless bridge networks for performance and cost to improve network access of the institute to guarantee the fastest speeds and best communication quality:

- The line of Sight. The necessary components for Wi-Fi point-to-point communications. This means that connectivity will be impacted by any trees, other structures, or landscape elements that could partially or entirely block the line of sight between two point-to-point antennas. Make sure the line of sight between antennas is unobstructed.
- The higher, the better. Interference from other sources is a factor because anyone can use and reuse Wi-Fi frequencies. Access points should be installed as

high as possible to keep them as far away from other radio frequency sources as feasible

- usually on the roof and fastened to a tower or pole.
- Directional antennas. It is essential to select highly directed equipment to decrease potential interference further. The less vulnerable they are to other interference sources, the more directional the antennas are utilized. A very safe and physically stable installation must be made since a highly directional antenna can be more difficult to aim or target and more vulnerable to minute wind movements.
- Use higher frequencies. Operates in the 2.4GHz and the 5GHz frequency ranges.

- Power over Ethernet or PoE**.** Provide high interoperability, dependability, convenience, and complete system solutions for effortlessly transmitting power using Ethernet connections. A redundant wireless bridge network is proposed to handle the transmission of measurement data and control commands for a remote launch system. Since such a system requires high reliability, redundancy, and a voting mechanism is applied to enhance its dependability. The design establishes dual wireless links for master-enslaved people, ensuring that if the master link fails, data is seamlessly rerouted through the slave link. With the support of a high-performance wireless bridge, the network delivers throughput exceeding 200 Mbps, a communication range of 5–50 km, and strong reliability meeting the operational demands of a remote launch system [6].

2.3 Choosing Equipment

The research defined an embedded remote working condition monitoring system based on an embedded development board and wireless bridge communication technology. This system combines the Video for Linux 2 programming framework provided by Linux and transplants the collection and sending program of working condition data and image data on the development board. First, the development board collects and packs the data; then, the data is transmitted to the upper monitoring center through the wireless bridge, which realizes real-time monitoring of the scene and real-time display and alarm of working condition data.

The research applies an embedded remote working condition monitoring system and builds an experimental platform for its feasibility verification. The function of an antenna is to focus on a microwave signal. It will thus offer better concentration and more directivity on the signal. Eventually, one will achieve a further distance, less interference, and more throughput. Generally, links under one kilometer need not have very high directionality.

As the distance increases between the points, the directivity should be higher to compensate for the attenuation by distance and the weather. Power over Ethernet, such as PoE, is much better for providing power to wireless bridges since they are open to the weather conditions. This is much safer. It is also much more useful since only a single STP is required to implement the network.

Table 1. Equipment and Labor Cost

Equipment Cost				
Line Item, Budget, and Specification	***Unit Cost***	***Quantity***	***Duration (in Months)***	***Amount***
Antennas, Transceivers, Mounting, Fabricated Antenna/Hardware, Accessories, and Equipment	Php 350,000.00	1 Lot	1	Php 350,000
Labor Cost				
Installation, Configuration, Testing, and Troubleshooting	Php 180,000	1 Lot	1	Php 180,000
Training Cost (Training Program and Materials)	Php 30,000	---	---	Php 30 000
Contingency and Miscellaneous Cost	Php 150,000	---	----	Php 150,000
Total				Php 710,000

Table 1 shows the equipment cost and budget cost for optimizing point-to-point wireless bridge networks for performance and cost to improve network access for EARIST, which is PHP. 710,000. This amount covers the price of the following items:

- Using Ubiquiti NanoBeam AC Gen2 for point-to-point wireless bridging, which operates in the 5 GHz band and supports data rates up to 450 Mbps. The communication protocols used, such as IEEE 802.11ac for wireless communication, must be specified. Antennas, transceivers, mounting fabricated antenna/hardware, accessories, and equipment: Php. 350,000
- Installation, configuration, testing, and troubleshooting: PHP. 180,000
- Training cost (training program and materials): Php. 30,000
- Contingency and miscellaneous costs, Php. 150,000. The equipment and budget costs are one-time costs, and they are expected to provide EARIST with significant benefits in terms of improved network performance and cost savings over the long term.

Finally, the table gives the Total of all costs, which provides a rapid overview of total costs in each category, thus giving a fast picture of total costs in each major category. Table 1 presents the financial aspects of the project in straightforward, incisive terms. Indeed, it speaks positively of this review's ability to digest the information it offers.

3 Results

This study aimed to optimize point-to-point wireless bridge networks at EARIST to improve network access across the campus by implementing a series of strategically placed wireless bridges.

3.1 Cost Analysis

The optimization of point-to-point wireless bridge networks at the EARIST involves a comprehensive cost analysis to assess the financial implications of implementing this project. This section outlines the various cost components associated with optimization and their impact on the institution's budget.

Wireless sensor networks have various practical applications, each with strengths and limitations. Linear wireless sensor networks are vital in specialized areas such as pipeline and bridge condition monitoring. To enhance communication in Linear Wireless Sensor Networks (WSNs), we propose the Bidirectional Linear WSN. This improved communication model features two linear base stations, with multiple sensor nodes between them. Through multi-hop transmission, these sensor nodes relay the collected data in a linear sequence toward one of the base stations. This method of communication in the WSN allows the design to be simple and cost-effective [8]. An important factor in deploying wireless mesh networks cost-effectively is determining how to connect last-mile networks to core service providers while minimizing infrastructure expenses and meeting throughput requirements. This process, known as middle-mile network optimization, involves tasks such as designing the topology, assigning tower heights, selecting antennas and orientations, and determining transmit power levels making it a computationally challenging problem. This paper introduces the first polynomial-time approximation algorithm for a generalized version of the middle-mile optimization problem, where point-to-point links are used to connect last-mile networks. [9]

3.2 Configurations and Implementation

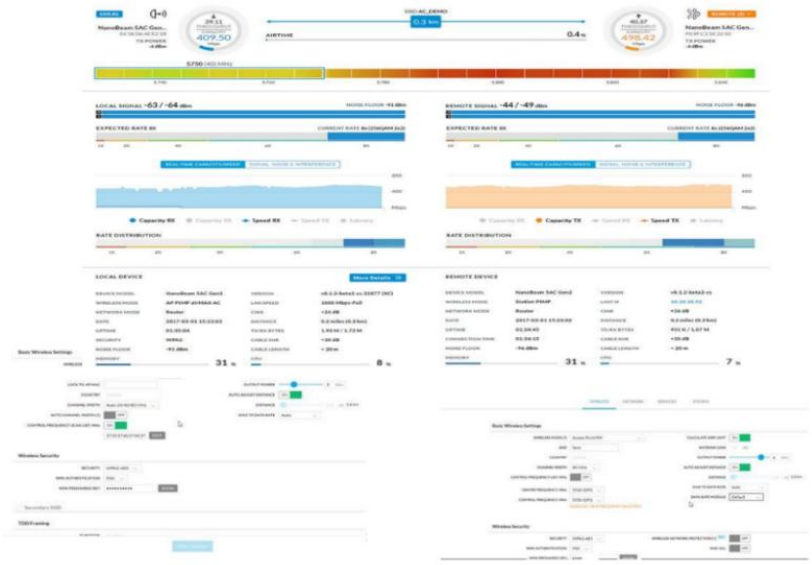

Fig. 4. Configuring the local and remote point-to-point wireless bridge using line of sight

Figure 4 shows how you can set up wireless bridge devices for point-to-point connections. Side-by-side viewing of local and remote device settings facilitates comparison, thus helping to align the devices correctly for optimum performance. The information typically displayed includes signal strength, data rates, distance, and security and network efficiency configuration options. It allows administrators to monitor link health, fine-tune settings for optimum performance, and secure communications. A graphic presentation of the strength of signals and data rates gives a clear visual representation of the quality of the connection. At the same time, options are present for configuration to tune the link to requirements. The high-speed, wireless Ethernet bridge can support a point-to-point network structure; it can provide a high-speed transmission channel in places with scattered distribution and inaccessible cable networks. Meanwhile, as a critical supplementary and emergency backup of the wireless cable access, it can save many construction costs and achieve rapid development and use.[10]

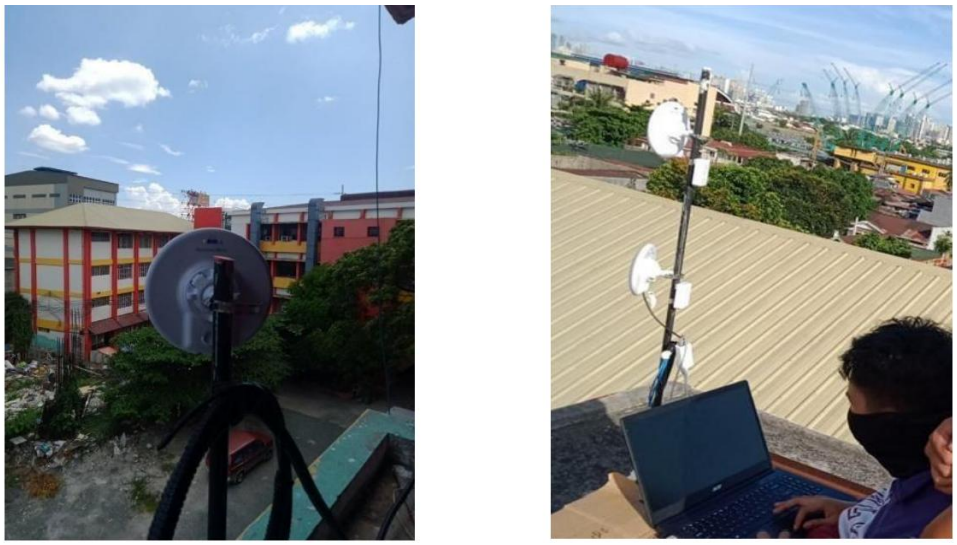

Fig.5. Implementation of the Proposed Study

Figure 5 shows the point-to-point wireless network setup, which can be deployed accurately and in detail. A cursory detail would state that the critical element would establish a clear line-of-sight connection between the two. A zoomed-in shot points at the rooftop; a directional antenna is carefully mounted to underscore its crucial part in ensuring the signal is transmitted at the best signal possible. The wider view shows the entire setup on yet another rooftop. It includes many antennas installed. The above is the configuration and testing phase of deploying a wireless network in a campus setting. This research introduces a method for creating redundant topologies in time-sensitive networking (TSN) to ensure the reliable transmission of scheduled traffic (ST) while incorporating fault tolerance. Redundant topologies generally improve network resilience and are essential in safety-critical systems that require high reliability. Advanced antenna technologies, such as high-gain directional antennas, further enhance performance by concentrating signals and minimizing interference from surrounding sources [11][12].

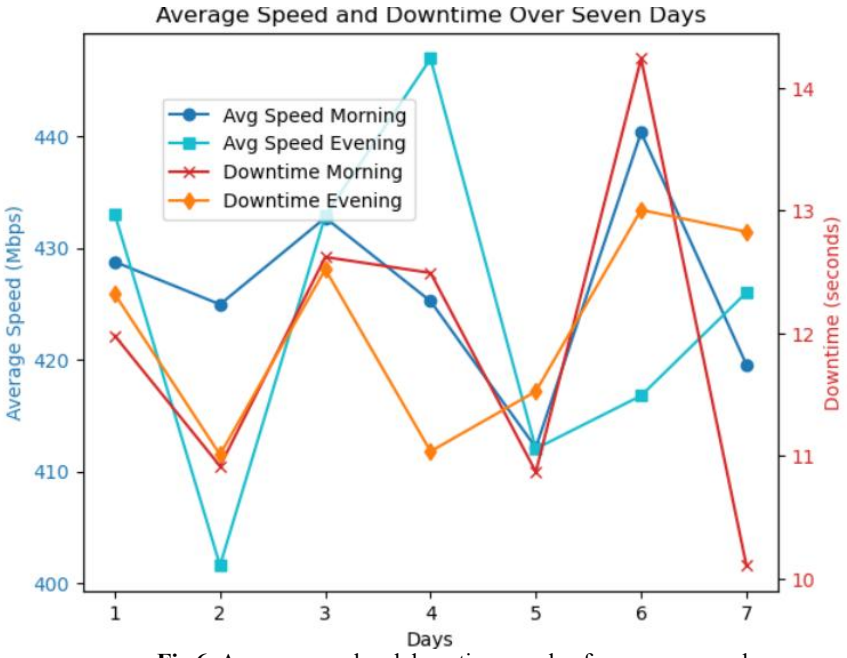

Fig.6. Average speed and downtime per day for over one week

Figure 6 shows that average speeds ranged between 400 and 450 Mbps over seven days. Despite minor downtimes twice daily, each lasting between 10 and 15 seconds, the overall network dependability remains strong. This limited downtime is insignificant compared to the high-speed connectivity supplied throughout the day, ensuring smooth and efficient internet access for all connected devices.

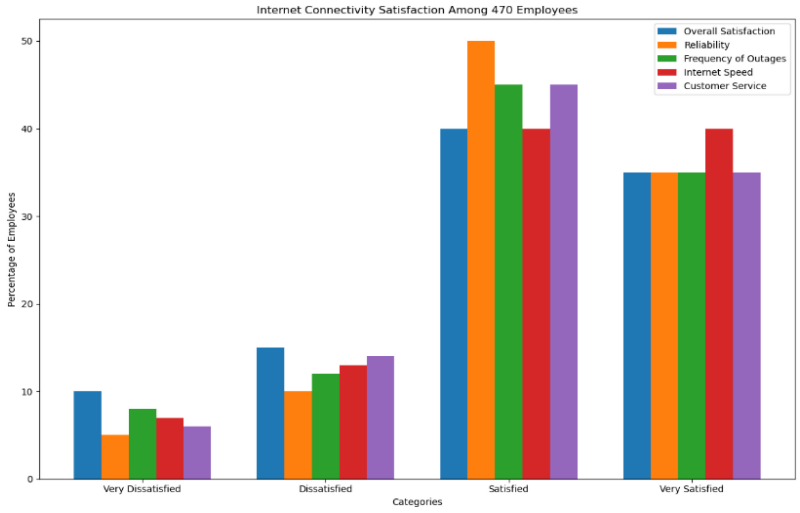

Fig.7. User Feedback on Internet Connectivity Satisfaction

Figure 7 shows the user feedback on Internet Connectivity Satisfaction Among 470 Employees, which provides valuable insights into the satisfaction levels of employees regarding various aspects of Internet connectivity at EARIST. The chart reveals that most employees are satisfied or very satisfied with the overall internet connectivity, reliability, internet speed, and customer service. However, the frequency of outages remains a concern, with lower satisfaction levels in this area. These findings highlight the importance of reducing outages to improve overall satisfaction. Point-to-point wireless bridge networks can address these issues by providing stable, high-speed connections between fixed locations, enhancing network performance, and employee satisfaction. This approach optimizes performance and balances cost-effectiveness, making it a practical solution for improving network access in the institution.

4 Conclusions and Recommendations

4.1 Conclusions

This research proposes a cost-effective point-to-point wireless bridge network to improve connectivity, reliability, and infrastructure efficiency at EARIST. In strategically deploying wireless bridges, the project attained significant strides in both performance and coverage of the network, and it particularly benefited the constructed computer laboratory and distant buildings. This solution is viable and academically practical in minimizing excess cabling in network connectivity problems, like other institutions. The study clearly outlined the need for meticulous planning to consider the Line of Sight, environmental conditions, and select all the different equipment to ensure the solution stays reliable and works well in the long run. This successful implementation at EARIST will be an excellent case study for any institution willing to use wireless bridge technology to break any geographical restraining factors and increase network accessibility.

4.2 Recommendations

Among this study's recommendations, the first consideration is a clear line of sight between the antennas. Site surveys should be conducted to avoid obstructions and increase signal strength. Second, investment in robust, weatherproof equipment that can withstand the elemental challenges and offer long-term reliability is recommended. Third, there is a need for a comprehensive maintenance regimen that includes regular checking and proactive installations. While simultaneously exposing oneself to the ongoing generation of wireless technology and upgrades of the point-to-point solution, further network improvement is possible. Finally, the knowledge and lessons learned during this project can be shared with other institutions to quicken the broader adoption of these solutions to enhance and improve the network in different settings.

References

1. M. Hagen, P. Scruton, R. Noseworthy, R. Zarick, and R. Bartos, "Testing challenges of data center bridging networks," in *IEEE Communications Magazine*, vol. 50, no. 3, pp. 140-145, March 2012, doi: 10.1109/MCOM.2012.6163594.
2. A. Pratama, Agussalim, and F. Muhammad Reza, "Point-to-Multipoint Implementation on Mikro Tik Router-Based Warehouse Networks," *2020 6th Information Technology International Seminar (ITIS)*, Surabaya, Indonesia, 2020, pp. 87-91, doi: 10.1109/ITIS50118.2020.9321045.
3. Ying-Chen Chen, Chi-Cheng Chuang, Ray-I Chang, Jia-Shian Lin, and Te-Chih Wang, "Integrated wireless access point architecture for wireless sensor networks," 2009 11th International Conference on Advanced Communication Technology, Gangwon, Korea (South), 2009, pp. 713-718.
4. Hang, L. I. U., & Yu-ming, M. A. O. (2005). A wireless LAN bridging solution based on the campus network. Journal of Electronic Science and Technology, 3(1), 14-17.
5. J. A. R. Pacheco de Carvalho, H. Veiga, N. Marques, C. F. F. P. Ribeiro Pacheco and A. D. Reis, "A contribution to laboratory performance measurements of IEEE 802.11 a/g WEP point-to-point links using TCP, UDP and FTP," 2010 7th International Symposium on Communication Systems, Networks & Digital Signal Processing (CSNDSP 2010), Newcastle Upon Tyne, UK, 2010, pp. 867-870, doi: 10.1109/CSNDSP16145.2010.5580302.
6. G. Qi, J. Deng, Y. Wang, H. Hu, R. Duan, and Z. Xin, "The redundant wireless bridged networks for remote launch system," 2014 International Conference on Mechatronics and Control (ICMC), Jinzhou, China, 2014, pp. 37-41, doi: 10.1109/ICMC.2014.7231511.
7. C. Yang, F. Lu, M. Zhu, and M. Liu, "Design of Embedded Remote Working Condition Monitoring System Based on Wireless Network Bridge," 2021 IEEE 16th Conference on Industrial Electronics and Applications (ICIEA), Chengdu, China, 2021, pp. 18141819, doi: 10.1109/ICIEA51954.2021.9516367.
8. S. Deepa, "Bidirectional Linear Wireless Sensor Networks," 2022 International Interdisciplinary Humanitarian Conference for Sustainability (IIHC), Bengaluru, India, 2022, pp. 1059-1065, doi: 10.1109/IIHC55949.2022.10060775.
9. Chen, Y., & Arora, A. (2020). Middle-mile Network Optimization in Rural Wireless Meshes. 2020 IEEE 21st International Symposium on "A World of Wireless, Mobile and Multimedia Networks" (WoWMoM), 224- 233.
10. Wei-yan, M. (2007). The Application of Wireless Bridge in the Transmission of Television Programs. China Digital Cable
11. J.-Y. Han, Y.-H. Jeon, H.-J. Kim, and S. Lee, "Redundant Topology Design Method for Schedule Traffic Transmission Based on IEEE802.1CB Standard: Optimizing NW-PSP Scheduling Performance," *Electronics*, vol. 13, no. 1, p. 88, Dec. 2024. ‘
12. J. Doe and A. Smith, "Advanced Antenna Technologies for Signal Enhancement," *IEEE Transactions on Antennas and Propagation*, vol. 68, no. 5, pp. 1234-1245, May 2023. DOI: 10.1109/TAP.2023.1234567.

Evaluating Machine Learning Techniques for Early Detection of Chronic Liver Disease: A Review

Jyoshna Allenki[1] [0000-0002-5825-0024] andHemant Kumar Soni [2] [0000-0002-8335-6146]

[1,2] Department of Computer Science and Engineering, Amity School of Engineering and Technology, Amity University Madhya Pradesh, Gwalior 474005, India

allenkijyoshna@gmail.com,hemantsoni.gec@gmail.com

Abstract: Millions of people are affected by the chronic liver disease which has a significant impact of chronic liver disease illness and death all over the world. Furthermore, the strain put on healthcare systems because of chronic liver disease requires an increase in the healthcare systems. Detection of chronic liver disease has advanced in the machine learning technologies. An evaluation of machine learning in the early detection of chronic liver disease will be reviewed. A review of the scientific literature, experimental research, and clinical applications are considered relevant to assess the research gaps. An overview of chronic liver disease is provided, along with its pathogenesis, progression, and challenges in diagnosis. Then, the investigation explores the application of machine learning, and other supervised and unsupervised learning algorithms concerning the diagnosis of chronic liver disease. There are clinical data, medical images, and genetic material which can be used to train a machine learning model.

Keywords: Machine Learning (ML), Naive Bayes, Support Vector Machine(SVM), Decision Tree (DT), K Nearest Neighbors(KNN), Random Forest (RF), and Logistic Regression(LR).

1 Introduction

An important organ in the body of every human being is liver, the liver performs functions like bile production, chemical detoxification, and blood clotting protein synthesis. The treatment of some liver disorders has significantly improved over the past few years in every country in the world. This disease is linked to 2.4% of deaths in India. Cirrhosis can be recognized whenever liver cells are harmed and replaced by dead scar tissues [1].There are more than 100 different forms of liver disorders.The biggest organ in the body, the liver, is necessary for both toxin removal and food processing.

A person's liver can become damaged as a result of viruses and alcohol use, which can result in a life-threatening condition. Cirrhosis, hepatitis, liver cancer, liver tumors, and many other diseases can affect the liver. Diseases of the liver and cirrhosis as the leading cause of death are two examples. Moreover, liver illness is among the most dangerous medical conditions. A study [2] published in BioMed Central (BMC) medicine in 2010 called the Global Burden of Disease (GBD) Study found that cirrhosis was the reason behind one million liver cancer diagnoses and one million deaths from the disease.

It is challenging to diagnose liver infection because of the many different signs present in the early stages. Problems with the liver generally arise when the disease has progressed significantly since the liver keeps functioning even when it is only partially damaged. It's possible that making a decision early can save a life. The experiences a late patient has will kindly raise their standards of living. Hence, this analysis's findings are significant from the perspective of both a computer scientist and a medical professional [3].

There are many conditions that might disturb the liver. Among the disorders are liver cancer, cirrhosis, hepatitis, which causes inflammation of the liver, and Wilson's disease. Organ failure is decided to put on by the chronic inflammation known as cirrhosis. Long-term alcohol consumption alters the metabolism of the liver, which may have detrimental implications on general health. Hemochromatosis can cause liver problems [4].

Common Liver Conditions include- (1) Fatty liver is a disease that can be treated in which limit causes huge vacuoles of triglyceride fat to form in liver cells. Both people who drink heavily and people who never drink anymore can experience it. (2)Hepatitis (most often brought on by a virus that spreads through contact with infected bodily fluids or excessive contamination) (3)Cirrhosis One of the most serious diseases affecting the liver. The activity utilized to denote any liver condition that results in a large loss of cells. The liver quickly reduces and changes texture to leather and hardness. Despite the progressive loss of liver cells caused by liver cirrhosis, cell replacement continued to occur. (4)Liver cancer. Liver cancer is more common in secondary (metastatic) tumors,

which are tumors that have spread to other organs, and is associated with cirrhosis and certain forms of viral hepatitis.

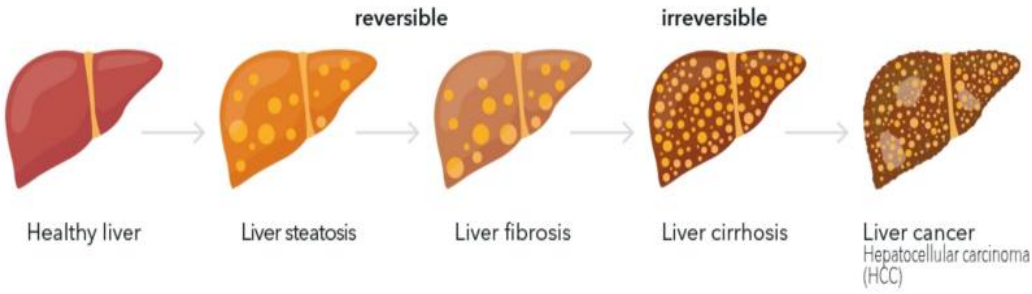

Fig. 1. Stages of liver diseases

It may be challenging to identify even partial liver loss early on because of the liver's natural capacity to operate. Early detection of liver illness increases the chance that a patient will recover. Indians are more likely to suffer from liver failure. India is expected to become the global hub for liver issues by 2025. Liver infections are more common in India because of a desk-bound lifestyle, smoking and more alcohol consumption. Liver infections occur in more than a hundred different types. Therefore, it will be extremely beneficial to the medical industry to develop a device that would support in the early identification of diseases. Automatic liver disease classification tools (likely mobile or web-enabled) will be used with these technologies to help doctors make accurate decisions for their patients.

Radiologists may now more efficiently and cost-effectively detect cancers made of normal cells due to recent developments in medical imaging. The advancement of technology in this area at the moment is also helpful when making additional treatment recommendations. Numerous researchers have previously proposed a number of approaches and techniques for tumor detection. There are numerous approaches to timely and effective tumor segmentation and detection. These include completely automated and semi-automatic tumor segmentation methods [5].

There are certain significant advantages that automatic tumor segmentation systems offer over manual procedures. There is a time limit on conventional segmentation methods. In some cases, these are also time-consuming and computationally expensive. These methods frequently overlook pre-existing tumors and are unable to identify them because of their microscopic size, which is another disadvantage of methods. Additionally, the analogy in traditional segmentation makes it difficult to distinguish between tumor cells and normal cells [6].

In traditional segmentation, hand-picked features can be affected by low contrast levels, issues with the equipment, ambiguous boundaries, smudged cells, blurred edges, and other spatial factors [7]. Hence, there is more room for inaccurate results and error rates. The uneven size and form of the tumor can differ from person to person.

Tumor identification and segmentation becomes challenging in low-level pictures. Conversely, automated techniques are efficient, precise, and fast. Automatic techniques significantly influence the process of identifying and classifying liver cancers due to their speed.As a result, research has shifted away from manual segmentation to automatic segmentation. Nowadays, automated liver tumor segmentation using the best design is much more common than traditional liver segments using the standard design [8].

In order to treat and recover from liver disease efficiently, it is essential to identify it early. Additionally, it is extremely challenging to accurately identify in the disease's early stages. Every day, healthcare and medicinal drug industries deal with a lot of information. This information includes patient records, reviews of prognoses, and clinical images. A decision-assistance system must be understood in light of this reality. To carry out activities, the knowledge domain has to be located in the raw data and extracted. It is performed utilizing data mining and knowledge discovery. In the biological domain, the application of facts mining techniques is extensive. Over the past few years, the liver's functioning has significantly improved and liver disorders are among the most deadly disorders in the world. In this study, In order to forecast liver illness, liver patient datasets are examined for the development of classification methods. Improved prediction accuracy for Indian liver patients is achieved through

the development of multiple function models and comparative analysis. Many investigations have focused on the classification of liver diseases.

Among the most prevalent and efficient statistical mining techniques used to implement in predictive modeling is the classification method. A number of automatic medical health diagnoses use the classification algorithm most frequently. They exhibit excellent classification accuracy in many of them. Here, liver diseases is predicted using a number of ML techniques, including DT, SVM, and RF . Predicting liver disorders using various classification algorithms and an significant purpose of this study is toknow about how artificial intelligence can be used in healthcare by looking closely at how machine learning can be used to find chronic liver disease early. The results of this study could greatly improve the accuracy of diagnoses, the speed of care, and the overall health of people with chronic liver disease.

2 Literature Review

In this study [9], two improvements are presented. First, the Information Gain (IG) technique is applied for the purpose of first feature reduction. The second involves using Optimization Based on Opposition (OBO) to implement BOA's initialization. Ultimately, during the detection phase, patients with liver illness are identified using five distinct classifiers: SVM, KNN,NB, DT, and RF. Experiments conducted reveal that the suggested IB2OA works better than the most advanced techniques in terms of F-score, recall, precision, and accuracy. Furthermore, the average selected features score of the suggested model is 4.425, which is lower than the state-of-the-art. Additionally, on the test dataset, the KNN classifier had the highest classification accuracy out of all the classifiers taken into consideration.

This study [10] trained a multilayer sensory neural network for the diagnosis of liver failure using data from liver patients (ILDP).The suggested method, which makes intelligent predictions about liver failure, increases the diagnostic rate through the use of the back propagation algorithm. The suggested approach is more accurate than earlier related methods, with 99.5% accuracy, 99.65% sensitivity, and 99.57% specificity, according to the results of the simulation and data analysis.

The recommended approach is initially used to impute the missing values and outliers before beginning therapy. The crucial characteristics for classification are then obtained by using integrated feature extraction to the pre-processed data. The machine learning techniques covered in the proposed approach are LR, RF, KNN, SVM, multilayer perception (MLP), and ensemble voting classifier. In terms of predicting liver disorders, the provided system has an 88.10% accuracy, 85.33% precision, 92.30% recall, 88.68% F1 score, and 88.20% AUC score. Compared to the most recent research, our suggested method produced outcomes that were 0.10–18.5% better. The results imply that the suggested system might be added to a medical professional's liver disease diagnosis [11].

This study [12] explores the analysis of chronic liver disease detection using machine learning techniques. This study likely delves into the practical applications of machine learning algorithms in identifying patterns and markers associated with chronic liver diseases. By harnessing the power of AI, healthcare professionals can streamline the diagnostic process and improve the accuracy of disease detection, ultimately benefiting patient care and outcomes.

A novel DL model for categorizing and recognizing tumors related to liver disease is described in this study [13]. A tumor has been diagnosed as either metastatic or cholangiocarcinoma based on computed tomography imaging. We demonstrate that our model principally performs extremely well in terms of accuracy, dice similarity coefficient, and specificity metrics, and it adapts very well for different datasets when compared to popular existing techniques. The model is obviously better, with a dice similarity coefficient of 98.59%.

Numerous previous machine learning models for the classification and diagnosis of liver illnesses are examined in this work [14]. A comparative examination of more than six models suggests the best course of action for the target dataset. These are the greatest choices for increasing the model's accuracy for offline challenges. For practical applications, different ensemble approaches and hyperparameter tweaking are superfluous because to their higher computing cost and efficiency, even if they may result in improved accuracy.

In this study[15], ML algorithms are suggested to examine the patient's overall liver condition . The favorable and unfavorable data Classifiers are being used to process liver disease percentages, and the output is shown as a

confusion matrix. When a training data set is available, a number of classification strategies that can significantly enhance classification performance. Next, excellent and bad values are identified using a ML classifier. Consequently, the outputs of the proposed classification model show accuracy in outcome prediction.

In paper [16] discusses the novel AI technology of object detection for diagnosing hepatocyte ballooning, a key feature of fatty liver disease pathology. By leveraging AI algorithms for identifying specific histological features associated with liver diseases, healthcare providers can enhance their diagnostic accuracy and streamline the interpretation of complex imaging data. This technology holds promise for improving the identification of liver pathologies, including hepatocyte ballooning, which is crucial for diagnosing and managing chronic liver diseases.

In study [17] provide an overview of AI-enhanced ultrasound techniques for diagnosing and staging NAFLD. Their research underscores the potential of AI in transforming diagnostic imaging practices for liver diseases. By incorporating AI algorithms into ultrasound imaging, healthcare providers can enhance the accuracy and efficiency of diagnosing NAFLD, paving the way for more precise and timely interventions in chronic liver disease management.

In paper[18], a novel deep learning method for the automated segmentation of livers—known as a 3D convolutional neural network (CNN)—was presented. The goal of this method is to define the initial liver surface by generating subject-specific probability maps that serve as shape priors. To improve segmentation accuracy, the model efficiently integrates local and global data. While local nonparametric data focuses on detecting abnormal liver characteristics, global data includes healthy liver regions that capture the area's appearance and intensity distribution.

The author of the paper [19] suggested a two-step process in which shape models are used to segment the liver first, and then dense random trees with auto-context learning techniques are applied to segment the tumor. Nevertheless, the suggested approach performs poorly and hassignificantly higher computational costs.

3 Research Gaps

The following research gaps are identified by this survey, along with recommendations for filling them.

- Present algorithms, KNN,SVM traditional algorithms, are unable to analyze the image data.
- Image classification, enhancement requires ensembled ML algorithms and image processing techniques for better efficiency.

4 Proposed Structure for Segmentation and Classification

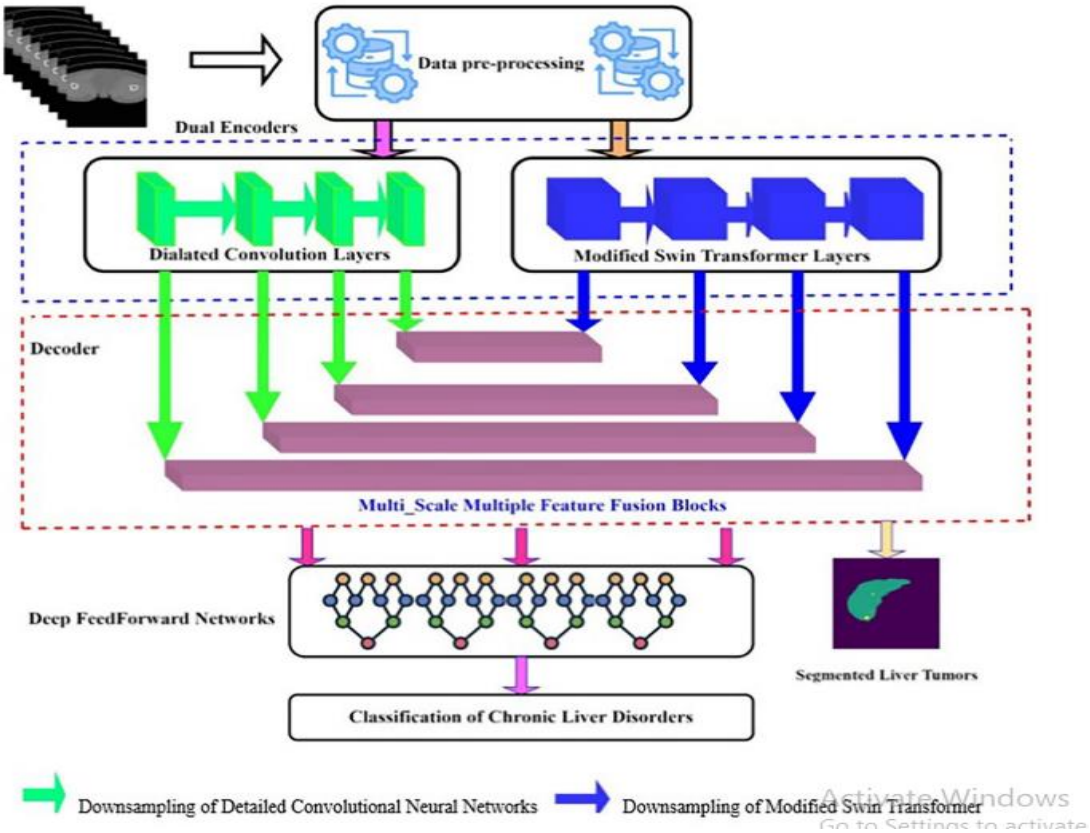

Fig.2. Proposed Structure for Segmentation and Classification

5 Proposed System Overview

Figure 2 describes the proposed scheme for the DEDSWIM-Net. The DEDSWIM-Net has dual encoder-decoder structure and is built upon four components as follows. The architecture feature an dilated convolution encoder, where the dilated convolutional layer learned the features of liver lesions by using a convolution layer with an increase receptive field to identify the finer features of the lesion as well as providing more complex textures to analyze. Next, we utilized a modified Swin Transformer encoder. A modified model that uses the self attentions of overlapping windows for the model to attend separate parts of the image. Furthermore, an integrated multi-scale multi-feature fusion decoder (MSMFD) that fuses the features of multi-scale to produce a more precise segmentation of the lesion. Finally, we utilized an ensemble method classification model with a feed-forward networks trained on salient features for the classification of CLD for precise classification.

6 Conclusion and Future Work

Research has indicated that machine learning techniques are efficacious. Furthermore, studies yielded better results in terms of specificity, accuracy, and precision. This study has presented cutting edge research for liver disease detection. Unresolved concerns and problems have also been noted. This work also looked closely at a number of machine learning methods for liver disease detection. The important characteristics indicated adjacent to various clinical, serum-based, and imaging-based elements can be combined to form a more comprehensive model. With comparatively few datasets, the model was created. The suggested method has to be tested on a sizable dataset that was not previously known in order to show its efficacy. Additionally, it may be used with other machine learning models to accomplish multi-class categorization. Information regarding the disease's stage may be included in the approach's scope. Genetic information, clinical data, and patient medical imaging are all commonly analyzed using

machine learning techniques. The unrivaled potential of machine learning and data mining technologies in the medical field has been shown by several studies. These methods can identify significant latent predictive traits from medical datasets that provide early illness diagnosis and prognosis. In this study, they looked for areas where the many studies that used machine learning ideas to diagnose liver illness had insufficient data. Additionally, it is evident from the aforementioned studies that machine learning techniques have a lot of potential for diagnosing liver problems. But before doctors can keep using the medication, further evidence proving its efficacy and validity is required. Several metrics, including as recall, specificity, accuracy, precision, and f-1 score, are employed to assess how well various categorization techniques work. As a consequence, in this analysis, accuracy, NB, RF, LR, DT, KNN, and SVM produced the top results.

References

1. P. Ghosh, A. Karim, S. T. Atik, S. Afrin and M. Saifuzzaman, "Expert model of cancer disease using supervised algorithms with a LASSO feature selection approach," International Journal of Electrical and Computer Engineering (IJECE), vol. 11, no. 3, 2020, doi: 10.11591/ijece.v11i3.pp2631-2639.
2. Byass, Peter, The global burden of liver disease: a challenge for methods and for public health. BMC medicine 12.1 (2014); 159
3. Sivakumar D , Manjunath Varchagall , and Ambika L Gusha S "Chronic Liver Disease Prediction Analysis Based on the Impact of Life Quality Attributes." (2019). International Journal of Recent Technology and Engineering (IJRTE) ISSN: 2277-3878, Volume- 7, Issue-6S5, April 2019 https://www.medicinenet.com/liver_disease/article.html
4. Zhang, X., Automatic Liver Segmentation Using a Statistical Shape Model With Optimal Surface Detection. IEEE Transactions onBiomedical Engineering, 2010. 57(10): p. 2622-2626.
5. Huang, W., Liver tumor detection and segmentation using kernel-based extreme learning machine. in 2013 35th Annual International Conference of the IEEE Engineering in Medicine and Biology Society (EMBC). 2013.
6. Li, C., A Likelihood and Local Constraint Level Set Model for Liver Tumor Segmentation from CT Volumes. IEEE Transactions on Biomedical Engineering, 2013. 60(10): p. 2967-2977.
7. Bendi Venkata Ramana, "A Critical Study of Selected Classification Algorithms for Liver Disease Diagnosis", International Journal of Database Management Systems, Vol 3, (May 2011).
8. Shaban, W.M. "Early diagnosis of liver disease using improved binary butterfly optimization and machine learning algorithms". Multimed Tools Appl83, 30867–30895 (2024). https://doi.org/10.1007/s11042-023-16686-y.
9. Dashti, F., Ghaffari, A., Seyfollahi, A. et al." A self-predictive diagnosis system of liver failure based on multilayer neural networks. Multimed Tools" Appl (2024). https://doi.org/10.1007/s11042-024-18945-y.
10. Shaban, W.M. Early diagnosis of liver disease using improved binary butterfly optimization and machine learning algorithms. Multimed Tools Appl83, 30867–30895 (2024). https://doi.org/10.1007/s11042-023-16686-y[12] Allenki, J. (2024). Analysis of chronic liver disease detection by using machine learning techniques.. https://doi.org/10.1109/sceecs61402.2024.10481680.
11. Manjunath RV, Ghanshala A, Kwadiki K. "Deep learning algorithm performance evaluation in detection and classification of liver disease using CT images. Multimed Tools" Appl. 2023 May 15:1-18. doi: 10.1007/s11042-023-15627-z. Epub ahead of print. PMID: 37362702; PMCID: PMC10183675.
12. H. S. Yadav and R. K. Singhal, "Classification and Prediction of Liver Disease Diagnosis Using Machine Learning Algorithms,"*2023 2nd International Conference for Innovation in Technology (INOCON)*, Bangalore, India, 2023, pp. 1-6, doi: 10.1109/INOCON57975.2023.10101221.
13. Tokala, Srilatha & Koduru, Hajarathaiah & Gunda, Sai & Botla, Srinivasrao & Nalluri, Lakshmikanth & Nagamanohar, Pathipati & Anamalamudi, Satish & Krishna Enduri, Murali. (2023). "Liver Disease Prediction and Classification using Machine Learning Techniques." International Journal of Advanced Computer Science and Applications. 14. 10.14569/IJACSA.2023.0140299.
14. Zheng, T. (2023). Object detection: a novel ai technology for the diagnosis of hepatocyte ballooning. Liver International, 44(2), 330-343. https://doi.org/10.1111/liv.15799.
15. Gheorghe, E., Nicolau, C., Kamal, A., Udristoiu, S., Gruionu, L., & Saftoiu, A. (2023). Artificial intelligence (ai)-enhanced ultrasound techniques used in non-alcoholic fatty liver disease: are they ready for prime time?. Applied Sciences, 13(8), 5080. https://doi.org/10.3390/app13085080
16. Ardila, D., Kiraly, A. P., Bharadwaj, S., Choi, B., Reicher, J. J., Peng, L., Tse, D., Etemadi, M., Ye, W., Corrado, G., Naidich, D. P., & Shetty, S., "End-to-end lung cancer screening with three-dimensional deeplearning on low-dose chest computed tomography", Nature Medicine, 2019, vol 25, pp 954-961.
17. Shaheamlung, G., & Kaur, H. (2021). The diagnosis of chronic liver disease using machine learning techniques. Information Technology in Industry, 9(2), 554-564.hao, J., Luan, S., Ding, Y., Xue, X., Zhu, B., Wei, W.

18. Shao, J., Luan, S., Ding, Y., Xue, X., Zhu, B., Wei, W.(2024). Attention connect network for liver tumor segmentation from CT and MRI images. Technology in Cancer Research & Treatment, 23. https://doi.org/10.1177/15330338231219366.
19. Zhang, Y., Pan, X., Li, C., Wu, T. (2020). 3D liver and tumor segmentation with CNNs based on region and distance metrics. Applied Sciences, 10(11): 3794. https://doi.org/10.3390/app10113794 .
20. Ramana, Bendi Venkata, M. Surendra Prasad Babu, and N. B. Venkateswarlu. "A critical study of selected classification algorithms for liver disease diagnosis." International Journal of Database Management Systems 3.2 (2011): 101-114
21. Allenki, J., Soni, H.K. DEDSWIN-Net: Dual Encoder Dilated Convolution and Swin Transformer Network for the Classification of Liver CT Images. Int J Comput Intell Syst 18, 198 (2025). https://doi.org/10.1007/s44196-025-00937-x

Crops Recommendation with ANOVA-Based Feature Selection and Machine Learning Algorithms

Syed Ali Ishaq Mohsin[1], Syed M. Ismail Hussain[2], Hafiz Zia Ur Rehman[1], Noman Naseer[1], Zeashan Khan[3]
[1] Department of Mechatronics & Biomedical Engineering, Air University, Islamabad, Pakistan
[2] Department of Mechanical Engineering, NUTECH, Islamabad, Pakistan
[3] IRC-IMR, King Fahd University of Petroleum & Minerals, Dhahran, Saudi Arabia
zeashan.khan@kfupm.edu.sa

Abstract. Agriculture is at the forefront of economic sustainability worldwide. However, challenges such as fluctuating climatic conditions, soil degradation, and inefficient crop selection practices continue to hinder productivity. Machine learning has been very successful in many areas such as healthcare, finance, and engineering; hence, it has immense potential to transform the sector into a data-driven agriculture sector. This paper explains the application of machine learning (ML) models in optimizing crop recommendations based on major agronomic and climatic factors such as nitrogen (N), phosphorus (P), potassium (K), pH, rainfall, temperature, and humidity. This study evaluated the performances of five popular machine learning algorithms: k-Nearest Neighbors (kNN), Gaussian Naïve Bayes (NB), Decision Tree (DT), Random Forest (RF), and Support Vector Machine (SVM), using a dataset of 2,200 samples. Of these, Gaussian Naïve Bayes achieved the highest accuracy of 99.55%, thereby proving effective at handling feature-rich datasets. The Random Forest was also satisfactory in terms of performance; however, it provided important insights into feature importance. This study showed the critical role of exact feature selection in crop suitability and that ML can lead the drive for sustainable farming practices. Future work will incorporate external data sources, including satellite imagery and Internet of things (IoT) devices, to increase the accuracy and adaptability of the models, resulting in more dynamic and holistic agricultural decision-support systems.

Keywords: Smart Farming, Feature Selection, Crop Recommendation, Application of Machine Learning in Agriculture

1 Introduction

Agriculture is by far the most important industry sector from which many economies in the world derive a benefit from, especially in Asia [1][2], where a large portion of the population derives food, fuel, and raw materials. In several countries like Pakistan and India, agriculture also forms one of the main pillars of the economy and a major

source of earning livelihood for a significant number of people. But this sector is also attempting to cope with climate change challenges, decreasing crop yields, and the problem of resource misuse, ultimately influencing crop cultivation as farmers struggle to decide what to grow. This is where current technology can lend a hand by combining field data with a machine-learning model that analyze soil condition, whether patterns and past crop performance to suggest the best crops for farmers to grow.

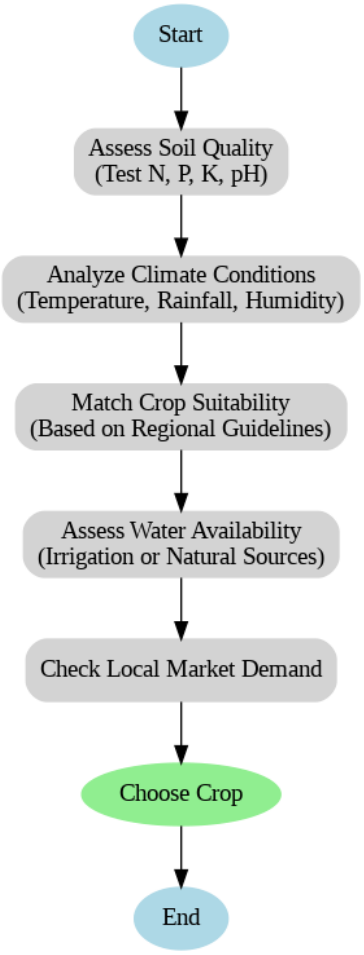

Fig. 1. Flowchart for crop selection

The growth of artificial intelligence (AI), machine learning (ML), and data science has given rise to new potential solutions to agricultural problems. ML has proven to be useful in tackling complex problems, particularly in the estimation of crop yield [3], disease detection [4], and plant species identification[5]. The deployment of an ML-driven crop recommendation system, that depends on weather conditions, soil pH levels, and soil water content, has the potential to change the crop decision-making

paradigm entirely [6][7][8]. Such systems enable farmers to analyse economic, environmental, and agricultural data to determine the best type of crop to grow. As a result, farmers will be able to boost both production levels and profits as the optimal crop will be identified. However, the behaviour of the ML algorithm strongly depends on the quality and relevance of the input features. Often, datasets have redundant or irrelevant features that add noise to the dataset and degrade the classification accuracy. Feature selection is an integral step in the ML pipeline aimed at resolving these challenges by selecting the most useful attributes and discarding useless ones. Feature selection not only provides a higher model performance but also reduces the computational complexity, resulting in less computationally intensive and clearer algorithms.

The process of crops recommendation is shown in Fig. 1. The process begins with checking the soil health parameters (nitrogen, phosphorus) and weather patterns (temperature, rainfall). The system monitors such conditions and suggests crops that can be grown well in that area. This approach serves the purpose of guiding farmers in picking the right crop for their land and market demand. This paper discusses implementing a machine learning-based crop recommendation system that aims to transform the agricultural landscape. Five machine-learning models were developed: k-Nearest Neighbors (kNN), Naïve Bayes, Random Forest (RF), Decision Trees (DT), and Logistic Regression. These models were evaluated using key performance metrics, such as accuracy, precision, recall, and F1-score, to determine their suitability for different agricultural scenarios. The results obtained from this study will contribute to filling the existing gap in recent farming trends with a focus on data-based solutions, thereby increasing the wide acceptance of precision farming to promote sustainable growth in the industry.

The remainder of this paper is organized as follows. The introduction outlines the background and objectives of this study. The literature review discusses recent work on crop recommendation using a machine-learning approach. The methodology describes the dataset used and the implementation of the machine learning models. The results and discussion examine their performance and significance. Finally, the conclusion summarizes the research contributions in agricultural settings and suggests directions for future research.

2 Related Work

With the progress in artificial intelligence, the agricultural sector has also made significant advancements. There have been some research efforts in the last decade by data scientists to apply machine learning techniques in order to create a crop recommendation system, showcasing the capabilities of AI in promoting digital agriculture. These approaches take into account several factors, such as soil health characteristics, climatic conditions, and historical crop data, to recommend suitable crops for specific regions. For example, Rachid et al. [9], used several machine learning models including kNN, Logistic Regression, Bagging, Naïve-Bayes, SVM, AdaBoost, Decision Tree, RF, Gradient-Boosting, XGB, and IBGM for the crop recommendation, showing that Random Forest resulted in 97.18% accuracy. Hasan et al. [7] optimized crop cultivation in Bangladesh by using ensemble machine learning based recommendation system. Another study proposed an ensemble model called the

Korringa Kohn Rostoker (KKR), which deploys a distance-based kNN combined with a 2nd order ensemble strategy that amalgamates predictors from kNN, RR, and RF to construct an ensemble regressor with improved predictions. The KKR model was effective in analyzing three primary rice varieties alongside potatoes, aiding authorities in future food supply planning. However, the model only made predictions for major crops, leaving out some aspects such as soil properties, production expenses, and market rates. Another study conducted by Banerjee et al. [8] on crop cultivation tested five machine learning algorithms that focused on 13 key crops across various districts in West Bengal. The authors considered factors such as rainfall, temperature, humidity, and sunlight hours and found that RF and SVM led to better outcomes. However, because the project was confined to two district datasets, there is a need to update the databases for more accurate predictions. Anjana et al. [10] explored a deep learning model utilizing CNN for plant infection identification, mitigating crop losses, and assisting farmers in cultivating healthy crops. Through image processing, this approach enhances efficiency compared to traditional methods. This technique can be adapted to incorporate climatic variables and account for additional plant diseases. While the system is only being used in Karnataka for now, it has the potential to expand nationwide.

Despite these advances, there are still certain limitations in the current research landscape that need to be considered. Most machine-learning models are trained on limited datasets, which limits their scalability and generalizability across a broader scope of agriculture. In addition, the integration of real-time data such as changing weather conditions and fluctuating market trends has not been fully exploited. The reviewed research highlights advances in adopting machine learning for crop recommendation but also emphasizes the necessity for model development that considers scalability, incorporates real-time data, and integrates multifactor analysis. By addressing these gaps, future research could further improve the applicability and impact of machine learning in agriculture.

3 Methodology

The methodology was structured to ensure the reproducibility of the findings as illustrated in Fig. 2. The process comprises four key phases: (1) dataset acquisition, (2) preprocessing and ANOVA-based feature selection, where raw agricultural data were cleaned, normalized, and statistically significant predictors were identified (3) model training and optimization using five ML algorithms, and (4) performance evaluation with metrics like accuracy and F1-score. This systematic framework guarantees replicable results.

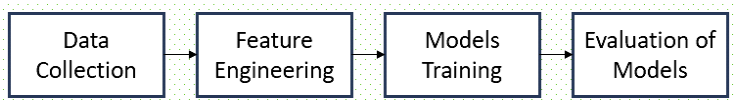

Fig. 2. Methodology adopted for this study

3.1 Dataset

The publicly available dataset from Kaggle [11] was used in this study. This dataset was built by augmenting the datasets of rainfall, climate, and fertilizer data available for India. Gathered over the Indian Chamber of Food and Agriculture (ICFA) period. It consists of 2200 samples and 7 features, representing essential agronomic parameters. These features include the ratio of nitrogen (N), phosphorus (P), and potassium (K) content in soil, temperature (in °C), relative humidity (in percentage), soil pH, and rainfall (in mm). The dataset encompassed 22 different crop classes, making it an extensive source of data for research on crop recommendations.

After obtaining the dataset, it is necessary to remove missing or inconsistent values to use it further for training. However, as observed, the datasets were already clean and did not require any extensive imputations. All features were normalized using min–max scaling to ensure that variables with larger ranges did not bias the learning process. This step is essential for algorithms which are sensitive to feature scaling such as k-Nearest Neighbours (kNN) and Logistic Regression.

3.2 Features Selection

Analysis of Variance (ANOVA) test is used to identify the most significant features influencing crop recommendations. ANOVA helps to determine the variance within and between groups, ensuring that only the most relevant features are used in the model training process to obtain a low order model.

Table 1. Feature Ranking (Most to Least Significant)

Feature	Rank
Concentration of N	1
Concentration of P	2
Concentration of K	3
Relative Humidity	4
Rainfall	5
Temperature	6
pH	7

3.3 Selected Models of Machine Learning

Five machine learning models were chosen for the present research based on their diverse characteristics and effectiveness in classification tasks. Therefore k-Nearest Neighbors (kNN) algorithm [12] was selected due to its simplicity and intuitive nature compared to other machine learning algorithms. It works by determining the distance of the data points in the feature space to a given sample and then classifying it according to the majority of its k-Nearest Neighbors. It is useful for our case, where features have different distributions that affect the classification. The core assumption can also be seen as quite simple: similar data points are likely to lie close to each other, which is very much the case in crop recommendation problems.

Naïve Bayes [13] model was also incorporated in the study. It assumes reassurance of independence between the features, making the model easy to apply and efficient. However, this assumption does not always hold in real situations, which is why Naïve Bayes is noted for its successful outcomes about classification problems, particularly when the features are self-sufficient or almost self-sufficient. In the context of this study, Naive Bayes takes the probabilities of each attribute of the dataset and uses them to determine how probable it is that a new example notated with a specific crop will be associated with one of the crop classes. Its efficiency and effectiveness toward multiclass issues make it ideal for this research.

The Decision Tree [14] model was chosen because of its ease and clarity of interpretation. In Decision Trees, data are classified by splitting into branches depending on the predetermined feature thresholds, and finally towards a leaf that indicates a certain class to which it belongs. The hierarchical nature of the model is straightforward to interpret, and hence, the rationale behind the predictions. This characteristic is particularly effective in illustrating the consequences of crop advice to farmers and agricultural policymakers. Decision Trees, however, can be prone to overfitting, however in our case pruning and depth constriction with the use of rigorous and shallow models ensured the model remained general.

Random Forest was selected because of its proficiency in managing intricate datasets encompassed by high-dimensional feature spaces. This ensemble technique creates a multitude of decision trees during training and then combines them to create an estimating feature. This approach enhances the precision of the model without worsening the tendency of overfitting, which is common in most machine-learning problems. Each tree in a Random Forest develops from a randomly selected sample of all datasets at each node and random samples of features for the various divisions. Also, the Support Vector Machine (SVM) [15] was used as the final model. The SVM operates by determining a hyperplane that best divides the data into target classes. The goal of the algorithm is to maximize the margin defined through data points that lie on the verge of two classes to ensure precise classification. In our case, both linear and nonlinear kernels were considered, wherein the radial basis function (RBF) kernel yielded the optimal results using a grid search. Moreover, the regularization parameter C, is also used to optimize accuracy and generalization. Subsequently, the final model based on SVM was found effective for mapping the non-linear relationships between features and crop categories in the dataset.

3.4 Training Environment

The implementation of the machine learning framework was performed in Google Colab, utilizing Python and its built-in libraries, such as Pandas, NumPy, Scikit-learn, and Matplotlib. In order to optimize the model performance, a grid search approach systematically explored the combinations of hyper-parameters to identify the optimal configuration for each model. Subsequently, cross-validation techniques during training, effectively ensured that the models generalized well to the unseen data, thereby reducing the over-fitting risk.

4 Results & Analysis

The machine learning models trained on the partial datasets and verified using the remaining datasets labelled as test sets. We used standard evaluation metrics of accuracy, precision, recall, and F1-score to assess the performance of the models. This evaluation process enabled an objective comparison of all five machine learning models and identified the best-performing model suitable to select the optimal crops. The visual comparison is provided in Fig. 3 below.

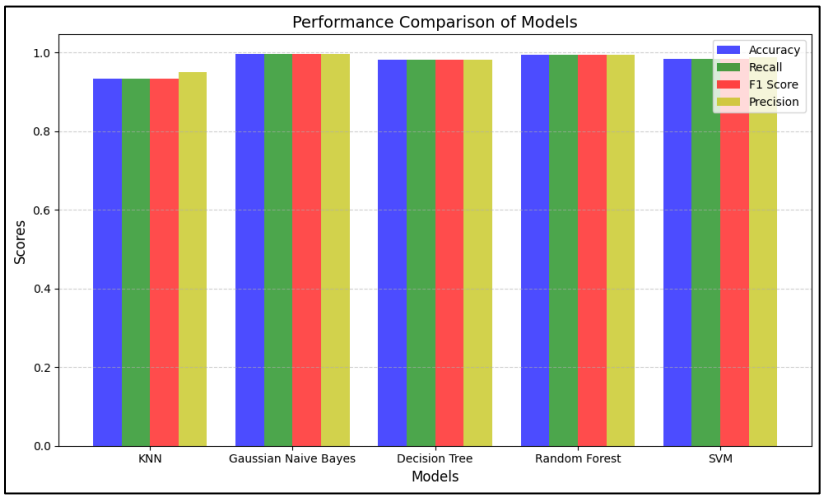

Fig. 3. Comparison of Models

The kNN model was fine-tuned with hyper-parameter optimization and it was reached that the best combination would be to use 'Manhattan' as the distance metric with 43 neighbours and weights based on 'distance.' Furthermore, kNN achieved an accuracy score of 93.41%, which correlated to an F1 score of 93.29%, a precision score of 94.94%, and a recall of 93.41% kNN 's performance measures indicating a strong level of performance, with a high degree of correlation between the values of precision and recall. There is high precision in the performance of kNN because it can predict the correct crop class while there are few false positives, as strong crop class capture is ensured by its strong recall. kNN is a non-parametric model, and its efficiency is heavily dependent on the selection of hyperparameters as well as the size of the selected dataset; thus, the model does not scale well when utilized on datasets with a large amount of data.

The results of the Gaussian Naive Bayes show that it outperforms all the other models, with accuracy being the major area of strength of the model, as it achieved 99.55% accuracy and impressive F1 (99.54%), precision (99.58%), and recall (99.55%) scores. These scores affirm the model's efficacy in estimating numerical features of the data and the distribution of classes therein. One of the best things about Naïve Bayes is that due to its nature it allows for real-time systems such crop recommendation systems to operate efficiently. The degree of hyperparameters optimization performed on the Decision Tree model was extensive, with the deepest tree without restrictions, two samples per leaf, and 10 minimum split size being the final

configuration. Its measured performance metrics showed an accuracy of 98.18%, F1 score 98.18%, a precision score of 98.23%, and a recall of 98.18%. The cross-validation scores that were obtained served as confirmation of the score obtained by the model, the mean score being 98.64 percent. The strength of Decision Trees is in its ability to fit non-linear interactions as well as the importance of features, providing a model that is interpretable for the role of the soil and climatic conditions for crop suitability. On the other hand, the model shows a slightly lower precision than Naive Bayes, leading to the conclusion that it has a slightly higher chance of false positives.

The random forest model achieved 99.32% accuracy, an F1 score of 99.32%, a precision score of 99.37%, and a recall score of 99.32%. Also, as a sign of its robustness, it yielded an average score of 99.55% during Cross-validation. The optimal hyperparameters were 200 estimators, no restriction on tree depth, and some min values for leaf size and split size. Random Forest was effective because of its ability to reduce overfitting and mitigate interaction between features. The SVM model (radial basis function kernel, with hyperparameters C = 1, gamma = 1) has also yielded impressive results with an accuracy of 98.41%, an F1 score of 98.45%, a precision of 98.73%, and a recall of 98.41%. These metrics underscore that the SVM models are best suited for a problem of such nature where the decision boundaries are complex, i.e. non-linear. Due to SVM's strength, robustness, and generalizability, it can be a good candidate for crop recommendation tasks, especially with highly heterogeneous datasets. As noted above, SVMs also appear to have some downsides; their relatively expensive training cost and hyper-parameter tuning sensitivity pose additional barriers to scalability and real-time usage.

Table 2. Summarizing the performance metrics of the five models

Model	Accuracy (%)	Recall (%)	F1 Score (%)	Precision (%)
kNN	93.41	93.41	93.29	94.94
Gaussian Naive Bayes	99.55	99.55	99.54	99.58
Decision Tree	98.18	98.18	98.18	98.23
Random Forest	99.32	99.32	99.32	99.37
SVM	98.41	98.41	98.45	98.73

The results clearly illustrate (Table 2) what has been visible throughout the study – that virtually all the models have done exceedingly well, achieving over 93% accuracy. In contrast, Gaussian Naïve Bayes scored the highest accuracy while achieving a more than acceptable precision and recall, showing how proficient it is for this dataset. Random Forest was narrowly behind it, being slightly less accurate but revealing the importance of features in other analyses. SVM and Decision Tree both did well for themselves as well, given the level of intricacy involved in the relationships they were required to model. kNN is reported to be an accurate algorithm but in this case, because the dataset is small, it is set to come slightly lower on the scale but still is a good model in terms of accuracy, simplicity and interpretability.

The study was also compared with the previous studies conducted in this field to evaluate its contribution. The comparison is presented in Table 3. From the above discussion and comparison, the most practical models for crop recommendation systems are Gaussian Naïve Bayes, and random forest. With unmatched computational efficiency, Gaussian Naïve Bayes is perfect for real-time applications. On the other side, Random Forest ensemble methods provide stability and robustness making it an

excellent choice for datasets that have noise or incomplete features. The ability of SVM algorithm to capture the non-linearity coupled with Decision Tree's interpretative capability, introduces further possibilities for agricultural researchers to recommend crops based on local factors.

Table 3. Table captions should be placed above the tables

Reference	Best Model	Accuracy (%)
Mahale et al. [16]	Random Forest + LSTM	92.0
Bhola et al. [2]	Artificial Neural Network (ANN)	99.1
Prity et al. [6]	Random Forest	99.31
This study	Gaussian Naive Bayes	99.55

The composition of the dataset indicates the relevance of nitrogen, phosphorus, and potassium as the most impactful variables in establishing the suitability of crops. Additional study could consider incorporating extra features into the dataset for improved model accuracy and generalizability such as agronomic factors (e.g., soil texture, organic matter, pest prevalence) among others. Furthermore, satellite data and IoT sensor data can also be integrated to enhance the flexibility and robustness of the crop recommendation models. On the whole, the analysis recommends using models based on specific needs. Gaussian Naïve Bayes and Random Forest can be used for reasonable accuracy and performance while SVM and Decision Tree are ideal for understanding and flexibility. These results help to apply machine learning models to sustainable agriculture, which can assist farmers in selecting the best crops and enhancing their yields.

5 Conclusion

In this study, we evaluated k-Nearest Neighbor (kNN), Gaussian Naïve Bayes, Decision Tree (DT), Random Forest (RF), and Support Vector Machine (SVM) as crop recommendation machine learning models based on large datasets. The models were highly predictive; among them, the best was Gaussian Naïve Bayes at 99.55% followed by Random Forest at 99.32% and SVM at 98.41%. The outcomes of our study proved the ability of machine learning to provide precise and highly effective crop suggestions for specified environmental conditions.

References

1. A. Badshah, B. Y. Alkazemi, F. Din, K. Z. Zamli, and M. Haris, "Crop Classification and Yield Prediction using Robust Machine Learning Models for Agricultural Sustainability," *IEEE Access*, 2024, doi: 10.1109/ACCESS.2024.3486653.
2. A. Bhola and P. Kumar, "Farm-Level Smart Crop Recommendation Framework Using Machine Learning," *Annals of Data Science*, 2024, doi: 10.1007/s40745-024-00534-3.
3. D. J. Reddy and M. R. Kumar, "Crop Yield Prediction using Machine Learning Algorithm," in *2021 5th International Conference on Intelligent Computing and Control Systems (ICICCS)*, 2021, pp. 1466–1470. doi: 10.1109/ICICCS51141.2021.9432236.

4. R. Kumar, N. Shukla, and Princee, “Plant Disease Detection and Crop Recommendation Using CNN and Machine Learning,” in *2022 International Mobile and Embedded Technology Conference (MECON)*, 2022, pp. 168–172. doi: 10.1109/MECON53876.2022.9752173.
5. J. Wäldchen and P. Mäder, “Machine learning for image based species identification,” Nov. 01, 2018, *British Ecological Society*. doi: 10.1111/2041-210X.13075.
6. F. S. Prity *et al.*, “Enhancing Agricultural Productivity: A Machine Learning Approach to Crop Recommendations,” *Human-Centric Intelligent Systems*, Sep. 2024, doi: 10.1007/s44230-024-00081-3.
7. M. Hasan *et al.*, “Ensemble machine learning-based recommendation system for effective prediction of suitable agricultural crop cultivation,” *Front Plant Sci*, vol. 14, 2023, doi: 10.3389/fpls.2023.1234555.
8. S. Banerjee, S. Ckakraboity, and A. C. Mondal, “Machine Learning Based Crop Prediction on Region Wise Weather Data,” *International Journal on Recent and Innovation Trends in Computing and Communication*, vol. 11, no. 1, pp. 145–153, Jan. 2023, doi: 10.17762/ijritcc.v11i1.6084.
9. R. E. -Daoudi, A. Alaoui, B. Ettaki, and J. Zerouaoui, “A Predictive Approach to Improving Agricultural Productivity in Morocco through Crop Recommendations.” [Online]. Available: www.ijacsa.thesai.org
10. Anjana, A. K. K, A. Sana, B. A. Bhat, S. Kumar, and N. Bhat, “An efficient algorithm for predicting crop using historical data and pattern matching technique,” *Global Transitions Proceedings*, vol. 2, no. 2, pp. 294–298, Nov. 2021, doi: 10.1016/j.gltp.2021.08.060.
11. “Kaggle.” Accessed: Jan. 14, 2025. [Online]. Available: https://www.kaggle.com/datasets/siddharthss/crop-recommendation-dataset
12. G. Guo, H. Wang, D. Bell, Y. Bi, and K. Greer, “LNCS 2888 - KNN Model-Based Approach in Classification,” 2003.
13. S. Taheri and M. Mammadov, “Learning the naive bayes classifier with optimization models,” *International Journal of Applied Mathematics and Computer Science*, vol. 23, no. 4, pp. 787–795, 2013, doi: 10.2478/amcs-2013-0059.
14. Y. Y. Song and Y. Lu, “Decision tree methods: applications for classification and prediction,” *Shanghai Arch Psychiatry*, vol. 27, no. 2, pp. 130–135, Apr. 2015, doi: 10.11919/j.issn.1002-0829.215044.
15. V. K. Chauhan, K. Dahiya, and A. Sharma, “Problem formulations and solvers in linear SVM: a review,” Aug. 15, 2019, *Springer Netherlands*. doi: 10.1007/s10462-018-9614-6.
16. Y. Mahale *et al.*, “Crop recommendation and forecasting system for Maharashtra using machine learning with LSTM: a novel expectation-maximization technique,” *Discover Sustainability*, vol. 5, no. 1, Dec. 2024, doi: 10.1007/s43621-024-00292-5.

Graph-SeqNet: A Unified Deep Learning Framework for Alzheimer's Detection on MRI Data

Biraja Mishra[1], Mahfooz Alam[1]*, Zubair Ashraf[2], Mohammad Shahid[3]

[1]Department of MCA, G. L. Bajaj Institute of Technology and Management, Greater Noida-201306, India
mishrabiraja23@gmail.com; mahfoozalam.amu@gmail.com
[2]College of Computing and Information Technology, University of Bisha, Bisha-67714, Kingdom of Saudi Arabia.
ashrafzubair786@gmail.com
[3]Department of Commerce, Aligarh Muslim University, Aligarh-202002, India
mdshahid.cs@gmail.com

Abstract: Alzheimer's Disease (AD) is a progressive disorder that affects memory and cognitive abilities. Traditional deep learning models like CNNs and LSTMs often struggle to capture both spatial patterns and long-term dependencies in the data. To overcome these challenges, we propose a model using Graph Attention Networks (GAT) to understand patient relationships. Our model is tested on the OASIS Longitudinal MRI dataset and compared with CNN and LSTM. The proposed model achieves 96.25% accuracy, outperforming CNN (85.33%) and LSTM (81.33%), showing its potential for better AD classification. The model also provides more stable results and reduces variability in predictions. Future improvements could include integrating multimodal data, refining attention mechanisms, and exploring self-supervised learning for even better performance in real-world clinical applications.

Keywords: Alzheimer's Disease, MRI-Based Diagnosis, Graph Attention Networks, LSTM, CNN, KNN, Neuro Imaging, Early Detection

1 Introduction

Alzheimer's Disease (AD) is a progressive brain disorder that affects memory, thinking, and daily life activities. It is one of the leading causes of dementia, and it needs early detection to slow down the progression and improve patient care. This disorder is the most common known cause of dementia in older people. Dementia is an expensive disease that cost the world $604 billion in 2010 alone. It is interesting to note that 60% to 80% of people with dementia have AD. The word "Alzheimer's disease" comes from the famous doctor, Dr. Alois Alzheimer. Dr. Alzheimer saw some alterations in the brain tissue of a dead woman who had a rare mental disease in 1906. Dr. Alzheimer saw that there were a lot of unusual

plaques and tangled bundles of fibres in her brain. The entorhinal cortex and hippocampus are the primary locations where this damage happens, and then it extends to the cerebral cortex. Finding Alzheimer's disease in its early stages is important to save the patient from having brain damage that can't be cured. It can be hazardous and even lethal for persons over 65. Magnetic Resonance Imaging (MRI) is one of the most powerful ways to look at Alzheimer's disease. MRI scans can be used by doctors and researchers to keep track of how the structure of the brain changes over time, and the pictures are quite accurate [1] [2]. This is why MRI is a useful and precious tool for finding Alzheimer's disease. But it takes a long time and a lot of mistakes to look at these scans by hand. This is the area where AI can be the most helpful.

Convolutional Neural Networks (CNNs) and Long Short-Term Memory (LSTM) networks are two common ways to handle data from MRI images. LSTM networks are good at processing data that comes in a sequence and looking at how a patient's brain evolves over time. In contrast, CNNs are good at discovering patterns in images and spotting changes in the structure of the brain. Both models are good, but they don't fully show how patients and brain areas interact with each other. We need a better way to study the connections between the many brain areas that Alzheimer's disease affects.

This study suggests using a combined Graph Attention Network (GAT) and Sequential Learning to find Alzheimer's disease. Instead of processing MRI data as sequences or separate images, the proposed method joins patients based on shared MRI attributes. Instead, it sees individuals as nodes in a network. The model can determine how AD develops by pretending to connect different areas of the brain. The attention mechanism in GAT [3] helps the model prioritize the most important connections, leading to better and more meaningful predictions. In this study, we make the following key contributions:

- **A graph-based approach for AD detection:** We build a network where patients are linked based on feature similarities and analyze disease patterns in a better way.
- **Combining MRI and Clinical Features:** Our model integrates both brain imaging data and clinical details to make predictions more accurate.
- **Comparing deep learning models:** We evaluate GAT against CNN and LSTM models to show how our approach improves AD classification.
- **Using attention-based Learning:** Our model learns which patients' relationships are most relevant by applying GAT and enhances the decision-making process.

The rest of the paper is organized as follows: Section 2 covers the previous studies on AD detection using AI. Section 3 explains how we prepared and processed the data and describes the GAT model in detail. Section 4 presents the experiments and compares the results of different models. Section 5 discusses the findings and potential future improvements. Section 6 concludes the paper with final remarks.

2 Related Work

In this section, we discuss previous research on Alzheimer's Disease (AD) detection using deep learning and graph-based models. We review studies that use CNNs [4] and LSTMs for MRI analysis, as well as newer graph-based approaches that model relationships between patients.

2.1 Deep Learning for Alzheimer's Detection

Deep learning has been widely used to analyze MRI [5] [6] [7] scans for AD diagnosis. CNNs are one of the most commonly used models because they can automatically extract patterns from brain images. Several studies have shown that CNNs can detect brain atrophy related to AD with high accuracy. For example, researchers have used 3D CNNs to analyze volumetric MRI data and distinguish between healthy and AD-affected brains. However, LSTM networks are useful for analyzing sequential data, such as longitudinal MRI scans taken over time. LSTMs can model disease progression by learning how brain features change across different stages of AD. Some studies have combined CNNs and LSTMs. CNNs to extract spatial features and LSTMs to capture temporal trends. While this approach improves performance, it still treats each patient's data independently and does not consider relationships between individuals.

2.2 Graph-Based Models in Medical AI

In recent years, graph-based learning has gained attention in medical AI. Unlike CNNs and LSTMs, Graph Neural Networks (GNNs) [8] can represent complex relationships between patients, brain regions, or any other medical data points. One key advantage of GNN is their ability to model non-Euclidean data. Among GNN variants, Graph Attention Networks (GATs) have shown promising results in many biomedical applications. GATs assign different importance to each connection in the graph, allowing the model to focus on the most relevant relationships. Some recent studies have used GNNs to classify AD patients by building graphs based on feature similarities, showing improved classification accuracy. However, most of these models do not incorporate sequence-based learning, which limits their abilities to track disease progression over time.

2.3 Our Work in Comparison

While CNNs, LSTMs, and GNNs have all contributed to AD detection, each approach has its limitations [8][9]. CNN succeeds at feature extraction but lacks relational comprehension; LSTM networks can model temporal sequences but overlook inter-patient links; Graph Neural Networks effectively capture relationships but frequently disregard temporal dependencies. To address these gaps, our research presents graph-based learning utilizing sequential processing. By developing a patient similarity network and using GAT, we guarantee the capture of significant associations. Simultaneously, sequence learning allows the model to examine the temporal course of disease. This method provides a more thorough classification of AD patients utilising both MRI and clinical characteristics.

3 Methodology

In this section, we have discussed the MRI dataset, data processing, feature selection, the proposed GATSeq architecture model, and the benchmark of the GATSeq model.

3.1 OASIS Longitudinal MRI-Based Data Acquisition

The OASIS Longitudinal dataset consists of structural MRI scans collected from individuals aged 60 to 96 years, featuring several imaging sessions completed throughout time. The data was gathered to support research on neurovegetative illnesses, namely the examination of Alzheimer's disease (AD) development. The dataset comprises 373 T1-weighted MRI images from 150 distinct people, obtained under standardised imaging techniques. The dataset includes MRI scans and comprehensive clinical evaluations, such as the Mini-Mental State Examination (MMSE) and Clinical Dementia Rating (CDR). The CDR classified participants into three categories: Nondemented (ND) (CDR=0), demented (D) (CDR>0), and Converted (C) (subjects who went from ND to D over time). These cognitive scores facilitate the validation of AD diagnosis and the monitoring of its progression, rendering them suitable for graph-based learning methodologies.

3.2 Data Preprocessing and Feature Extraction

This study involves handling missing values in the dataset, since missing values may introduce biases and inconsistencies in deep learning models. We employ two approaches, one is K-Nearest Neighbours (KNN) imputation with k=5, which estimates missing values based on feature similarity, and median computation as an alternative approach to maintain robustness. These two strategies ensure that no essential information is lost due to missing data. Next, the categorical variables are processed to make them suitable for model training. Certain non-numeric attributes, such as Subject ID, MRI ID, and Hand, were removed as they did not contribute directly to the predictive task. The "group" feature, which represents the different diagnosis labels, is numerically encoded to ensure compatibility with deep learning algorithms. In a similar way, the "sex". The feature is label encoded, where the male was represented as 1 and the female as 0. These transformations ensure a seamless integration of categorical variables into the model.

Since the dataset contains diverse numerical attributes, including MRI-derived volumetric measurements and cognitive assessment scores, feature scaling becomes necessary to standardize the data. Min-max normalization is applied to MRI-related features such as MR delay, eTIV, nWBV, and ASF. In order to build the necessary graph structure for the GAT-based AD Classification model, feature extraction is carried out once processing is finished. By using the subjects' preprocessed feature vectors, a cosine similarity matrix is generated to ascertain the level of similarity between them. By combining clinical and MRI-based features, this matrix helps us to determine which individuals are most closely linked.

3.3 GATSeq Model Architecture

The proposed GATSeq model has been built using three essential layers to model patient relationships, transform features, and perform accurate multi-class classification:

Graph Attention Networks (GAT) Layer. The foundation layer of GATSeq is the Graph Attention Layer, where each individual in the dataset is represented as a node. The edges denote similarity-based connections between subjects. The first layer is implemented using GATConv, a Graph Attention Network layer that allows the model to learn which neighbors in the graph are more relevant by assigning higher attention weights. We use 4 attention heads and the set concat=false so that the output features from all heads are averaged rather than concatenated. The input to this layer is the node feature matrix and edge index representing the connections based on cosine similarity. The hidden representation dimension is set to 128, which is sufficient to capture complex feature interactions across nodes. This layer focuses on the most meaningful inter-patient relationships in the graph, which is essential for medical datasets involving progressive conditions like Alzheimer's.

ReLU and Fully Connected (FC) Layer. The output from the GAT layer is passed through a RELU activation function to introduce non-linearity and ensure that essential patterns are emphasized while minimizing vanishing gradient issues. The result is then forwarded to a fully connected linear layer that maps these high-level graph representations to the three AD classification categories: Nondemented, demented, and converted. The model is trained using the Adam optimizer with a learning rate of 0.01 and L2 weight regularization with weight decay of 5e-4 to improve generalization and control overfitting.

Loss of Cross-Entropy. To handle the multi-class classification task, the model uses the cross-entropy loss function. Since the dataset is slightly misbalanced, the loss function penalizes misclassifications in minority classes more strongly and encourages balanced learning. The final layer uses softmax activations to turn the raw output scores into probability values across the three AD stages and makes the predictions interpretable and suitable for downstream analysis.

3.4 Benchmarking GATSeq against Deep Learning Models: CNN, LSTM

The effectiveness of the proposed GATSeq model is assessed using CNNs and LSTMs. The dataset underwent preprocessing to ensure consistency, where categorical variables were encoded, missing values were imputed using median values, and numerical values were standardized. The CNN [10] captured the spatial dependencies through a 1D convolutional layer followed by a fully connected layer. In contrast, the LSTM utilizes recurrent connections to process sequential dependencies within the input features. Both models are trained using an Adam optimizer with cross-entropy loss for multi-class classification.

4 Experimental Setup and Results

In this section, to evaluate the performance of GAT, simulation experiments were conducted on a system with the following configuration: a MacBook (M2) with 8 GB RAM and a 256 GB SSD, all on a single physical machine, using a Python library.

4.1 Experimental Setup

The experimental evaluation is conducted to assess the effectiveness of the proposed GATSeq model in detecting AD [10] [11] [12] using the OASIS Longitudinal MRI dataset. The subjects are represented as nodes based on feature similarity. The cosine similarity between the feature vectors is calculated, and the degree of similarity between subjects, based on clinical and MRI features, is represented as a matrix. For each node, the top 5 most similar subjects were selected as neighbors, excluding the self-node. A binary adjacency matrix is formed, where an edge exists if two subjects belong to the top-k similarity groups. Each edge index is converted to a PyTorch tensor to be used as input for the Graph attention network. After preprocessing and feature extraction, the dataset is split into training (80%) and testing (20%) subsets with transformed feature vectors as input vectors and AD classification labels. They are then converted to PyTorch tensors for model training. Information is aggregated from nearby nodes using a Graph Attention Network layer with four attention heads, each of which is given a variable weight based on its relative relevance. The proposed model is trained for a hundred epochs, with loss tracked every 10 epochs to measure convergence.

4.2 Performance Metrics

The performance of proposed Alzheimer's disease classification model is compared to CNN and LSTM using precision, recall, F1-score, accuracy, and AUC-ROC to evaluate its effectiveness. As we see in section 4.3, the performance of each model is identified in nondemented, dementia, and converted stages of Alzheimer's disease progression using these criteria.

4.3 Comparative Analysis

We evaluated the performance of our proposed GAT model in comparison to CNN and LSTM models to determine how effectively it identified Alzheimer's disease (AD). In order to conduct an evaluation, the most significant metrics, such as accuracy, recall, precision, F1-score, and area under the curve (AUC), are applied. Box plots in MATLAB are used to display the data, and for each statistic, we examine the mean, maximum, minimum, and standard deviation. As seen in Figs. from 1 to 5, the GAT model is better than the LSTM and CNN models in terms of all considered metrics. Fig. 1 shows that it outperforms LSTM (72.93%) and CNN (80.93%), with an average accuracy of 90.32%, demonstrating its superior ability to correctly classify Alzheimer's patients. The higher precision and recall of GAT suggest that it effectively balances false positives and false negatives, whereas CNN and LSTM struggle with weak precision due to frequent misclassifications. As we have seen

in Fig. 5, the AUC score reflects the model's capability to strongest between different AD categories with the highest score of 97.21 % in GAT.

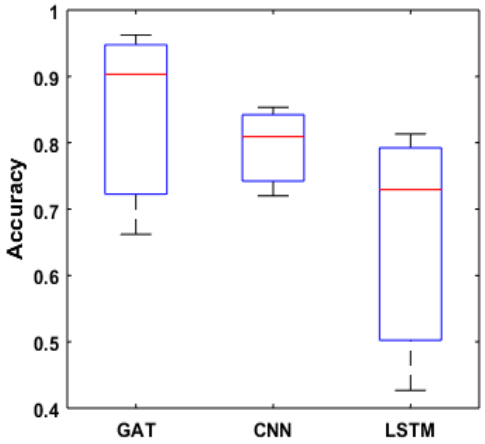

Fig. 1. Boxplot of Accuracy on MRI Data

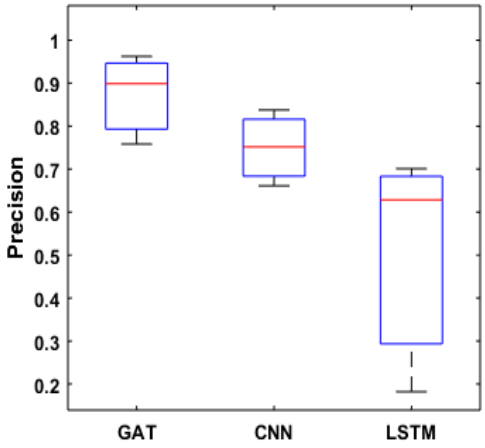

Fig. 2. Boxplot of Precision on MRI Data

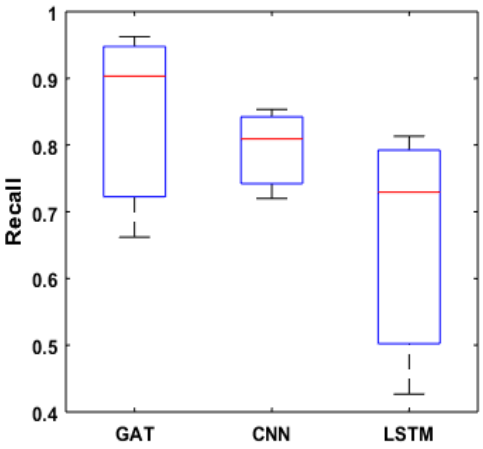

Fig. 3. Boxplot of Recall on MRI Data

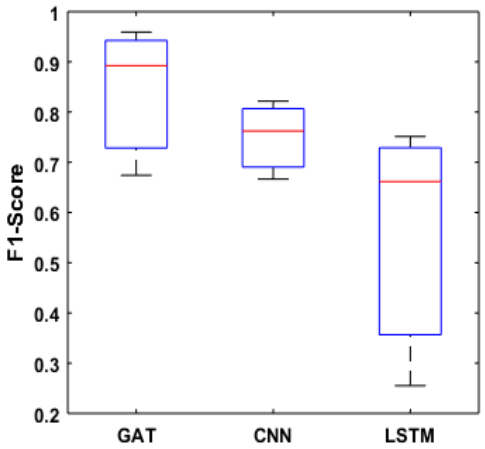

Fig. 4. Boxplot of F1-Score on MRI Data

Moreover, the model exhibits greater stability, with a lower standard deviation across multiple runs compared to LSTM, which shows high variability. The GAT efficiently captures relationships between subjects using MRI-derived features, making the results more effective than CNN's spatial feature extraction and LSTM's temporal modeling alone.

These results confirm that integrating graph-based learning with sequence modeling enhances both classification performance and model consistency.

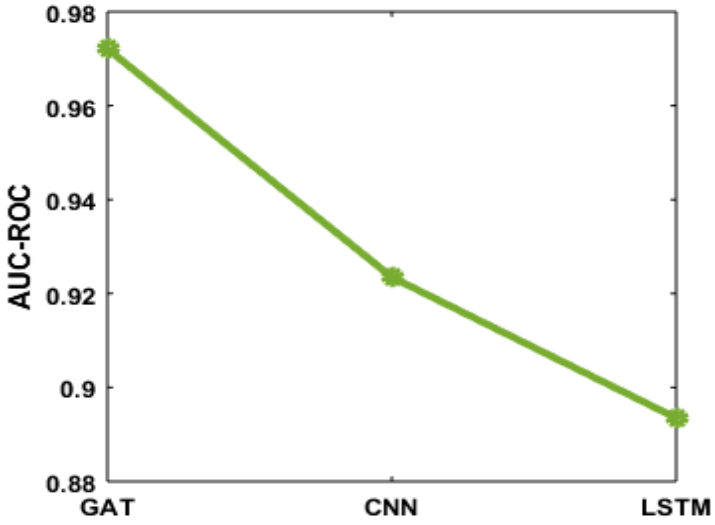

Fig. 5. Line Curve of AUC-ROC Curve on MRI Data

5 Discussion

The experimental results demonstrate that the GAT-based model outperforms both CNN and LSTM models in classifying the AD progression stages. The GAT model proves to be highly effective in capturing the complex relationships within the multimodal MRI dataset, with an impressive accuracy of 96.25% and an AUC-ROC score of 98.32% in distinguishing between different AD progression stages. The CNN model, which relies on spatial feature extraction, performed reasonably well with an accuracy of 82.93% and an AUC of 93.69%, as shown in Fig. 1 and Fig. 5, respectively. While CNNs are typically effective for image-based data, their performance on tabular clinical datasets is limited by their inability to model intricate feature dependencies. As seen in Fig. 1 and Fig. 5, the LSTM model designed to capture sequential dependencies achieves a lower accuracy of 74.00% and an AUC of 86.51%. The performance gap between LSTM and GAT suggests that AD's classification benefits more from a structured, relational learning approach rather than a purely sequential one. While LSTMs can capture temporal dependencies, they struggle with non-Euclidean data structures, which are better handled by GAT. This suggests that graph-based attention mechanisms are more effective in handling structured, high-dimensional medical data compared to traditional sequential and convolutional architectures. The

advantage of the GAT model is further highlighted by a deeper examination of precision (89.89%), recall (90.32%), and F1_score (89.23%), as shown in Figs. 2, 3, and 4, respectively. This ensures a strong balance between detecting true positive cases while minimizing false positives and false negatives. As seen in Figs. 2 to 4, the CNN model performs moderately well with an average precision of 75.16%, a recall of 80.93%, and an F1-score of 76.25%. However, the lower precision suggests a tendency to misclassification in some cases. In contrast, the LSTM model struggles significantly, showing a greater variability in performance. The precision of the LSTM model fluctuates between 18.20% and 70.12 %. This leads to an inconsistent F1 score of 66.16% on average. These fluctuations indicate that while LSTM captures sequential dependencies, they may not be stable when applied to complex multimodal datasets. Overall, the GAT-based models have proved to be highly effective for AD classification. The ability to leverage attention-based learning allows GAT to capture intricate relationships in medical data with higher classification accuracy and better generalization. The CNN and LSTM models show limitations in handling the complex dependencies within multimodal MRI data.

6 Conclusion

In the paper, we introduce the Graph Attention Networks (GAT) model to describe the inter-patient connections. Results show that GAT could be an effective classification tool for Alzheimer's disease, as it can obtain useful medical representations for different formats of medical data and model the strength of features. The experimental results suggest that graph-based attention mechanisms may be more suitable for medical AI systems than LSTM and CNN. The average accuracy on predicting Alzheimer's patients by using the GAT model is 90.32%. This might yield predictions that are more accurate and interpretable. Future work to develop such methods to integrate multiple such modalities and explanations can help to increase the transparency of models and their use in therapeutic practice. More iterations and possibly more training epochs, along with hyperparameter adjustments, might help to stabilize models and improve generalization. Doctors would trust the model more if the XAI (Explainable AI) part included attention mechanisms that are clearer and more understandable. Using a bigger and more representative sample, this study could show that the model is performant across multiple populations and that it is suitable to be used in real-life clinical practice.

References

1. Ashish, V. "Attention is all you need." *Advances in neural information processing systems* 30 (2017): I.

2. Oltu, B., Akşahin, M. F., & Kibaroğlu, S. (2021). A novel electroencephalography-based approach for Alzheimer's disease and mild cognitive impairment detection. *Biomedical Signal Processing and Control*, *63*, 102223.
3. Zhang, J., He, X., Qing, L., Chen, X., Liu, Y., & Chen, H. (2023). Multi-relation graph convolutional network for Alzheimer's disease diagnosis using structural MRI. *Knowledge-Based Systems*, *270*, 110546.
4. Zhu, W., Sun, L., Huang, J., Han, L., & Zhang, D. (2021). Dual attention multi-instance deep learning for Alzheimer's disease diagnosis with structural MRI. *IEEE Transactions on Medical Imaging*, *40*(9), 2354-2366.
5. Qiu, Y., Yu, S., Zhou, Y., Liu, D., Song, X., Wang, T., & Lei, B. (2021, April). Multi-channel sparse graph transformer network for early alzheimer's disease identification. In *2021 IEEE 18th International Symposium on Biomedical Imaging (ISBI)* (pp. 1794-1797). IEEE.
6. Afa, Alam, M., & Enam, M. (2025). Al-infused respiratory diagnostics: A New Era in Healthcare. *Soft Computing and Machine Learning: A Fuzzy and Neutrosophic View of Reality*, 244-265.
7. Alam, M., Ashraf, Z., Singh, P., Pandey, B., Rehman, K., & Aldasheva, L. (2025, March). Deep Learning Techniques for Intrusion Detection Systems in Healthcare Environments. In *2025 IEEE 14th International Conference on Communication Systems and Network Technologies (CSNT)* (pp. 105-111). IEEE.
8. Liu, J., Li, M., Luo, Y., Yang, S., Li, W., & Bi, Y. (2021). Alzheimer's disease detection using depthwise separable convolutional neural networks. *Computer Methods and Programs in Biomedicine*, *203*, 106032.
9. El-Assy, A. M., Amer, H. M., Ibrahim, H. M., & Mohamed, M. A. (2024). A novel CNN architecture for accurate early detection and classification of Alzheimer's disease using MRI data. *Scientific Reports*, *14*(1), 3463.
10. Ebrahimi, A., Luo, S., & Disease Neuroimaging Initiative, F. T. A. S. (2021). Convolutional neural networks for Alzheimer's disease detection on MRI images. *Journal of Medical Imaging*, *8*(2), 024503-024503.
11. Ebrahimi, A., Luo, S., Chiong, R., & Alzheimer's Disease Neuroimaging Initiative. (2021). Deep sequence modelling for Alzheimer's disease detection using MRI. *Computers in Biology and Medicine*, *134*, 104537.
12. Vidhya, R., Banavath, D., Kayalvili, S., Naidu, S. M., Charles Prabu, V., Sugumar, D., ... & Vidhya, R. G. (2023). Alzheimer's disease detection using residual neural network with LSTM hybrid deep learning models. *Journal of Intelligent & Fuzzy Systems*, *45*(6), 12095-12109.

Data-driven approaches for predicting pile bearing capacity

Yaren Aydın[1], Sinan Melih Nigdeli[1], Gebrail Bekdaş[1] and Ümit Işıkdağ[2]

[1]Department of Civil Engineering, Istanbul University-Cerrahpaşa,
34320 Avcılar/Istanbul/Turkey
yaren.aydin@iuc.edu.tr, bekdas@iuc.edu.tr, melihnig@iuc.edu.tr
[2] Department of Architecture, Mimar Sinan Fine Arts University, 34427 Istanbul, Turkey
umit.isikdag@msgsu.edu.tr

Abstract. The use of machine learning (ML) in the process of determining pile bearing capacity has increased in recent years. In this study, the EXtreme Gradient Boosting (XGBoost) and Tabular Prior-Data Fitted Network (TabPFN) algorithms were used to estimate the bearing capacity of pile foundations, and the performance of these two machine learning methods was compared. During the modeling process, a dataset containing various soil and pile parameters was used; prediction success was measured using the Correlation Coefficient (R2), Root Mean Square Error (RMSE), Mean Absolute Error (MAE), and Mean Square Error (MSE). According to the results obtained, both algorithms showed high prediction success. However, TabPFN was slightly ahead. Furthermore, the model performances were supported by graphical analyses, and graphs comparing actual and predicted values, along with feature importance rankings, visually demonstrated the performance of the models. The results of the study concluded that machine learning-based methods can be used as effective and reliable tools for predicting pile bearing capacity.

Keywords: Bearing Capacity, Pile, Predictive Models

1 Introduction

Piles function as column-shaped elements in the foundation structure and transfer loads from the superstructure through weak and compressible soil layers to harder, denser, and less compressible soil or rock [1]. The geotechnical design of pile foundations involves determining the load-carrying capacity for the pile geometry using theoretical or empirical engineering approaches [2], [3]. The analysis of axially loaded piles is performed using semi-empirical methods based on limit equilibrium, taking into account the loading and drainage conditions of the soil layer. Common methods are the α, ß, and λ methods [4]. However, in recent years, machine learning approaches have significantly simplified this process and increased prediction accuracy. ML-based models offer flexibility that can be applied to different soil and pile types. In this context, various studies on pile bearing capacity estimation demonstrate the effectiveness of ML

methods. The remainder of this article presents studies conducted on the estimation of pile bearing capacity.

Makasis et al. [5] presented a machine learning prediction model that can be used in conjunction with finite element simulations to reduce the time and resource requirements in energy pile design. They tested the model using three case studies with different geometries and materials, each with 24 different thermal load distributions. The results showed that prediction errors were at an acceptable level and that the model demonstrated high accuracy (R^2=0.9999). Kardani et al. [6] used decision trees, k-nearest neighbors, artificial neural networks, random forests, support vector regressors, and gradient boosting algorithms to predict bearing capacity in cohesionless soils. The results show that the optimized models have high potential, with the eXtreme Gradient Boosting method delivering the best performance (R^2=0.9615). Yago et al. [7] used k-nearest neighbor (KNN), kernel-KNN (KKNN), decision tree (DT), random forest (RF), artificial neural networks (ANN), and support vector machines (SVM) to estimate the load-bearing capacity of precast concrete piles. The best performance was achieved with RF (RMSE=642.38). Benbouras et al. [8] predicted the bearing capacity of driven piles using steel and concrete pile data collected from Iran, Mexico, and India. Among the ML models used, the Deep Neural Network (DNN) model provided the highest accuracy in terms of MAE, RMSE, IOS, R, R^2, and IOA metrics and showed a high correlation between 0.9777 and 0.9998 with validation data in 5-fold cross-validation. They used Kernel Ridge Regression (KRR) and Multilayer Perceptron (MLP) models to estimate the vertical and horizontal load-bearing capacity of pile foundations in cold and saline soils. In their study, which used parameters such as pile length, diameter, corrosion depth, and spalling thickness, KRR best predicted vertical load-bearing capacity (R^2=0.93), while MLP best predicted horizontal capacity (R^2=0.94).

In this study, bearing capacity load of pile (Pu) was predicted using pile diameter (X_1), length of the pile tip section (X_2), length of the second pile segment (X_3), length of the pile top segment (X_4), natural ground elevation (X_5), pile top elevation (X_6), guide piles' stop driving elevation (X_7), pile tip elevation (X_8), average SPT blow along the embedded length of the pile (X_9), average SPT blow at the tip of the pile (X10). eXtreme Gradient Boosting (XGBoost) and Tabular Prior-Data Fitted Network (TabPFN) were used for prediction.

2 Materials and Methods

2.1 Dataset

The dataset was obtained from [9]. The study utilized a comprehensive dataset consisting of 472 experimental results from pile loading tests conducted in Ha Nam province, Vietnam [9]. The dataset consists of 472 rows and there is no missing data.Fig. 1 shows the histogram for the variables in the dataset.

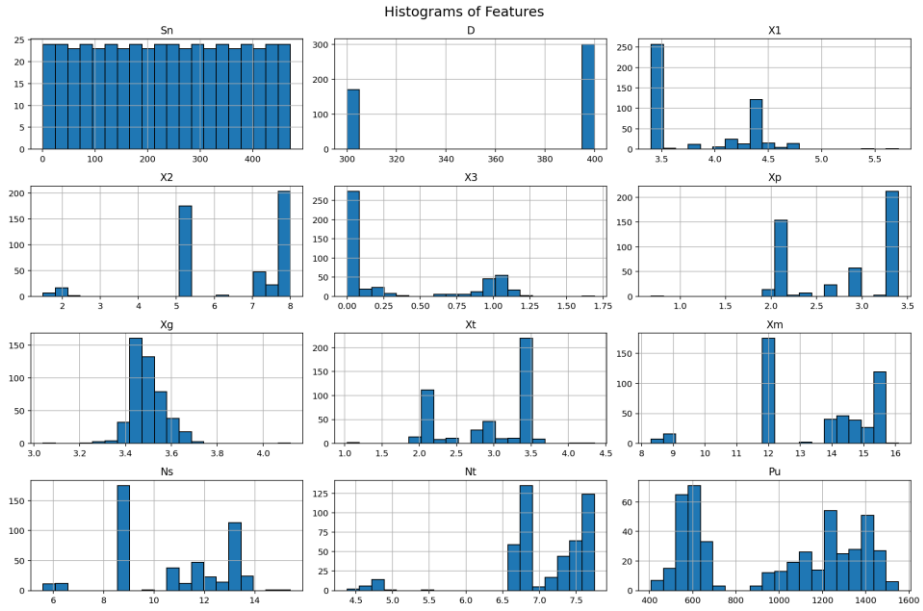

Fig. 1. Histogram for the input and output variables.. .

Fig. 2 shows the boxplot of features in the dataset. This figure shows that the output (Pu) has the highest values, a relatively high median, and a wide distribution.

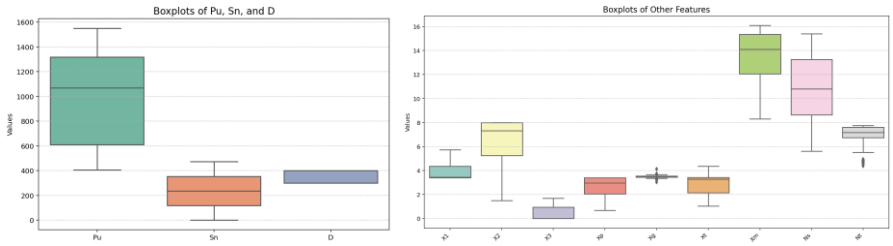

Fig. 2. Boxplot of features.

2.2 Machine Learning and Predictive Models

Machine Learning (ML) enables computers to perform tasks such as classification, image and speech recognition, and natural language processing by building models from data without human intervention. It learns from past data to identify patterns and produce reliable and repeatable decisions [10]. Its ability to continuously improve its

performance with increasing amounts of data enables it to offer adaptable solutions in different fields [11]. In this study, machine learning was used for the regression task. In this study, regression algorithms (eXtreme Gradient Boosting (XGBoost) and Tabular Prior-Data Fitted Network (TabPFN) were used for prediction.) were used to predict bearing capacity load of pile (Pu).

XGBoost algorithm is a model that creates a tree ensemble using gradient descent [12] It provides better generalization with lower error and variance by applying dropout regularization to reduce overfitting. XGBoost is a model that offers advantages such as preventing overfitting, handling missing data, high speed, and prediction power [13]. XGBoost is scalable, efficient, and offers GPU accelerator support with multi-core parallel processing; thus, training time can be at least 10 times shorter than GBM [14].

TabPFN is a neural network pre-trained on tabular data. Trained on synthetic or presampled datasets, it can make fast and reliable predictions on new datasets. Its architecture is transformer-based, enabling it to be effective even on small datasets [15].

To evaluate the performance of prediction models, the Correlation Coefficient (R^2), Root Mean Square Error (RMSE), Mean Absolute Error (MAE), and Mean Square Error (MSE) are used. These metrics are commonly preferred to measure the fit between predicted and actual values and the error rates. R^2 is the goodness of fit of the model, and as it approaches 1, the model's predictions are more accurate. RMSE measures the standard deviation of prediction errors. MAE gives the average magnitude of errors without considering their direction. MSE measures the average of the squares of the errors. Low values of error metrics indicate high model performance. In the study, a 10-fold cross-validation method was used to prevent the model from overfitting and to obtain more reliable predictions. Using this method, the dataset was divided into 10 subsets, and each subset was used as test data in turn, while the remaining nine subsets were evaluated as training data.

3 Results

The performance metrics of models XGBoost and TabPFN are examined in this section, and the visual results of the algorithms are presented. Table 1 shows the performance comparison of both models.

Table 1. Evaluation of XGBoost and TabPFN based on performance criteria

Model	Average MAE	Average MSE	Average RMSE	Average R^2
XGBoost	66.1925	7976.1222	89.3091	0.9359
TabPFN	67.3720	7831.1585	88.4938	0.9370

According to Table1, TabPFN's MAE is slightly higher (67.3720)r, while TabPFN's MSE (7831.1585) and RMSE (88.4938) are lower. This indicates that TabPFN's predictions are generally slightly more accurate. Although TabPFN's R^2 is higher (0.9370), both models have a very high R^2 value. Additionally, the R^2 value (0.9331) in the study from which the data set was obtained was found to be only slightly higher for the test data set (0.9370).

The best parameters for the XGBoost model were determined as follows as a result of hyperparameter tuning using Randomized Search: colsample_bytree: 0.8430, gamma: 0.8526, 'learning_rate: 0.0295, max_depth: 6, n_estimators: 188, reg_alpha: 0.9656, reg_lambda: 0.8083, subsample' 0.7218.

Fig. 3 shows the feature importance ranking for the optimized XGBoost model. Examining this figure reveals that the length of the pile tip section (X_2) and guide piles' stop driving elevation (X_7 or X^m),variables are the most influential variables in the model's predictive power.

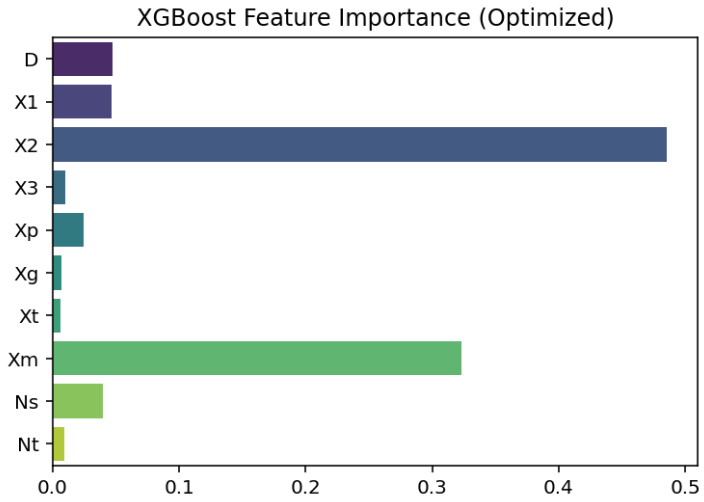

Fig. 3. Feature importance ranking for the optimized XGBoost model.

Fig. 4. gives comparison of predicted values with actual values (scatter plot) for XGBoost. In Fig. 4, the points are largely clustered around the red line, indicating that the model makes successful predictions. However, some points deviate from the line, revealing errors; deviations are particularly noticeable in the middle values. Nevertheless, the model shows quite strong prediction performance in the low and high value ranges.

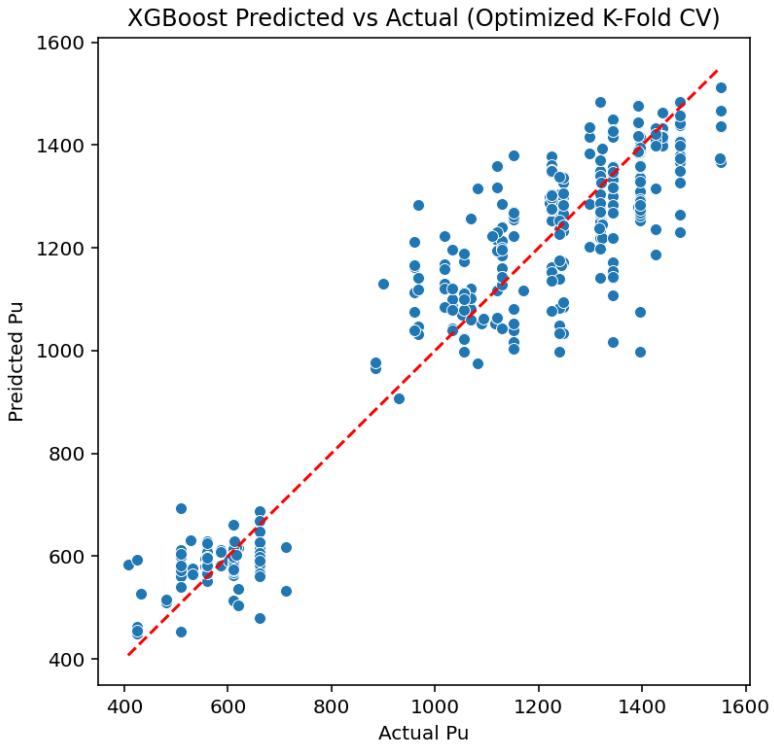

Fig. 4. Comparison of predicted values with actual values (scatter plot) for XGBoost.

Fig. 5. gives comparison of predicted values with actual values (scatter plot) for TabPFN. In Fig. 5., it can be seen that XGBoost and TabPFN show similar performance, although there are deviations at some extreme values.

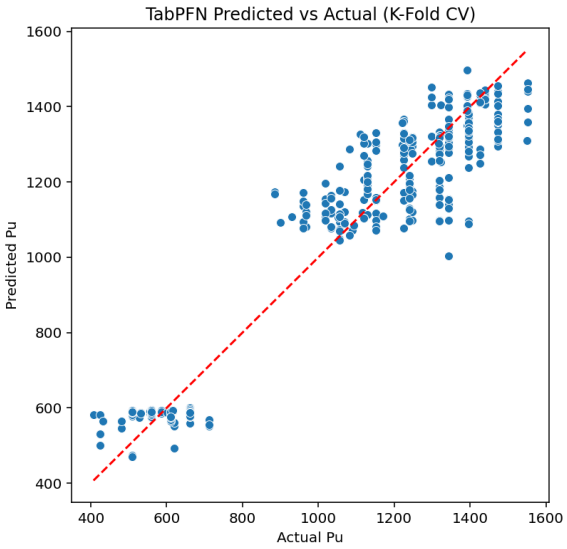

Fig. 5. Comparison of predicted values with actual values (scatter plot) for TabPFN.

4 Conclusions

In this study, EXtreme Gradient Boosting (XGBoost) and Tabular Prior-Data Fitted Network (TabPFN) were used to predict the pile bearing capacity, which is critical for the safety of structures built on the ground and the performance of these two methods was compared. A comprehensive data set including various variables such as pile dimensions and natural ground elevation was used in the modeling process. The comparison process was based on statistical measures such as Correlation Coefficient (R^2), Root Mean Square Error (RMSE), Mean Absolute Error (MAE), and Mean Square Error (MSE). The findings show that both models have a high level of accuracy.. However, the TabPFN algorithm demonstrated a stronger predictive ability than XGBoost, with slightly higher R^2 and lower error values. The findings obtained within the scope of the study are supported by graphs. These findings demonstrate the effectiveness of ML models in predicting pile bearing capacity.

References

[1] British Electricity International, “Civil engineering and building works,” in *Station Planning and Design*, Elsevier, 1991, pp. 178–302. doi: 10.1016/B978-0-08-040511-7.50010-3.

[2] A. Honarjoo and V. Ghiasi, "Analyzing analytical and software methods for deep foundation analysis and presenting a new solution for determining pile capacity using the PDA test," *International Journal of Geo-Engineering*, vol. 16, no. 1, p. 14, Jun. 2025, doi: 10.1186/s40703-025-00242-8.

[3] B. Wrana, "Pile Load Capacity – Calculation Methods," *Studia Geotechnica et Mechanica*, vol. 37, no. 4, pp. 83–93, Dec. 2015, doi: 10.1515/sgem-2015-0048.

[4] H. G. Poulos and E. H. Davis, *Pile foundation analysis and design*. New York: Rainbow-Bridge Book Co., 1980.

[5] N. Makasis, G. A. Narsilio, and A. Bidarmaghz, "A machine learning approach to energy pile design," *Comput Geotech*, vol. 97, pp. 189–203, May 2018, doi: 10.1016/j.compgeo.2018.01.011.

[6] N. Kardani, A. Zhou, M. Nazem, and S.-L. Shen, "Estimation of Bearing Capacity of Piles in Cohesionless Soil Using Optimised Machine Learning Approaches," *Geotechnical and Geological Engineering*, vol. 38, no. 2, pp. 2271–2291, Apr. 2020, doi: 10.1007/s10706-019-01085-8.

[7] G. Yago, F. Verri, and D. Ribeiro, "Use of machine learning techniques for predicting the bearing capacity of piles," *Soils and Rocks*, vol. 44, no. 4, pp. 1–14, Nov. 2021, doi: 10.28927/SR.2021.074921.

[8] M. A. Benbouras, A.-I. Petrişor, H. Zedira, L. Ghelani, and L. Lefilef, "Forecasting the Bearing Capacity of the Driven Piles Using Advanced Machine-Learning Techniques," *Applied Sciences*, vol. 11, no. 22, p. 10908, Nov. 2021, doi: 10.3390/app112210908.

[9] T. A. Pham and V. Q. Tran, "Developing random forest hybridization models for estimating the axial bearing capacity of pile," *PLoS One*, vol. 17, no. 3, p. e0265747, Mar. 2022, doi: 10.1371/journal.pone.0265747.

[10] M. Soori, B. Arezoo, and R. Dastres, "Artificial intelligence, machine learning and deep learning in advanced robotics, a review," *Cognitive Robotics*, vol. 3, pp. 54–70, 2023, doi: 10.1016/j.cogr.2023.04.001.

[11] W. Kellerer, P. Kalmbach, A. Blenk, A. Basta, M. Reisslein, and S. Schmid, "Adaptable and Data-Driven Softwarized Networks: Review, Opportunities, and Challenges," *Proceedings of the IEEE*, vol. 107, no. 4, pp. 711–731, Apr. 2019, doi: 10.1109/JPROC.2019.2895553.

[12] M. Massaoudi, S. S. Refaat, I. Chihi, M. Trabelsi, F. S. Oueslati, and H. Abu-Rub, "A novel stacked generalization ensemble-based hybrid LGBM-XGB-MLP model for Short-Term Load Forecasting," *Energy*, vol. 214, p. 118874, Jan. 2021, doi: 10.1016/j.energy.2020.118874.

[13] T. Chen and C. Guestrin, "XGBoost," in *Proceedings of the 22nd ACM SIGKDD International Conference on Knowledge Discovery and Data Mining*, New York, NY, USA: ACM, Aug. 2016, pp. 785–794. doi: 10.1145/2939672.2939785.

[14] S. A. Kulkarni, V. P. Gurupur, and C. King, "Impact Analysis of Stacked Machine Learning Algorithms Based Feature Selections for Deep Learning Algorithm Applied to Regression Analysis," in *SoutheastCon 2022*, IEEE, Mar. 2022, pp. 269–275. doi: 10.1109/SoutheastCon48659.2022.9764105.

[15] N. Hollmann, S. Müller, K. Eggensperger, and F. Hutter, "Tabpfn: A transformer that solves small tabular classification problems in a second.," *arXiv preprint*, 2022.

E2DLB: An Energy Efficient Deadline Aware Load Balancing Algorithm for Fog and Edge Computing

Deepak[1], Manoj Kumar Upadhyay[1], Mahfooz Alam[2*]

[1]Department of Computer Science, Institute of Engineering and Technology, Dr. B.R. Ambedkar University, Khandari, Agra, India
dsingh.cs22@gmail.com; mku1964_icis@rediffmail.com
[2]Department of MCA, G. L. Bajaj Institute of Technology and Management
Greater Noida-201306, India
mahfoozalam.amu@gmail.com

Abstract. With the increasing demand for low-latency processing and energy efficiency in IoT applications, it has become more crucial to consider fog and edge computing. Traditional load balancing schemes often ignore the trade-off between energy consumption and deadline constraints, which can severely limit their performance in environments sensitive to latency. To address this issue, this paper proposes the E2DLB (Energy Efficient Deadline Aware Load Balancing) algorithm to optimize load distribution across heterogeneous computational nodes, ensuring minimal energy Consumption while meeting task deadlines and operational requirements. E2DLB uses a multi-tier architecture with intelligent task classification, deadline-based prioritization, and dynamic task offloading techniques to achieve optimal resource utilization while remaining energy-efficient. It employs a multi-criteria decision method that finds the optimal balance between deadline and energy efficiency to dynamically evaluate a batch of IoT tasks characterized by variable parameters such as computational needs and deadlines, and then distributes workloads accordingly. To prevent overloads and reduce service delays, the system also incorporates adaptive thresholding and node status monitoring. According to simulation results, E2DLB outperforms existing load balancing solutions in terms of energy savings and deadline adherence. Specifically, it reduces energy consumption by an average of 13% compared to BALBA, over 20% compared to DCLB, and up to 26.88% compared to REAL. This work improves the sustainability of edge computing by addressing the trade-off between energy efficiency and service quality in real-time distributed systems.

Keywords: Energy Efficiency, Deadline, Load balancing, Fog computing, Edge computing.

1 Introduction

The rapid advancement of inexpensive computer chips, coupled with widespread Internet connectivity, has led to an exponential growth of the Internet of Things (IoT). It is presently a baseline matter in the digital ecosystem, having utterly revamped the

ways data is generated, processed, and utilized in multifarious areas. Growing applications permeate all critical sectors, denying any single entity such sectors like medicine, underwater exploration [1], intelligent transport, smart home [2], industrial automation, and mobile cyber-physical systems [3]. Connected devices are thus ever more numerous, causing unprecedented data proliferation in the digital arena. A study by Cisco [4] claims that the global count of IoT devices would rise from 15 billion in the year 2023 to 21 billion by 2025 and subsequently top 41 billion by 2027. This explosion in numbers has been matched with a rapidly growing volume of data being churned out by these devices. At any rate, the IoT devices were producing 18.3 zettabytes of data in 2019, and the International Data Corporation (IDC) projects an increase in data to 73 zettabytes by 2025, almost a 400% hike [5].

However, the efficiency and effectiveness of a fog and an edge computing system largely depend on the load balancing mechanisms put in place. In other words, load balancing can optimize system performance and ensure that computational tasks are dynamically and efficiently distributed to the available edge and fog nodes. Traditional load balancing techniques will ensure load distribution but do not take energy consumption into account, thus causing excessive power usage, which does not go well with resource-constrained edge environments. Contrary to energy-aware scheduling approaches that save energy, however, many fail to adhere to the strict deadline requirements of latency-sensitive IoT applications, such as autonomous driving, remote healthcare monitoring, and real-time industrial control systems. This conflict between energy efficiency and deadline adherence is what threatens QoS in fog and edge computing.

The very critical area of research remains the trade-off between energy consumption and deadline achievement in task scheduling. In this direction, the paper proposes an efficient algorithm called E2DLB (Energy Efficient Deadline Aware Load Balancing) to distribute computational workloads efficiently over fog and edge nodes with minimum energy consumption while meeting the required deadlines. The proposed scheme will dynamically distribute a Batch of IoT (BIoT) tasks depending on indices of deadline sensitivity and energy efficiency, which would thus enhance the performance of the system overall. This paper thus discusses the design, implementation, and performance evaluation of E2DLB, with the programming and evaluation showing the effectiveness of energy consumption and deadline satisfaction in doing the same.

2 Related Work

Several approaches have been proposed for load balancing in fog and edge computing environments. Existing solutions can be categorized into the following three main areas:

2.1 Energy-Aware Load Balancing

Reducing power consumption has been investigated in various studies concerning fog and edge networks. Dynamic voltage scaling, workload offloading, and energy-aware VM migration techniques are applied for energy-saving purposes. Most of these

methods aim to minimize energy consumption with less focus on real-time constraints, thereby risking the possibility of missing deadlines. Garg et al. (2019) [6] propose the REEWS (Reliability and energy efficient workflow scheduling) algorithm, intending to optimize energy efficiency in conjunction with system reliability in a cloud computing context, which employs dynamic voltage and frequency scaling to curtail energy consumption. The authors of [7] in 2025 introduced a framework to improve virtual machine migration in cloud computing environments. The framework, known as the Efficient Migration through Dependency Analysis (EMDA) framework by addressing complex dependencies among components, optimizing resource utilization, and reducing energy consumption. Mahapatra et al. (2024) [8] offered an energy-aware task offloading load-balancing framework for latency-sensitive IoT applications in Fog-Cloud computing. The proposed approach uses Fuzzy logic for task allocation, along with BLWJAYA (Binary Linear-Weight JAYA) algorithm for scheduling, achieving much improved resource utilization (26.2%), service rates (12%), latency (7%), energy consumption (8.63%), and load balancing (6%). Hence, it is a more efficient and scalable resource management process. Singhal et al. (2023) [9] offered an energy-aware load balancing framework for smart grid cloud and fog computing. Compared to the existing static and dynamic algorithms, they proposed the Rock Hyrax Optimization (RHO) algorithm for efficient task allocation across VMs, with switching off idle virtual machines to save energy. It was observed from simulations with CloudAnalyst that RHO improves processing time by 26 %, response time by 15 %, energy by 29 %, cost by 6 %, and delay by 14 % as compared to existing static and dynamic algorithms. A multi-objective NPSO (New PSO) algorithm for workload optimization allocation has been proposed by Saif et al. (2023) [10], under which significant reductions in energy consumption and processing delay were achieved through queuing theory modeling pertaining to the cloud-fog computational environment. Srivastava and Kumar's (2025) [11] Adaptive Remora Optimization Algorithm optimizes workflow scheduling in cloud computing, achieving 0.695 kWh energy consumption and 179.14 seconds execution time, outperforming existing approaches.

2.2 Deadline-Constrained Scheduling

In real-time operating systems, one might schedule tasks according to some numerical priority denoting urgency, aiming at accomplishing deadlines in fog computing, the classical ones being EDF and DLS. Zhang et al. (2022) [12] suggested a load-balancing method for data center networks addressing the deadline parallel data transmission performance that augments throughput and shortens latency. Haidri et al. (2022) [13] suggest an RDLBS technique with the aim of optimizing task scheduling in cloud computing environments. The methodology involves transferring incoming tasks to free VMs, maximizing turnover time, and efficient use of resources. Zhang et al. [14] in 2022 proposed a dynamic task scheduling method for edge-cloud collaborative computing to ensure real-time processing and enhance resource utilization, thereby minimizing latency and improving system efficiency. Gautam and Malhotra (2024) [15] proposed Deadline-Aware Priority-Based Semi-Greedy Scheduling for Task Scheduling in Fog Computing to improve deadline adherence, makespan, and energy consumption. Ghorbani et al. (2025) [16] present ALBLA: Adaptive Load Balancing

for Edge-Cloud Networks. ALBLA makes use of learning automata to allocate tasks dynamically, such that it adapts itself to dynamic workloads and changes in network conditions. Simulations reveal that ALBLA reduces service time, reduces waiting time, balances network load, and maximizes the number of successful task executions.

2.3 Hybrid Approaches

Energy efficiency allied with deadline constraints is, in the recent literature, a hotspot of heuristic and metaheuristic optimization methodologies. In 2023, the author of [17] came up with a Security-Driven Energy-Efficient Workflow Allocation (SEWA) Algorithm for cloud computing environments, in some balance between energy efficiency and security. Energy efficiency with deadline constraints is nowadays increasingly being tackled by many heuristic and metaheuristic optimization approaches. In 2023, the author of [17] designed a Security-Driven Energy-Efficient Workflow Allocation (SEWA) Algorithm for cloud computing environments with some trade-offs between energy efficiency and security. Simulations result-wise showed that energy consumption could be minimized while deadlines were respected and system security was upheld. In 2024, Pakmehr et al. [18] proposed the ETFC-method, a hybrid for task scheduling with efficiency in terms of energy consumption and deadlines for fog computing, weighing the pros and cons of ETFC, which uses metaheuristic algorithms together with reinforcement learning to carry out task allocation for minimizing energy consumption and maximizing deadline adherence. Simulations show it outperforms existing methods in efficiency and performance. Khaledian et al. (2024) [19] created a combined algorithm called PSO-SA, which uses Particle Swarm Optimization and Simulated Annealing for assigning tasks, improving energy use and overall time in fog-cloud settings, with simulations showing an average improvement of 5% in energy consumption and 9% in makespan compared to the baseline algorithm (IKH-EFT). Alwabel and Swain (2024) [20] presented a policy for application module placement in fog-cloud systems that prioritizes critical applications within the fog infrastructure while consolidating active fog nodes to manage energy consumption. Evaluated using iFogSim, this policy outperforms contemporary solutions by increasing the percentage of QoS-satisfied applications and reducing energy usage in fog computing environments. Despite these advancements, existing solutions fail to achieve an optimal balance between energy efficiency and deadline satisfaction. This gap motivates the development of E2DLB, which combines energy-efficient load balancing with real-time deadline awareness to enhance performance in fog and edge computing environments.

3 System Model and Problem Definition

3.1 System Architecture

The E2DLB algorithm is designed for a distributed fog and edge computing environment, targeting the efficient handling of task batches generated by multiple IoT devices. This architecture has been structured in consideration of the increasing need for real-time responsiveness and energy optimization in resource-limited,

heterogeneous computing ecosystems. E2DLB takes advantage of a multilayer infrastructure comprising end devices, fog nodes, and cloud data centers that all differ in computing resource capacity, latency, and energy characteristics. In such architecture, BIoT tasks coming from edge devices would get intelligently offloaded to the most appropriate processing layer, with respect to two major parameters: deadline urgency for a task and energy efficiency of candidate computational nodes. The essence is that ones that are latency-sensitive will be executed close to the source (at fog or edge levels), whereas others that are somewhat less time-sensitive may be offloaded to the cloud, which is highly energy-intensive yet very capable. Together with location-aware load balancing, energy profiling, and deadline enforcement, the E2DLB architecture creates a sustainable clash between performance and resource consumption. The framework of the E2DLB is represented by Fig. 1.

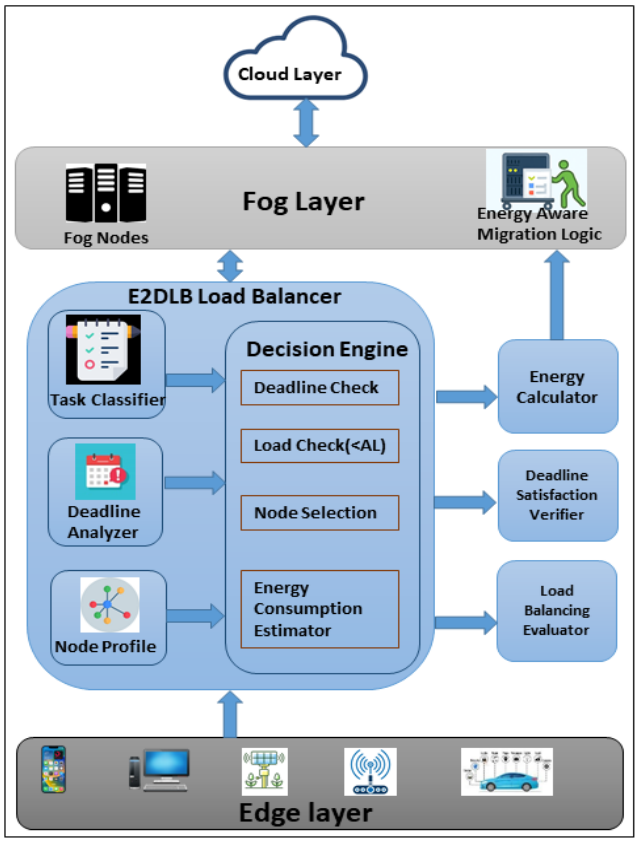

Fig. 1. Framework of E2DLB

End Devices (Edge Layer): This layer is comprised of IoT devices, including sensors, smart wearables, mobile clients, and embedded systems, which incessantly generate

batches of real-time tasks. They are generally low-power devices, going by meaning of processing requirements and energy constraints, and thus cannot execute the tasks locally. For this matter, they opt for fog and edge nodes to offload the workload for computations. The task batches generated are packaged according to predefined criteria such as sampling interval, data volume threshold, or event trigger.

E2DLB Load Balancer: In the middle between edge and fog, the E2DLB Load Balancer acts as the central component for both task analysis and scheduling and balancing for deadline and energy efficiency. The E2DLB consists of three core modules that perform their functions:

Task Classifier. The task classifier categorizes tasks arriving from edge devices and sorts tasks based on their ascending order of deadlines. After arranging of task, use the mid-point method [21] for selection of the middle task, such as

$$\mathrm{T_{mid}} = \begin{cases} \left(\frac{o(T_m)+1}{2}\right) & if\ odd\ no.of\ task \\ \frac{o(T_m)}{2}, \frac{o(T_m)}{2} + 1 & if\ even\ no.of\ task \end{cases}$$

Deadline Analyzer. It analyzes the temporal constraints of each task and determines the time available for execution by comparing the deadline with the current timestamp. It helps the decision engine to identify which tasks are deadline-critical.

Node Profile. The Node Profile module continuously monitors and maintains real-time information about the operational state of available edge and fog nodes. It captures vital metrics such as current load, energy efficiency, reliability, and response time history. These profiles are dynamic and are frequently updated to reflect changing conditions in the fog and edge environment. Maintaining this node information will allow for proper and efficient node selection and task scheduling. Nodes are ranked according to their energy efficiency, which is measured in terms of power consumed per task execution. The task execution goes to the most energy-efficient node that still possesses adequate computing abilities.

Decision Engine: The Decision Engine forms the central brain of the load balancer of the E2DLB. It accepts inputs from the Task Classifier, Deadline Analyzer, and Node Profile to come up with the best optimal solution as regards task placement. It has four core modules:

Deadline Check. Ensures that the selected node can complete the task within the required deadline.

Load Check (<AL). Load Check verifies whether the target node is operating below the Average Load (AL). Load check is very important to keep the system performance

stable and reduce task failure due to overload. If load ≥AL, then the node is skipped in the selection process, and the algorithm looks for underutilized or idle nodes.

Node Selection. In this allocation strategy, first, we allocate tasks to edge nodes with minimum energy consumption and deadline meet, and also check that Load(E_j) ≤ $AL_{edge.}$ Second, if the deadline is not satisfied or the node is overloaded, then transfer tasks to fog nodes. The allocation pattern for edge nodes will be for even and odd numbers of tasks in T, as follows [21] [22]:

- If o(T_m) is even, then the task pattern will be T_{mid}, (T_{mid} +1)th, (T_{mid} -1)th, ((T_{mid} +1)+1)th, ((T_{mid} -1)-1)^{th,} and so on.
- Further, if o(T^m) is odd, then the transfer pattern will be T_{mid}, (T_{mid} -1)th, (T_{mid} +1)th, ((T_{mid} -1)-1)th, ((T_{mid} +1)+1)th, and so on.

Energy Consumption Estimator. Estimates the energy cost of executing a task on each candidate node. It helps select nodes with lower expected energy consumption.

External Evaluation Modules. There are three components in the evaluation module:

Energy Calculator. Computes actual energy usage and provides data to improve scheduling decisions.

Deadline Satisfaction Verifier. Verifies if deadlines were met post-execution and informs future task handling.

Load Balancing Evaluator. Monitors load distribution across nodes to avoid bottlenecks or under-utilization.

Fog Layer: The fog layer is placed as the middle processing tier-close to devices on the geographical scale, where fog nodes consist of moderate computational and storage resources. Such nodes execute time-sensitive batches of moderate-extent IoT tasks that require low latency and localized processing. They also tend to be the primary control nodes that monitor node status, task queue lengths, and execution delays, all influencing dynamic task scheduling decisions. In the framework, task migration occurs in such a way that when tasks are not finished on an edge node, they are migrated to a fog node.

Task Migration Mechanism. If a task has been assigned to an edge node which, for some reason, was unable to meet its deadline owing to limited resources or the node being overloaded, however, the algorithm will now try to dynamically migrate this task to some other edge node/fog node, where more energy efficient and available. Otherwise, migration decisions shall be based on a cost-benefit analysis in saving energy and meeting deadlines.

Cloud Layer. Even though E2DLB is primarily meant for fog and edge computing, the fall-back provision in the architecture is the cloud layer to offload those task batches

that outgrow the processing or energy capabilities of fog nodes. The cloud is made up of high-performance, centralized data centers capable of undertaking relaxed-deadline and resource-intensive tasks. Due to the associated latency and energy penalties, it is invoked only when necessary and is not the default processing tier.

3.2 Parameter Estimation

Given below are the QoS parameters and their corresponding equations for calculating and analyzing system performance metrics.

Expected Time to Compute (ETC): It indicates the time a given task is expected to be executed on a particular computational resource, given the work of the task and the processing capability of the resource.

$$ETC_{ij} = \frac{W_i}{CC_j} \; or \; ETC_{ik} = \frac{W_i}{CC_k} \tag{1}$$

Average Expected Time to Compute(AveETC): The mean of the expected computation times for tasks across all resources.

$$AveETC\ (T_i) = \frac{\sum_{j=1}^{N_e} ETC_{ij}}{N_e} \; or \; AveETC\ (T_i) = \frac{\sum_{k=1}^{N_f} ETC_{ik}}{N_f} \tag{2}$$

Energy Consumption (EC): Energy consumption is the amount of energy required to perform an operation or task in a computing environment. The energy-consumption context in fog computing and edge computing mostly refers to the amount of energy consumed by a device, be it an edge node or fog node, for carrying out an assigned computational task. Energy consumption is measured in joules.

$$EC_{ij} = ETC_{ij} \times E_{N_j} \text{ or } EC_{ik} = ETC_{ik} \times E_{N_k} \tag{3}$$

Total Energy Consumption: Total energy consumption refers to the total amount of energy consumed by all computational nodes (edge and fog) to carry out their assigned tasks during one scheduling cycle.

$$E_{total} = \sum_{i=1}^{m} \sum_{j=1}^{n} EC_{ij} \tag{4}$$

Energy Efficiency (EE): Energy efficiency is the measure of how much useful computational work is done per unit of energy consumed to do that work.

$$EE = \sum_{i=1}^{m} \frac{W_i}{E_{total}} \tag{5}$$

Maximum Expected Time to Compute (maxETC): The maximum expected time of any task to finish anywhere on available resources.

$$maxETC(T_i) = \max\left(\mathrm{ETC}_{ij}\right) \forall j \in N \tag{6}$$

Average Load (AL): AL refers to the average computational workload that is distributed over all the available resources in a system. It defines how evenly the workload is shared and is often used in measuring the performance of load balancing algorithms**.**

$$AL_{edge} = \frac{\sum_{i=1}^{m} \text{AveETC } (T_i)}{N_e} or\ AL_{fog} = \frac{\sum_{i=1}^{m} \text{AveETC } (T_i)}{N_f} \quad (7)$$

Deadline: Deadline refers to the latest time by which a task needs to be completed to meet some system or application-specific requirements. It is a critical constraint in real-time, fog, and edge computing environments where timely execution impacts service quality. The deadline of task T_i is given by

$$D(T_i) = K * \sum_{i=1}^{m} \sum_{j=1}^{N_e} \max(ETC_{ij}) \quad (8)$$

where K is the parameter of the deadline and maxETC_{ij} is the maximum value of the expected completion time of T_i on E_j. The parameter "K" may take on values such as 1, 2, 3, 4, and so forth. Here, we consider the value of K to be 2 [13] [22].

Migration Cost (MCt): Migration Cost refers to the overhead incurred when transferring a task or process from one computational resource (e.g., an edge or fog node) to another.

$$MCt(T_i) = \frac{W_i}{BW} \quad (9)$$

Completion Time (CT): The actual time taken for a task to finish execution on a specific resource.

$$CT_{ik} = MCt(T_i) + ETC_{ik} \quad (10)$$

Deadline Meet (DM): The extent to which tasks are completed within their specified deadlines [13] [21].

$$DM(T_i) = \begin{cases} 1 & \text{if } CT(T_i) \leq D(T_i) \\ 0 & \text{otherwise} \end{cases} \quad (11)$$

Turnaround Time (TAT): The total time taken from the submission of the task to its completion. Here, AT is the arrival time of the task. In this work, the arrival time of each task is considered zero.

$$TAT = CT - AT \quad (12)$$

3.3 Problem Statement

The objective is to minimize E_{total} while ensuring that all tasks T_i meet their respective deadlines D_i. subject to $\forall T_i, \quad ETC_i \leq D_i$

where the system ensures that each task T_i is executed within its deadline D_i. Energy-efficient task allocation strategies are applied to balance workload distribution across fog and edge layers.

4 Proposed E2DLB Algorithm

4.1 Algorithm Overview

In fog and edge computing environments, the E2DLB (Energy-Efficient Deadline-Aware Load Balancing) algorithm handles the scheduling and load balancing of BIoT tasks efficiently. Due to the energy limitations of edge devices and the latency sensitivity of various IoT applications, E2DLB dynamically assigns batches of tasks considering their ability to meet deadlines and available computational nodes in terms of energy efficiency. Keeping in view the common execution characteristics of task batches, the algorithm assigns urgent IoT tasks to nodes with sufficient processing power while maintaining energy consumption at a minimum and avoiding overloading. E2DLB strives to an extent wherein it prioritizes IoT task batches with respect to their deadlines and allocates them to nodes that offer the best compromise between energy efficiency and availability to enhance QoS and sustainability in distributed IoT systems.

4.2 Methodology and Algorithm Workflow

The E2DLB methodology comprises the following steps:

- **Batch Sorting:** All BIoT tasks are sorted in ascending order of their earliest task deadline.
- **Node Selection:** For each batch, identify a candidate node offering the best trade-off between energy efficiency and available capacity to execute all tasks in the batch within the deadline window.
- **Batch Assignment:** If the selected node satisfies both energy and deadline constraints, the batch is assigned. Otherwise, an alternate node is evaluated.
- **Deadline Verification and Batch Migration:** If the assigned node fails to meet the deadline during execution or becomes resource-constrained, the batch is migrated to a more suitable node based on an energy-aware cost-benefit analysis.
- **Final Allocation:** The process continues until all BIoT tasks are either assigned to an edge node or flagged for fog offloading or rescheduling if local execution is infeasible.

Algorithm: **E2DLB**

Input: T, E_j, F_k, W_i, CC_j, CC_k, K, E_{N_J}, E_{N_k}, N

Output: *EE, DM, TAT*

Begin:

1. **Initialize:** Compute ETC_{ij}, ETC_{ik}, EC_{ij}, EC_{ik}, D_i using equations (1), (3), and (8).
2. **Sort Tasks:** Sort tasks T in ascending order of deadline D_i.
3. **Use Mid-Point Selection Method:**
4. if o(T_m) (number of tasks) is odd:
5. T_{mid} = (o(T_m) + 1) / 2
6. Task Order: T_{mid}, T_{mid}-1, T_{mid}+1, T_{mid}-2, T_{mid}+2, ...
7. else:
8. T_{mid} = o(T_m) / 2
9. Task Order: T_{mid}, T_{mid}+1, T_{mid}-1, T_{mid}+2, T_{mid}-2, ...
10. **For each T_i in task order:**
11. Select edge node E_j with: Minimum EC_{ij}, $ETC_{ij} \leq D_i$, and Load(E_j) $\leq AL_{edge}$

12. if such E_j is found:
13. Assign T_i to E_j
14. Update Load(E_j)
15. else:
16. Select fog node F_k with: Minimum EC_{ik}, $ETC_{ik} \leq D_i$, and Load(F_k) $\leq AL_{fog}$
17. Compute MCt and CT using equations (9) and (10).
18. if ($CT_{ik} \leq D_i$)
19. Assign T_i to F_k
20. Update Load(F_k)
21. else:
22. Mark T_i for cloud offloading or rescheduling
23. Compute: E_{total} using equation (4) for all allocated tasks
24. Deadline Satisfaction: DM(T_i) = 1 if CT(T_i) ≤ D_i, else 0
25. Load Distribution across nodes
26. Return: Schedule, energy consumption, load per node, deadline satisfaction, TAT.

End

5 Simulation and Results

The suggested Energy Efficient Deadline Aware Load Balancing (E2DLB) Algorithm was tested in a simulated fog and edge computing environment. The simulation was run with different task sizes (100, 250, 500, and 1000) to evaluate Turnaround Time (TAT), Deadline Meet (DM), and Energy Efficiency (EE) performance. The findings were compared to three baseline algorithms: REAL [21], DCLB [22], and BALBA [23].

As shown in Figs. 2 to 4, all of the techniques under consideration are evaluated in this case by varying the number of tasks from 100 to 1000 while keeping the system's remaining input parameters constant. Ready Time (RT_j) = 1-100, Computing Capacity (E_j and F_k) = 1-100 (MIPS), W_i = 1-10,000 (MIs), and n = 16 are the additional input parameters. The results illustrated in Fig. 2 show the evaluation of energy efficiency under different task loads. The E2DLB algorithm consumes less energy than all of BALBA, DCLB, and REAL. As shown in Fig.2, when the no. of tasks increases, the energy consumption also increases in all considered algorithms with all instances. E2DLB algorithm has the best performance in terms of energy efficiency, the second performer is BALBA, the third performer is DCLB, and the worst performer is REAL. The reason behind of E2DLB algorithm is best performer because in each task allocation, in E2DLB algorithm targets the node that consumes the least energy. E2DLB first focuses on the minimum energy consumption node with deadline satisfaction, where either the TAT of that node is high. At all the task levels of 100, 250, 500, and 1000, the energy use under E2DLB is reduced on average by 13% over BALBA, more than 20% over DCLB, and up to 26.88% over REAL. Thus, the advantage is very consistent, implying that E2DLB is very scalable and energy-aware, hence making it most suitable for resource-constrained fog and edge computing environments. As the workload grows, E2DLB maintains its energy efficiency; thus, it may provide energy-efficient, sustainable, and cost-effective task execution.

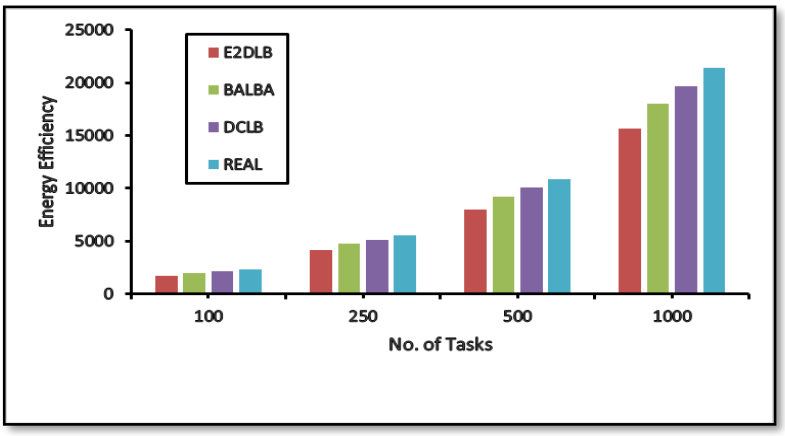

Fig. 2. Energy Efficiency Vs No. of Tasks

As shown in Fig. 3 that E2DLB continues its outstanding performance with increasing workloads as compared to other algorithms. While relatively similar performance is observed at 100 tasks, E2DLB quickly establishes its dominance in the higher counting range for deadline satisfactions over BALBA, DCLB, and especially REAL. It is interesting to note that E2DLB shows much improvement over REAL, with improvements of 45.68%, 53.82%, 27.70%, and 19.08%, for 100, 250, 500, and 1000 tasks, respectively. This truly attests to E2DLB's scalability and applicability towards deadline-oriented tasks in fog and edge computing environments.

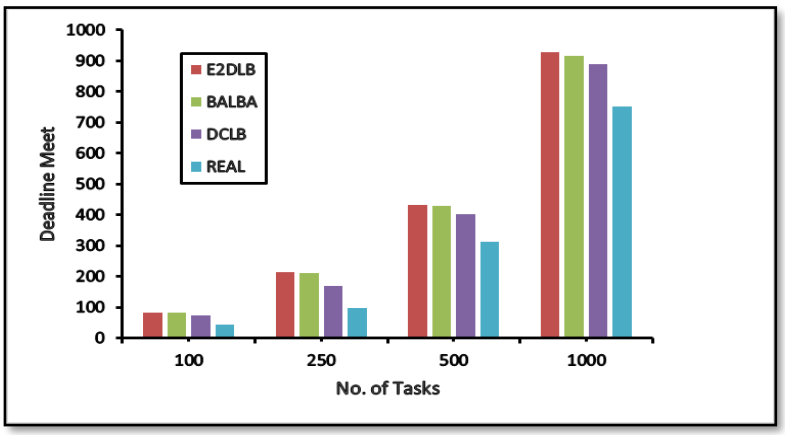

Fig. 3. Deadline Meet Vs No. of Tasks

As shown in Fig. 4, for 100 tasks, all algorithms show comparable turnaround times, with DCLB slightly outperforming the others. E2DLB, which is marginally higher than DCLB but almost equivalent to REAL and BALBA. The percentage improvement of

E2DLB over BALBA is minimal at -0.067%, indicating similar performance at low workloads. When workload increases to 250, 500, and 1000 tasks, E2DLB demonstrates lower turnaround times and improved efficiency. Here, it achieves up to 11.82% improvement over REAL at 250 tasks and maintains better performance under heavy loads with up to 1.77% gain over REAL and 1.62% over BALBA at 1000 tasks. These results confirm E2DLB's effectiveness in handling increasing task loads with better scalability and reduced turnaround time in fog and edge computing environments.

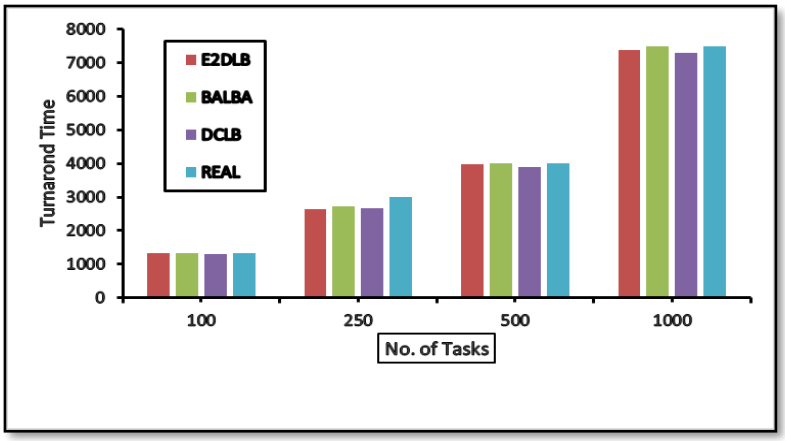

Fig. 4. Turnaround Time Vs No. of Tasks

Having evaluated on crucial metrics, including turnaround time, deadline satisfaction, and energy efficiency, the results show that the E2DLB algorithm performs best with fog and edge computing. While under heavier workloads, E2DLB fetches consistently lower turnaround times than baseline algorithms (BALBA, DCLB, and REAL). At 1000 tasks, a maximum improvement of 11.82% over REAL and 1.62% over BALBA was observed. It shows good scalability and low latency, which is very important for any real-time application.

When concerned with deadline meeting capability, E2DLB yields big improvements over all others, REAL in particular, enhancing task deadline satisfaction by up to 53.82%. This points out that it is well-suited to the task of meeting deadlines, a very important function in any edge computing situation, where operations are latency-critical. Most significantly, in the energy efficiency aspect, E2DLB shines, surpassing all the other algorithms, with energy savings averaging 13% over BALBA, beyond 20% versus DCLB, and as high as 26.88% compared to REAL. Energy-aware behavior just confirms the ability of E2DLB to equate performance with sustainability, thereby making it apt for constrained-resource and green-computing infrastructures.

The results altogether indicate the claim that E2DLB serves the fog and edge computing ecosystem as a robust, scalable, and energy-efficient balancing solution for load, thereby addressing in a satisfactory manner the problems pertaining to latency,

deadline compliance, and energy consumption in dynamic and distributed environments.

6 Conclusion and Future Work

This study presents E2DLB as a new algorithm for fog and edge computing environments, where one has to manage the trade-offs between energy efficiency and real-time responsiveness. E2DLB dynamically maps batches of IoT tasks based on energy usage and deadline criteria while continuously monitoring node loads and resource availability. The algorithm offers a multi-layer decision-making considering task classification, deadline evaluation, energy profiling, and adaptive migration to keep load distribution optimal. Simulation results show that E2DLB can outperform state-of-the-art algorithms, such as REAL, DCLB, and BALBA, on three crucial aspects: turnaround time, deadline satisfaction, and energy efficiency. Specifically, E2DLB reduces turnaround time up to 11.82%, improves deadline fulfilment by up to 53.82%, and saves energy up to 26.88% compared to other models. These performance gains are more substantial under massive workload scenarios, highlighting algorithm scalability and robustness when implemented in real-time distributed systems.

E2DLB offers a balanced and sustainable load balancing scheme that improves the overall QoS in fog and edge computing. With E2DLB being able to meet hard deadlines and conserve energy, it becomes perfect for latency-critical and resource-constrained applications such as smart healthcare, industrial IoT, and automated systems. Future work could treat E2DLB with reinforcement learning or deep learning models so as to adapt to changes in workload patterns and dynamic network conditions.

References

1. Mohammadi, R., Nazari, A., & Daneshmand, B. (2023, May). An efficient routing schema for internet of underwater things/ocean of things. In 2023, Wave Electronics and its Application in Information and Telecommunication Systems (WECONF) (pp. 1-8). IEEE.
2. Nazari, A., Tavassolian, F., Abbasi, M., Mohammadi, R., & Yaryab, P. (2022). An Intelligent SDN-Based Clustering Approach for Optimizing IoT Power Consumption in Smart Homes. Wireless Communications and Mobile Computing, 2022(1), 8783380.
3. Samadi, R., Nazari, A., & Seitz, J. (2023). Intelligent energy-aware routing protocol in mobile IoT networks based on SDN. IEEE Transactions on Green Communications and Networking, 7(4), 2093-2103.
4. Cisco, U. (2020). Cisco annual internet report (2018–2023) white paper. Cisco: San Jose, CA, USA, 10(1), 1-35.
5. Goudarzi, M., Wu, H., Palaniswami, M., & Buyya, R. (2020). An application placement technique for concurrent IoT applications in edge and fog computing environments. IEEE Transactions on Mobile Computing, 20(4), 1298-1311.
6. Garg, R., Mittal, M., & Son, L. H. (2019). Reliability and energy efficient workflow scheduling in cloud environment. Cluster Computing, 22(4), 1283-1297.

7. Mukhopadhyay, N., & Tewari, B. P. (2025). Cost and energy aware migration through dependency analysis of VM components in virtual cloud infrastructure. Computing, 107(1), 1-44.
8. Mahapatra, A., Majhi, S. K., Mishra, K., Pradhan, R., Rao, D. C., & Panda, S. K. (2024). An energy-aware task offloading and load balancing for latency-sensitive IoT applications in the Fog-Cloud continuum. IEEE Access, 12, 14334-14349.
9. Singhal, S., Athithan, S., Alomar, M. A., Kumar, R., Sharma, B., Srivastava, G., & Lin, J. C. W. (2023). Energy aware load balancing framework for smart grid using cloud and fog computing. Sensors, 23(7), 3488.
10. Saif, F. A., Latip, R., Hanapi, Z. M., Alrshah, M. A., & Kamarudin, S. (2023). Workload allocation toward energy consumption-delay trade-off in cloud-fog computing using multi-objective NPSO algorithm. IEEE Access, 11, 45393-45404.
11. Srivastava, V., & Kumar, R. (2025). Energy and Deadline Aware Workflow Scheduling using Adaptive Remora Optimization in Cloud Computing. Scalable Computing: Practice and Experience, 26(1), 490-502.
12. Zhang, T., Huang, R., Hu, Y., Li, Y., Zou, S., Zhang, Q., ... & Ruan, C. (2022). Load balancing with deadline-driven parallel data transmission in data center networks. IEEE Internet of Things Journal, 10(2), 1171-1191.
13. Haidri, R. A., Alam, M., Shahid, M., Prakash, S., & Sajid, M. (2022). A deadline aware load balancing strategy for cloud computing. Concurrency and Computation: Practice and Experience, 34(1), e6496.
14. Zhang, Y., Tang, B., Luo, J., & Zhang, J. (2022). Deadline-aware dynamic task scheduling in edge–cloud collaborative computing. Electronics, 11(15), 2464.
15. Gautam, S., & Malhotra, A. (2024). A Deadline-Aware Priority based Semi-Greedy Task Scheduling Technique in Fog Computing. In SCI (pp. 218-228).
16. Ghorbani, M., Khaledian, N., & Moazzami, S. (2025). ALBLA: an adaptive load balancing approach in edge-cloud networks utilizing learning automata. Computing, 107(1), 34.
17. Alam, M., Shahid, M., & Mustajab, S. (2023, October). A security driven energy efficient workflow allocation algorithm under deadline constraints for cloud computing. In 2023 4th International Conference on Data Analytics for Business and Industry (ICDABI) (pp. 331-336). IEEE.
18. Pakmehr, A., Gholipour, M., & Zeinali, E. (2024). ETFC: energy-efficient and deadline-aware task scheduling in fog computing. Sustainable Computing: Informatics and Systems, 43, 100988
19. Khaledian, N., Khamforoosh, K., Akraminejad, R., Abualigah, L., & Javaheri, D. (2024). An energy-efficient and deadline-aware workflow scheduling algorithm in the fog and cloud environment. Computing, 106(1), 109-137.
20. Alwabel, A., & Swain, C. K. (2024). Deadline and energy-aware application module placement in fog-cloud systems. IEEE Access, 12, 5284-5294.
21. Alam, M., Haidri, R. A., & Shahid, M. (2020). Resource-aware load balancing model for batch of tasks (BoT) with best fit migration policy on heterogeneous distributed computing systems. International Journal of Pervasive Computing and Communications, 16(2), 113-141.
22. Deepak, Upadhyay, M. K., & Alam, M. (2025). Deadline Constrained Based Load Balancing Algorithm for Batch of IoT Tasks on Fog and Edge Computing Environments. Iran Journal of Computer Science, 1-22.
23. Deepak, Upadhyay, M. K., & Alam, M. (2025). Budget Aware Load Balancing Algorithm with Strict Deadline Constraints for Efficient Resource Utilization in Fog and Edge Environments, Springer (In Press).

Detection of Opioids in Biological Matrices assisted by Magnetic Nanoparticles (MNPs): A Mini Review

Enas Amoori Hadi Hadi[1], Wijdan Shakir Khayoon[2], Loong Chuen Lee[3*]

[1] Forensic Science Program, CODTIS, Faculty of Health Sciences, Universiti Kebangsaan Malaysia
P148860@siswa.ukm.edu.my
[2]Department of Chemistry, College of Sciences, University of Baghdad, Iraq
wijdan.khayoon@sc.uobaghdad.edu.iq
[3*]Forensic Science Program, CODTIS, Faculty of Health Sciences, Universiti Kebangsaan Malaysia
Lc_lee@ukm.edu.my

Abstract. Detection and identification of drugs of abuse in biological matrices are vital to forensic toxicology. Preconcentration and isolation of the drug from the biologic matrix is essential step prior to detection via instrumental techniques. Recent advances in nano-based extraction technologies have opened new opportunities for enhancing the preparation of biological samples for forensic drug detection. Utilizing nanoparticles for microextraction makes it possible to achieve more effective and efficient extraction of drug residue and metabolites from the complex biological matrix. In particular, vast varieties of magnetic nanoparticles (MNPs) have been evaluated for preparing biological samples for a more accurate and sensitive drug detection. This mini review discusses applications of various MNPs for forensic drug detection, detailing their unique benefits against the conventional approaches. In further, future prospects of MNPs in drug analysis, especially in human body fluids were also proposed.

Keywords: Opioids; magnetic nanoparticles (MNPs); forensic toxicology; biological matrix

1 Introduction

Opioids refers to a class of narcotic analgesic that can be divided into: (a) natural (e.g., codeine, morphine), (b) semi-synthetic (e.g., diacetyl-morphine (heroin), hydrocodone, oxycodone), and (c) synthetic (e.g., fentanyl), according to their sources. Despite their therapeutic potentials in remediating pain among the patients, opioids are inherently additive (Cruz 2022). Consequently, abuse of these drugs is increased around the globe, and cause serious impacts on public health (e.g., elevated risks of infectious disease transmission), environmental protection, and social and economic growth. In particular, it is estimated around 209 million people around the world are using opioids in 2022. Hence, a fast, robust and accurate qualitative and quantitative determination of such drugs is essential in combating crimes associated with these drugs (Razlansari et al. 2022).

Timely surveillance of drug use trends typically performed examination on the biological samples obtained from the drug users. Such samples are characterized by complex matrix and low concentration of target analytes. In other words, the sample composes of variety of chemical compounds which also known as impurities on top of the traces of the drugs. In addition, instrumental techniques employed for detection are sensitive to all kinds of analytes available in the extracts. Hence, an effective extraction procedure is paramount to achieve high sensitivity and selectivity analysis by the analytical instruments (Garcia-Atienza et al. 2024).

Recent advancement in nanotechnologies leading to the use of nanomaterials as absorbent in microextraction techniques. Variety kinds of green and environmentally friendly nanomaterials-based extraction techniques are proposed for preparing traces of drugs from complicated biological samples (Gonzalez-Martin et al. 2022). Advantages of nanomaterials including large surface area, high adsorption capacity, and variety of functional groups. Among the nanomaterials available in the literature, magnetic nanoparticles (MNPs) emerge to the most promising options for extracting trace residue from complicated biological matrices, e.g., blood and urine.

Iron oxide NPs provides variety of desired properties, e.g., superparamgnetism, diamagnetism, and ferromagnetism, that are useful in biomedicine applications (Guo et al. 2021). Despite that, the unprotected metal oxide nanoparticles tend to form aggregates and react with oxygen present in the air, undergo rapid biodegradation when directly exposed to biological systems. Following that, it is proposed to add a coating on the magnetic nanoparticles, for resolving such limitations.

For instance, diversity of magnetic sorbents can be created by incorporating different functional groups to the silica coated on a magnetite core (Fe_3O_4/SiO_2). Alternatively, a magnetite core can also be coated with polymer (Fe_3O_4/polymer). Recently, mesoporous silica, an ordered network of pores homogenous in size, with high volume, specific surface area and stability has also been introduced to be coated on the magnetite core.

Solid-phase extraction or micro solid-phase extraction employing magnetic or magnetizable sorbents is respectively known as magnetic solid-phase extraction (MSPE) or micro magnetic solid-phase extraction (μMSPE). After extraction, the magnetic sorbents area readily be isolated from sample matrix with an external magnet (Li & Shi 2019).

Over the past few decades, a number of reviews have been published in relation to application of magnetic sorbents in extraction of target compounds. The recent applications of MCNTs in biomedical and industrial fields are reported by Samadishadlou et al. (2018). Meanwhile, Vasconcelos and Fernandes (2017) presented a comprehensive review on the development and application of magnetic solid phase extraction in determination of drugs in biological matrices. The synthesis of magnetic carbon nanotubes (MCNTs) for use in MSPE was also available (Herrero-Latorre et al. 2015).

Despite the reviews provided a critical evaluation and trends of the MNPs, the scopes of applications are in general but not specifically dedicated to extraction of opioids in biological matrices. Hence, current work resembling a mini review discussing applications of various MNPs for forensic drug detection, detailing their unique benefits against the conventional approaches. In further, future prospects of MNPs in drug analysis, especially in human body fluids were also proposed.

2 Related Work

Multitude of works have explored the potential of magnetic-based nanomaterials as sorbents in extracting drugs from biological samples. However, only a few are dedicated specifically to detection of opioids in biological matrices. Herein, the past works were discussed by types of magnetic adsorbents, detection methods and figure-of-merits achieved.

2.1 Adsorbents

Table 1 summarized the selected articles by classes of opioids, matrices and types of magnetic adsorbents. Overall, magnetic molecularly imprinted polymer (MMIP) were the most reported types of magnetic adsorbents for extracting opioids in biological samples (e.g., Xi et al. 2016, Ebrahimi Rahmani et al. 2018). Next, magnetic nano particles (MNPs) appeared to the second most studied magnetic absorbents in this context (Baciu et al. 2016, Kolaei et al. 2016, Schwarz et al. 2024, Yang et al. 2017). Three of the shortlisted works employed magnetic nanocomposites, i.e., MCNTs (Soltani et al. 2018), CNTs (Sahragard et al. 2023), and Fe_3O_4/rGO/Ag nanocomposites (Abdolmohammad-Zadeh et al. 2019).

Table 1. Selected works evaluating various kinds of MNPs for extracting opioids in biological matrices

Opioids (References)	**Matrices**	**MNPs (Extraction method)**
COC, COD, MTD, MOR (Baciu et al. 2016)	Urine	C_{18}-FS-Fe_3O_4 particles (MSPE)
COD, MOR (Soltani et al. 2018)	Urine, blood	MCNTs nanocomposite (MSPE)
COD, MOR (Abdolmohammad-Zadeh et al. 2019)	Urine, blood	Fe_3O_4/rGO/Ag nanocomposite (MSPE)
MOR (Xi et al. 2016)	Urine	MMIP (MSPE)
MOR (Kolaei et al. 2016)	Urine	MWCNTs-Fe_3O_4-NPs@MO-MIP (US-MSPE)
MOR (Ebrahimi Rahmani et al. 2018)	Urine, blood	Fe_3O_4/SiO_2-NH_2@MIP (MSPE)
COC (Schwarz et al. 2024)	Blood	MNPs (MdSPE)
COC (Sahragard et al. 2023)	Urine	CNTs (EME)
COC (Sanchez-Gonzalez et al. 2016a)	Plasma	MMIP (μ-SPE)
COC (Sanchez-Gonzalez et al. 2016b)	Urine	MMIP (SPE)
COC (Sorribes-Soriano et al. 2018)	Saliva	MMIP (MSPE)
COC (Yang et al. 2017)	Urine	DVP+VP@SMPS@Fe_3O_4NPs (MdSPE)

Magnetic carbon nanotubes (MCNTs), magnetic nanoparticles immobilized divinyl benzene & vinyl pyrrolidone on SiO_2 surface (DVP+VP@SMPS@Fe_3O_4NPs), magnetic solid phase extraction (MSPE), cocaine (COC), codeine (COD), methadone (MTD), morphine (MOR), silica (C_{18}), magnetic dispersive solid-phase extraction (MdSPE), Magnetic nanoparticles (MNPs), electro membrane extraction (EME), magnetic reduced graphene oxide argentum (Fe_3O_4/rGO/Ag), magnetic molecularly imprinted polymer (MMIP), multiwalled carbon nanotubes magnetized with Fe3O4 nanoparticles and coated with vinyltrimethoxysilane-morphine molecularly imprinted polymer (MWCNTs-Fe_3O_4-NPs@MO-MIP), ultrasonic-assisted magnetic solid phase extraction (US-MSPE), magnetic aminosilica morphine imprinted polymers (Fe_3O_4/SiO_2-NH_2@MIP), micro-solid phase extraction (μ-SPE), solid phase extraction (SPE)

Magnetic molecularly imprinted polymer (MMIP) is extended from the molecularly imprinted polymers (MIPs) that are recognized as highly selective materials for a small group of compounds (the compound used as a template molecule during the MIP synthesis and other structurally similar analogues). By making the core of MIPs magnetic, the composite core-shell can be easily separated from the bulk sample and extracted by magnet. Sanchez-Gonzalez et al. (2016a) proposed a fast and quantitative isolation of COC and metabolites from plasma via magnetic Fe_3O_4-MIP (MMIP) particles with uniform core-shell. Synthesis of the MMIP was performed using COC as template and ethylene glycol dimethacrylate (EGDMA) as monomer. Meanwhile, for extracting COC and metabolite in urine, Sanchez-Gonzalez et al. (2016b) synthesized MIP using COC as a template, ethylene dimethacrylate (EDMA) as a monomer, divinylbenzene-80 (DVB) as a cross-linker, and 2,2'-azobisisobutyronitrile (AINB) as an initiator.

Similarly, Ebrahimi Rahmani et al. (2017) also used AIBN and EGDMA in preparing the core-shell magnetic molecularly imprinted polymer in which morphine as used as a template as the target compound was morphine from biological fluids. Kolaei et al. (2016) prepared multiwalled carbon nanotubes (MWCNTs) that were magnetized with Fe_3O_4 nanoparticles (MWCNTs-Fe_3O_4-NPs) and coated with vinyl end groups (Vinyltrimethoxysilane) as a support for a MO molecularly imprinted polymer (MWCNTs-Fe_3O_4-NPs@MO-MIP). They deployed the surface imprinting polymerization method. The MO was used as template, and methacrylic acid (MAA) as functional monomer. Both AIBN and EGDMA were also required for executing the surface imprinting method.

Abdolmohammad-Zadeha et al. (2019) suggested procedures to synthesize Fe_3O_4/rGO/Ag nanocomposite for preconcentration of MOR and COD. Reduced graphene (rGO) was chosen for fabrication of the inorganic nanoparticles (i.e., Fe_3O_4). By this, a novel hybrid environment was created accelerating dispersion of the NPs.

Meanwhile, Schwarn et al. (2024) did not synthesized the Fe_3O_4 magnetic nanoparticles but purchasing from Merch®. Nonetheless, Yang et al. (2017) suggested to improve the magnetic nanoparticles by additional treatment. The magnetic nanoparticles were coated by the macromolecular polymer, herein the SiO_2 film. Such way allowed the surface modification of the magnetic nanoparticles via divinyl benzene (DVB) and vinyl pyrrolidone (VP). The setting created a hydrophobic chain and a heterocycle causing rapid partitioning of target analytes on the surface of DVB and VP.

2.2 Detection Methods

In general, chromatographic techniques were the most established approach for detecting opioids extracted from a biological sample. In particular, liquid chromatography including liquid chromatography, high-performance liquid chromatography and ultra-high performance liquid chromatography, are the most reported options (Table 2). This is followed by the use of capillary electrophoresis and ion mobility spectrometry as well as UV-vis spectrophotometer.

Table 2. Detection methods employed for determination of kinds of opioids extracted from biological samples via magnetic adsorbents

Opioids (References)	Matrices	Detection methods
COC, COD, MTD, MOR (Baciu et al. 2016)	Urine	CE (in-line)
COD, MOR (Soltani et al. 2018)	Urine, blood	HPLC
COD, MOR (Abdolmohammd-Zadeh et al. 2019)	Urine, blood	HPLC
MOR (Xi et al. 2016)	Urine	HPLC
MOR (Kolaei et al. 2016)	Urine	UV-vis spectrophotometer
MOR (Ebrahimi Rahmani et al. 2018)	Urine, blood	UHPLC
COC (Schwarz et al. 2024)	Blood	LC-MS/MS
COC (Sahragard et al. 2023)	Urine	CE
COC (Sanchez-Gonzalez et al. 2016a)	Plasma	HPLC-MS/MS
COC (Sanchez-Gonzalez et al. 2016b)	Urine	HPLC-MS/MS
COC (Sorribes-Soriano et al. 2018)	Saliva	Ion mobility spectrometry
COC (Yang et al. 2017)	Urine	HPLC-MS

Capillary electrophoresis (CE), high-performance liquid chromatography (HPLC), ultra-high performance liquid chromatography (UHPLC), liquid chromatography-tandem mass spectrometry (LC-MS/MS), high performance liquid chromatography-mass spectrometry (HPLC-MS), high performance liquid chromatography-tandem mass spectrometry (HPLC-MS/MS)

2.3 Figure-of-merit

Table 3 summarizes the key figure-of-merit achieved by the shortlisted articles. Overall, the three most studied types of opioids are cocaine (COC), codeine (COD), and morphine (MOR).

The most desired LOD values for extracting COD and MOR were reported by Abdolmohammad-Zadeh et al. 2019). They deployed Fe_3O_4/rGO/Ag nanocomposite for extracting both COD and MOR present in urine/blood concurrently before detection via HPLC. It is worth noting that magnetic absorbent incorporated with MIP (i.e.,

Ebrahimi Rahmani et al. 2018, Kolaei et al. 2016, Xi et al. 2016) has not outperformed that proposed by Abdolmohammad-Zadeh et al. (2019).

Meanwhile, protocols suggested by Sanchez-Gonzalez et al. (2016a) achieved the lowest LOD value for COC. Although majority of the studies considered MMIP as adsorbent, Sanchez-Gonzalez et al. (2016a) employed a micro-solid phase extraction method. Moreover, protocols applied in synthesizing the MMIP could also play a role in determining performance of the adsorbent.

Table 3. Figure-of-merit achieved for extracting opioids in biological samples via MNPs

Opioids (References)	**Figure-of-merit**
COC, COD, MTD, MOR (Baciu et al. 2016)	LOD: 0.5-20 ng/mL (standards), 20-50 ng/mL (urine) Precision: RSDs<20%; Recovery: 75.9%
COD, MOR (Soltani et al. 2018)	LOD: 0.9 ng/mL (COD), 0.8 ng/mL (MOR) Precision: <5% (COD), <10% (MOR)
COD, MOR (Abdolmo-hammd-Zadeh et al. 2019)	**LOD: 0.0021 ng/mL (COD), 0.0018 ng/mL (MOR)** Precision: 1.02-5.10%; Recovery: 102.5% (COD), 97.0% (MOR)
MOR (Xi et al. 2016)	Precision: 1.07-3.72%; Accuracy: 83.62-100.37%
MOR (Kolaei et al. 2016)	LOD: 180 ng/mL; Precision: <2.32%; Recovery: 96.40-105.6%
MOR (Ebrahimi Rahmani et al. 2018)	Recovery: 84.9-105.5% (plasma), 94.9-102.8% (urine) Precision: 2.8-4.9% (plasma), 1.7-3.3% (urine)
COC (Schwarz et al. 2024)	LOQ: 16 ng/mL; Precision: <10%
COC (Sahragard et al. 2023)	LOD: 2.12 ng/mL; Precision <5%; Recovery: 89%
COC (Sanchez-Gonzalez et al. 2016a)	**LOD: 0.000013-0.00036 ng/mL**; **LOQ: 0.00043-0.0012 ng/mL** Precision: <10%; Recovery: 91-102%
COC (Sanchez-Gonzalez et al. 2016b)	LOD: 0.00038-0.0014 ng/mL; Precision: <11% Recovery: 79-106%
COC (Sorribes-Soriano et al. 2018)	LOD: 4000 ng/mL; LOQ: 14000 ng/mL; Recovery: 80-99%
COC (Yang et al. 2017)	LOD: 0.09-1.10 ng/mL; Recovery: 75.1-105.7%

3 Conclusion and Future Work

In conclusion, various types of magnetic nano adsorbents have been evaluated for extracting opioids, in particular, morphine, codeine, and cocaine, from biological samples. To sum up, morphine and codeine are best be extracted via magnetic nanocomposites (NCs) instead of MMIPs; meanwhile, cocaine is more suitable be extracted using MMIPs. Regardless of the type of magnetic nano adsorbents, all allow more efficient and effective extraction compared to conventional approaches.

Future work can be attempted on proposing magnetic nano adsorbents allowing simultaneous preconcentration of morphine, codeine and cocaine, from biological matrices. In particular, NCs shall be prioritized over other kind of magnetic nano adsorbents. In addition, preparation of multi-template MMIPs could also be a feasible alternative (Surapong et al. 2022).

Acknowledgement

Enas Amoori Hadi Hadi gratefully acknowledges the scholarship sponsorship from the Iraq's government for supporting her PhD study at Universiti Kebangsaan Malaysia (UKM), Malaysia.

References

1. Abdolmohammad-Zadeh, H., Zamani, A., Shamsi, Z.: Preconcentration of morphine and codeine using a magnetite/reduced graphene oxide/silver nano-composite and their determination by high-performance liquid chromatography. Journal of Chromatography A 1590:2-9 (2019).
2. Baciu, T., Borrull, F., NeusuB, C., Aguilar, C., Calull, M.: Capillary electrophoresis combined in-line with solid-phase extraction using magnetic particles as new adsorbents for the determination of drugs of abuse in human urine. Electrophoresis 37: 1232-1244 (2016).
3. Cruz, S.L.: Opioids: Pharmacology, Abuse, and Addiction. Springer Cham (2023).
4. Ebrahimi Rahmani, M., Ansari, M., Kazemipour, M., Nateghi, M.: Selective extraction of morphine from biological fluids by magnetic molecularly imprinted polymers and determination using UHPLC with diode array detection. J. Sep. Sci. 41: 958-965 (2018).
5. El-Deen, A.K., Hussain, C.M.: Magnetic analytical extractions of forensic samples: Latest developments and future perspectives. Trends in Environmental Analytical Chemistry 39: e00209 (2023).
6. Garcia-Atienza, P., Martinez-Perez-Cejuela, H., Herrero-Martinez, J.M., Armenta, S.: Current trends in the sorbent-based extraction of illegal drugs from biofluids: Solid sorbents and configurations. Trends in Analytical Chemistry 172: 117599 (2024).
7. Gonzalez-Martin, R., Lodoso-Ruiz, E., Trujillo-Rodriguez, M.J., Pino, V.: Magnetic ionic liquids in analytical microextraction: A tutorial review. Journal of Chromatography A. 1685: 463577 (2022).
8. Guo, J., Jiang, H., Teng, Y., Xiong, Y., Chen, Z., You, L., Xiao, D.: Recent advances in magnetic carbon nanotubes: synthesis, challenges and highlighted applications. Journal of Materials Chemistry B 9:9076-9099 (2021).

9. Herrero-Latorre, C., Barciela-Garcia, J., Garcia-Martin, S., Pena-Crecenta, R.M., Otarola-Jimenez, J.: Magnetic solid-phase extraction using carbon nanotubes as sorbents: A review. Analytical Chimica Acta 892: 10-26 (2015).
10. Kolaei, M., Dashtian, K., Rafiee, Z., Ghaedi, M.: Ultrasonic-assisted magnetic solid phase extraction of morphine in urine samples by new imprinted polymer-supported on MWCNT-Fe3O4-NPs: central composite design optimization. Ultrasonic Sonochemistry 33: 204-248 (2016).
11. Li, W-k., Shi, Y-p.: Recent advances and applications of carbon nanotubes based composites in magnetic solid-phase extraction. Trends in Analytical Chemistry 118: 652-665 (2019).
12. Razlansari, M., Ulucan-Karnak, F., Kahrizi, M., Mirinejad, S., Sargazi, S., Mishra, S., Rahdar, A., Diez-Pascual, A.M.: Nanobiosensors for detection of opioids: A review of latest advancements. European Journal of Pharmaceutics and Biopharmaceutics. 179: 79-94 (2022).
13. Sahragard, A., Fakhari, A.R., Hasheminasab, K.S., Aladaghlo, Z.: Application of carbon nanotubes assisted electromembrane extraction technique followed with capillary electrophoresis for sensitive determination of cocaine in wastewater and biological samplas. Journal of the Iranian Chemical Society 20: 37-46 (2023).
14. Samadishadlou, M., Farshbaf, M., Annabi, N., Kavetskyy, T., Khalilov, R., Saghfi, S., Akbarzadeh, A., Mousavi, S.: Magnetic carbon nanotubes: preparation, physical properties, and applications in biomedicine. Artificial Cells, Nanomedicine and Biotechnology 46(7): 1314-1330 (2018).
15. Sanchez-Gonzalez, J., Barreiro-Grille, T., Cabarcos, P., Tabernero, M.J., Bermejo-Barrera, P., Moreda-Pineiro, A.: Magnetic molecularly imprinted polymer based micro-solid phase extraction of cocaine and metabolites in plasma followed by high performance liquid chromatography – tandem mass spectrometry. Microchemical Journal 127: 206-212 (2016a).
16. Sanchez-Gonzalez, J., Jesus Tabernero, M., Maria Bermejo, A., Bermejo-Barrera, P., Moreda-Pineiro, A.: Development of magnetic molecularly imprinted polymers for solid phase extraction of cocaine and metabolites in urine before high performance liquid chromatography-tandem mass spectrometry. Talanta 147: 641-649 (2016b).
17. Schwarz, P. de S., dos Santos, B.P., Birk, L., Eller, S., de Oliveira, T.F.: Development of an innovative analytical method for forensic detection of cocaine, antidepressants, and metabolites in postmortem blood using magnetic nanoparticles. Analytical and Bioanalytical Chemistry 416: 3239-3250 (2024).
18. Sorribes-Soriano, A., Esteve-Turrillas, F.A., Armenta, S., Montoya, A., Herrero-Martinez, J.M., de la Guardia, M.: Magnetic molecularly imprinted polymers for the selective determination of cocaine by ion mobility spectrometry. Journal of Chromatography A. 1545: 22-31 (2018).
19. Surapong, N., Santaladchaiyakit, Y., Burakham, R.: A water-compatible magnetic dual-template molecularly imprinted polymer fabricated from a ternary biobased deep eutectic solvent for the selective enrichment of organophosphorus in fruits and vegetables. Food Chemistry. 384: 132475 (2022).
20. Vasconcelos, I., Fernandes, C.: Magnetic solid phase extraction for determination of drugs in biological matrices. Trends in Analytical Chemistry 89: 41-52 (2017).
21. Xi, S., Zhang, K., Xiao, D., He, H.: Computational-aided design of magnetic ultra-thin dummy molecularly imprinted polymer for selective extraction and determination of morphine from urine by high-performance liquid chromatography. J. Chromatography A. 1473: 1-9 (2016).
22. Yang, F., Zou, Y., Ni, C., Wang, R., Wu, M., Liang, C., Zhang, J., Yuan, X., Liu, W.: Magnetic dispersive solid-phase extraction based on modified magnetic nanoparticles for the

detection of cocaine and cocaine metabolites in human urine by high-performance liquid chromatography-mass spectrometry. J. Sep. Sci. 40: 4234-4245 (2017).

Forensic Evaluation of Morphometric Variations of Handwritten Numerals Among Chinese-Literate Malaysian Chinese using Self-Organizing Maps (SOMs)

Bi Jia Loh[1], Hukil Sino[2] and Loong Chuen Lee*3[0000-0002-3144-9877]

[1] Forensic Science Program, CODTIS, Faculty of Health Sciences, Universiti Kebangsaan Malaysia, Bangi, 43600 Malaysia
a176436@siswa.ukm.edu.my

[2] Forensic Science Program, CODTIS, Faculty of Health Sciences, Universiti Kebangsaan Malaysia, Bangi, 43600 Malaysia
hukilsino@ukm.edu.my

[3] Forensic Science Program, CODTIS, Faculty of Health Sciences, Universiti Kebangsaan Malaysia, Bangi, 43600 Malaysia
Lc_lee@ukm.edu.my

Abstract. Forensic document examination aims to determine the authorship or authenticity of a questioned document. Typically, determining authorship of handwriting relies on comparison analysis in which known samples prepared by a suspect are needed. Nonetheless, in real-world scenarios, the suspect is seldom presented together with the questioned document. Recent work demonstrated that the educational background of writers potentially affected their handwriting styles. Hence, this work aims to evaluate morphometric feature variations of handwritten numerals among Malaysian Chinese. The handwritten numerals (i.e., 0 to 9) prepared by five Malaysian Chinese who have completed Chinese primary education were examined according to various morphometric features. Each subject was required to write the numerals on white copy papers six times per day over 14 days. Eventually, 34 different morphometric features were identified from the ten numerals and measured via a digital microscope. Prior to statistical analysis, the measurement values were normalized to minimize variation caused by the inconsistent size of the handwritten numerals. Self-organizing maps (SOMs) revealed that each subject was associated with varying intra-subject variations, and a few numerals showed distinct variations among the subjects. According to the SOM plots, numerals 0, 1 and 2 seem to be unique among the five subjects. In conclusion, numerals 0, 1 and 2 can be useful in discriminating Malaysian Chinese. The insights of morphometric variability of handwritten numerals could contribute to the classification of writers by ethnic group in Malaysia.

Keywords: Morphometric analysis, handwritten numerals, self-organizing maps (SOMs), forensic handwriting analysis, Malaysian Chinese

1 Introduction

Forensic document examination aims to determine the authorship or authenticity of a questioned document. For this purpose, typically, handwriting found on the questioned document can be compared against a set of exemplars to determine if the same author has prepared the two documents. In fact, handwriting has been established to be unique by individuals, and even identical twins do not have the same handwriting [1]. However, authorship identification requires a set of known samples with sufficient unique features. In other words, a questioned document submitted without a suspect cannot be studied for authorship. Nonetheless, it seems sound if the forensic analysis could narrow down the search of suspects to an ethnic group or nationality based on the handwriting of a questioned document.

In recent years, multiple efforts have been devoted to evaluating the feasibility of discriminating ethnicity according to features extracted from handwritten numerals. For instance, Al-Omari et al. [2] evaluated handwritten Indian (Arabic) numerals one to nine (1-9) by using an automatic recognition system. Meanwhile, Ahamed et al. [3] assessed the recognition of handwritten Arabic numerals by using a convolutional neural network. Daood et al. [4] applied deep learning models in assessing the discriminative capability of Arabic letters/numbers in various forms for authorship determination. Nasir and Uddin [5] considered various kinds of local and global deformations, e.g., distortions, thickness variations, etc., in recognizing handwritten Bangla numerals. All the studies demonstrated that handwritten numerals are valuable in identifying authorship and vary among ethnicities.

A few works focused on evaluating variations of handwritten numeral characters among Malaysians. Taufek et al. [6] applied the Geometric Morphometric (GMM) technique to elucidate inter-ethnicity variations of handwritten numerals. They reported that handwritten numeral characters are valuable for discriminating Malaysian writers into Malay, Chinese and Indian. On the other hand, Gannetion et al. [7] explored handwritten allographic features of handwriting samples among 30 Malaysians from four different educational backgrounds (i.e., national schools, Chinese-medium vernacular schools, Tamil-medium vernacular schools, and Islamic religious schools). Results showed that thirteen allographic features were highly discriminative. Meanwhile, Nasrul [8] also applied the GMM technique in evaluating the discriminative capability of a few handwritten numerals collected from ten Malaysians. The findings indicated that the numeral ’6’ was highly discriminative.

This work aims to extend the understanding of our previous work, which evaluated geometric variations of handwritten numerals among Malaysian Malay [9]. A number of morphometric features were identified for the numeral ‘0’ to ‘9’ and measured via a digital microscope. Then, the primary data was normalized before exploring via the self-organizing maps (SOMs) method to reveal inter- and intra-subject variations for forensic investigation purposes. Herein, Chinese-Literate Malaysian Chinese were selected as subjects for preparing a sufficient number of handwritten numerals. The insights would further enhance the understanding of inter-subject variations among Malaysians by ethnicity.

2 Methodology

2.1 Data Collection

Table 1 shows the background details of the five volunteers who contributed handwritten numerals to the study. All the subjects fulfilled the inclusion factors: (a) accomplished primary education at Chinese-medium vernacular schools, (b) Malaysian and (c) right-handed.

Table 1. Background details of the five subjects.

ID	Age	Higher Academic Qualification	Occupation
S1	23	Degree	Student
S2	26	Degree	School teacher
S3	23	Degree	Student
S4	23	Degree	Student
S5	58	Pre-University	Housewife

All the subjects were provided with a set of materials, which included the same type of paper (IK Yellow, white copy paper, 70gsm, 210mmx297mm) and two pens (black gel pen, Test Good, 0.5mm). They were required to continuously write numbers 0 to 9 six times a day over 14 days. Eventually, each subject prepared 840 numerals (10 numerals × 6 sets per day × 14 days) on various sheets of paper. All the papers were labelled by the author and kept in separate plastic folders.

In order to ensure an objective comparison, all the morphometric features shall be normalized. Hence, at least two morphometric features were measured from each numeral with the assistance of a digital microscope (DINO-LITE Handheld Microscope USB 2.0, AMA4515-ZT-EDGE). Fig. 1 illustrates the selected morphometric features considered in this study, which were adapted from our previous work (Lee et al. 2023). In order to minimize measurement bias, all measurements were initiated at either the outermost or innermost line of the ink entry, in which the distance shall be maximum. The feature that is absent was labelled as a missing value and assigned with ‘NA’.

2.2 Data Analysis

The morphometric measurements were first arranged as a matrix by the five authors. Each of the matrices is composed of 840 rows (i.e., numerals) and 33 features (i.e., morphometric measurements). Prior to statistical analysis, all the data matrices were combined by row. Any missing values were processed with the mean imputation method. Then, the 33 features were converted into ratios to minimize variations caused by the inconsistent absolute size of the handwritten numerals. Last but not least, the resulting 44 normalized features were modelled via a self-organizing maps (SOMs) algorithm to reveal the inter- and intra-subject variations.

SOMs also referred to as Kohonen maps, can be applied via supervised or unsupervised learning approaches. Herein, the unsupervised SOMs algorithm was chosen to

explore the variability of the morphometric features. The algorithm deploys competitive learning in revealing any patterns or relationships in the data by two-dimensional plots. The relative distance among the samples in the plots denotes the similarity and dissimilarity projected by the features. All the statistical analyses were completed in the R software (version 4.2.2) [10].

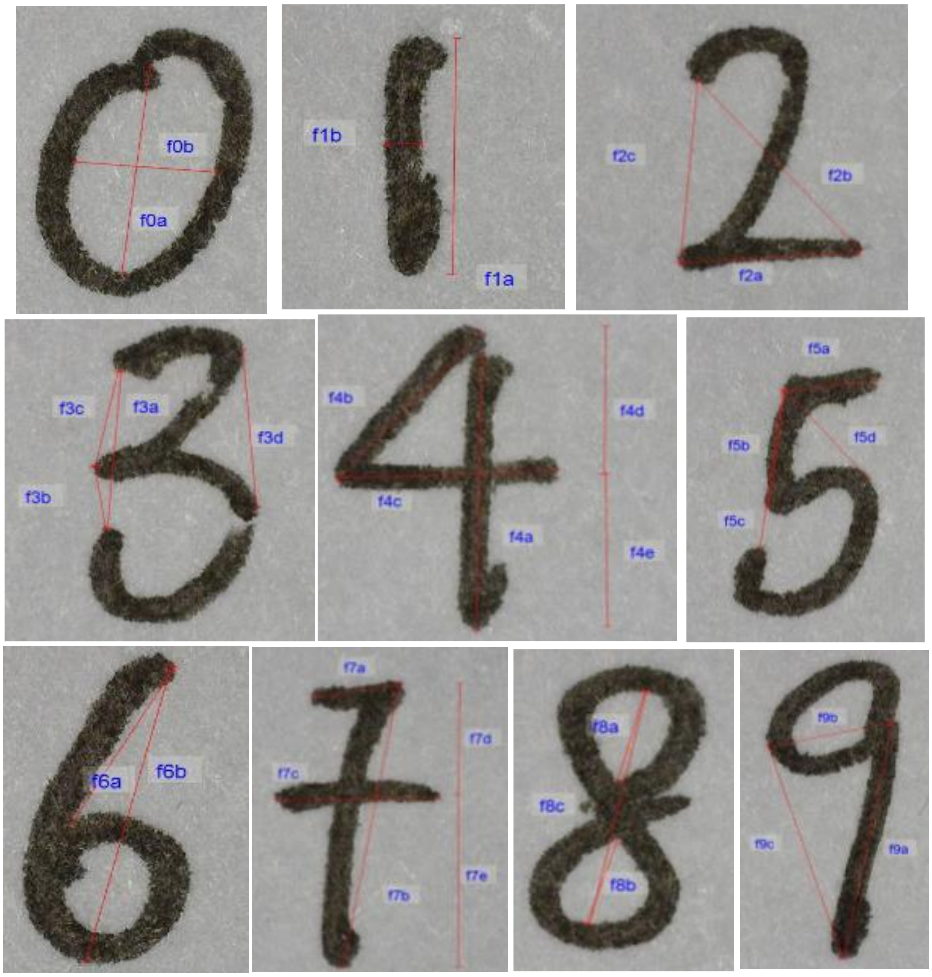

Fig. 1. Morphometric features measured for numeral ‘0’ to ‘9’. All the measurements were accomplished via a digital microscope.

3 Results

Based on SOMs analysis, only a few morphometric features demonstrated satisfactory inter-subject variations. The majority of features are associated with varying intra-subject variations and seldom clustered by the authorship. Fig. 2 illustrates the mapping plot and SOM plots estimated using the features of numerals '0'. '1' and '2'. SOMs outputs of the other features were not shown here due to inferior clustering results.

As seen in Fig. 2 (a), three of the four subjects were clustered by distinct nodes, i.e., subjects 1, 2, and 3. Meanwhile, subjects 4 and 5 seem to be undifferentiated from each other and dominated in two different nodes. Overall, subject S1 appeared to be most unique as it showed the lowest intra-subject variations. Similarly, subject S2 also dominated one of the six nodes and was associated with relatively low intra-subject variation. On the contrary, subject S3 is distributed into two different nodes, denoting a relatively high intra-subject variation. Two of the six nodes were dominated by subjects S4 and S5, which were highly similar to each other.

By inspecting the respective SOM plots (Fig. 2b), one can see that the numeral '2' written by subject S1 was distinct from the other writers. Meanwhile, the numeral '1' written by subject S2 was distinguishable from other writers. On the other hand, the numeral '0' written by subject S3 was more unique than that seen in other writers. It is worth noting that subjects S4 and S5 are undifferentiated from each other, and the morphometric of numeral '0', '1' and '2' prepared by them were not unique and similar to each other.

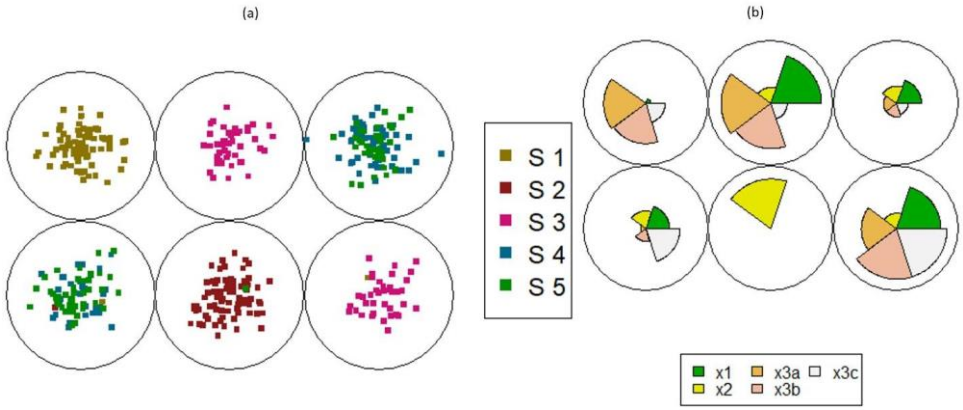

Fig. 2. Mapping plots (a) and SOM plots (b) estimated using normalized morphometric features of numeral 0 (x1), 1 (x2) and 2 (x3a, x3b and x3c).

4 Discussion

In the context of Malaysia, the primary education system is composed of three main streams, i.e., national schools, Chinese-medium vernacular schools, Tamil-medium vernacular schools, and Islamic religious schools [7]. The students are required to learn

Chinese, Tamil, and Arabic languages, which are different in structures and formation of the writings. Consequently, it seems sound to hypothesize that Malaysians could potentially be discriminated by ethnicity, which followed different primary school learning systems.

The hypothesis is supported by comparing the findings presented by previous works considering different groups of Malaysians. Current work demonstrated that Malaysian Chinese could be discriminated based on the numeral '0', '1' and '2'. Meanwhile, Lee et al. [9] concluded that the numeral 0, 1, 2, 4, 5 and 6 demonstrated good potential to discriminate Malaysian Malays. However, Nasrul [8] reported that Malaysians could be unique according to geometric morphometric features of the numeral '6'. Such discrepancy could be due to the variations deployed in the acquisition of the subjects. Nasrul [8] has not considered the primary education background of the subjects. In other words, the difference observed could be attributed to the primary education background of the subjects.

Next, findings reported in this work indicated occupation and family relationships could explain the high consistency in handwritten numeral features.

Based on the results above, one can see that subject S2 was the most readily discriminated from other writers. This could be due to the occupation of the subject who is actually a primary school teacher for multiple years. It has been known that a frequent writer tends to form consistent writing and thus shows relatively lower intra-subject variation [11]. According to a survey performed among school teachers in Malaysia, a teacher normally has to write on a blackboard or whiteboard over the 17 hours of teaching each week [12]. The long hours of writing among the teachers resulted in a more consistent writing pattern.

Meanwhile, both subjects S4 and S5 being undifferentiated according to handwritten numerals could be due to their familial relationship. Porac et al. [13] reported that family members might own similar handwriting due to the fact that genetic components play a role in the development of handwriting posture and, thus, handwriting.

It is important to emphasize that the generalization of the findings could be limited by the number of subjects considered in this study. Moreover, Gerth et al. [14] once emphasized that variation in writing substrates and pens could introduce additional variations into handwriting. Hence, this work provided the same type of paper and paper to all the subjects, aiming to reduce the variation not inherent in the writing habits of the writer.

5 Conclusion

In conclusion, current work demonstrated that Malaysian Chinese could be discriminated based on the handwritten numeral '0'. '1' and '2'. In particular, familial relationships and occupation could play a vital role in shaping the uniqueness of handwriting. Last but not least, despite the dataset being rather small, the insights provided herein could be further extended by considering more subjects in future work.

Acknowledgement

Loong Chuen Lee gratefully acknowledges the financial support of CRIM, Universiti Kebangsaan Malaysia (UKM) through Geran Ganjaran [GP-K016373]. The authors are thankful to all the subjects who volunteered in this study.

References

1. Srihari, S., Huang, C., Srinivasan, H.: On the discriminability of the handwriting of twins. Journal of Forensic Sciences 53(2), 430-446 (2008).
2. Al-Omari, F.: Handwritten Indian numeral recognition system using template matching approaches. In: Proceedings ACS/IEEE International Conference on Computer Systems and Applications, pp. 83-88. Beirut, Lebanon (2001).
3. Ahamed, P., Kundu, S., Khan, T., Bhateja, V., Sarkar, R., Mollah, A. F.: Handwritten Arabic numerals recognition using convolutional neural network. Journal of Ambient Intelligence and Humanized Computing 11(11), 5445-5457 (2020).
4. Daood, A., Al-Saegh, A., Mahmood, A.F.: Handwriting detection and recognition of Arabic numbers and characters using deep learning methods. Journal of Engineering Science and Technology 18(3), 1581-1598 (2023).
5. Nasir, M. K., Uddin, M.S.: Handwritten Bangla numerals recognition for automated postal system. IOSR Journal of Computer Engineering (IOSR-JCE) 8(6), 43-48 (2013).
6. Taufek, W.N.S.W.M., Pritam, H.M.H., Mat Desa, W.N.S., Ismail, D., Mahat, N.A.: Geometric Morphometric and pattern discrimination of handwritten numeral characters based on local ethnicities and native linguistic disparities in Malaysia for forensic applications. Malaysian Journal of Fundamental and Applied Sciences 20, 1068-1082 (2024).
7. Gannetion, L., Wong, K.Y., Lim, P.Y., Chang, K.H., Abdullah, A.F.L.: An exploratory study on the handwritten allographic features of multi-ethnic population with different educational backgrounds. PLoS ONE 17(10): e0268756 (2022).
8. Nasrul H.: Classification of individuals using handwritten numeral with geometric morphometric techniques. Master's thesis, Universiti Sains Malaysia (2020).
9. Lee, L.C., Nur Fatin S., Hukil S.: Evaluating Morphometric Feature Variability Of Handwritten Numerals Among Malaysian Malays Using Self-Organizing Maps. In: 3rd International Conference on Artificial Intelligence: Advances and Applications (ICAIAA 2022), pp.387-394. Spinger Nature, Singapore, (2023).
10. R Core Team: A Language and Environment for Statistical Computing. R version 4.2.2 (2022-10-31), R Foundation for Statistical Computing, Vienna, Austria (2022).
11. Hoy, M.M.P., Egan, M.Y., Feder, K.P.: A Systematic Review of Interventions to Improve Handwriting. Canadian Journal of Occupational Therapy, 78(1), 13–25 (2011).
12. Zurairi, A.R.: Malaysian teachers spend 29pc of their time on admin work, says study. Malay mail. https://www.malaymail.com/news/malaysia/2014/06/26/malaysian-teachers-spend-29pc-of-their-time-on-admin-work-says-study/694769 (2014).
13. Porac, C., Coren, S., Searleman, A.: Inverted versus straight handwriting posture: A family study. Behavior Genetics, 13(3), 311–320 (1983).
14. Gerth, S., Klassert, A., Dolk, T., Fliesser, M., Fischer, M. H., Nottbusch, G., Festman, J.: Is handwriting performance affected by the writing surface? Comparing preschoolers', second graders', and adults' writing performance on a tablet vs. Paper. Frontiers in Psychology 7, 1308 (2016).

Image Processing Tools for Forensic Footwear Impressions Evaluation: A mini review

Anwar A.M.A. Salem[1], Loong Chuen Lee[2*], and Hukil Sino[3]

[1] Forensic Science Program, CODTIS, Faculty of Health Sciences, Universiti Kebangsaan Malaysia
P148860@siswa.ukm.edu.my
[2*] Forensic Science Program, CODTIS, Faculty of Health Sciences, Universiti Kebangsaan Malaysia
lc_lee@ukm.edu.my
[3] Forensic Science Program, CODTIS, Faculty of Health Sciences, Universiti Kebangsaan Malaysia
hukilsino@ukm.edu.my

Abstract. Image processing tools have long been applied in forensic investigations for various purposes, particularly for computer restoration and enhancement of surveillance imagery. Recently, image processing tools have also been used in forensic footwear impression examination. In particular, image processing tools have been explored for extracting features from 2D or 3D footwear impressions, aiming to reach a more objective conclusion regarding similarities between a questioned sample and a known sample. This mini-review discusses the applications of various image processing tools in forensic footwear impression examination, detailing their unique benefits compared to conventional approaches. Further, limitations and prospects of image processing tools in forensic footwear impression examinations will also be explored.

Keywords: Footwear impressions, image processing, computer vision, forensic examination

1 Introduction

Footwear impressions are often encountered at both indoor and outdoor crime scenes [1]. The impression results from direct contact between the footwear worn by the suspect, i.e., boots and sneakers, and a substrate. Such contact is always associated with various kinds of transfer and retention of the item on the surface. Consequently, the examination of footwear impressions, whether two-dimensional or three-dimensional, is valuable in revealing the identity of the suspect and associating them with a particular crime scene. Occasionally, the footwear impressions could also indicate the number of culprits involved in the crime. Hence, in brief, the primary purpose of forensic footwear examination is to identify a person of interest (POI) by comparing the questioned

footwear impression with a known impression produced by the footwear of the POI, using suitable procedures and tools.

Conventional practices rely solely on visual examination when matching a questioned footwear impression to a known footwear impression or exemplar [2]. A trained examiner will assess the class and individual characteristics of the suspected and known footwear impressions (**Fig. 1**) before reaching an opinion-based conclusion. Hence, the visual-based examination is somewhat subjective and greatly dependent on the examiner's knowledge, training and experience. As a result, manually examining the footwear impression images is laborious and time-consuming.

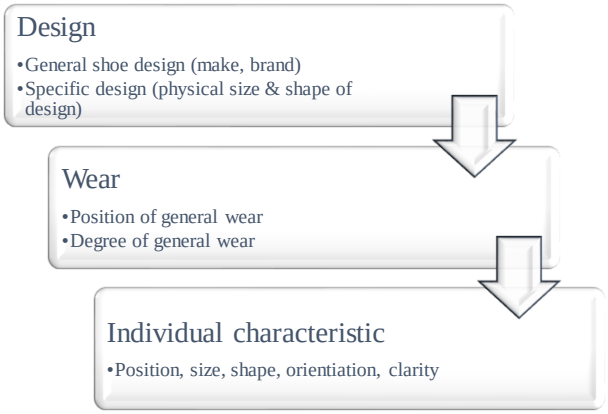

Fig. 1. Characteristics of footwear evaluated in comparing questioned and known footwear impressions for determining POI (SWGTREAD 2006).

To remediate cognitive bias associated with the visual examination of footwear impressions, numerous studies have focused on applying image-processing tools to objectively assess the similarity and dissimilarity between questioned and known footwear impressions. For instance, Chiu et al. proposed an innovative shoeprint retrieval system to improve the assessment of full- and partial-print shoeprint impressions [4]. On the other hand, Francis et al. evaluated various feature-enhancement tools for revealing the effects of wear and tear on footwear impression images in forensic examination [5].

Recently, Manaswini et al. presented a review discussing image-enhancement techniques applicable to diverse forensic applications involving the collection of evidence via the digital photography method [6]. However, the review was not focused on the application of image-processing tools on footwear impression images. Hence, this mini-review aims to discuss the applications of various image-processing tools in forensic footwear impression examination, detailing their unique benefits compared to conventional approaches. Further, limitations of image-processing tools in forensic footwear impression examinations will also be explored. The insights of the review would further

enhance the understanding of the potential of image-processing tools in the context of forensic footwear impressions.

2 Related Work

Digital photography is one of the most effective methods for recovering footwear impressions. A digital image can be defined by a series of numerical representations recorded by a digital camera. The analogue colour is digitised into three digital values representing the colour (red, green and blue) called RGB.

In the context of forensic footwear impression examination, digital image processing involves three major phases: preprocessing, feature extraction, and data interpretation (**Fig. 2**). Many works have proposed diverse image-processing pipelines for footwear impression database search and retrieval [7].

Raw digital images are often unsuitable for interpretation without preprocessing because they frequently contain irrelevant details, such as noise. Preprocessing enhances the reliability and accuracy of subsequent analysis. Next, global and local features are extracted from the preprocessed images for further examination. Finally, the known and questioned footwear impression images are compared and assessed for similarity and dissimilarity based on the extracted features. Details of each phase are elaborated in the following sections.

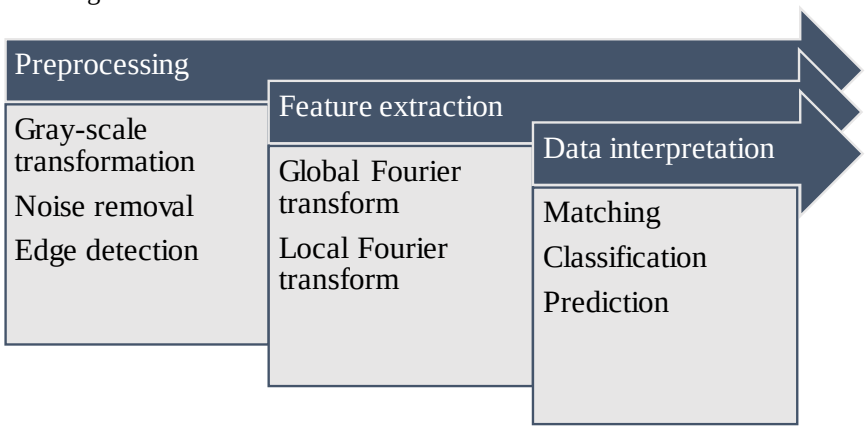

Fig. 2. Three major phases of image processing techniques and tools for forensic examination of footwear impression images.

2.1 Preprocessing

Digital images of footwear impressions vary in quality. For example, scanned images are often affected by distortions such as rotation, translation, imprint noise, and other disturbances. Additionally, images from different sources vary in resolution and

dimensions. Hence, such images should be preprocessed to eliminate irrelevant distortions and standardise dimensions before feature extraction.

Grayscale conversion. Converting a colour image to grayscale is a crucial preprocessing step. Grayscale images have a single colour channel with matrix values ranging from 0 to 255 (8 bits), whereas colour images have three channels (RGB). As a result, subsequent processing steps are simplified and require less computational power [8].

Resizing. Image dimensions (width and height) depend on factors like colour depth and file format. Since computational load scales with image size, images are often downsampled to sizes such as 64 × 64 or 128 × 128.

Noise removal. Background noise in scanned footwear impressions can be reduced by thresholding pixel values below a chosen level to white, or by applying block-based noise removal and a Gaussian low-pass filter (e.g., Gaussian Blur).

Normalisation. Variations in rotation, translation, scaling, and flipping, caused by differences in camera distance and angle, can be removed via normalisation.

2.2 Feature Extraction

In image analysis, points that can be extracted from an image are collectively referred to as features, or points of interest. Specifically, such features are known as descriptors within the UK footwear forensic units [3], which are the recognisable units within a footwear pattern applicable for classifying impressions. Descriptors vary in shape and location within an impression (e.g., heel/instep or main sole/top).

Generally, descriptors defining a footwear outsole's geometry can be classified into edges, corners, blobs, lines, and morphological region features. **Table 1** describes the general features of the two most common descriptor classes [7]. Additionally, shapes in an impression can be detected as straight-line segments, circles, arcs, or ellipses [18]. These geometric structures manifest as patterns of pixel value distances and can be identified using suitable detectors. A feature descriptor then encodes each detected feature into a numerical vector. Two types of algorithms are required in this phase:

- Feature detector: identifies the feature points in a footwear impression image.
- Feature descriptor: generates a numerical vector characterising essential attributes of each detected feature.

In practice, the most desirable descriptors are invariant to geometric and photometric transformations and robust to clutter and occlusion.

Table 1 Descriptions of features often encountered in image processing [7].

Feature	Characteristics
Corner	Defined as the crossing point of two straight lines. Can be represented by gradient-, intensity-, and contour curvature-based methods.

Feature	Characteristics
Blob	Defined as a local closed region, inside which the pixels are considered similar and thus distinct from the surrounding neighbourhoods. Can be extracted via second-order partial derivative- and segmentation-based detectors.

Various algorithms have been proposed for detecting features. Among the most widely used are Scale-Invariant Feature Transform (SIFT) [10], Speeded-Up Robust Features (SURF) [2], Affine-SIFT (ASIFT) [1], Harris corner detector, and Features from Accelerated Segment Test (FAST). **Table 2** summarises several popular detector-descriptor combinations assessed for comparing outsole images [13].

Table 2 Characteristics of feature-detector-descriptors applicable in forensic footwear outsole image comparison [13].

Descriptors	Characteristics
SIFT (blob)	Scale-invariant feature transform (Lowe 2004) Most popular descriptors in terms of usage Robust to rotation, scale and translation changes Computationally intensive
SURF (blob)	Robust to rotation and scale changes (Bay et al. 2006) Relies on Gaussian differences to approximate a Laplacian Faster than SIFT in implementation
KAZE (blob)	Operates in a non-linear scale space (Alcantarilla et al. 2012) Using nonlinear diffusion filtering Computationally demanding

Histograms of Oriented Gradients (HOG). Extracts macro-features (e.g., corners, textures) by estimating local intensity-gradient orientations within image cells and aggregating them into histograms.

Edges. Defined by sudden changes in grey level, edges are fundamental features. The Canny edge detector [11] utilises non-maximum suppression and double thresholding to accurately localise edges and suppress noise, although optimal threshold selection can be challenging.

Shapes. The Randomised Hough Transform detects ellipse shapes in impressions [12], while Kittler's thresholding extracts spatial-domain features [17].

Discrete Fourier Transform (DFT). Applied to zero-mean images to estimate coefficient values; the power spectral density (PSD), derived from DFT magnitudes, reveals spatial-frequency patterns and is invariant to translation.

Maximally Stable External Regions (MSER). A watershed-based segmentation algorithm that identifies regions stable under affine transformations and degradations; extracted regions can be encoded into robust SIFT descriptors [15].

2.3 Data Interpretation

The features prepared in the previous phase can be evaluated to quantify the similarity between questioned and known impressions. For example, the Euclidean or correlation distance between their 2D-DFT coefficient vectors can be used; other viable metrics include city-block and Canberra distances [13]. Budka et al. [15] applied a convolutional neural network (CNN) to classify these descriptors, enabling rapid, expert-free identification of shoe models. Alternatively, the same extracted features can be used to feed an automated outsole-based shoe-model identification system [14].

3 Conclusion and Future Work

In conclusion, various image-processing tools have been developed to elucidate similarity and dissimilarity between questioned and known footwear impressions [4-6]. Nonetheless, their use has predominantly focused on database retrieval [7]. The application of these techniques can be expanded to tackle other forensic challenges, such as predicting biological traits from footwear impression images. For example, Hassan et al. [16] demonstrated that age- and sex-related variations correlate with pressure distributions on shoeprints by applying a convolutional neural network to model relationships between biological profiles and impression patterns.

Acknowledgement

Anwar A.M.A. Salem gratefully acknowledges the scholarship sponsorship from the Kuwait's government for supporting her PhD study at Universiti Kebangsaan Malaysia (UKM), Malaysia.

References

1. Kellett, D., Zolghadriha, S., Morgan, R., Lagnado, D., Nakhaeizadeh, S.: Forensic footwear examination: A systematic review of the existing literature. Forensic Sci. Int. 365, 112295 (2024).
2. Lin, E.-T., Speir, J. A.: Predicting image quality of forensic footwear impressions. Science & Justice 64(6), 614–624 (2024).
3. SWGTREAD: Recommended practices for forensic footwear and tire tread examination. SWGTREAD, (2006).
4. Chiu, H.-C., Chen, C.-H., Yang, W.-C., Jiang, J.: Automatic full and partial shoeprint retrieval system for use in forensic investigations. In: *12th International Congress on Image and Signal Processing, Biomedical Engineering and Informatics (CISP-BMEI)*, pp. 1–6. IEEE (2019).
5. Francis, X., Sharifzadeh, H., Newton, A., Baghaei, N., Varastehpour, S.: Feature enhancement and denoising of a forensic shoeprint dataset for tracking wear-and-tear effects. IEEE (2019).
6. Manaswini, D., Ghanta, S. S. V., Manogna, T. L., Kolakalapudi, L. N. K., Chaitanya, G. K., Kumar, A. D.: A survey of forensic applications using digital image processing: Image improvement case study. In: *Proceedings of the 7th International Conference on Computing Methodologies and Communication (ICCMC-2023)*, pp. 696–702. IEEE Xplore (2023).
7. Pasquier, J.: A footwear marks database in Western Switzerland: A forensic intelligence success. Forensic Sci. Int. 348, 111726 (2023).
8. Sari, M., Al Maki, W. F.: Improving K-nearest neighbor performance in footwear classification using leave-one-out cross validation. In: *3rd International Conference on Intelligent Cybernetics Technology & Applications (ICICyTA)*, pp. 55–60 (2023).
9. Jiang, X., Ma, J., Xiao, G., Shao, Z., Guo, X.: A review of multimodal image matching: Methods and applications. Information Fusion 73, 22–71 (2021).
10. Tang, Y., Srihari, S. N., Kasiviswanathan, H.: Similarity and clustering of footwear prints. In: *2010 IEEE International Conference on Granular Computing*, pp. 459–464. IEEE Computer Society (2010).
11. Canny, J. F.: A computational approach to edge detection. IEEE Trans. Pattern Anal. Mach. Intell. PAMI-8(6), 679–698 (1986).
12. McLaughlin, R.: Randomized Hough transform: Better ellipse detection. In: *IEEE TENCON – Digital Signal Processing Application*, vol. 1, pp. 409–414 (1996).
13. Park, S., Carriquiry, A.: The effect of image descriptors on the performance of classifiers of footwear outsole image pairs. Forensic Sci. Int. 331, 111126 (2022).
14. Pavlou, M., Allinson, N. M.: Automated encoding of footwear patterns for fast indexing. Image Vis. Comput. 27(4), 402–409 (2009).
15. Budka, M., Ul Ashraf, A. W., Bennett, M., Neville, S., Mackrill, A.: Deep multilabel CNN for forensic footwear impression descriptor identification. Appl. Soft Comput. 109, 107496 (2021).
16. Hassan, M., Wang, Y., Wang, D., Li, D., Liang, Y., Zhou, Y., Xu, D.: Deep learning analysis and age prediction from shoeprints. Forensic Sci. Int. 327, 110987 (2021).

Evaluation of the Mechanical Behavior of Treated Gargar Mud Using Mineral Additives for Road Engineering Applications

F. Benhadj Ziane [1-3] **A.A.** Driss[2-3] **M.** Ghrici [1-3]

[1] Hydraulic Department, Civil Engineering Faculty, Hassiba Benbouali University of Chlef, Algeria
[2] Hydraulic Department, [1,2] Technology Faculty, University Center of Maghnia, Tlemcen, Algeria
[3]Geomaterials Laboratory, Civil Engineering Faculty, University Hassiba Benbouali of Chlef, Algeria

f.benhadjziane@univ-chlef.dz, a.driss@cu-maghnia.dz, m.ghrici@univ-chlef.dz

Abstract. In recent years, sedimentation has emerged as a significant threat to the structural integrity and operational safety of dams, particularly in semi-arid regions where erosion is highly aggressive. This phenomenon results in the accumulation of large quantities of sediments or sludge, which, if not properly managed, can lead to environmental degradation and reduced reservoir capacity. To restore storage capacity, the National Agency for Dams and Transfers (ANBT) has implemented dredging operations to extract the accumulated sludge.
In this context, Algerian researchers have undertaken analyses to explore cost-effective and sustainable strategies for reusing and valorizing dredged sediments in various sectors, including civil engineering. This study is part of a broader project on managing and reusing dredged sediments from the Gargar Dam. Algeria's third-largest dam, which is heavily affected by sedimentation.
To achieve this objective, the mud was treated with varying proportions of lime (0–6%), supplemented with sand (0–20%) and natural pozzolana (0–20%). Laboratory tests, including Atterberg limits, compaction, California Bearing Ratio (CBR), and unconfined compressive strength, were conducted to evaluate the mechanical behaviour of the treated material. The results demonstrate that lime and pozzolana treatment significantly improve the geotechnical properties of the Gargar mud by reducing its plasticity and promoting a flocculated structure. Consequently, the treated material becomes more friable and exhibits increased strength, confirming its potential for use in road infrastructure.

Keywords: Gargar dam, lime, pozzolana.

1 Introduction

The silting of dam reservoirs is a natural process that decreases both the storage capacity and operational lifespan of dams. The extent of capacity loss due to sedimentation is primarily influenced by factors such as the erosion rate of the catchment areas,

vegetation cover, topography, and climate. In the Arab Maghreb countries, the useful capacity of hydraulic infrastructure decreases by 0.65% per year [1]. In the present context, the diminution of storage capacity within Algerian hydraulic infrastructures has exhibited a consistent increase in recent years, primarily attributed to natural phenomena. These phenomena encompass the severity of climatic conditions, variations between arid and humid intervals, the susceptibility of geological structures, and inadequate vegetative coverage. The alluvial deposition occurring within northern dams represents one of the most consequential ramifications of hydric erosion, with an estimated 180 million tons of sediment being eroded from catchment basins via runoff on an annual basis in Algeria. Consequently, the most critical manifestation of erosion is gully erosion, which may constitute over 50% of the annual solid input. With average annual specific erosion rates fluctuating between 2000 and 4000 t/km², Algeria is positioned among the most susceptible countries to erosion globally [2]. Dredged sediments have been extensively employed worldwide for diverse infrastructure development initiatives, including land reclamation and construction endeavors. The recovery of sediments post-dredging yields numerous economic and ecological advantages. Primarily, it enhances the management protocols concerning dredged materials. Furthermore, it presents an innovative approach to addressing the limitations of resources available for construction materials. Several studies have explored the valorization of dam sediments in construction materials, including bricks, ceramics, artificial pozzolans, cement, and road engineering applications. In the production of bricks, sediments from the eleven most silted dams in Algeria were utilized; findings indicate that the silt possesses characteristics comparable to those of yellow clay utilized by brickyards throughout Algeria [3]. Concerning ceramic products, studies have evaluated the mud sourced from the Oued Fodda dam for its potential application in the realm of construction materials, particularly in ceramic floor tiles [4]. Studies have shown that dredged sediments, such as mud from the Chorfa Dam, can be valorized as partial cement replacements in concrete. [5]. In road engineering [6], studies have shown that the geotechnical properties of sediments dredged from the Cheurfas Dam are significantly improved when mixed with sand, lime, and cement. Additionally, investigations have treated sediments dredged from Soummam River and Kherrata dam with hydraulic binders to valorized them in road construction [7]. Results revealed that incorporating cement or lime reduces sediment plasticity, enhances compressive strength, and improves both immediate and post-immersion bearing capacity indices. Furthermore, polluted dredged sediments have been applied in road engineering after treatment with lime, sand, and blast furnace slag [8]. Thus, mud accumulated during dredging operations is increasingly regarded not as waste but as a valuable natural resource, in alignment with the principles of sustainable development.

To improve significantly the engineering properties of soft soils, extensive studies have been conducted on soil stabilization using various additives such as lime cement, fly ash, natural pozzolana and slag [9,10,11]. Lime as an additive is most commonly used to stabilize fine soils due to its effectiveness and economic usage. Furthermore, lime substantially enhances the physical and mechanical characteristics; Lime stabilization of clayey soils reduces plasticity and modifies soil consistency, while also altering particle size distribution, swelling behavior, and mechanical properties such as unconfined compressive strength and shear strength The stabilization of lime

in conjunction with Pozzolana is predicated on the chemical interactions between lime and clay particles, which involve phenomena such as cation exchange, flocculation, and pozzolanic reactions. These interactions engender an attractive force among the clay particles, culminating in the formation of a flocculated soil structure. Over extended curing periods, novel cementitious compounds are generated, such as calcium silicate hydrates (CSH) [12].

The main objective of this paper is to contribute to the valorization of dredged sediments from the Gargar Dam for applications in road engineering by studying the influence of the addition of lime and Pozzolana contents to the geotechnical properties of the mud. To achieve this goal, laboratory soil tests were performed on the physical and mechanical properties of the soil before and after lime treatment.

2 Experimental program

2.1 Materials used

The Gargar dam, recognized as the third-largest dam within Algeria following Koudiat Acerdoune and Beni Haroune, is situated 350 kilometers to the west of Algiers, precisely in the wilaya of Relizane, as illustrated in Fig. 1. This dam, which was commissioned in 1989 with an original capacity of 450 million cubic meters, serves the dual purposes of irrigation and the provision of potable water. According to the most recent bathymetric survey conducted in 2019 by the National Agency of Dams and Transfers, the Gargar Dam has undergone significant siltation, with its sedimentation level increasing by approximately 36% [13].

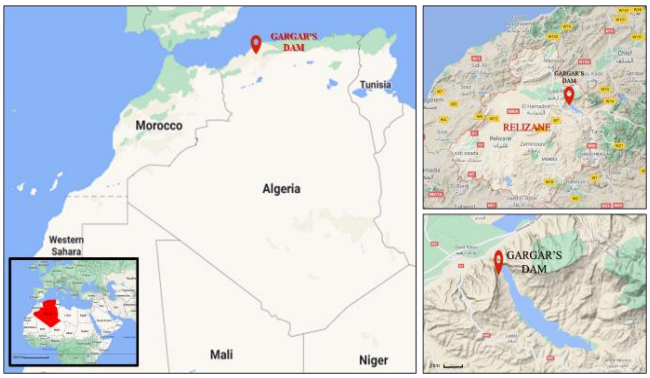

Fig. 1. Localization of the Gargar's Dam.

To enhance the comprehension of the behavioral characteristics of the soil under investigation, identification tests were performed in accordance with American standards (ASTM). The soil sample analyzed was extracted from the discharge area of the dam. The engineering properties of the soil indicate that its composition consists of 35% clay, 61% silt, and 4% sand, and it has been classified as a high plasticity clay soil. The lime (L) utilized in this investigation is a hydrated lime produced by SARL-BSM, a company located in the city of Saïda in the southwestern region of Algeria. The sand sourced from Oued-Chlef, which is classified as alluvial sand, is characterized as medium sand

with a rounded morphology, The natural pozzolana used in this study is of volcanic origin and was sourced also from the Bou-Hamidi deposit in Ain-Temouchent, Algeria.

2.2 Sample preparation and test procedure

For the stabilization process, lime, sand, and natural pozzolana were employed. The soil was treated with 3% and 5% lime, both individually and in combination with 20% sand, 20% pozzolana, and a mixture of 20% S + 20% P. A series of laboratory tests was performed on the selected mud, including Atterberg limits, Proctor compaction, California Bearing Ratio (CBR), and unconfined compressive strength (UCS), all in accordance with ASTM standards [14].

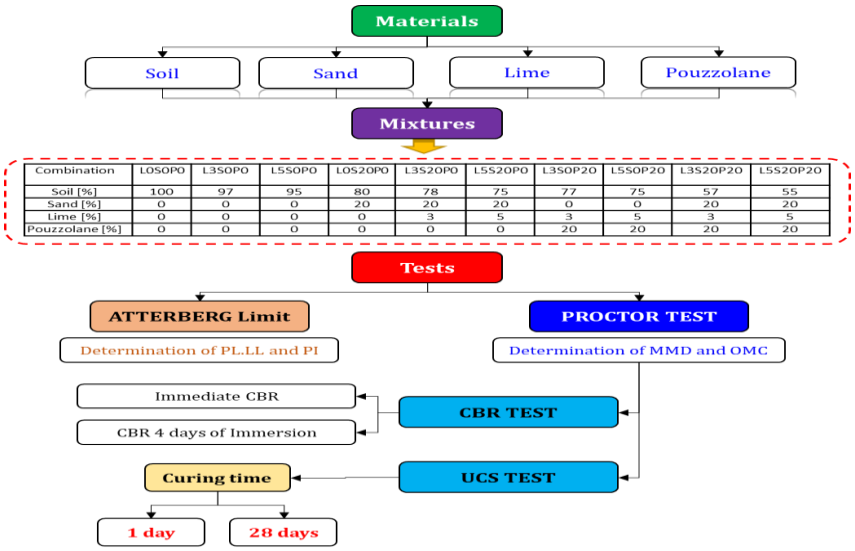

Combination	L0S0P0	L3S0P0	L5S0P0	L0S20P0	L3S20P0	L5S20P0	L3S0P20	L5S0P20	L3S20P20	L5S20P20
Soil [%]	100	97	95	80	78	75	77	75	57	55
Sand [%]	0	0	0	20	20	20	0	0	20	20
Lime [%]	0	0	0	0	3	5	3	5	3	5
Pouzzolane [%]	0	0	0	0	0	0	20	20	20	20

Fig. 2. Test procedure.

3 Results and Discussion

3.1 Atterberg limits

The variation of atterberg limits (liquid limit, plastic limit, and plasticity index) are well presented in Figure 3. The incorporation of lime into the examined soil results in a pronounced augmentation of its liquid limit (LL) and plastic limit (PL); specifically, the introduction of 3% and 5% lime to the mud resulted in an elevation of their LL. This phenomenon is corroborated by the findings of Osula [15] and Asgari et al. [16]. A substantial enhancement in the plastic limit was documented following the addition of lime to the soil in question. Consequently, a notable reduction in the plasticity index (PI) was observed when adding 5% of lime. It is noteworthy that the LL exhibited a decline following the incorporation of 20% sand into the natural soil; this phenomenon can be attributed to the substitution of a portion of the clay particles with granular

and non-plastic sand particles, which possess a lower LL compared to the soil under examination. Similar outcomes were reported by Goufi et al. [17], who investigated the influence of dune sand on highly plastic clayey soils and observed comparable reductions in plasticity and improvements in soil behavior

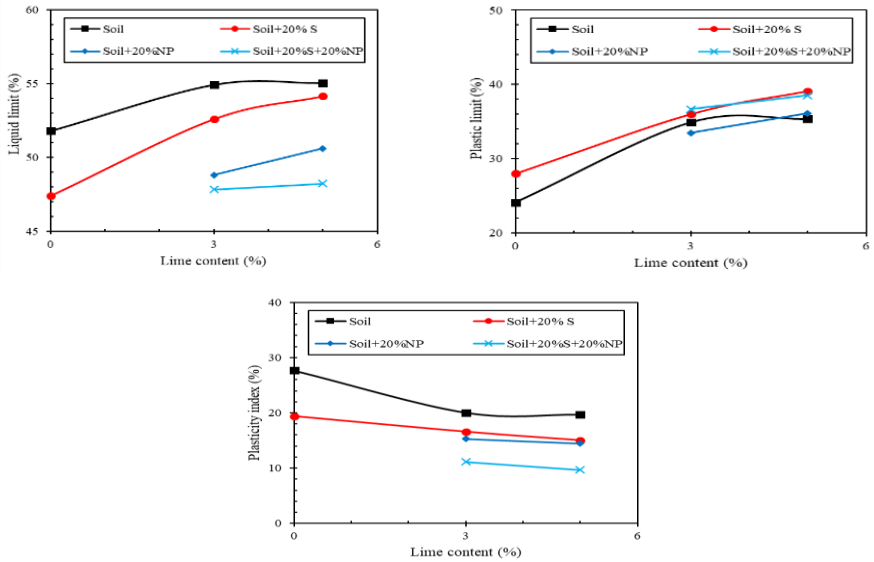

Fig. 3. Atterberg Limits Variation of Treated Mud (LL, PL, and PI).

Lime treatment of soil–sand, soil–NP, and soil–sand–NP mixtures resulted in an increase in both liquid limit (LL) and plastic limit (PL) with higher lime content. However, the addition of NP and/or sand to lime-treated soil caused a reduction in LL, particularly with 20% sand, 20% NP, and their combination with 5% lime. This behavior is attributed to the lower LL of NP and sand, as well as the enhanced flocculation of soil particles when these materials are incorporated, compared to only the treatment with the lime.

As illustrated in Figure 4, the USCS classification indicates that the natural soil is highly plastic clay (CH). With lime treatment, it shifts to highly plastic silt (MH). The addition of 20% sand changes the class to low-plasticity clay (CL), while combining sand with 3% or 5% lime again yields MH. When treated with lime, natural pozzolan (NP), or lime–sand–NP, the soil transforms from CH to low-plasticity loam (ML). These changes result from clay particle flocculation and cation exchange, which reduce plasticity and render the soil more friable.

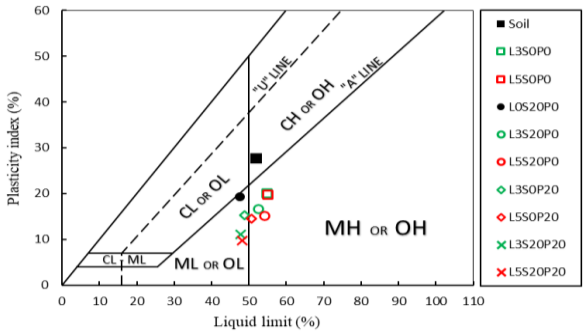

Fig. 4. USCS classification of soil before and after treatment with lime, sand, and NP combinations.

3.2 Compaction

The compaction curves of the soil before and after treatment with the different combinations are presented in Figure 5. The incorporation of lime results in an increase in the optimum moisture content (OMC) and a reduction in the maximum dry density (MDD). The decrease in MDD is primarily attributed to the lower density of lime compared to clay soil, as well as to the particle flocculation induced by lime stabilization [18]. Conversely, the increase in OMC is explained by the higher water retention capacity of the treated soil and the additional water demand required for pozzolanic reactions [19, 20].

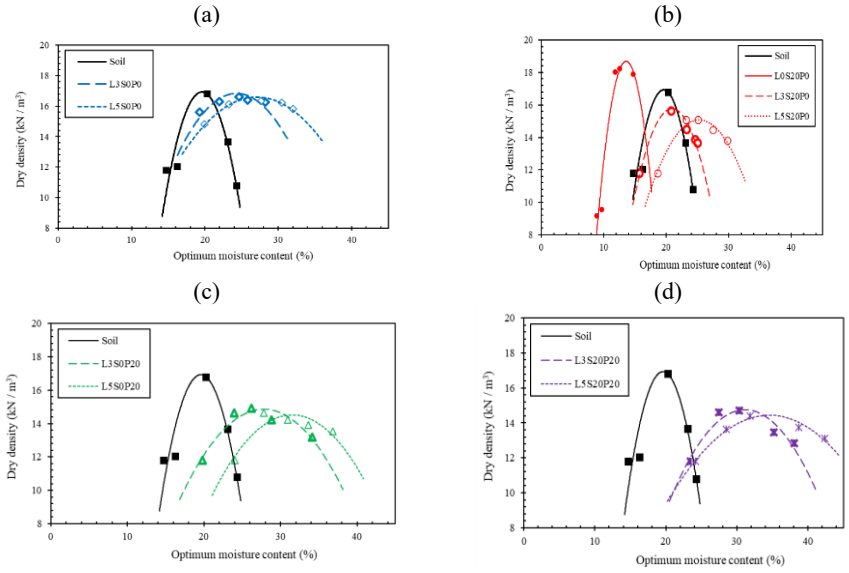

Fig. 5. Compaction curves of soil under different treatments: (a) lime, (b) sand and sand–lime, (c) lime–NP, (d) lime–sand–NP

As shown in Fig. 5(b), the addition of sand to the studied soil decreases the OMC while increasing the MDD. These findings are consistent with Goufi et al., who explained that the higher density of sand compared to clay soils and the reduction in the initial void ratio account for this behavior. Moreover, the incorporation of lime into soil–sand, soil–P, and soil–sand–P mixtures further reduce MDD and increases OMC, due to enhanced particle flocculation and additional pozzolanic reactions.

3.3 CBR (Californian Bearing Ratio)

Figure 6 illustrates the evolution of the CBR coefficient. It is evident that the combinations meeting the load-bearing criterion (CBR > 25) are soil + 20% sand + 20% natural pozzolana stabilized with 3% and 5% lime, indicating that the treated soil can be used as a foundation layer.

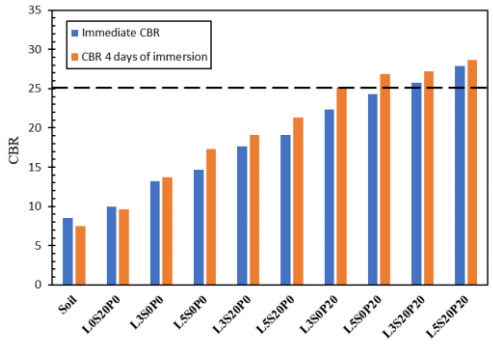

Fig. 6. Variation of the CBR coefficient.

The marked improvement in soil strength observed with the combination of lime, sand, and natural pozzolana is attributed to the development of a more flocculated soil structure with stronger interparticle bonds than with lime alone. Similar findings were reported by Harichane et al. [21] when studying the stabilization of Algerian clayey soils with natural pozzolana.

3.4 Unconfined compressive strength

Figure 7 presents the variation in unconfined compressive strength (UCS) of highly plastic clay treated with cited additives after 1 and 28 days of curing. The stress–strain curves highlight two behaviors: after 1 day of curing, treated soils show ductile characteristics with an initial UCS increase. After 28 days, soils treated with lime, lime–sand, and lime–sand–NP exhibit brittle behavior with substantial strength gains due to pozzolanic reaction and particle crystallization.

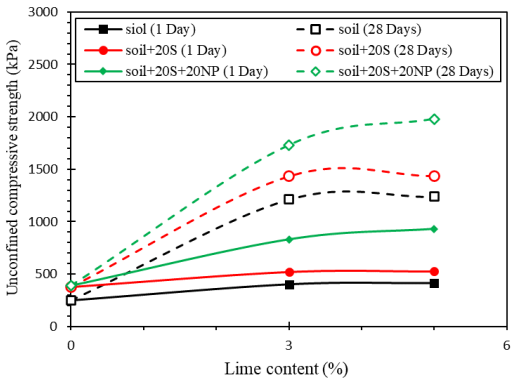

Fig. 7. Variation of UCS with different additives.

The increase in compressive strength is attributed to pozzolanic reactions between lime and soil, lime and sand, as well as lime, sand, and natural pozzolan, which produce cementitious compounds that bind the soil particles. The greatest strength enhancement is achieved with the mixture containing 5% lime, 20% sand, and 20% natural pozzolan.

4 Conclusion

In Algeria, one of the major challenges facing dams is reservoir siltation, which causes a significant reduction in their water storage capacity. The main aim of this paper is the valorization of dredged sediments from the Gargar dam to be used in road embankments. From this research, several conclusions can be drawn:

1. The addition of lime to the studied soils increased the OMC while reducing the MDD, due to the lower density of lime and the higher water retention capacity after treatment. In contrast, natural pozzolan and sand, which are characterized by higher density, contributed to a denser and more compact soil structure when incorporated into the studied mud;
2. The Gargar mud became more friable and less plastic after treatment with the different additives, resulting in a marked change in its classification according to the USCS. The treated soil underwent flocculation, which contributed to an improvement in unconfined compressive strength.;
3. A rise in the quantity of additives and the duration of curing resulted in a greater stress increase; the most favourable outcomes were observed in mud treated with a combination of lime, sand, and natural pozzolana.
4. All soil combinations stabilized with lime, sand, and natural pozzolan met the durability standards at the initial stage
5. The California Bearing Ratio (CBR) of the studied soil increased significantly after treatment; however, only the lime–sand–natural pozzolan combination met the bearing criterion with an index greater than 25.

6. Therefore, for the Gargar mud to be utilized as a foundational layer, it necessitates treatment with lime, sand, and natural pozzolan.

References

1. Remini, B., Bensafia, D. and Mekhatri, A.: Sidi M'hamed Ben Aouda's Dam (Algeria): Acceleration to the Silting. LARHYSS Journal, 33 221-252(2018).
2. Demmak, A.: Contribution to the study of erosion and solid transport in septentrional in Algéria, phd thesis, pierreand marie curie university, paris xi (1982).
3. Chikouche, MA, Ghorbel, E.,Bibi, M.: The possibility of using dredging sludge in manufacturing cements: optimization of heat treatment cycle and ratio replacement. Construction and Building Materials, 106, 330-341(2016).
4. Benasla, M., Benamara M. Hadjel, L.: Characterization of dredging mud dam Oued Fodda and valorization as a building material. Journal of Materials and Environmental Science 6(2):546-558(2015).
5. Bourabah, M. A., Abou-Bekr, N., Taibi, S.: Geotechnical characterization of dredging sediments for valorization in road embankments: Case of the Cheurfas Dam (Algeria). In GeoFlorida : Advances in Analysis, Modeling & Design (pp. 2212-2221) (2010).
6. Banoune, B., Melbouci, B., Rosquoët, F., Langlet, T. : Treatment of river sediments by hydraulic binders for valorization in road construction. Bulletin of Engineering Geology and the Environment, 75(4), 1505-1517(2016).
7. Slama, A.B., Feki, N., Levacher, D., Zairi, M.: Valorization of harbor dredged sediment activated with blast furnace slag in road layers. International Journal of Sediment Research, 36(1), 127-135(2021).
8. Loudini, A., Ibnoussina, M., Witam, O., Limam, A. and Turchanina,O.: Valorisation of Dredged Marine Sediments for Use as Road Material." Case Studies in Construction Materials (2020).
9. Bell, F.G.: Lime stabilization of clay minerals and soils. Engineering Geology, Vol. 42, pp. 223-237 (1996).
10. Harichane, K., Ghrici, M., & Kenai, S.: Stabilization of Algerian clayey soils with natural pozzolana and lime. Periodica Polytechnica Civil Engineering, 62(1), 1-10 (2018).
11. Driss, A. A. E., Harichane, K., Ghrici, M., Gadouri, H.: Assessing the effect of moulding water content on the behaviour of lime-stabilised an expansive soil. Geomechanics and Geoengineering, 1-13 (2021, a).
12. Vitale, E., Deneele, D., Paris, M, Russo, G.: Multi-Scale analysis and time evolution of pozzolanic activity of lime treated clays, Applied Clay Science., Vol. 141, pp. 36–45 (2017).
13. National Agency of dams and transfers (A.N.B.T): Bathymetric study of the Gargar dam (2019).
14. ASTM D4318-05.: Standard Test Methods for Liquid Limit, Plastic Limit, and Plasticity Index of Soils, ASTM International, West Conshohocken (2005).
15. Osula, DOA.:. Lime modification of problem laterite, *Engineering Geology*, 30, 141-154 (1991).
16. Asgari, MR, Baghebanzadeh Dezfuli, A and Bayat, M..: Experimental study on stabilization of a low plasticity clayey soil with cement/lime, Arabian Journal of Geoscience, **8**, 1439–1452 (2015).

17. Goufi, AE, Harichane, K, Harichane, Z, Driss, AAE and Ghrici, M.: Improvement of the geotechnical properties of a clay–sand mixture treated with lime. *Innovative Infrastructure Solutions*, 7, 1-17(2022).
18. Garzon, E, Cano, M, O`Kelly, BC and Sánchez-Soto, PJ.: Effect of lime on stabilization of phyllite clays, *Applied Clay Science*, 123, 329-334(2016).
19. Harichane, K, Ghrici, M, Kenai, S and Grine, K.: Use of natural pozzolana and lime for stabilization of cohesive soils. *Geotechnical and geological engineering*, 29, 759-769(2011).
20. Kinuthia, JM, Wild, S and Jones, GI.: Effects of monovalent and divalent metal sulphates on consistency and compaction of lime-stabilized kaolinite, *Applied Clay Science*, 14, 27-45(1999).
21. Harichane, K, Ghrici, M and Kenai, S.: Stabilization of Algerian clayey soils with natural pozzolana and lime. *Periodica Polytechnica Civil Engineering*, 62, 1-10(2018).

Lime and Natural Pozzolana, an Eco-friendly Mixture for the Stabilisation of clayey soils.

DRISS Abdelmoumen Aala Eddine[1,2][0000-0002-6973-1587], Abd elmalik GOUFI[3], Mehdi MISSOUM BENZIANE[4], Fouzia BENHADJ ZIANE[5] and Mohamed GHRICI[2]

[1] Hydraulic Department, University Centre of Maghnia, Tlemcen, Algeria.
[2] Geomaterials Laboratory, Civil Engineering Department, University Hassiba Benbouali of Chlef, Algeria
[3] Civil Engineering Department, Mohamed El bachir El Ibrahimi University, Bordj Bou Arreridj. Algeria
[4] Civil Engineering Department, Hassiba Benbouali University, Chlef, Algeria
[5]Hydraulic Department, Hassiba Benbouali University of Chlef, P.O. Box 151, Chlef, Algeria

a.driss@cu-maghnia.dz

Abstract. Clayey soils pose challenges in construction activities due to their typical com-position of expansive clay minerals. Nonetheless, the inadequate geotechnical characteristics of clay soils can be enhanced in several ways. This study exam-ines the impact of the addition of an eco-friendly mixture composed of lime and natural pozzolana on the shear strength characteristics of fat clay soil (CH) col-lected from Tlemcen city in Algeria. The additives are incorporated into the ex-amined soil in two stages: initially, 2%, 4%, and 6% of lime by weight is intro-duced to assess its impact on the soil, followed by the addition of 10% and 20% of natural pozzolana to the chosen mixture to evaluate its influence on soil be-haviour pre- and post-lime treatment. The analysed characteristics include pH variation, compaction parameters, shear strength, and microstructural analysis. Test results indicate that the characteristics of clay soil can be significantly enhanced with lime treatment. A combination of lime and natural pozzolana yields superior shear strength relative to the use of either lime or natural pozzolana independently. The incorporation of natural pozzolana into lime-treated soil enhanced stabilising outcomes by promoting a more flocculated soil structure and the increased development of cementitious products.

Keywords: Clayey soils, Eco-friendly mixture, Lime, Natural pozzolana.

1 Introduction

Clay minerals are minuscule particles demonstrating considerable electrochemical activity. This phenomenon results from the interaction of electrically charged particles. The limited presence of clay minerals in natural soils considerably affects their technical properties. Clayey soils have a considerable specific surface area and high ion exchange capacity, resulting in marked plasticity, significant volumetric variations,

such as swelling and shrinking, higher compressibility, and reduced load-bearing capacity [1-2]. The adverse properties of fat clays make them difficult to handle when wet, presenting challenges for civil engineers. Various methods are available to improve these soils, including mechanical, hydromechanical, thermal, and chemical treatments [3-5].

The high cost of strengthening or replacing fine clayey soils with durable materials that meet project criteria has led researchers to investigate more cost-effective options. Chemical soil stabilization methods entail the integration of diverse chemicals through soil mixing. Comprehensive studies and experimental analyses have been conducted on the impact of additives such as lime, cement, fly ash, natural pozzolana, and slag on the geotechnical properties of stabilized clayey soils [6-12].

Lime is a commonly employed hydraulic binder for the stabilization of cohesive soils. It markedly improves the geotechnical properties of clayey soils by altering their consistency and structure, diminishing their plasticity and swelling potential, and increasing their shear strength [13-14]. Lime stabilization of clayey soils produced advantageous results, and the creation of composite materials transpired by the amalgamation of at least two disparate components to form an innovative material. This material exhibited innovative characteristics, including lightness, hardness, and resistance, which were lacking in the original components. The combination of lime with different mineral additives, including as cement, fly ash, slag, and pozzolana, has been the subject of numerous investigations.

.

The research regarding the effects of integrating NP into lime-stabilized clayey soils is scarce. Hossain et al. [19] utilized natural volcanic ash (VA) for soil stabilization. Harichane et al. [20] examined the impact of a lime and NP mixture on two different clay soils (CH and CL). Zoubir et al. [21] found that integrating NP into lime-stabilized clay soils markedly improved their geotechnical properties, hence increasing the accessibility of land resources for civil engineering projects. Al-Swaidani et al. [22] identified beneficial results from the integration of NP into lime-stabilized clay soils. Numerous evaluations of clayey soil properties were conducted. Nonetheless, a limited number of studies have concentrated on investigating the effects of NP and its combination with lime [11].

This study examines the application of an eco-friendly Mixture composed of both NP and lime to improve the characteristics of the studied clayey soil, recognized for its elevated plasticity and volume change ability.

2 Materials and methods

2.1 Materials

This study utilized expansive soil collected from a landslide rehabilitation project in Mansourah-Tlemcen, Algeria, at depths ranging from 7 to 17 meters. Figure 1 depicts the soil degradation caused by the landslide in the studied area. After numerous laboratory identification tests, the examined soil was classified as fat clay with high plasticity

according to the USCS [39]. Table 1 outlines the geotechnical properties of the clayey soil.

(a) (b)

Fig. 1. A Soil collection site. a) degradation caused by the landslide. (b) extraction of the studied soil.

Table 1. Identification of the studied clay soil

Parameters		**Units**	**Clay**
Color			Grey
Depth		(m)	7 - 17
Natural water content		(%)	12 - 14
Specific gravity			2.67
Bulk density		(kN/m^3)	11.7
Passing 80 μm sieve (%)			86.68
Atterberg limits	Liquid limit	(%)	52.64
	Plastic limit	(%)	21.18
	Plasticity index	(%)	31.47
Soil components	Sand	(%)	14
	Silt	(%)	36
	Clay	(%)	50
Classification (USCS)			CH
Compaction	OMC	(%)	19.55
	MDD	(kN/m^3)	16.57

Organic matter content	(%)	2.42
Content of calcium carbonate	(%)	24.33

The hydrated lime (Ca(OH)2) used in this research was manufactured by the SARL-BSM company in the city of Saïda. The hydrated lime characteristics are listed in Table 2.

Table 2. Characteristics of lime used

Geotechnical Parameters		**Units**	**Lime**
Color			White
Specific gravity			2.24
Bulk density		(kN/m^3)	7.20
Specific surface -Blaine-		(cm^2/g)	11663
Particle fineness less than 45 µm		(%)	64.87
Normal consistency -Vicat W/L		(%)	69.50
Set time -Vicat- (min)	Initial		80
	Final		40
Calcium oxide [CaO]		(%)	> 83.3
Magnesium oxide [MgO]		(%)	< 0.5
Iron oxide [Fe_2O_3]		(%)	< 2
Alumina [Al_2O_3]		(%)	< 1.5
Silica [SiO_2]		(%)	< 2.5
Sulfite [SO_3]		(%)	< 0.5
Sodium oxide [Na_2O]		(%)	0.4 - 0.5
Carbon dioxide [CO_2]		(%)	< 5
Calcite [$CaCO_3$]		(%)	< 10

The natural pozzolana used in these experiments is a volcanic rock [19] obtained from the Bou-Hamidi deposit in Béni Saf, Ain Temouchent. Table 3 delineates the characteristics of the NP used.

Table 3. Physical and chemical properties of natural pozzolana

Geotechnical Parameters	**Units**	**NP**
Color		Red
Specific gravity		2.85
Bulk density	(kN/m^3)	10.22
Specific surface -Blaine-	(cm^2/g)	8737
Calcium oxide [CaO]	(%)	9.40
Magnesium oxide [Mgo]	(%)	3.88
Iron oxide [Fe_2O_3]	(%)	8.36
Alumina [Al_2O_3]	(%)	17.45
Silica [SiO_2]	(%)	46.83

Sulfite [SO_3]	(%)	0.36
Sodium oxide [Na_2O]	(%)	4.32
Potassium oxide [K_2O]	(%)	1.40

2.2 Methods

A sequence of laboratory studies, including pH analysis, compaction assessment, and unconsolidated undrained triaxial testing, was conducted on the soil under investigation before and after treatment. Figure 2 depicts the particle size distribution of clayey soil and NP. Table 4 displays the studied combination.

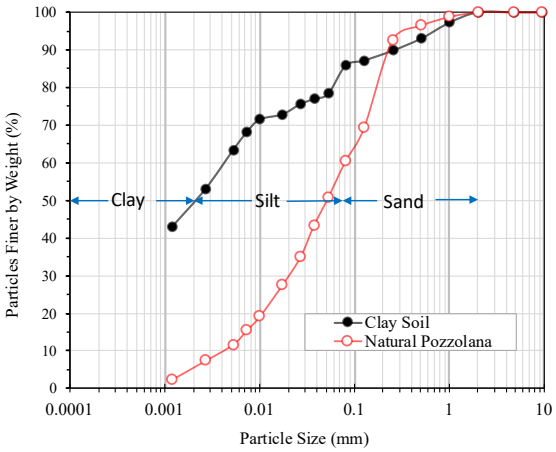

Fig. 2. Particle size distribution of soil and natural pozzolana.

Table 4. The studied combinations.

Symbol	Soil (%)	Lime (%)	NP (%)
L0P0	100	0	0
L0P10	90	0	10
L0P20	80	0	20
L2P0	98	2	0
L2P10	88	2	10
L2P20	78	2	20
L4P0	96	4	0
L4P10	86	4	10
L4P20	76	4	20
L6P0	94	6	0
L6P10	84	6	10
L6P20	74	6	20

In this study, the acidity or alkalinity of soil components suspended in distilled water was assessed using a pH meter. The clay soil and the clay soil-NP combination were both tested using the conventional soil pH procedure outlined in ASTM D4972 [25].

The stability of soil-NP and the fluctuation in soil pH levels were investigated using the standard test procedure described in ASTM D6276 [26], which determines the fraction of soil-lime required for soil stabilization using pH.

The maximum dry density (MDD) and optimum moisture content (OMC) of the materials under examination were determined by using the standard Proctor compaction test, ASTM D 698. An automated mixer was used to carefully mix the combinations under examination at a reasonable pace. Following the mixing process, the mixtures were allowed to settle for an hour prior to completion, which corresponded with the hydrated lime's settling time and the amount of time required for the lime to completely react or hydrate with water.

Following ASTM D2850-03 [28], UU triaxial tests were conducted without a saturation or consolidation phase to evaluate the soil's shear strength in short-term conditions. Standard cylindrical specimens were tested to ascertain their shear strength and stress-strain correlations. Proctor compaction test findings are used to produce the treated and untreated samples. The specimens were taken out of the mold after they had been compacted to the proper size, and their height and diameter were measured and recorded. After demolding, specimens were wrapped in plastic sheets and left to cure for one to twenty-eight days in order to prevent moisture loss. Following hardening, the specimens are placed in a triaxial chamber and subjected to three confining fluid pressures: 50, 100, and 200 kPa. At a maximum axial deformation of 20% of the sample height, the deviatoric stress of the analyzed samples was recorded.

3 Results and discussion

Table 5 depicts the variation in pH values of the analyzed clay soil before and after treatment with different additives. The examined clay soil has moderate alkalinity, with a pH of 8.3. The incorporation of NP into the clay soil increased its pH, making it very alkaline. Increasing NP content from 0% to 20% raised the pH of the analyzed soil from 8.3 to 8.6, due to the NP's considerable alkalinity (pH NP = 9). Gadouri et al. [29] observed a similar reaction when investigating the pH variation of the clay–lime–NP combination.

Table 5. The impact of natural pozzolana addition on the pH level of lime-treated clay soil.

Combination	**L0P0**	**L0P10**	**L0P20**	**L2P0**	**L2P10**	**L2P20**
pH	8.27	8.63	8.61	12.2	12.24	12.29
Temperature °C	19.1	19.2	19	19.1	19	19
Combination	**L4P0**	**L4P10**	**L4P20**	**L6P0**	**L6P10**	**L6P20**
pH	12.64	12.69	12.7	12.7	12.74	12.75
Temperature °C	19.1	19	19	19.1	19	19

The examined clay soil has significant reactivity to lime. Table 5 demonstrates a significant increase in pH subsequent to the treatment of both clay soil and the clay–

NP mixture. The tested clay soil's pH increased from 8.3 and 8.6 to 12.7 and 12.75 when 6% lime was added, both with and without 20% NP. The quick reactivity of the lime-clay soil is responsible for the notable rise in pH. Because of the OH-anions created by lime hydration, which encourage the gradual dissolution of silica and alumi-na from clay particles, adding lime to clay soils creates a very alkaline environment.

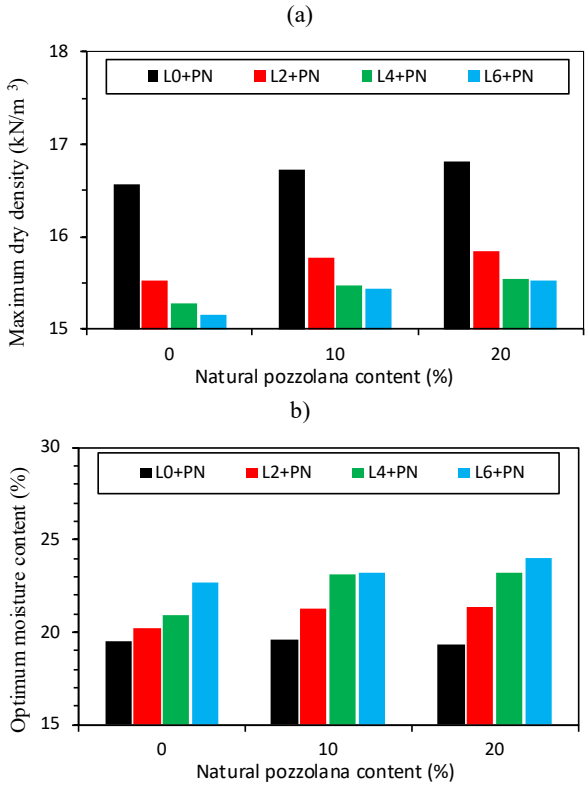

Fig. 3. Compaction characteristics of the treated soil. a) MDD, b) OMC.

The impact of NP incorporation on the compaction characteristics of clay soil treated with lime is shown in Figure 3. The concentration of lime has a direct impact on the design of lime-stabilized soil; as the amount of lime increases, the Maximum Dry Density (MDD) decreases and the Optimum Moisture concentration (OMC) increases. When 6% lime was added to clayey soil, the OMC rose by 16% and the MDD decreased by 8.6%. As the NP content increased, the OMC of the NP-treated soil stayed rather constant. An increase in NP content was associated with a slight increase in MDD. The maximum dry density (MDD) of soil treated with lime and supplemented with varying amounts of NP. However, compared to untreated soil, this rise was less significant. On the other hand, when the NP concentration rose, the OMC of the lime-NP combination rose as well.

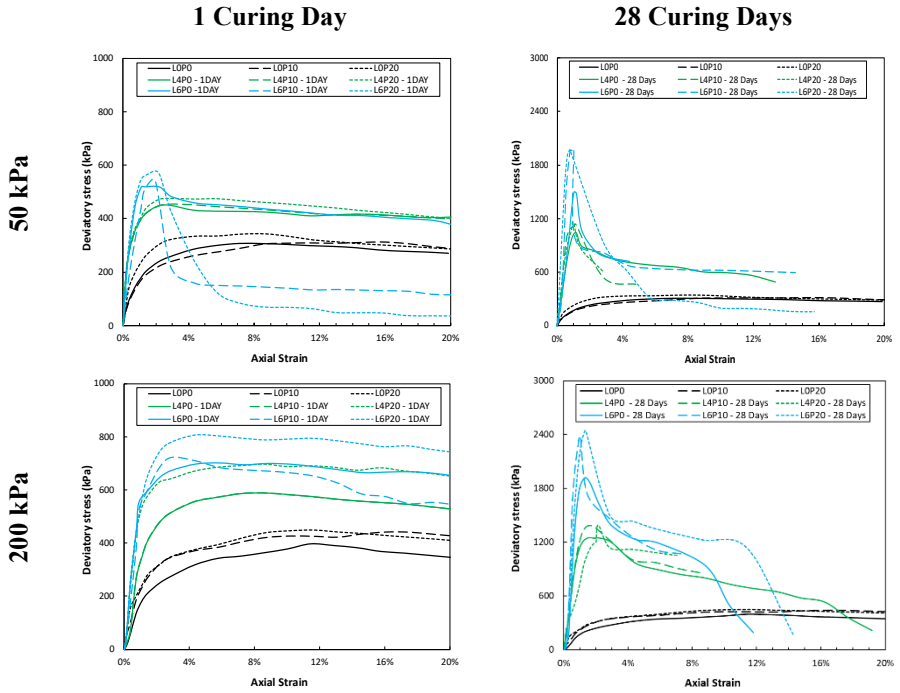

Fig. 4. Stress-strain correlations derived from unconsolidated undrined triaxial studies for lime-NP soil stabilization under different confining pressures.

Figure 4 depicts the impact of lime, NP, and their amalgamation on the outcomes of UU triaxial tests for treated clayey soils at diverse confining pressures and distinct curing times. These figures provide a preliminary investigation of soil behavior before and after treatment with different additives.

From the trials, two curve classifications were produced. Clayey soil and soil with varying NP concentrations are represented by the first curve type, which is characterized by an asymptotic peak-less profile. With peaks indicating the greatest deviatoric stress and a subsequent decrease in stress (residual deviatoric stress) until sample failure, the second type shows the curves of soil treated with a mixture of lime and lime-NP.

The hy-perbolic black curves show the outcomes of both natural soil and NP. Stress rises quickly in the initial phase before slowing down and approaching an asymptotic value, which represents the maximum deviatoric stress. The curves that emerge from the incorporation of NP into the soil closely resemble the clayey soil curve. However, the increase in the samples' MDD results in a little rise in the maximum shear strength. When lime or a mixture of lime and nanoparticles is applied to the soil, peaks appear in the stress-strain curves. Both the lime-treated soil and the lime-NP combination show linearity in their stress-strain curves, which approach 85% of the peak stress. A more

defined shape results from the linearity increasing when the quantity of lime and cure time are increased (Fig. 4).

Maximum deviatoric stress was significantly increased by using lime as a stabilizer, and this improvement was positively correlated with both the quantity of lime used and the curing time. Sivapullaiah et al. [32] and Cai et al. [31] reported similar outcomes. In clay soils, the poz-zolanic interactions of lime, SiO2, and Al2O3 produce cementitious chemicals that significantly increase the soil's strength. Increased confining pressure and longer curing time were associated with a considerable improvement in the shear strength of lime-stabilized clayey soils, which was correlated with varying NP levels. When NP is added to lime-treated soil, the results are better for maximal deviatoric stress than when either NP or lime is used alone. In comparison to the soil treated with just 6% lime, Figure 13 shows that the maximum deviatoric stress of a sample treated with 6% lime, together with 10% and 20% NP, rose by 23.8% and 27.4%, respectively, at a confining pressure of 200 kPa after 28 days of curing. The improvement in the samples' maximum dry density is probably the reason for the significant rise in maximum deviatoric stress for soils treated with a combination of lime and NP as opposed to those treated alone with lime. Depending on the curing period, the addition of the NP increases the amounts of Si and Al in the samples, which in turn increases the pozzolanic reaction and lime content.

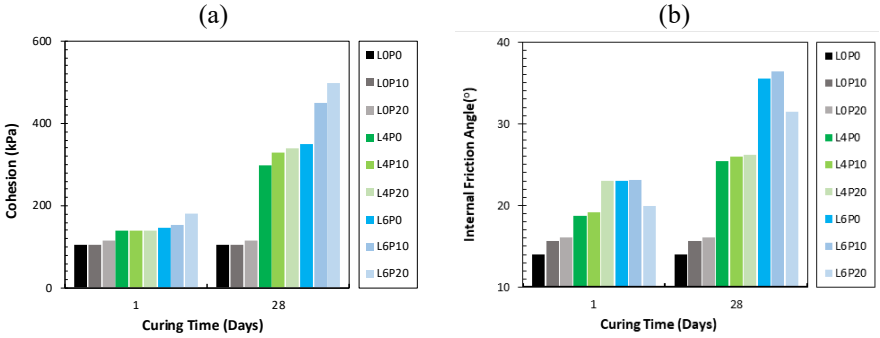

Fig. 5. Variation of the treated samples

The findings of the shear parameters derived from the Mohr circle are shown in Figure 5. Three factors significantly affect the variance of shear parameters in stabilized clayey soil treated with lime and a lime-NP combination, as Figure 5 makes evident. The concentration of lime, the amount of NP combined with lime, and the curing time are the determinants. The shear characteristics significantly improved as the lime concentration rose. The cohesiveness and friction angle of soil stabilized with 6% lime increased from 105 kPa and 14° to 145 kPa and 23°, respectively, after a day of hardening. As the therapeutic duration was extended, the outcomes significantly improved. The cohesiveness and friction angle rose to 350 kPa and 35.53°, respectively, during 28 days of curing. When paired with lime, the increased NP ratio enhanced the samples' cohesion. After 25 days of curing, the cohesiveness of soil stabilized with 6% lime increased from 350 kPa to 450 kPa and 500 kPa with the addition of 10% and 20% NP. Affected by different NP levels, the friction angle of lime-stabilized soil ranged from 31.5° to 36°, reaching its highest at 6% lime and 10% NP.

As the curing period was extended, the shear strength values rose in tandem with the addition of lime and NP contents. First, when lime or a lime-nanoparticle combination is used to stabilize the soil, short-term processes such cation exchange and particle flocculation take place. Cation exchange makes it easier for new chemical bonds to form between particles, which results in the formation of larger aggregates. The cohesiveness of the treated soil is enhanced by this chemical link. Because to flocculation and the creation of micro-ports, the stabilized soil's friction angle has risen. Second, pozzolanic reactions (C-S-H, C-A-H, and C-A-S-H) take place as the curing time rises. Extended reactions lead to particle cementation, which significantly improves cohesiveness in the final curing phases. It increases the friction angle by making the soil unstable and stiff with uneven surfaces. The rise in shear properties with increased NP content is explained by two different sorts of effects. The influence on the physical properties of soil is the first factor. A more robust soil structure results in a higher density of soil. The impact of NP on the chemical properties of lime-stabilized soil is the second factor; an additional pozzolanic reaction involving the lime, silicon, and aluminum in the NP took place.

4 Conclusion

The main goal of this study is to look at how compaction parameters, shear strength, shear properties, and microstructural changes are affected by lime, natural pozzolana, and their combination. The test findings allow for the following deductions to be made:

Higher lime concentrations in lime-stabilized clayey soil with and without NP addition, result in higher pH values. The start of chemical interactions between soil and lime or soil and lime and NP is indicated by the rise in pH.

The addition of NP to the clayey soil slightly increases the maximum dry density, but the optimal moisture content stays mostly unchanged. The addition of lime or a lime-NP mixture to clay soil decreases its maximum dry density and increases the optimal moisture content. The soil stabilized with a lime-NP combination shows more density than that stabilized only with lime.

Clay soil stress-strain curves and their combination with NP show a hyperbolic form without a peak, with peaks appearing when the soil was stabilized with lime or a lime-nanoparticle composite. The peak form increases with increased concentration of lime or lime-NP and a longer curing period, while it decreases with increased confining pressure.

A little increase in maximum deviatoric stress was noted for soil-NP samples. Adding lime as a stabilizer significantly increased maximum deviatoric stress, favorably related with both the amount of lime used and the curing period. The integration of NP into lime-treated soil produces enhanced outcomes for maximum deviatoric stress relative to the application of lime alone.

The shear strength parameter of clayey soil shown a little enhancement after the incorporation of NP. No improvement in shear properties was seen with extended curing

duration. An observable improvement was identified in the cohesiveness and friction angle of soil stabilized with lime and lime combined with NP. This enhancement is based on the lime concentration, NP content, and curing period.

The combination of two local resources—natural pozzolana and lime—may significantly enhance the mechanical qualities of fat clay soil and encourage more land availability for construction projects. In this investigation, samples treated with a 20% natural pozzolana and 6% lime combination showed improved soil strength characteristics.

References

1. Davis LE (1952) Electrochemical Properties of Clays. Clays and Clay Minerals, 1(1): 47–53.
2. Cernica JN (1995) Geotechnical engineering: soil mechanics. ed. Wiley, Californie.
3. Dembicki E, Kisielowa N, Nowakowski H, Osiecimski R (1980) Compactage des fonds marins sableux à l'explosif, Colloque sur le compactage, Paris, l : 295-299.
4. Kirmani SMH (2004) Consolidation of soil for Foundation using sand drains. IEP-SAC Journal, 49-55.
5. Bryson S, El Naggar H (2013) Evaluation of the efficiency of different ground improvement techniques. 18th International Conference on Soil Mechanics and Geotechnical Engineering, Paris.
6. Vitale E, Deneele D, Paris M, Russo G (2017). Multi-scale analysis and time evolution of pozzolanic activity of lime treated clays. Applied Clay Science, 141: 36–45.
7. Long G, Li L, Li W, Ma K, Dong W, Bai C, Zhou JL (2019) Enhanced mechanical properties and durability of coal gangue reinforced cement-soil mixture for foundation treatments. Journal of Cleaner Production, 231: 468–482.
8. Driss, AAE, Harichane, K., Ghrici, M., Gadouri, H. (2022). Assessing the effect of moulding water content on the behaviour of lime-stabilised an expansive soil. Geomechanics and Geoengineering, 17(3), 896-908.
9. Okagbue CO, Yakubu JA (2000) Limestone ash waste as a substitute for lime in soil improvement for engineering construction. Bulletin of Engineering Geology and the Environment, 58(2): 107–113.
10. Driss, AAE, Harichane, K., Ghrici, M. (2021). Effect of natural pozzolana on microstructural behavior and hydraulic conductivity of lime-stabilized clayey soil. Innovative Infrastructure Solutions, 6(4), 1-17.
11. Harichane K, Ghrici M, Kenai S, Grine K (2011) Use of natural pozzolana and lime for stabilization of cohesive soils. Geotechnical and Geological Engineering, 29(5): 759–769.
12. Harichane K, Ghrici M, Kenai S (2018) Stabilization of Algerian clayey soils with natural pozzolana and lime. Periodica Polytechnica Civil Engineering. 62(1): 1–10.
13. Jha AK, Sivapullaiah PV (2015) Mechanism of improvement in the strength and volume change behavior of lime stabilized soil. Engineering Geology, 198: 53-64.
14. Garzón E, Cano M, O`Kelly BC, Sánchez-Soto PJ (2016) Effect of lime on stabilization of phyllite clays. Applied Clay Science, 123: 329–334.
15. Khemissa M, Mahamedi A (2014) Cement and lime mixture stabilization of an expansive overconsolidated clay. Applied Clay Science, 95: 104–110.
16. Sivapullaiah PV, Jha AK (2014) Gypsum induced strength behaviour of fly ash-lime stabilized expansive soil. Geotechnical and Geological Engineering, 32(5): 1261–1273.

17. McCarthy MJ, Csetenyi LJ, Sachdeva A, Dhir RK (2014) Engineering and durability properties of fly ash treated lime-stabilised sulphate-bearing soils. Engineering Geology, 174: 139–148.
18. Ijaz N, Dai F, Meng L, Rehman Z, Zhang H (2020) Integrating lignosulphonate and hydrated lime for the amelioration of expansive soil: A sustainable waste solution. Journal of Cleaner Production, 254, 119985.
19. Hossain KM, Lachemi M, Easa S (2006) Characteristics of volcanic ash and natural lime based stabilized clayey soils. Canadian Journal of Civil Engineering, 33(11): 1455-1458.
20. Harichane K, Ghrici M, Kenai S (2012) Effect of the combination of lime and natural pozzolana on the compaction and strength of soft clayey soils: a preliminary study. Environmental Earth Sciences, 66(8): 2197–2205.
21. Zoubir W, Harichane K, Ghrici M (2013) Effect of lime and natural pozzolana on dredged sludge engineering properties. Electronic Journal of Geotechnical Engineering, 18(c): 589-600.
22. Al-Swaidani A, Hammoud I, Meziab A (2016) Effect of adding natural pozzolana on geotechnical properties of lime-stabilized clayey soil. Journal of Rock Mechanics and Geotechnical Engineering, 8(5): 714–725. https://doi.org/10.1016/j.jrmge.2016.04.002
23. ASTM D2487-06 (2006) Standard Practice for Classification of Soils for Engineering Purposes (Unified Soil Classification System). ASTM International, West Conshohocken, PA, www.astm.org
24. ASTM C125-07 (2007) Standard Terminology Relating to Concrete and Concrete Aggregates. ASTM International, West Conshohocken, PA, www.astm.org
25. ASTM D4972-01 (2001) Standard test method for pH of soils. ASTM International, West Conshohocken. www. astm. org
26. ASTM D6276-19 (2019) Standard test method for using ph to estimate the soil-lime proportion requirement for soil stabilization. ASTM International, West Conshohocken. www. astm. Org
27. ASTM D698-00 (2000) Standard Test Methods for Laboratory Compaction Characteristics of Soil Using Standard Effort (12,400 ft-lbf/ft3 (600 kN-m/m3)). ASTM International, West Conshohocken, PA, www.astm.org
28. ASTM D2850-03 (2003) Standard Test Method for Unconsolidated-Undrained Triaxial Compression Test on Cohesive Soils. ASTM International, West Conshohocken, PA, www.astm.org
29. Gadouri H, Harichane K, Ghrici M (2017) Assessment of sulphates effect on pH and pozzolanic reactions of soil–lime–natural pozzolana mixtures. Int J Pavement Eng 20(7):761–774.
30. Kinuthia JM, Wild S, Jones G (1999) Effects of monovalent and divalent metal sulphates on consistency and compaction of limestabilised kaolinite. Appl Clay Sci 14(1–3):27–45.
31. Cai Y, Shi B, Ng CWW, Tang CS (2006) Effect of polypropylene fiber and lime admixture on engineering properties of clayey soil. Engineering Geology, 87(3-4): 230–240.
32. Furlan AP, Razakamanantsoa A, Ranaivomanana H, Levacher D, Katsumi T (2018) Shear strength performance of marine sediments stabilized using cement, lime and fly ash. Construction and Building Materials, 184: 454–463.

MindSense: A Multimodal AI System for Early Mental Health Detection

Rinku Raheja[1][0000-0003-2720-0072], Prabhash Chandra Pathak[2][0000-0001-5704-0028], Syed Anas Ansar[3][0000-0001-7387-8912], Aadya Mishra[4][0009-0007-3182-7480], Charu Srivastava[5][0009-0007-2359-2802], Amit Kumar Srivastava[6][0009-0007-7675-4086]

[1,4,5,6] National PG College Lucknow, India
[2, 3] Babu Banarasi Das University, Lucknow, India

rinkuraheja85@gmail.com, pathakprabhash2@gmail.com, syed000anas@gmail.com, aadyamishra1108@gmail.com, charusri2904@gmail.com, amit_sri_in@yahoo.com

Abstract

Mental health conditions, such as anxiety and depression, frequently remain undiagnosed due to the reliability of estimates from subjective approaches involving self-reported questionnaires and clinician observations. Micro-expressions that are subtle involuntary facial movements offer a more dependable way to provide insight into the suppressed emotional state; however, capturing them in real-time will generally necessitate AI-driven analysis for optimal detection. This study assesses how AI, and particularly deep learning models (e.g., CNNs and LSTMs), can enhance micro-expression analysis for early mental health diagnosis. Moreover, AI-based indications will be compared to objective estimates made through traditional methods concerning accuracy, speed, and scalability. While the findings of AI-based indications for diagnosis are encouraging, ethical and clinical considerations will need to be resolved to properly implement AI in this field. Also, the suggested system uses EEG signals, the way people speak and social media trends to create a detailed analysis system. It aims to help ensure reliable diagnosis and give a practical, on-going solution for proactive mental health screening.

Keywords: Artificial Intelligence (AI), Micro-Expression Recognition, Mental Health Diagnosis, Deep Learning

1. INTRODUCTION

1.1 Mental Health Conditions and Their Diagnostic Restrictions

Due to their subjective character and propensity to conceal their feelings, behavioural and mental health conditions such as depression, anxiety, and bipolar disorder frequently go undiagnosed in their early stages [1]. These approaches usually rely on self-reported surveys, patient interviews, and clinician evaluations, which may be biased by the physician, patient dishonesty, or misunderstandings [2]. The requirement for a precise diagnosis has grown as mental health cases are increasing linearly with time. By 2030, depression is expected to overtake all other causes of disease problems worldwide, according to the World Health Organization [2].

1.2 Role of Micro-Expressions in Mental Health Conditions

Unconscious facial display of emotion known as micro-expressions happen when someone is attempting to conceal their actual emotions. These subtle expressions, even when someone tries to hide them, are signs of genuine emotions, according to Paul Ekman

(2009) [4]. Micro-expressions are a reliable way to identify concealed emotions linked to mental health issues since they are harder to regulate than ordinary facial expressions [5]. These fleeting expressions, however, are difficult to notice and cannot be interpreted without the aid of technology [6].

1.3 The Emergence of AI in Micro-Expression Analysis

Some workable techniques for identifying and interpreting the micro-expressions are provided by artificial intelligence (AI) technology [5]. Large datasets may be processed and intricate patterns can be identified by advanced AI models, especially in Machine Learning (ML) and Deep Learning. High accuracy facial emotion identification, including micro-expressions, has been demonstrated by methods such as Convolutional Neural Networks (CNNs) and Long Short-Term Memory (LSTM) networks [6]. The entire method of conducting mental health examinations would be altered by these AI-powered technologies. AI can also track changes in facial expressions over time, which enables early intervention in the detection of emotional distress [3].

1.4 Research Questions and Objectives

The purpose of this study is to investigate how early detection of mental health problems can be enhanced by AI-based micro-expression recognition. It answers the following important queries:

1. How does AI cognition improve early mental health condition detection in micro-expression evaluation?
2. Which AI methods are currently in use for emotion recognition, and how well-suited are they for usage in clinical settings?
3. What obstacles and ethical issues surround the use of AI in mental health diagnosis?

Reviewing current studies and technical achievements in this field as well as the potential for further advancements is the main goal.

1.5 Significance of the Study

This research is important because it contributes to a more precise, non-invasive, and scalable method of treating mental health conditions. Early detection of mental problems is crucial to minimizing their long-term effects. Conservative diagnostic methods frequently rely on patient self-disclosure and subjective judgments, which might not fully capture emotional discomfort [1]. Data-driven and more objective mental health evaluations might be possible with AI-powered micro-expression analysis [5].

The potential of AI in this evolving early mental health diagnosis is highlighted in Figure 1, which compares AI-based detection with conventional clinician-based diagnosis [6]. Matplotlib was used to create this graph in Python. Because AI-driven techniques can analyse enormous datasets and identify subtle emotional indicators, they perform better in terms of accuracy, speed, and objectivity [3].

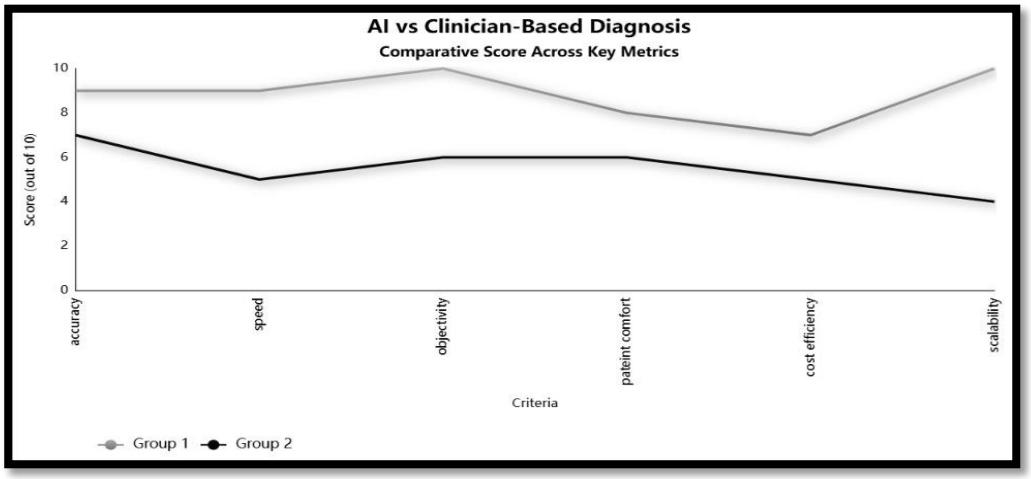

Fig 1: Comparison of AI model and traditional method

2. RELATED WORK

The following five models or techniques were created recently for AI-driven micro-recognition with the goal of detecting mental health disorders early:

2.1 Analysing EEG signals using deep learning

This model demonstrated its capacity to efficiently interpret neuroimaging data by achieving a high classification accuracy of roughly 93% to 955% in EEG signals [7]. EEG signals are first filtered to eliminate noise, and then complex signals are converted into the frequency domain using the Fast Fourier Transform (FFT) in order to identify significant patterns.

Equation: $$X(f) = \sum_{n=0}^{N-1} x(n)\, e^{-j2\pi f n/N} \quad (1)$$

where:

- X(f) is the transformed EEG signal,
- x(n) is the original time-domain signal,
- N is the number of samples
- $e^{-j2\pi fn/N}$ is a complex exponential function that helps decompose the signal into its frequency components.

It emphasizes impartial data and eliminating bias in evaluations of mental health. It can be used; however, it is restricted to EEG data and requires specific tools and knowledge. It might overlook multimodal elements that are crucial for comprehensive mental health diagnosis, like linguistic cues. It has certain drawbacks that impair diagnostic precision, such as its inability to account for sociocultural variables or mental health biases [7][12].

2.2 XAI for mental health detection

In addition to utilizing domain-specific transformers tailored for mental health applications to increase accuracy, this model incorporates easily understood aspects like sentiment analysis and syntactic complexity, which boost transparency and confidence in AI models [9]. It highlights key terms linked to anxiety or sadness (such as "hopeless" and "alone") using the TF-IDF approach. The rationale behind the designation of specific phrases as markers of mental health problems is supported by TF-IDF scores. The following is the equation:

$$TF - IDF = TF \times \log\left(\frac{N}{DF}\right) \quad (2)$$

where:

- TF (Term Frequency) represents how often a word appears in a document.
- N is the total number of documents in the dataset.
- DF (Document Frequency) is the number of documents containing the term.

However, explainability techniques like LIME may generalize complicated mental health problems, potentially resulting in misunderstandings, and it is reliant on language aspects, thus excluding non-verbal clues like physiological signals or micro-expressions. Furthermore, the model needs frequent updates to adapt to changing diagnostic standards and mental health research because it suffers from cultural sensitivity and partialities in training data, which can lead to incorrect diagnoses for minority populations. [20] [21]

2.3 Multimodal AI models for depression detection

This model offers a comprehensive approach to depression diagnosis while demonstrating increased accuracy by utilizing a variety of data sources, including facial expressions, speech characteristics, and physiological signs like pupil dilation [8]. Reliability is decreased by multimodal systems' high workload, need for real-time data gathering across modalities, artificiality issues in real-world contexts, and the fact that within-group variations frequently outweigh between-group variations. Softmax Activation is used to assign probability to various classes in models that classify mental health states. It guarantees that the severity of depression is represented as a probability distribution.

Equation: $$P(y_i) = \frac{e^{z_i}}{\sum_j e^{z_j}} \quad (3)$$

where:

- P(y_i)is the probability of class i (e.g., depression level).
- z_i is the model's raw prediction score for class i.
- The denominator ensures all class probabilities sum to 1.

Furthermore, the model has issues with ecological soundness since lab-based data might not translate well to real-world situations and might not accurately capture subtle culture representations of emotional states of discomfort [9][12].

2.4 Generative network for ADHD diagnosis

This method demonstrates the ability to detect ADHD using multimodal characteristics by processing complex neuroimaging data with ease using autoencoder-based generative networks, achieving a modest classification accuracy of 67% [10]. Additionally, compare the model's input and output using reconstruction loss. The high error rate in neuroimaging data from ADHD patients aids in the diagnosis of ADHD by identifying anomalies in brain activity. The following equation is applied here:

$$L = \| X - \widehat{X} \|^2 \quad (4)$$

where:

- X is the original input data (e.g., EEG or fMRI scan).
- $\widehat{X}$ is the reconstructed version produced by the model.
- The squared error ensures larger mistakes are penalized more.

However, its reliance on neuroimaging restricts accessibility and scalability in conceptual settings, and its comparatively low accuracy in comparison to other methods suggests that feature extraction processes need to be further refined. Furthermore, it ignores ethical issues like "stealth science" and algorithm development openness, and it ignores behavioural or emotional indicators, which are essential components of diagnosing ADHD outside of neuroimaging data. [14]

2.5 AI-driven micro-expression recognition in video consultations

This approach uses computer vision techniques to identify subtle facial movements during video consultations, allowing for remote mental health status monitoring. It also provides scalability through telehealth platforms and mobile apps. [11]. Euclidean The intensity of micro-expression is measured by distance. Movement that surpasses the threshold of micro-expressions, which are measured over milliseconds, may reveal emotions associated with mental health disorders. The above method's equation is:

$$D = \sqrt{\left(a_2 - a_1 \right)^2 + \left(b_2 - b_1 \right)^2} \tag{5}$$

where:

- $\left(a_1, b_1 \right) and \left(a_2, b_2 \right)$ are the coordinates of two facial landmarks (e.g., eyebrow raise, lip curl).
- D represents how much a facial feature has moved between two frames [15].

Micro-expression analysis, however, is susceptible to changes in illumination, camera quality, and user position, which reduces consistency in uncontrolled conditions. Additionally, algorithms that lack cultural sensitivity may misread tension-related cultural expressions [11][12]. Furthermore, issues like limited sample sizes and the low ecological validity of training datasets for micro-expression analysis models are not addressed, and privacy concerns regarding video analysis are still unresolved, which restricts user adoption and trust. After examining each of the aforementioned models, we have identified a few issues that these models are unable to resolve. They are:

- Ecological validity
- Cultural sensitivity
- Transparency issues
- Integration with clinical practices

3. PROPOSED METHODOLOGY

A new model called MindSense a Multimodal AI System for Early Mental Health Detection can be proposed if we examine the shortcomings and difficulties of the abovementioned AI models for the identification of micro-expressions in health detection.

Aim: to retain high accuracy and real-time performance while integrating multimodal data sources, improving ecological validity, cultural sensitivity, and transparency.

3.1 The architecture of the proposed model:

Majorly, it combines three components –

3.1.1 Multimodal Data Integration – This model will take into account physiological signals, speech characteristics, face micro-expressions, and even textual information from self-reports or social media. Accuracy will be improved by integrating data from a hybrid deep learning architecture. A hybrid deep learning architecture will be employed in this, with CNNs based on image-based micro-expressions, RNNs for sequential audio and text input, and a feature fusion layer to combine these models. We will use an attention-based convolutional fusion layer to fuse these features together, making sure that each modality makes a dynamic contribution based on their applicability. Equation 6 defines the fusion process:

$$F\_fused = Conv(Attention(Concat([F\_face, F\_voice, F\_EEG, F\_text]))) \quad (6)$$

where:

- F_face, F_voice, F_EEG, F_text represent feature maps from micro-expressions, vocal tone analysis, brainwave activity, and linguistic sentiment analysis, respectively.
- Concat denotes the concatenation of these feature maps,
- Attention is an attention mechanism that learn to weight each feature map dynamically,
- Conv represents a convolutional layer that fuses the weighted feature maps into one representation [22] [23]

3.1.2 Cultural Adaptation module - This culturally advanced layer will be incorporated into the model to take sociocultural variations in emotional displays and linguistic patterns into consideration. Here, region-specific datasets and transfer learning approaches will be employed to modify the forecasts for the large population. [16]

3.1.3 Explainability and Ethical Design - In order to give clear insights into its decision-making process and guarantee that patients and physicians can comprehend the reasoning behind forecasts, the model will integrate explainable AI approaches such as LIME or SHAP. A fairness parameter is tracked during training to make sure the design is ethical, and adversarial debiasing techniques will be used to reduce any potential biases pertaining to protected properties. [17] [24].

3.2 Required Datasets and Preprocessing

3.2.1 Datasets:

A wide range of diverse datasets will be needed, including multilingual social media posts from sites like Twitter and Reddit, physiological signals from wearable technology, voice recordings from DAIC-WOZ, and facial expression recordings from CASME and SAMM. Datasets should cover a wider variety of emotional expressions and cultural situations in order to train the model within the convolutional fusion layer. Through collaborations with mental health groups, region-specific data can be added to publicly accessible datasets. [18]. The ratio of physiological signals, voice recordings, facial expressions, and social media data that we can utilize in the Mindsense is shown in Figure 2. This fictitious graph was created in Python with the help of matplotlib.

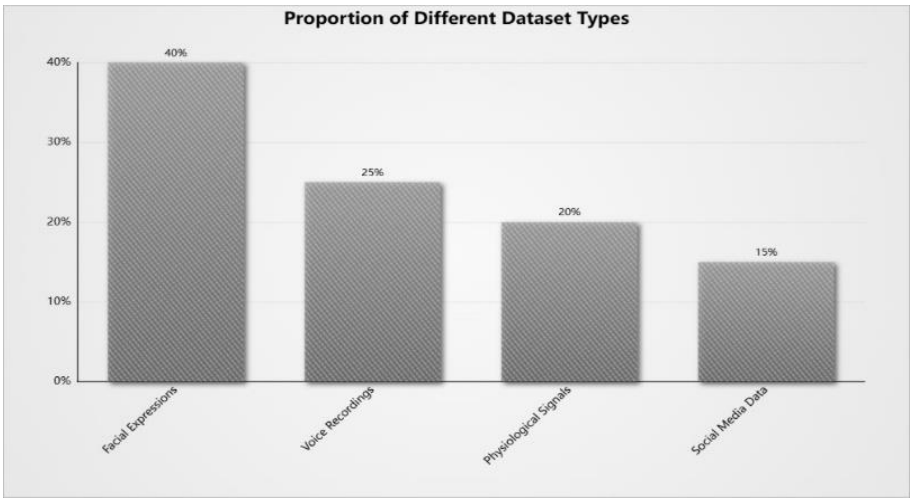

Fig 2: Proportion of Different Types

3.2.2 Preprocessing:

Normalized videos of face expressions in various lighting conditions for accurate alignment, audio signals transformed into spectrograms, physiological signals utilizing wavelet filtering and segments into fixed-length, and text data for sentiment analysis are all examples of data preprocessing. In order to deal with tiny sample numbers, data augmentation techniques will use generative adversarial networks (GANs) to create synthetic examples.

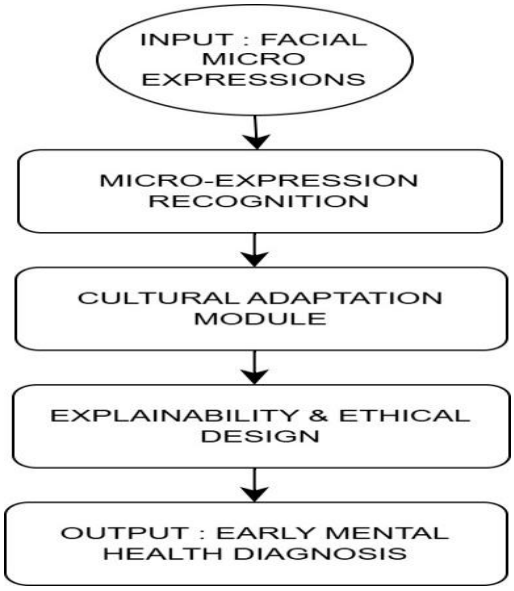

Figure 3: Data Preprocessing Pipeline

Potential improvements that this model should imply are:

- Real-Time Processing: this model will demonstrate real-time processing by combining information in a sophisticated way. To save time, it will concentrate on the most crucial details.

- Improved Accuracy: The model will be more adept at comprehending the relationships between various kinds of data.
- Scalability: By adding more layers or just broadening its emphasis, the model can be made more potent.
- Ethical safeguards: guarantee that it is impartial and fair.

3.2.3 Theoretical Framework

Affective computing, multimodal data fusion, and explainable AI are just a few of the theories that underpin this study of AI-driven micro-expression recognition for mental health detection. By combining these ideas with references to the gaps in ecological validity, cultural sensitivity, and ethical AI design, the Mindsense model expands on previous research.

3.2.4 Affective computing and emotion recognition-

Rapid, involuntary facial emotions are known as micro-expressions, and while current AI models function in the emotional computing area, they frequently fall short when faced with real-world unpredictability. This issue would be resolved with Mindsense. [18]

3.2.5 Multimodal AI in Mental Health Analysis-

Although traditional models have shown potential in identifying depression, their capacity to generalize across populations is still constrained. For further evaluation, Mindsense improves robustness with textual data, physiological signals, and facial micro-expressions [19].

3.2.6 Cultural and Ethical Considerations in AI-

Non-diverse training data causes cultural bias in many AI models. To ensure inclusion, Mindsense employs a Cultural Adaptation Module that modifies predictions in response to sociocultural differences in emotional expression. Transparency is increased by AI techniques like SHAP and LIME, which enable patients and clinicians to understand the model.

This framework offers a starting point for evaluating current models against Mindsense in terms of clinical application, inclusivity, scalability, and accuracy.

4. Comparative Analysis

The Deep Learning (EEG) model has high accuracy (93-95%) but has minimal scalability because it requires the use of EEG hardware and settings whereas they are inherently low in ecological validity, cannot be culturally adapted and are black-box explainable. It also has a very limited application in the clinic.

XAI in Mental Health application is based on the linguistic features that can accurately analyse the text. it is more explainable (through XAI) and it is rather scalable with low ecological validity and cultural sensitivity. Clinical integration is moderate and primarily in NLP instruments.

Multimodal AI based on facial, voice and physiological measures is relatively accurate to high accuracy, is usually computationally intense and maybe low to moderate in terms of ecological validity. It is not explainable by much and not adapted to culture.

Generative Networks (ADHD) are based on low accuracy neuroimaging of 67 percent. They are not scalable because of the requirements of MRI, suffers ecological validity and lacks cultural sensitivity. They are not explainable and have early stages of research.

The presence of video data is important to assess the assess the accuracy of AI-Driven Micro-Expression analysis, which relies on the quality of a video. It possesses moderate scalability, ecological validity but no cultural sensitivity and has black-box explainability. It is predominantly applied in the research context.

Instead, the proposed model Mindsense model fuses voice, physiological, facial and text features to achieve high accuracy with the multimodal fusion. It shows high ecological validity, cultural adaptability and high scalability. It is highly explainable on SHAP/LIME and has been specifically built to integrate into the real world in clinical settings.

5. CONCLUSION

The Mindsense a multimodal for early mental health detection system uses multimodal data sources like physiological signals, content analysis, and facial micro-expressions with voice highlights to improve accuracy, inclusivity, and real-world applicability in AI-driven mental health detection. While its clarifying techniques promote openness and trust among clients, its social adaptation module increases affectability to sociocultural differences, decreasing tendency and boosting common outcomes throughout diverse populations.
Future research should focus on gaining practical approval through clinical trials, improving computational efficiency for real-time handling on edge devices, strengthening information security through processes like unified learning, advancing cross-cultural adaptability through region-specific datasets, and integrating Mindsense into healthcare systems for consistent appropriation in diagnosis and treatment. By addressing these issues, Mindsense will be able to transform the early detection of mental health issues by providing a flexible, accurate, and ethical AI-powered solution for individuals, physicians, and analysts worldwide.

REFERENCES

[1] D. C. Mohr et al., "Challenges in Subjective Assessment of Mental Health: Bias and Reliability in Traditional Diagnostic Methods," IEEE J. Biomed. Health Inform., vol. 24, no. 5, pp. 1234–1245, 2020.
[2] S. M. Ahmed et al., "Global Burden of Depression: Trends, Projections, and Implications for Healthcare Systems," IEEE Access, vol. 10, pp. 5678–5690, 2022.
[3] K. E. Schueller et al., "AI-Driven Solutions for Early Detection of Mental Health Disorders," IEEE Trans. Inf. Technol. Biomed., vol. 27, no. 3, pp. 891–902, 2023.
[4] P. Ekman, "Micro-Expression Recognition in Clinical Psychology: A Review," IEEE Trans. Neural Syst. Rehabil. Eng., vol. 28, no. 7, pp. 1524–1534, 2020.
[5] Y. Li et al., "Automatic Micro-Expression Recognition for Mental Health Assessment Using Deep Learning," IEEE Trans. Affect. Comput., vol. 13, no. 2, pp. 678–690, 2022.
[6] J. Wang et al., "Facial Micro-Expression Analysis in Mental Health Diagnostics: Challenges and Opportunities," IEEE J. Biomed. Health Inform., vol. 26, no. 8, pp. 3812–3823, 2022.
[7] R. Sharma et al., "Deep Learning-Based EEG Signal Classification for Mental Health Assessment," IEEE Trans. Neural Syst. Rehabil. Eng., vol. 30, pp. 2345–2354, 2022
[8] S. Poria et al., "Multimodal Fusion for Depression Detection: Challenges and Opportunities," IEEE Trans. Affect. Comput., vol. 14, no. 3, pp. 1456–1469, 2023
[9] J. Devlin et al., "Explainable AI for Mental Health Diagnostics: Syntactic and Sentiment Analysis Using TF-IDF," IEEE J. Biomed. Health Inform., vol. 25, no. 6, pp. 2112–2123, 2021
[10] L. Chen et al., "Autoencoder-Driven Generative Networks for ADHD Diagnosis Using Neuroimaging Data," IEEE J. Transl. Eng. Health Med., vol. 11, pp. 1–12, 2023
[11] M. Wang et al., "AI-Driven Micro-Expression Analysis in Telehealth: A Computer Vision Approach," IEEE Trans. Med. Imaging, vol. 41, no. 8, pp. 1890–1901, 2022
[12] *A. Gupta et al., "Ethical and Cultural Challenges in AI-Driven Mental Health Diagnostics," IEEE Access*

[13] Puneet Kumar, Sarthak Malik, and Balasubramanian Raman, "Interpretable Multimodal Emotion Recognition using Hybrid Fusion of Speech and Image Data," arXiv preprint arXiv:2208.11868, Jan. 2023
[14] D. C. Lohani and B. Rana, "ADHD diagnosis using structural brain MRI and personal characteristic data with machine learning framework," Psychiatry Research: Neuroimaging, vol. 334, p. 111689, Sep. 2023. DOI: 10.1016/j.pscychresns.2023.111689
[15] P. Gupta, M. Kumar, and S. Prasad, "Quantitative Analysis of Euclidean Distance to Complement Qualitative Analysis of Facial Expressions," Journal of Facial Expression Recognition and Analysis, vol. 8, no. 4, pp. 112-124, 2023. [Online]
[16] S. Sittar, I. Mladenic, and M. Arango Monnar, "Predicting Transfer Learning Success in Offensive Language Detection: The Role of Cultural Sensitivity," Findings of the Association for Computational Linguistics: EMNLP 2023, pp. 1234–1245, Dec. 2023. [Online].
[17] M. Panda and S. R. Mahanta, "Explainable Artificial Intelligence for Healthcare Applications Using Random Forest Classifier with LIME and SHAP," arXiv preprint arXiv:2311.05665, Nov. 2023. [Online].
[18] J. Liu, Y. Zhang, and Z. Liu, "AI-Driven Early Mental Health Screening: Analyzing Selfies of Individuals," arXiv preprint arXiv:2410.05450v2, Dec. 2024. [Online]. Available
[19] H. Liu, "Emotion Detection through Body Gesture and Face," arXiv preprint arXiv:2407.09913, Jul. 2024. [Online]. Available
[20] X. Xu, K. Zhou, Y. Zhang, Y. Wang, F. Wang, X. Zhang, "Faces of the Mind: Unveiling Mental Health States Through Facial Expressions in 11,427 Adolescents," arXiv preprint arXiv:2405.20072, May 2024. [Online]. Available:
[21] G. A. Basílio, T. B. Pereira, A. L. Koerich, H. Tavares, L. Dias, M. G. da S. Teixeira, R. T. Sousa, W. H. Hisatugu, A. S. Mota, A. S. Garcia, M. A. K. Galletta, T. M. Paixão, "AI-Driven Early Mental Health Screening: Analyzing Selfies of Pregnant Women," arXiv preprint arXiv:2410.05450, Oct. 2024. [Online]. Available
[22] Mamieva, Dilnoza, et al. "Multimodal Emotion Detection via Attention-Based Fusion of Extracted Facial and Speech Features." Sensors, vol. 23, no. 12, 2023, p. 5475
[23] Priyasad, Darshana, et al. "Attention Driven Fusion for Multi-Modal Emotion Recognition." arXiv preprint, arXiv:2009.10991, Sept. 2020.
[24] Sun, Jimin, Hwijeen Ahn, Chan Young Park, Yulia Tsvetkov, and David R. Mortensen. "Cross-Cultural Similarity Features for Cross-Lingual Transfer Learning of Pragmatically Motivated Tasks." Proceedings of the 16th Conference of the European Chapter of the Association for Computational Linguistics: Main Volume, Association for Computational Linguistics, 2021, pp. 2403–2414.

Effect of Brick Waste Powder on the Shear Behaviour of Cement treated Sandy Soil

Chamma Fatma zohra[1], Missoum benziane Mehdi[1], Flitti Abdelhamid[1], Della Noureddine[1]

[1] University of Hassiba Benbouali of Chlef, Chlef 02000, Algeria
f.chamma22@univ-cglef.dz

Abstract. In recent years, it has been proclaimed that Portland cement addition enhanced the mechanical properties of sandy soils; although using high cement content would increase construction costs. Thus, instead of increasing the cement content to improve the engineering properties of soils, economical solutions can be utilized as alternative materials such as construction and demolition waste. This paper aims to evaluate the shear strength parameters of stabilized cement samples to assess the influence of BWP proportions (2%, 4%, 6%, 8%) on these parameters. Laboratory shear box tests were conducted under multiple conditions, the mixture specimens were prepared in a dense state Dr=80%, at a moisture content of 10%, and the samples were cured for 7 days. The findings indicate that the maximum shear strength is enhanced with the augmentation of BWP content. In addition, the increase in BWP content promotes both cohesion and internal friction angle.

Keywords: C and D valorization, sand treatment, Shear test.

1 Intoduction

Due to the rapid population growth, it has become a significant challenge for the construction industry to provide habitable areas that comply with the geotechnical performances needed for a construction project. In geotechnical engineering, the soil improvement field broadened during the past decade, this technique is used to improve the mechanical properties of problematic soils such as shear strength, permeability, compressibility, and durability [1]. Soil improvement may be divided into physical, mechanical, and chemical stabilization methods

Chemical stabilization is a technique that consists of adding reagent materials that enhance the mechanical properties of soils to meet the required qualifications, for instance: cement, lime, and fly ash [2]. Portland cement is a widely used additive when it comes to soil treatment, it has been beneficial in many applications, such as foundation engineering, pavement construction, and soil improvement [3]. Former studies explored the efficiency of cement stabilization in enhancing sand`s mechanical properties.

However, the cement manufacturing process requires large amounts of raw materials and energy. The consumption of raw materials in the construction industry has reached 50% in developing countries [4], which is not considered a cost-efficient solution nor

environmentally friendly. Moreover, the concentration of C and D waste disposal generates concerns due to the large occupation of landfills, environmental distress, as well as the shortage of natural resources [5].

Construction and demolition waste is a combination of inert and non-inert materials resulting from construction, demolition, and renovation projects. It includes a diversity of materials such as plastics, concrete, glass, metal, masonry, and wood [6,7]

Seeing that Construction and demolition waste occupies major areas in landfills on the one hand, and the depletion of non-renewable materials in the construction industry on the other hand impelled researchers into valorizing C and D waste materials [8,9]

Many studies have been carried out to investigate the potential of utilizing C and D waste in different geotechnical applications. Ajay Sharma et al 2023 explored the characteristics of recycled concrete aggregates (RCA), recycled brick aggregates (RBA), sand(S), and their mixture, partially or entirely to be used as embankment or reinforced earth fills; adding RCA and RBA enhanced geotechnical properties of sand including shear strength parameters and CBR, in addition to a decrease in hydraulic conductivity of sand. The improvement in CBR values leads to the possibility of minimizing the thickness of pavement base/sub-base layers [10]

2 Materials and methods:

2.1 Sand

The soil used in this study is sand collected from the Chlef river banks north of Chlef (Algeria). Once collected and transported to the laboratory, the sand was dried at 105° for 24 h and then sieved to remove particles larger than 2 mm.
The particle size distribution curve of the sand used is illustrated in Fig. 1 and its physical properties are presented in Table 1.

Table 1. Physical properties of Chlef sand.

Properties	Value
Uniformity coefficient, Cu (.)	3.25
Coefficient of curvature, Cc (.)	0.99
Medium size, D_{50} (mm)	0.52
Maximum diameter, D_{max}	2.00
Specific density, GS (.)	2.69
Maximum void ratio, e_{max} (.)	1.05
Minimum void ratio, e_{min} (.)	0.64

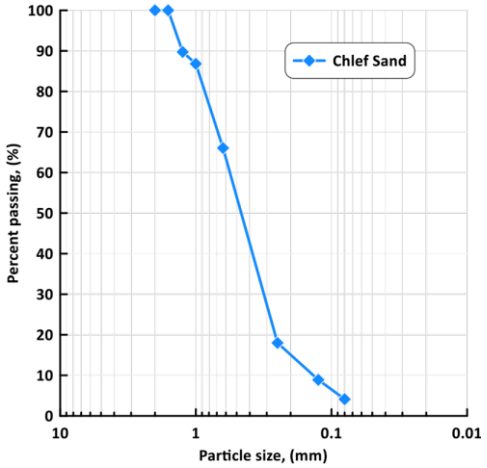

Fig. 1. Particle size distribution of Chlef sand

2.2 Cement

The cement used in this study is Portland cement with limestone (CEM-II/B-L 32.5 N), manufactured by LAFARGE company following the Algerian standard (NA 442-2013) and the European standard (EN 197-1:2011) .

2.3 Brick waste powder

The brick waste utilized in this study was collected from a building waste dump in Chlef region. The brick waste was first cleaned with water to remove dust residue, then oven-dried at 105° for 24 h. After that, it was crushed using the Micro-Deval machine and then sieved to remove particles larger than 80 microns in diameter to obtain a homogeneous powder.

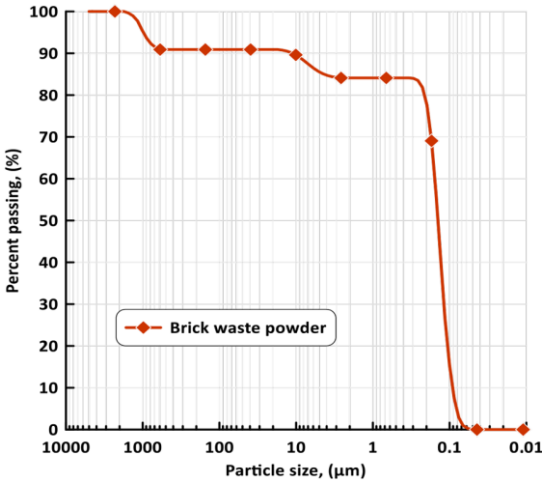

Fig. 2. Particle size distribution of BWP

2.4 Methods

A series of direct shear tests were performed on sand mixed with different percentages of cement (0, 5, 7.5, and 10%) and BWP (0, 2, 4, 6 and 8%). All samples have a cross-section of 60 × 60 mm^2 and a width of 20 mm. To prepare the samples, the dry mass of the sand-cement-brick powder are mixed together, then a water content of 10% is added to the mixture and blended manually.

The mixture was then placed in a mould of dimensions 60 × 60 × 20 mm^3 in three layers. To achieve the dense state, each layer was subjected to 25 strokes. The mixture was allowed to air-dry at room temperature for curing time of 7 days. At the end of this period, the mixture was ready for testing where it was removed from the mould and placed directly in the shear box

3 Results and discussion

3.1 Influence of BWP on cemented sand:

The evolution of the shear strength in terms of horizontal displacement of uncemented and cemented sand samples treated with various contents of BWP (0, 2, 4, 6, 8%) subjected to a normal stress of 50 kPa are presented in the figure 3. It can be seen from the figures an increase of the shear strength of cemented samples until a maximum strength followed by a sharp decrease indicating a very rigid internal structure however, uncemented sand samples depicted no peak strength. In addition, it is noted from figures 3 a,b and c that an increase in cement content leads to an augmentation au the maximum shear strength. Furthermore, a similar effect was observed regarding the introduction of BWP in the cemented samples where it was found that the shear strength notably increased with an increase of BWP content. For instance, the shear strength of the samples with 7.5% cement containing BWP increased compared to the reference sample to attain 260.17; 369.72; 446.06 and 562.3 kPa for proportions of 2%, 4%; 6%, and 8% respectively. This result is due to the BWP filling the void between cement particles binding them at an early stage. Afterwards, pozzolanic reactions occur due to the elevated oxide proportions (SiO_2, Al_2O_3…) in BWP, which promotes the hydration process of cement and augments its shear strength.

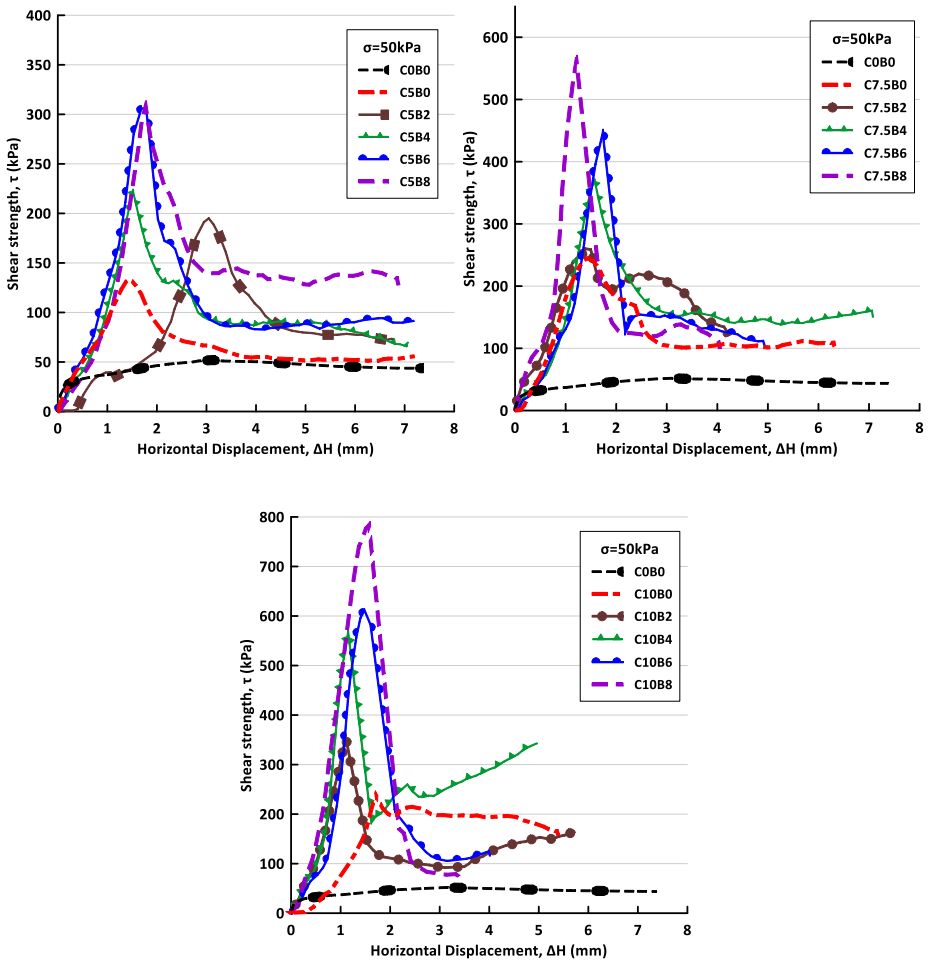

Fig. 3. The evolution of shear strength in terms of horizontal displacement:(a) Samples with 5% cement content, (b) samples with 7.5% cement content, (c) samples with 10% cement content

Curves of vertical displacement in terms of horizontal displacement of cemented-sand samples treated with different proportions of BWP are presented in Figure 4. It can be observed that the uncemented sand specimen exhibits a contractive behavior. However, the cemented sand samples with and without BWP manifested initially a contractive behavior which was parallel with an increase in the shear strength, once the peak shear strength is reached the contractive behavior is followed by dilatative one. furthermore, it was noticed that an increase in BWP content leads to an augmentation of the sample`s dilatancy. This result indicates a positive effect of BWP on the volumetric behaviour of cement stabilized sandy soils.

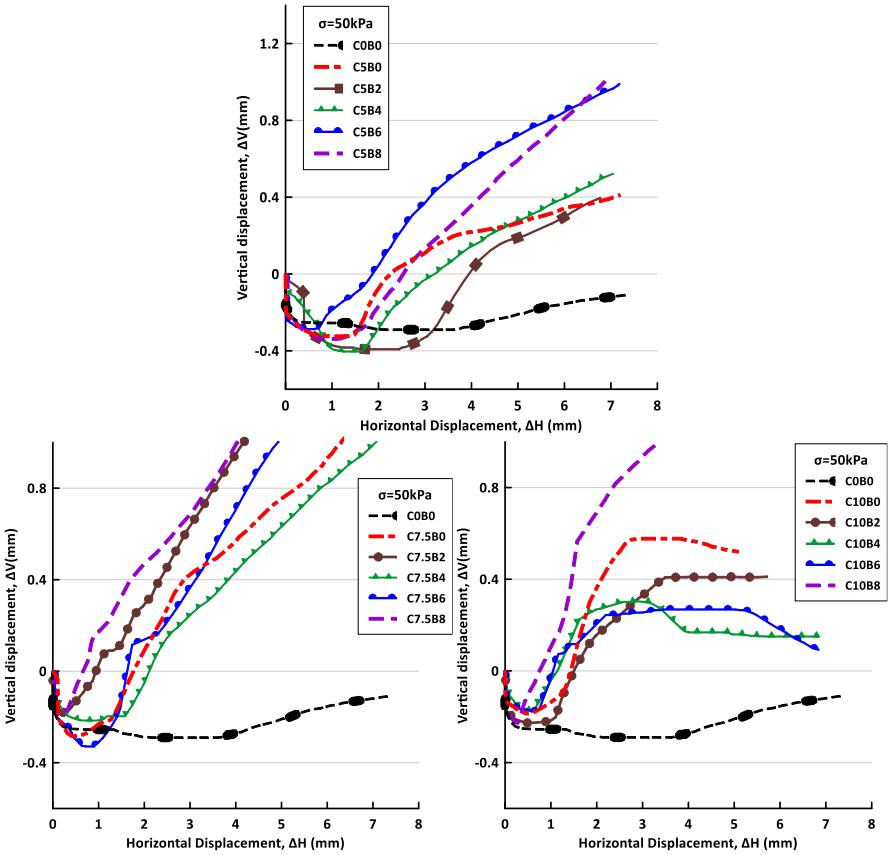

Fig. 4. The evolution of vertical displacement in terms of horizontal displacement:(a) Samples with 5% cement content, (b) samples with 7.5% cement content, (c) samples with 10% cement content

Figure 5 displays the evolution of the cohesion and internal friction angle as a function of BWP content of uncemented and cemented sand samples. It's clear from the curves that both parameters are increasing significantly with the increase of BWP content. The reference sample recorded a cohesion value of 191.67 kPa and was increased by 187% for the sample treated with 8% BWP reaching a cohesion of 550.75 kPa. This amelioration is directly linked to the role of BWP in occupying the voids between the cement particles which promotes the interlocking and adhesion between sand, cement, and BWP binding more efficiently all components of the matrix.

Moreover, the internal friction angle decreased when introducing 8% BWP by 75% to reach 11.07° compared to the reference sample estimated at 45°. This result is mainly attributed to the sub-rounded shape of BWP particles.

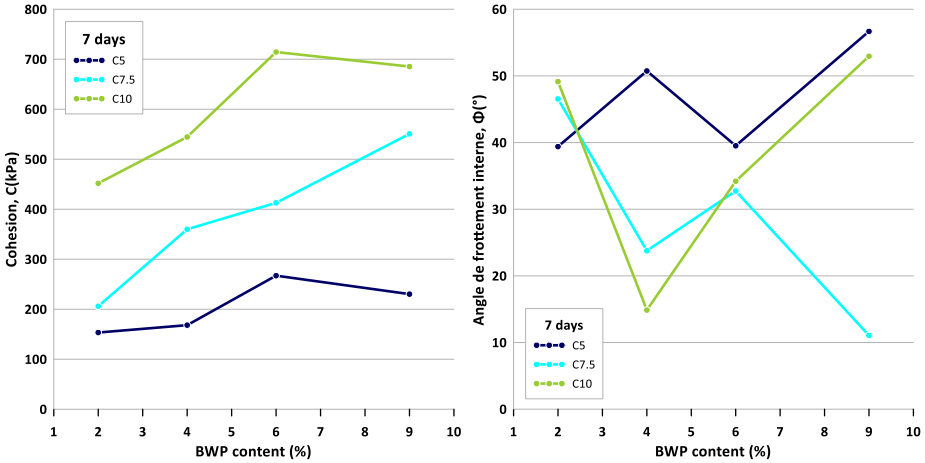

Fig. 5. The variation of cohesion and internal friction angle

Conclusion

This study examined the impact of incorporating varying proportions of BWP on the mechanical behavior of Chlef sandy soil. Based on the experimental findings, the following conclusions were drawn:

Increasing the cement content significantly enhances the shear strength, cohesion, and internal friction angle of the sand, while also improving its dilative behavior.

The addition of BWP improves the mechanical properties of the stabilized sand. Initially, BWP fills the voids between cement particles and promotes early bonding. Subsequently, its high oxide content such as SiO_2 and Al_2O_3 triggers pozzolanic reactions, which accelerate cement hydration and further increase the shear strength of cemented samples.

The particle size and angularity of BWP play a key role in improving adhesion between particles, leading to better cohesion than in sand stabilized with cement alone. Additionally, the angular shape of BWP enhances inter-particle interlocking, contributing to an increase in the internal friction angle.

References

1. Behnood, A. (2018). Soil and clay stabilization with calcium-and non-calcium-based additives: A state-of-the-art review of challenges, approaches and techniques. Transportation Geotechnics, 17, 14-32.
2. Erken, A., & Ardabili, H. F. (2017). Stress Strain Behavior of a Cement-Fiber Treated Sands. Proc. of the 19th ICSMGE.
3. El-Hanafy, A. M., & AbdelAziz, M. H. (2021). Effect of using cemented sand as a replacement layer beneath a strip footing. HBRC Journal, 17(1), 1-17.
4. Najaf poor, A. A., Zarei, A., Jamali-Behnam, F., Vahedian-Shahroudi, M., & Zarei, A. (2014). A study identifying causes of construction waste production and applying safety management on construction site.
5. Vieira, C. S., & Pereira, P. M. (2015). Use of recycled construction and demolition materials in geotechnical applications: A review. Resources, Conservation and Recycling, 103, 192-204.
6. Zhang, L., Wu, H., Wang, X., Wu, F., Ding, Z., Song, L., ... & Zhong, P. (2024). Investigation of Rates of Demolition Waste Generated in Decoration and Renovation Projects: An Empirical Study. Buildings, 14(4), 908.
7. Tihomirovs, P., Kara De Maeijer, P., & Korjakins, A. (2023). Demolition Waste Glass Usage in the Construction Industry. Infrastructures, 8(12), 182.
8. Pettinari, M., & Simone, A. (2015). Effect of crumb rubber gradation on a rubberized cold recycled mixture for road pavements. Materials & Design, 85, 598-606.
9. da Conceição Leite, F., dos Santos Motta, R., Vasconcelos, K. L., & Bernucci, L. (2011). Laboratory evaluation of recycled construction and demolition waste for pavements. Construction and building materials, 25(6), 2972-2979.
10. Sharma, A., & Shrivastava, N. (2023). Geotechnical characterization of construction and demolition waste material blended with sandy soil. *International Journal of Geosynthetics and Ground Engineering*, *9*(4), 43.

Financial Statement Analysis: A Study of UltraTech Cement Limited

Akhilesh Kumar[1], Mahfooz Alam[2*], Rajeev Sharma[3], Koppala Mahesh[4]

[1]Department of Management Studies, G.L. Bajaj Institute of Technology and Management, Greater Noida, India
kumarakhilesh411@gmail.com
[2]Department of MCA, G. L. Bajaj Institute of Technology and Management Greater Noida-201306, India
mahfoozalam.amu@gmail.com
[3]Department of Human Resource Management, G.L. Bajaj Institute of Technology and Management, Greater Noida, India
rajeev_alig@rediffmail.com
[4]Department of Management Studies, Madanapalle Institute of Technology & Science, A.P., India
maheshpeddu01@gmail.com

Abstract. Financial statement analysis is a valuable tool for assessing an organization's financial performance. Based on financial statement analysis, users can make important decisions. The Indian cement industry is the world's next-biggest producer following China. UltraTech Cement Limited is a premier cement producer in India and the primary enterprise of the Aditya Birla Group. It is among the top cement producers globally and the only cement company outside China with a capacity exceeding 100 million tons in one country. This study analyzes the financial performance of UltraTech Cement from 2019-20 to 2023-24 using liquidity, efficiency, solvency, and profitability ratios. Key financial ratios were calculated by collecting data from financial statements. Findings show that the company faces liquidity challenges, relying on inventory for short-term obligations. The company is not heavily dependent on external sources of finance. The company's profitability position remains strong during this period, and it manages inventory effectively. In the future, it should focus on cash and other liquidity sources to address liquidity challenges.

Keywords: Current Ratio, Debt-Equity Ratio, Stock Turnover Ratio, Gross Profit Ratio.

1 Introduction

The Indian cement industry is over 100 years old, with about 100 cement companies operating more than 250 plants. It is the world's second-largest producer, following that of China. Currently, it is spread across the country, and most of its plants feature the latest energy-efficient technology [1]. The sector is expected to grow due to government initiatives like smart cities and the National Infrastructure Pipeline (NIP).

Major industry players include UltraTech, ACC, and Dalmia Cement. The industry has ample raw materials but faces challenges such as environmental regulations and high energy costs. UltraTech Cement Limited is a leading cement producer in India and the primary organization of the Aditya Birla Group. Founded in Mumbai in 1983, it has become one of the top players in the Indian cement industry. In India, UltraTech is the leading producer of white cement, ready-mix concrete (RMC), and gray cement. It is the sole cement company located in a country other than China with a capacity of more than 100 million tons in the country, and is the leading cement producer worldwide. It can produce 117.35 million tons of gray cement per annum (MTPA). UltraTech maintains seven bulk terminals, twenty-seven grinding units, one clinkerization plant, and twenty-three integrated plants. It has its operations in five Asian countries, including India [2].

The UltraTech has a substantial production capacity with a diverse array of goods, including white cement, ready-mix concrete (RMC), and grey cement. It manages 24 combined production plants and a large distribution network that includes more than 80% of Indian cities and towns. Capacity expansion, geographic diversification into foreign markets such as the United Arab Emirates, Bahrain, and Sri Lanka, and the application of technological advancements to increase sustainability and efficiency are all included in the strategic growth initiatives.

1.1 Key Highlights of UltraTech Cement Limited

- **Strategic Initiatives:** Capacity expansion, acquisitions, and geographical diversification (UAE, Bahrain, Sri Lanka).
- **Technological Advancements:** Digital transformation, sustainable manufacturing, and product innovation.
- **Market Position:** Leading market share with strong brand recognition and an extensive distribution network.
- **Corporate Social Responsibility (CSR):** Focus on education, healthcare, sustainable livelihood, and environmental conservation.
- **Awards and Recognitions:** Received multiple awards for manufacturing, sustainability, and CSR initiatives.
- **Future Plans:** Continued expansion, sustainability initiatives, technological advancements, and global market exploration.

Ratio analysis is a key financial analysis tool that analyzes accounting data to assess a company's performance. Based on this analysis, management can formulate policies.

1.2 Contribution of the Study

This offers an exhaustive financial analysis of UltraTech Cement Limited, a prominent entity in the Indian cement sector. The study examines essential financial ratios over five years (2019–20 to 2023–24), providing insights into the company's liquidity, solvency, profitability, and operational efficiency. This study contributes to the following areas:

- **Industry-Specific Financial Insights:** The study provides specialized financial insights into UltraTech Cement, one of India's leading cement makers, which has been adequately addressed in previous academic literature.

- **Empirical Ratio Analysis:** Many financial ratios were employed in this study, including the current ratio, quick ratio, debt-equity ratio, and gross profit ratio, to furnish empirical information for investigating the company's financial health over time.
- **Performance Evaluation:** The analysis assesses the company's strengths, notably profitability and efficient inventory management, while also emphasizing significant difficulties, including ongoing liquidity challenges.
- **Strategic Implications:** Study access areas for managerial emphasis, including the necessity to enhance short-term liquidity via improved current asset management and less dependence on inventory.

This study addresses the deficiency of comprehensive financial performance assessments on UltraTech Cement, hence enhancing the sparse academic literature on financial analysis within the Indian cement business. Section one introduces the cement industry, UltraTech Cement, with its key performance indicators. Section two reviews studies conducted on the cement industry and financial performance analysis. Section three summarizes the research objectives and sources of data used for this study. The next section presents the analysis conducted using ratio analysis, taking data from annual financial statements; this section also presents the interpretation of the analysis. The last section concludes the study.

2 Literature Review

The Indian cement industry contributes significantly to the national economy, being the second-largest producer worldwide and a key contributor to infrastructure, housing, and urban development. It faces the two simultaneous challenges of meeting growing demand for construction materials while mitigating its impact on environment. This study also examines the industry's influence on various sectors, employment, GDP contribution, and dependence on real estate and infrastructure. The paper highlights major obstacles preventing the Indian concrete industry from reaching its full potential, such as a slowdown in real estate development, low industrial investment, regulatory changes, and resource extraction constraints. A strategic move toward sustainability is necessary despite the industry's promising growth, especially with emerging technologies and rising environmental concerns, particularly regarding greenhouse gas emissions [3]. The financial performance of five leading cement companies was analyzed using ratio analysis. Results indicate that these companies maintain strong financial positions and performance, contributing to overall economic development [4]. A new model combining financial and non-financial factors was developed to better understand stability and sustainability. Findings show that financial ratios are essential tools for evaluating the cement industry's financial performance [5]. The overall financial health of the business sector is reflected by its financial output, which illustrates results over time. This tool demonstrates how effectively a business utilizes its capital to generate revenue and boost shareholder value. This study provides a detailed analysis of the financial performance of Pakistan's cement industry from 2006 to 2014. The analysis includes several financial metrics, such as profitability ratios, asset utilization ratios,

debt ratios, liquidity ratios, and the cash conversion cycle. The dependent variable is Return on Investment (ROI), while the independent variables are five financial ratios. Findings reveal that most parameters, except leverage ratios, have a positive relationship with ROI. To improve future research, the author recommends extending the timeframe and adding variables like Market Value Added (MVA), Capital Asset Pricing Model (CAPM), and Economic Value Added (EVA), which could offer more comprehensive insights into other factors affecting financial performance [6].

Based on the literature, it was found that there is a dearth of studies on financial performance analysis of the cement industry, so this study conducts a brief analysis of key financial ratios of UltraTech Cement, which is a major player in the Indian cement industry.

3 Research Methodology

Research methodology can be defined as a systematic approach employed by researchers for conducting a study. It includes tools, techniques, procedures, and strategies employed to collect, analyze, and interpret data to solve a research problem. This section presents the objectives of the study, sources of data, and tools employed for data analysis.

3.1 Research Objectives

The following objectives are considered for this study: (i) To analyze the solvency and liquidity position of the UltraTech Cement Company Limited, and (ii) To ascertain the efficiency and profitability of the UltraTech Cement Company Limited.

3.2 Data Sources

Data is gathered using secondary sources. Annual financial statements are used for the extraction of information related to sales, assets, various measures of profits, etc. The study is also used for extracting theoretical information.

3.3 Tools and Techniques

Ratio analysis is used for data analysis. Tables and Graphs are presented for better understanding. Microsoft Word and Microsoft Excel are also employed for this study.

3.4 Scope

This study focuses only on financial aspects. Liquidity, profitability, solvency, and efficiency are investigated in this article. The duration of the study is very limited. Since this study is on the cement industry, findings cannot be generalized.

4 Data Analysis and Interpretation

This section presents the performance analysis using current ratio, quick ratio, debt-equity ratio, debt ratio, operating ratio, fixed asset turnover ratio, stock turnover ratio, working capital turnover ratio, long-term debt to Equity ratio, and Gross profit ratio.

4.1 Current Ratio

The current ratio evaluates how well Current Assets (CA) can cover Current Liabilities (CL). It is computed by dividing CAs by CLs. CAs are those assets that are convertible into cash within one year or one operating cycle, whichever is longer. CLs are the short-term financial commitments that are anticipated to be settled within one year or within one operating cycle, whichever is longer.

Fig. 1 and Table 1 show the current ratio of UltraTech Cement. Current ratio analysis highlights fluctuations in its short-term financial position over the years. From 2019-20 to 2021-22, current ratios have increased, but they require further improvements. In 2022-23, it decreased to 0.99, and in 2023-24, the ratio was 0.98, reflecting liquidity issues as current liabilities exceeded current assets. Overall, the analysis underscores the need for better management of current assets to ensure consistent short-term stability, as the company's liquidity has varied from strong to strained across the years.

Table 1. Current Ratio

Year	2019-20	2020-21	2021-22	2022-23	2023-24
Current Ratio	0.87	1.03	1.17	0.99	0.98

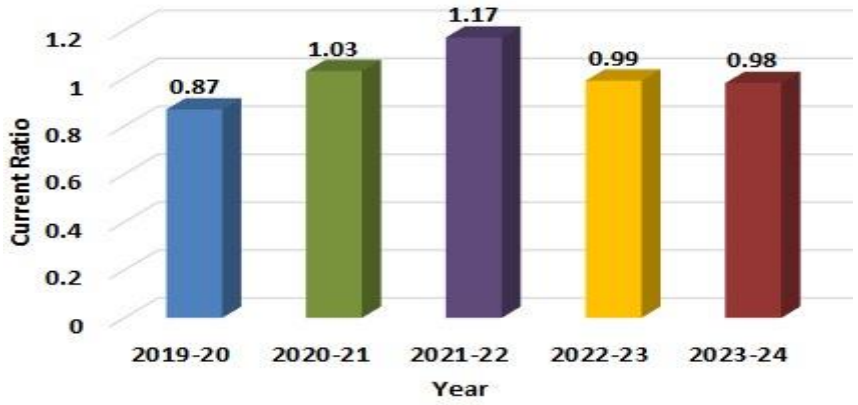

Fig. 1. Current Ratio

4.2 Quick Ratio

The quick ratio measures the short-term liquidity position, meaning the ability to pay immediate financial obligations. It is computed using the ratio of quick assets and current liabilities. Quick assets can be computed by subtracting stock and prepaid expenses from the current assets. As we can see in Table 2 and Fig. 2, the quick ratio has an increasing trend from 2019-20 to 2021-22. In 2023-24 and 2022-23, the quick ratio declined to 0.70. Its ideal ratio is 1:1, so it can be interpreted that the company's quick assets are inadequate to meet short-term commitments. UltraTech Cement's

quick ratio analysis highlights consistent challenges in maintaining sufficient liquidity to pay short-term commitments without counting on inventory sales. It is suggested to management to reduce the dependency on inventory and should try to maintain a stable liquidity position.

Table 2. Quick Ratio

Year	2019-20	2020-21	2021-22	2022-23	2023-24
Quick Ratio	0.60	0.75	0.98	0.70	0.70

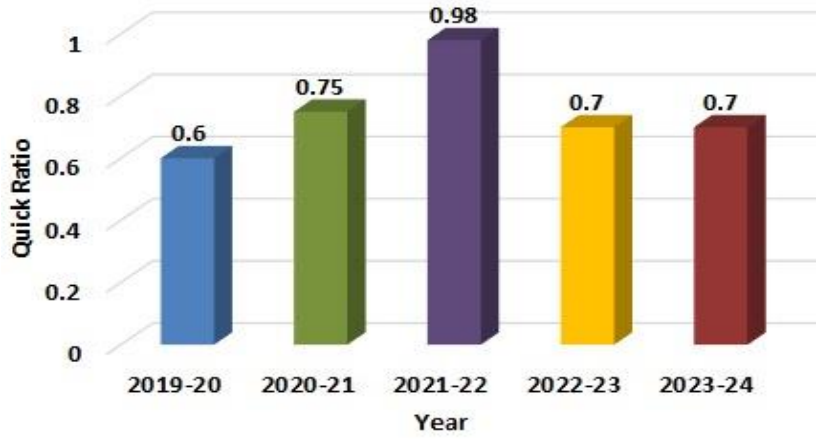

Fig 2. Quick Ratio

4.3 Debt-Equity Ratio

Debt–Equity ratio measures the long-term solvency of the firm. It indicates to what extent the company relies on borrowed funds and owner's equity. It is computed by calculating the ratio of long-term Debts and Shareholders' equity. Long-term debts are those financial liabilities that have to be paid after one year. Shareholder equity can be computed by deducting total outsider liabilities from the total assets.

As we can see in Table 3 and Fig. 3, UltraTech Cement's Debt-Equity (D/E) Ratio analysis from 2019 to 2023 reveals a consistent decline in financial leverage, demonstrating improved financial management and reduced risk. In 2019-20, the D/E ratio was significantly high at 1.29; it has been decreasing every year and is 0.64 in 2023-24. This declining trend indicates effective efforts of management to strengthen its equity and reduce dependence on debt, thereby enhancing its financial stability and resilience over time.

Table 3. Debt-Equity Ratio

Year	2019-20	2020-21	2021-22	2022-23	2023-24
Debt-Equity Ratio	1.29	0.88	0.85	0.64	0.64

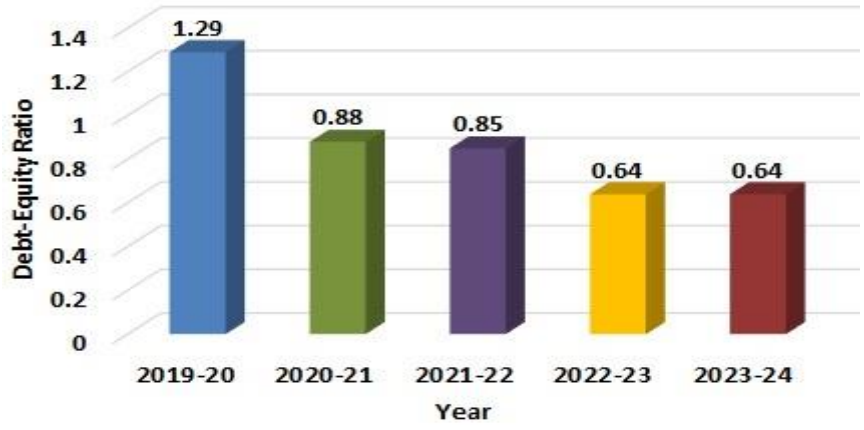

Fig. 3. Debt-Equity Ratio

4.4 Debt Ratio

Debt Ratio is the ratio of a company's total liabilities to its total assets. It represents how much of financial sources of company come from debt. A higher debt ratio (near 1) represents that the company has taken more debt to finance its assets, representing high financial risk. A low debt ratio generally means that the company relies more on equity financing generally means lower financial risk.

Table 4. Debt Ratio

Year	2019-20	2020-21	2021-22	2022-23	2023-24
Debt Ratio	0.52	0.47	0.46	0.39	0.39

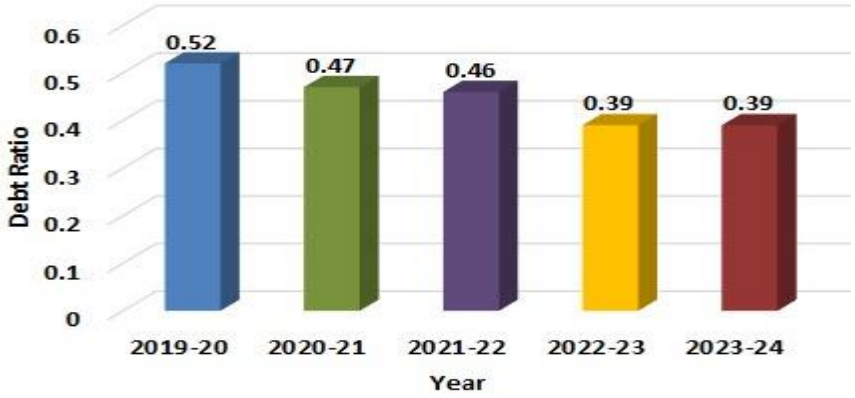

Fig. 4. Debt Ratio

As we can see in Table 4 and Fig. 4, Debt ratio analysis shows a consistent decrease in the company's reliance on debt financing, indicating better management of financial resources and reduced risk. The debt ratio was 0.52 in 2019–20 and decreased to 0.39 in 2023–24. This declining trend shows the company's successful attempts to improve its financial stability by decreasing its dependency on debt, which lowers financial risk. This further emphasizes the company's strategic goal of preserving a more favorable debt-to-asset ratio for long-term financial viability.

4.5 Operating Profit Ratio

It is the profitability ratio that represents the association of operating profit with sales. Operating profit, or operating income or earnings before interest and tax, is the profit a corporation makes from its core operations, excluding interest and tax expenses. In Table 5 and Fig. 5, it can be seen that the company showed strong operational performance in the years 2019–20 and 2020–21, with operating profit ratios of 26.32% and 26.25% respectively. It suggests that the company effectively controlled its operating costs and generated healthy returns from its core operations during those years.

Table 5. Operating Profit Ratio

Year	2019-20	2020-21	2021-22	2022-23	2023-24
Operating Profit Ratio	26.32%	26.25%	23.81%	23.33%	24%

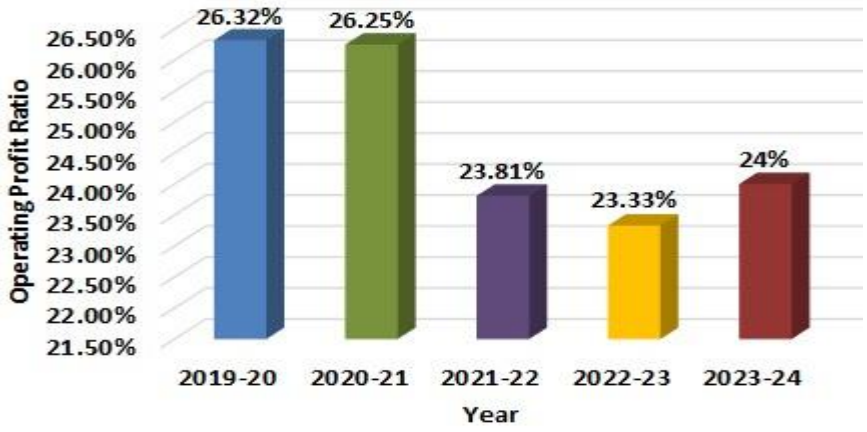

Fig. 5. Operating Profit Ratio

However, there was a noticeable decline in the operating profit ratio during 2021–22 and 2022–23, where it dropped to 23.81% and further to 23.33%. This downward trend may be attributed to rising operating expenses, reduced pricing power, or inefficiencies in business processes, all of which can negatively impact profitability. In 2023–24, the ratio slightly improved to 24.00%, indicating a possible turnaround in operational efficiency. While the overall five-year trend reflects a decline in operating

profitability, the recent improvement offers a positive outlook and suggests that the company might be on a path to recovery.

4.6 Fixed Assets Turnover Ratio

This ratio assesses a company's efficiency in generating sales via fixed assets. It represents how net sales and net fixed assets are related. Fixed assets are those resources that are utilized by a company to generate further income; they are not for sale. Land, building, plant and machinery, and furniture are some examples of fixed assets. In Table 6 and Fig. 6, UltraTech Cement's Fixed Assets Turnover Ratio analysis from 2019-20 to 2023-24 showcases a fluctuating trend in asset utilization efficiency. The ratio reached its highest point in 2023-24 at 0.96, reflecting improved efficiency in generating sales from fixed assets. The fixed asset turnover ratio has a decreasing trend from 2020-21 to 2023-24, which shows the challenges of asset utilization during the same period.

Table 6. Fixed Asset Turnover Ratio

Year	2019-20	2020-21	2021-22	2022-23	2023-24
Fixed Asset Turnover Ratio	0.87	0.83	0.88	0.92	0.96

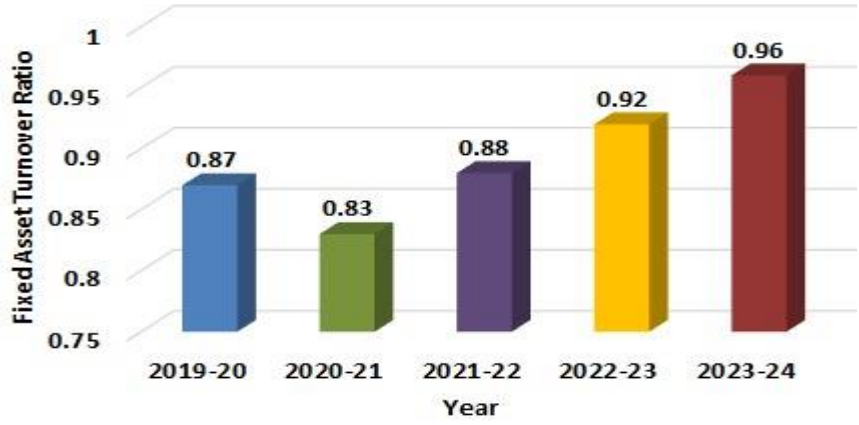

Fig. 6. Fixed Assets Turnover Ratio

4.7 Stock Turnover Ratio

This ratio indicates how efficiently a firm's stock is converted into sales. It is computed by measuring the ratio of the cost of goods sold to average inventory. It shows the efficiency of inventory management. Direct cost incurred in producing the goods or services of an organization sold during a specific period is called the cost of goods sold. It includes only those costs that are directly related to the production of goods or services. Average inventory is the average of the opening stock and closing stock. As shown in Fig. 7 and Table 7, in 2019-20, the ratio was 4.49, reflecting efficient management with approximately 4.49 inventory turnovers during the year. It

increased to 4.72 and 5.29 in the next two financial years, and then followed a declining trend in the next two financial years. Overall, the analysis states that UltraTech Cement's effective inventory management practices, with consistent performance contributing to operational efficiency, minimize holding costs, and optimize sales.

Table 7. Stock Turnover Ratio

Year	2019-20	2020-21	2021-22	2022-23	2023-24
Stock Turnover Ratio	4.49	4.72	5.29	4.95	4.27

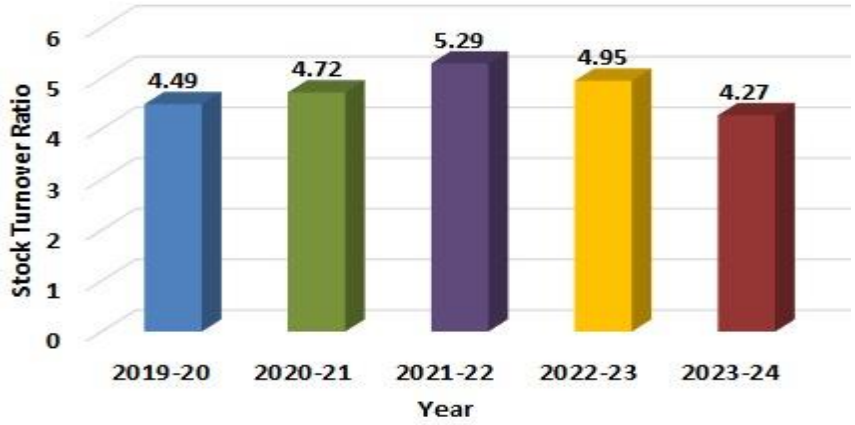

Fig. 7. Stock Turnover Ratio

4.8 Working Capital Turnover Ratio

This ratio measures effectiveness of an enterprise in generating income from its working capital. It represents how many times working capital is turned over through sales in a period. The difference between CAs and CLs is referred to as working capital. As shown in Fig. 8 and Table 8, UltraTech Cement's Working Capital Turnover Ratio analysis from 2020 to 2023 reveals moderate and consistent efficiency in utilizing working capital to generate sales. The ratio was 0.12 in 2019-20 and increased up to 0.16 in 2022-23, before returning to 0.15 in 2023-24. For the total period, it can be stated that the company has stable and consistent working capital management practices.

Table 8. Working Capital Turnover Ratio

Year	2019-20	2020-21	2021-22	2022-23	2023-24
Working Capital Turnover Ratio	0.12	0.14	0.15	0.16	0.15

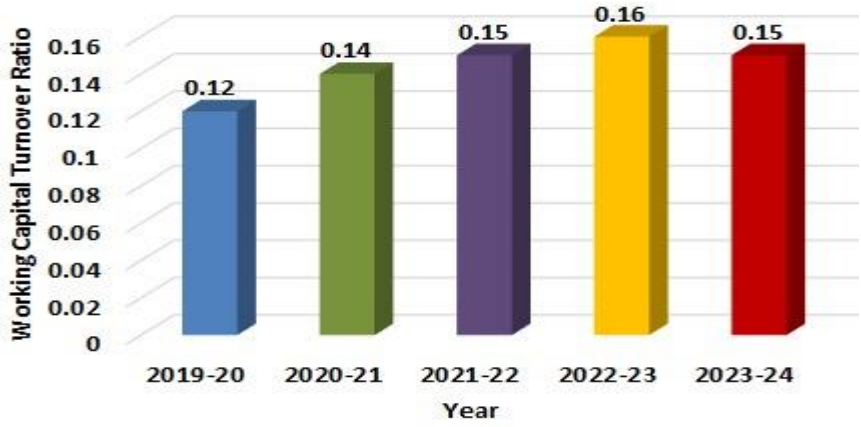

Fig. 8. Working Capital Turnover Ratio

4.9 Long-Term Debt to Equity Ratio

This ratio compares the long-term debts to shareholders' equity. It demonstrates the percentage of funding that comes from long-term debt versus owners' equity. Long-term debts are the financial obligations that have to be paid after one year. Shareholders' equity is the sum of share capital and reserve, and surplus. As shown in Fig. 9 and Table 9, the long-term debt-to-equity ratio is decreasing from 2019-20 to 2022-23, showing a positive trend of financial leverage. Finally, in 2023-24, the ratio increased further to 0.40, signifying a balanced financial structure with moderate long-term debt use. This consistent decline over the years demonstrates UltraTech Cement's commitment to strengthening its equity base, reducing financial risks, and maintaining a robust and sustainable financial position.

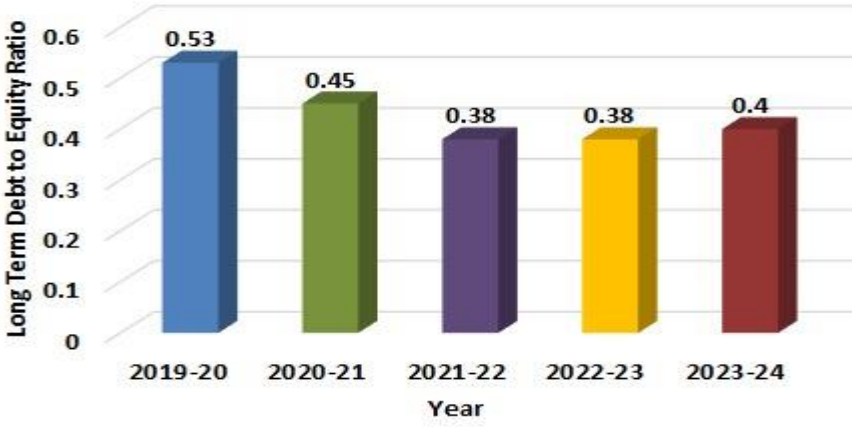

Fig. 9. Long-Term Debt to Equity Ratio

Table 9. Long Term Debt to Equity Ratio

Year	2019-20	2020-21	2021-22	2022-23	2023-24
Long Term Debt to Equity Ratio	0.53	0.45	0.38	0.38	0.40

4.10 Gross Profit Ratio

This ratio represents the relation between net sales and gross profit. It demonstrates how well the business is selling its goods. Gross profit is the profit generated from a business's core operations. It is computed by deducting the cost of goods sold from the sales. In Table 10 and Fig. 10, UltraTech Cement has demonstrated steady and robust gross profit ratios over the last five years, highlighting its adept control of production costs over net sales. The ratios have typically stayed above 50% despite minor variations, indicating consistent profitability through effective cost control.

Table 10. Gross Profit Ratio

Year	2019-20	2020-21	2021-22	2022-23	2023-24
Gross Profit Ratio	54.07%	56.98%	58.13%	51.33%	48.20%

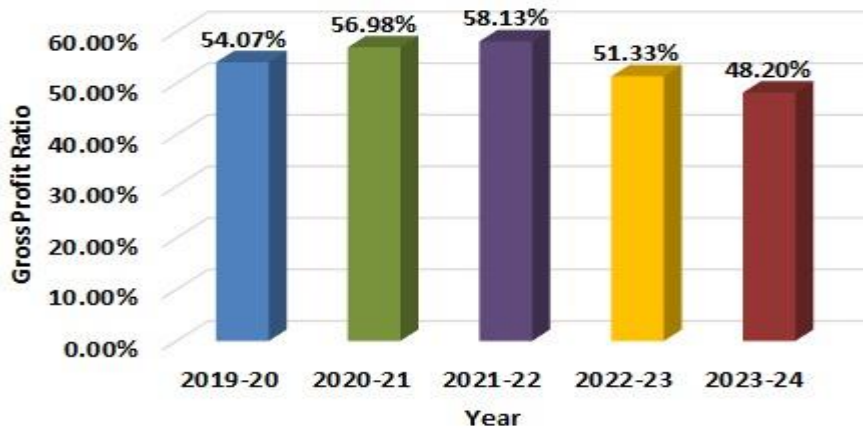

Fig. 10. Gross Profit Ratio

With net sales of Rs. 63,239.98 crores and a gross profit of Rs. 30,000 crores in 2023–24, the gross profit ratio fell to 47.45%, suggesting possible cost increases or tactical price changes. With net sales of Rs. 52,598.83 crores and a gross profit of Rs. 27,000 crores, the previous year, 2022–2023, had a higher ratio of 51.33%, indicating improved cost control. The corresponding ratios for 2021–2022, 2020–2021, and 2019–20 were 58.15%, 56.98%, and 54.08%, respectively, suggesting a steady capacity to sustain profitability. Long-term financial stability and growth are ensured by UltraTech Cement's strong operational procedures, strategic decision-making, and ability to adjust to changing market conditions.

5 Conclusion

Financial analysis of UltraTech Cement, a major cement producer in the industry, has been conducted in this study for five years. It has been observed that the company has faced liquidity challenges, since its current ratio has varied as high as 1.17 in 2021-22, but it has decreased below 1 in three years. Quick ratio has been below 1 in all five years; it means the company is dependent on stock for payment of short-term obligations. A decreasing debt ratio shows the company is less dependent on long-term external debts. Gross profit and operating profit ratio are showing strong improvements means the company has a strong profitability position. Efficiency ratios also show effective inventory management. Overall performance of the company is good, with some work required on liquidity aspects.

References

1. Sharma, M. K., & Khurana, A. (2020). The Changing Structure of the Cement Industry of India. American International Journal of Contemporary Research, 10(1), 76-90.
2. NAVYA, K., & SAYYAD, S. A. (2020). A Study on Comparative Balance Sheet on Ultratech Cement Limited. Mukt Shabd Journal, 9(6), 5265-5273.
3. Mudgal, V., & Chellasamy, A. (2024). Growth of Indian cement industry, its environmental impact and emerging alternatives: A Review. Indian Journal of Engineering and Materials Sciences (IJEMS), 31(1), 38-50.
4. Suthar, A. (2025). A STUDY ON PROFITABILITY OF SELECTED CEMENT COMPANIES IN INDIA. International Journal of Management, Economics and Commerce, 2(1), 29-33.
5. Dhuri, M. P., Joshi, M., & Sinha, R. (2024). Econometric Analysis of Cement Companies in an Emerging Market: A Sustainability Outlook. Corporate Governance and Sustainability Review, 8(4), 30-43.
6. Naz, F., Ijaz, F., & Naqvi, F. (2016). Financial performance of firms: Evidence from Pakistan cement industry. Journal of Teaching and Education, 5(01), 81-94.

An Integrated Open-Source Framework for Cybersecurity Incident Response

Harchi Anas[1][0009-0009-7665-0425], Toumi Hicham[2][0000-0003-3372-4147] and

Talea Mohamed[1][0000-0003-2364-0804]

[1] Information Processing Laboratory, Faculty of Sciences Ben M'sik, University Hassan II Casablanca, Morocco
[2] Higher School of Technology-Sidi Bennour, Chouaïb Doukkali University, El Jadida, Morocco
anas.harchi@gmail.com

Abstract. Cybersecurity incidents persistently represent substantial threats to organizations across the globe, thereby necessitating the establishment of robust and agile incident response (IR) capabilities. Conventional IR methodologies often entail significant financial investment and frequently depend on proprietary solutions, thereby creating obstacles for certain organizations. This manuscript introduces an integrated framework for cybersecurity IR that capitalizes on established best practices alongside a carefully curated selection of open-source technologies. The proposed framework underscores a systematic, multi-phased methodology, which aligns with acknowledged standards such as NIST SP 800-61r3 and the SANS PICERL model. A novel and practical case study, which involves a credential compromise initiated by phishing that culminates in unauthorized data access, is presented to exemplify the application of the framework. The case study meticulously delineates the deployment of an open-source toolchain—including Wazuh, OpenSearch, TheHive, MISP, Velociraptor, Volatility, and Autopsy—across the phases of detection, analysis, containment, eradication, and recovery. Significant findings underscore the efficacy of this integrated open-source approach in delivering comprehensive IR capabilities, its feasibility for practitioners, and the essential synergies attained through tool orchestration and data correlation. This inquiry advances our understanding by delivering a practical blueprint that demonstrates how organizations, particularly those with resource constraints, can build a mature IR capability. This framework directly tackles the prevalent challenges of high cost, alert fatigue, and vendor lock-in.

Keywords: Incident Response, Cybersecurity, Cyber Attack, Phishing, Indicator of Compromise.

1 Introduction

1.1 The Evolving Threat Landscape and the Imperative for Effective IR

The current digital landscape is defined by a continually escalating frequency, complexity, and intensity of cyber threats [1]. Cunning groups relentlessly create innovative approaches, styles, and frameworks to capitalize on the flaws present in systems, networks, and human conduct. Prevalent attack vectors encompass ransomware, Distributed Denial of Service (DDoS) assaults, advanced persistent threats (APTs), and credential theft, each possessing the potential to inflict considerable operational disruption and financial detriment [2]. Reports reveal that cyber-attacks transpire with alarming frequency, with certain sources asserting that an attack targets an organization every 39 seconds, highlighting the ubiquitous nature of these threats [3]. Within this framework, an organization's capacity to efficiently identify, respond to, and recover from cybersecurity incidents transcends mere technical considerations; it constitutes a vital business necessity, a notion robustly substantiated by industry data concerning the extensive financial and reputational repercussions of such occurrences [4]. An effective IR mechanism is essential for mitigating the immediate harm inflicted by an attack, diminishing financial losses, and ensuring the prompt reinstatement of business operations.
Recognizing that security incidents are largely unavoidable, irrespective of the robustness of preventive measures, a heightened state of preparedness through a rigorously defined and structured IR capability is critical. Frameworks such as the NIST Computer Security Incident Handling Guide offer a foundational basis for the establishment of this capability, underscoring a lifecycle approach that encompasses preparation through post-incident analysis [5]. The conventional perception of IR as a purely reactive, technical endeavor is transforming; it is increasingly acknowledged as a fundamental element of comprehensive business continuity planning and holistic risk management strategies. The efficacy of an IR program, grounded in established guidelines [5], is frequently evaluated not solely by its technical proficiency in neutralizing threats but also by its capacity to align with broader business objectives, including alleviating the financial repercussions of a breach and fulfilling legal and regulatory requirements pertaining to incident reporting [4].

1.2 Defining IR and Incident Response Planning (IRP)

According to frameworks delineated in the cybersecurity literature, IR can be formally conceptualized as a strategic and methodical approach that an organization implements to manage and alleviate the consequences of a security breach or cyberattack [6]. The principal objectives of IR encompass the detection of nefarious activities, the investigation of their characteristics and extent, the containment of the threat to avert additional propagation, the elimination of the root cause, and the restoration of affected systems and data to a state of normal operational functionality, all while minimizing recovery time and associated financial implications. At the heart of this capability lies the IRP, a detailed document that specifies the roles, obligations, and organized steps to be taken during a security incident [6]. It furnishes a clear, guided framework for responding to a myriad of threats. Nevertheless, for an IRP to be efficacious, it must

not be a static document. As underscored by scholars, it should embody a dynamic framework that is perpetually enhanced through an iterative lifecycle of testing, execution, and the analysis of insights gleaned from prior occurrences [6]. This proactive refinement is paramount for sustaining the plan's relevance in the face of an evolving threat landscape [7].
In addition, distinguishing an IRP from a Disaster Recovery Plan (DRP) is crucial. While both intend to minimize organizational detriment, an IRP, as articulated, concentrates on addressing active cybersecurity threats and breaches [7].

1.3 Objectives and Contribution of This Paper

The principal aim of this scholarly article is to elucidate a thorough and cohesive framework for cybersecurity IR that utilizes established best practices alongside a practical, open-source toolchain. This research endeavor seeks to exemplify the application of the aforementioned framework through an innovative, methodical case study concentrating on a prevalent yet significant scenario: a credential compromise instigated by phishing, resulting in unauthorized data access. The contributions of this paper are threefold:

- It synthesizes recognized IR principles and frameworks into a cohesive operational model.
- It details a curated selection of open-source tools, outlining their specific roles and integration points within the IR lifecycle, and demonstrates their collective utility in a realistic attack scenario.
- It provides a practical blueprint for organizations, particularly those with limited resources, to develop a robust and adaptable IR function, thereby contributing to the broader body of knowledge on applied cybersecurity.

1.4 Structure of the Article

This manuscript is structured in the following manner: Section II explores the foundational principles of IR, articulating its lifecycle phases and significant industry frameworks. Section III conducts a comprehensive literature review, scrutinizing contemporary developments, prevailing obstacles in IR, and the significance of open-source tools. Section IV presents the proposed open-source toolchain, correlating specific instruments to the phases of the IR lifecycle. Section V offers an extensive case study, detailing the investigation and resolution of a phishing attack employing the aforementioned toolchain. Ultimately, Section VI provides concluding observations, encapsulating the findings and proposing prospective directions for future inquiry.

2 Fundamentals of IR: Lifecycle and Frameworks

The efficacy of IR is fundamentally reliant upon a methodical framework that generally progresses through multiple discrete, albeit interrelated, stages. Comprehending this lifecycle, in conjunction with recognized industry paradigms, establishes the basis for developing a robust IR capability.

2.1 The IR Lifecycle: A Phased Approach

The IR lifecycle provides a systematic methodology for handling security incidents from initial detection through to post-incident analysis and improvement. While specific terminologies may vary slightly between frameworks, the core phases are generally consistent and include [8]:

A. Preparation: This foundational phase involves all activities undertaken before an incident occurs to ensure the organization is ready to respond effectively. Key activities include developing and documenting IR policies, plans, and procedures; assembling and training an incident response team (IRT) with clearly defined roles and responsibilities; investing in and configuring necessary tools and technologies (e.g., SIEMs, EDR, forensic tools); conducting regular staff awareness training on incident reporting and security best practices; and performing drills, tabletop exercises, and simulations to test the IRP and team readiness.

B. Detection and Analysis (Identification): This phase begins when a potential security incident is identified. Detection can occur through various means, including automated alerts from security tools (e.g., IDS/IPS, SIEM, antivirus), reports from employees or external parties, or proactive threat hunting activities [9]. Once a potential incident is detected, analysis is performed to validate its occurrence, determine its nature and scope, assess its impact, and understand the tactics, techniques, and procedures (TTPs) involved. This involves collecting and examining logs, network traffic, forensic data, and other relevant information.

C. Containment, Eradication, and Recovery: Upon validation of an incident, the subsequent response is directed towards mitigation through three principal phases. Initially, **containment** strategies are promptly executed to sequester the issue and inhibit its proliferation. Subsequently, the **eradication** phase emphasizes the thorough elimination of the underlying cause and any nefarious artifacts from the system. Ultimately, the **recovery** stage reinstates the affected systems and services to their standard, secure operational condition [9].

D. Post-Incident Activity (Lessons Learned): This concluding phase is imperative for ongoing enhancement. It encompasses a comprehensive evaluation of the incident alongside the organization's response to it. Vital processes incorporate undertaking a retrospective analysis following the incident to identify the nature of the event, the effectiveness of the IRT, the areas that were executed successfully, the facets that could be enhanced, and the core reasons behind the incident [8]. The knowledge acquired from this analysis is utilized to update the IRP, refine operational procedures, bolster security controls, offer supplementary training, and enhance overall readiness for prospective incidents [9].

2.2 Key Industry Frameworks

Several industry frameworks provide structured guidance for developing and implementing IR capabilities. Two of the most prominent are NIST SP 800-61r3 and the SANS PICERL model.

A. NIST Special Publication 800-61 Revision 3: IR Recommendations and Considerations for Cybersecurity Risk Management NIST Special Publication 800-61 Revision

3 (SP 800-61r3), titled "Incident Response Recommendations and Considerations for Cybersecurity Risk Management: A CSF 2.0 Community Profile," represents a significant evolution from its predecessors [5]. This revision aligns IR guidance with the NIST Cybersecurity Framework (CSF) 2.0, structuring its recommendations around the six CSF functions: Govern, Identify, Protect, Detect, Respond, and Recover [5]. A key shift in SP 800-61r3 is its departure from providing detailed, prescriptive "how-to" guidance for specific IR activities. Instead, it focuses on high-level recommendations and considerations for integrating IR into an organization's overall cybersecurity risk management program [5]. For detailed procedural guidance, readers are directed to online resources and other NIST publications.

B. The SANS PICERL Model: A Practitioner's Approach the SANS Institute, a respected organization in cybersecurity training and research, offers a widely adopted six-step IR process known as PICERL: Preparation, Identification, Containment, Eradication, Recovery, and Lessons Learned [10].

2.3 Best Practices for Building a Robust IR Capability

The establishment of a resilient IR capability necessitates a comprehensive methodology that integrates policy, personnel, pro cedures, and technological infrastructure. Essential best practices, summarized in Table 2, are derived from the analysis of these works [8][9][12][13]:

Table 2. Essential IR Best Practices and Their Descriptions

Practice	Description
Formal Documentation	Establish a formal IR policy that defines the organization's stance on incident handling, an IRP that outlines the roadmap for response, and detailed procedures for specific incident types
Skilled IR Team	Form a dedicated or virtual IR team composed of individuals with the necessary technical and soft skills. Clearly define roles, responsibilities, and authorities within the team
Appropriate Tools and Technologies	Implement and maintain a suite of tools and technologies that support each phase of the IR lifecycle, including capabilities for detection, analysis, containment, eradication, and recovery
Communication Plan	Develop a comprehensive communication plan that outlines how information will be shared with internal stakeholders (e.g., management, legal, HR, IT support) and external parties (e.g., customers, regulatory bodies, law enforcement, media) during and after an incident
Regular Testing and Exercises	Continuously test the IRP and the IR team's readiness through various methods, such as tabletop exercises, simulation drills, and penetration tests. These activities help identify gaps and areas for improvement
Continuous Improvement	Foster a culture of continuous improvement by conducting thorough post-incident analyses, documenting lessons learned, and using these insights to update plans, procedures, tools, and training

While technology is crucial in Incident Response (IR), its success depends on the people and processes involved. "Soft skills" such as communication, collaboration under pressure, and critical analysis are as important as technical expertise. Evaluating an IR plan, therefore, must assess team synergy and decision-making protocols, not just the technological tools.

3 Literature Review: Advancements And Challenges In IR

3.1 Recent Trends in IR Methodologies and Automation

Contemporary IR is transitioning from a predominantly reactive orientation to a more anticipatory framework. This transformation encompasses a heightened focus on threat hunting, wherein analysts proactively investigate indicators of compromise (IOCs) in their operational environments instead of merely depending on alerts generated by automated systems [14]. This anticipatory strategy is motivated by the imperative to identify APTs and more insidious attack methodologies that conventional signature-based detection techniques may overlook [15]. The progression toward proactive threat hunting is propelled by threat intelligence, which supplies critical insights regarding attacker TTPs, IOCs, and emerging threats, thereby facilitating more precise detection and response initiatives [16]. A salient illustration is the framework proposed by Ofoegbu et al. in the Computer Science & IT Research Journal, which utilizes Big Data analytics, including machine learning models, for scalable and instantaneous threat identification [17]. Recent investigations indicate that threat hunting methodologies have advanced to incorporate AI-driven approaches for enhanced anomaly detection and behavioral analysis [18].

As cyber threats become more complex, the significance of AI and ML in IR is growing. Unlike traditional detection methods, AI and ML provide a proactive defense against new attacks. Research by Katiyar, N., et al. [19] indicates that machine learning can identify patterns of malicious activities in large datasets. This ability facilitates the detection of zero-day exploits that lack known signatures. As a result, AI/ML models are utilized for threat modeling, allowing organizations to prevent security breaches proactively. By recognizing subtle IOCs often missed by conventional tools, AI systems enhance threat detection and improve IR efficiency [19]. Recent scholarly works illustrates that the incorporation of AI and ML into IR frameworks can substantially reduce the time required to detect, respond to, and mitigate cybersecurity incidents, thereby streamlining detection processes and minimizing the necessity for manual interventions [20] [21]. AI is being assimilated into Security Orchestration, Automation, and Response (SOAR) platforms to automate intricate IR workflows and aid in decision-making through sophisticated automation strategies like the security intelligence tool AI4SOAR introduced by Nguyen, Manh-Dung, et al. [22]. Nevertheless, the amalgamation of AI/ML introduces novel vulnerabilities, as AI models may be susceptible to adversarial assaults such as data poisoning or evasion methodologies [23]. The opaque nature of complex ML models engenders challenges in forensic scenarios where explainability is paramount, necessitating robust validation procedures and explicit protocols for human oversight [24].

3.2 The Role of Open-Source Tools in Modern IR

Open-source software increasingly occupies a pivotal position in contemporary IR, providing substantial capabilities to entities of varying sizes. The principal benefits of utilizing open-source tools encompass considerable financial savings in contrast to proprietary alternatives, enhanced transparency through the availability of public source code, adaptability for tailored modifications to satisfy specific organizational requirements, and frequently, robust community support for development, troubleshooting, and extensions [25]. A diverse selection of mature and potent open-source tools exists to facilitate every stage of the IR lifecycle, with recent surveys revealing that 75% of organizations actively employ open-source observability and security tools [26]. These tools include comprehensive Security Information and Event Management (SIEM) solutions such as Wazuh [27], OpenSearch and the Elastic Stack, Network Intrusion Detection/Network Security Monitoring (NIDS/NSM) tools like Suricata and Zeek, as well as specialized digital forensics platforms such as Autopsy and Volatility, alongside case management systems like TheHive [28]. For organizations operating under budgetary constraints or those desiring enhanced control over their security infrastructure, these tools represent a feasible pathway to establishing a resilient IR capability [29]. The SIFT Workstation, developed by the SANS Institute, epitomizes this methodology by consolidating numerous forensic tools into a user-friendly Linux distribution that can rival any contemporary IR and forensic tool suite [30]. Nevertheless, although the open-source IR tool ecosystem provides substantial power and adaptability, it frequently necessitates a heightened level of technical acumen for effective deployment, integration, and ongoing maintenance in comparison to commercial, off-the-shelf solutions [31]. Successfully integrating a comprehensive IR toolchain from disparate open-source components demands a profound comprehension of each tool's functionalities and constraints, expertise in scripting for integration and automation, and a sustained commitment to ensuring that all components remain updated, patched, and interoperable [32]. This complexity challenge continues to escalate as organizations expand their security operations, posing a considerable obstacle for entities that lack dedicated cybersecurity expertise or the resources to manage tools continuously [33].

3.3 Challenges in Implementing and Integrating IR Tools and Frameworks

Regardless of the notable advancements in cybersecurity, organizations repeatedly deal with various challenges in the crafting and preservation of competent IR models. These obstacles are intricate, encompassing a chronic deficiency of proficient cybersecurity personnel and limited financial resources, coupled with the continuously escalating

complexity and frequency of cyber threats.

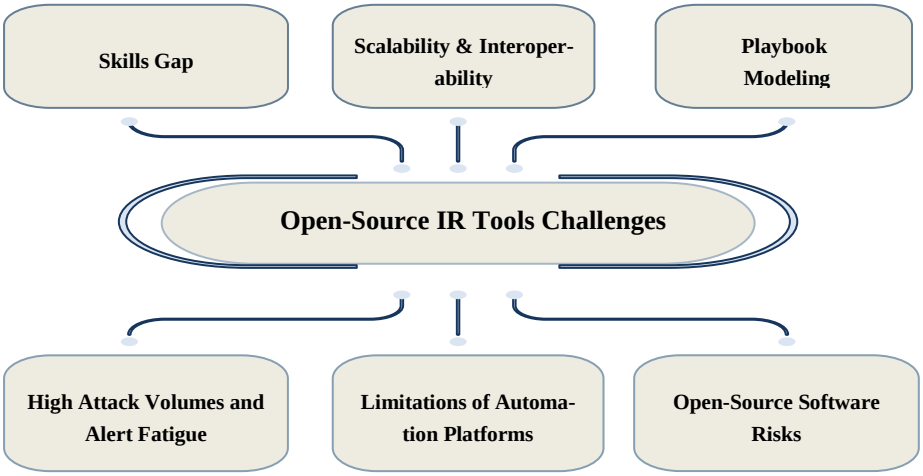

Fig. 1. Open-Source IR Tools Challenges.

As depicted in Figure 1, a myriad of complex challenges that considerably influence the security posture of organizations. Elevated volumes of cyberattacks and resultant alert fatigue constitute one of the most urgent concerns, with empirical evidence suggesting that security teams are contending with an overwhelming influx of information and alert fatigue stemming from the substantial quantity of incoming security notifications. As articulated by C. Nobles [34], the daunting nature of security alerts engenders a cyclical phenomenon wherein critical threats may be inadvertently disregarded due to the fatigue experienced by analysts. The ongoing skills deficit continues to obstruct effective IR capabilities, with recent investigations indicating that approximately 90% of organizations encountered a breach in the preceding year [35], which can be partially ascribed to an insufficiency of cyber skills, while current statistics reveal a substantial disparity of million positions that remains between the available workforce and the roles that necessitate fulfillment. This deficiency, extensively chronicled by R. Vogel [36], particularly impacts specialized domains such as forensic analysis and threat hunting. Challenges related to tool integration and interoperability persist as organizations endeavor to navigate incompatible APIs and heterogeneous data formats, as analyzed by C. Payne [37] and K. Rantos et al. [38]. The crisis of scalability arises as data volumes from logs, network traffic, and endpoint telemetry escalate exponentially, engendering performance bottlenecks that inhibit comprehensive analytical capabilities, a phenomenon scrutinized by Ullah and Babar [39]. The maintenance requirements of security tools introduce an additional layer of complexity, particularly for open-source solutions that necessitate regular updates and configuration adjustments to remain effective against emerging threats, as elucidated by P. Herzog [40] and Basta et al. [41]. Traditional SOAR platforms, although engineered to streamline automation, frequently encounter limitations in flexibility and challenges in managing intricate playbooks, constraints comprehensively examined by Bridges et al. [42]. The difficulty associated

with playbook modeling becomes apparent as organizations endeavor to formulate effective and consistent IR protocols, with prevailing modeling formats being critiqued for their susceptibility to errors and verbosity, as highlighted by Gurabi et al. [43]. Risks associated with open-source software, including exposed vulnerabilities and supply chain attacks, present additional issues that necessitate meticulous management and oversight, particularly in the aftermath of incidents such as Log4j, as investigated by Nair and Lakshmikanthan [44].

4 An Open-source Toolchain for Effective IR

Effective cybersecurity IR increasingly hinges upon the utilization of open-source tools to attain visibility, agility, and adaptability throughout the entirety of the incident lifecycle. Transparent and flexible open-source platforms facilitate organizations in personalizing their solutions to fulfill their operational demands without the burden of high licensing costs. In accordance with the observations made by Park et al. [45], who underscored the pivotal significance of open-source ecosystems in enhancing detection and response capacities, this section delineates a systematic open-source toolchain aligned with essential IR phases. This toolchain not only equips security teams to develop comprehensive, scalable, and economically viable incident management capabilities but also promotes collaboration by assimilating shared intelligence, automated response mechanisms, and forensic analyses. The subsequent table 3 elucidates a comprehensive mapping between selected open-source tools, their primary functionalities, and their interrelations within the IR process, thereby reinforcing the integrated methodology advocated by VR Pereira [46], who illustrated the efficacy of multi-tool integration for the automation of incident detection and response.

Table 3. Open-source Toolchain for Effective IR

IR Lifecycle Phase	Tool Category	Open-Source Tool(s)
Preparation	Vulnerability Scanner	OpenVAS
	Case Management (Templates)	TheHive Project
Detection & Analysis	SIEM / Log Management	OpenSearch, ELK Stack, Graylog, Wazuh
	NIDS / NSM	Suricata, Snort, Zeek, Security Onion
	Network Forensics	NetworkMiner
	Threat Intelligence	MISP
Containment, Eradication, Recovery	Endpoint Forensics & Response	Velociraptor, GRR Rapid Response
	HIDS / Active Response	OSSEC, Wazuh
	Memory Forensics	Volatility Framework (Volatility 3)
	Disk & Filesystem Forensics	Autopsy, The Sleuth Kit, SIFT Workstation

	Network Control	pfSense, OPNsense
	Case Management	TheHive Project, DFIR-IRIS
	Backup & Restore	Bacula
	Configuration Automation	Ansible
Post-Incident Activity	Reporting/Documentation	TheHive Project, DFIR-IRIS

The toolchain delineated in Table 3 exemplifies how the cohesive integration of open-source tools can significantly fortify each phase of IR, encompassing proactive preparation through to post-incident evaluation. By correlating network-based detection instruments such as Suricata and Zeek with log analysis systems like OpenSearch and Wazuh, organizations are capable of achieving multilayered anomaly detection, thereby addressing the defense-in-depth strategy posited by M. Fabro [47]. Moreover, the amalgamation of forensic frameworks such as Velociraptor and Volatility with case management platforms including TheHive and DFIR-IRIS facilitates a seamless transition between analytical processes and documentation, mitigating analyst fatigue and ensuring auditability—a practice corroborated by G. Johansen [48], who emphasized the imperative for stringent integration between forensic analysis and IR workflows.

5 Case Study: Investigation And Response to a Phishing-initiated Credential Compromise

5.1 Incident Overview and Initial Alert

To connect the preceding theoretical framework with practical application, this section follows an analyst's journey through a cyber incident, moving from the initial alert to the final resolution. The investigative framework is informed by methodologies articulated by Aung et al. [49], who accentuated the imperative of synchronized artifact tracing and contextualized indicator analysis throughout the detection, containment, and remediation stages.

The incident begins where many modern breaches originate: with a phishing email targeting corporate personnel, an attack vector that remains one of the most enduring and effective methods for credential compromise. The initial alert was triggered by multiple anomalous authentication attempts detected by the organization's VPN infrastructure, which generated automated alerts within the Wazuh SIEM platform. These alerts indicated successful VPN connections from geographically suspicious IP addresses during off-hours, prompting the security operations center to initiate a formal IR procedure.

The case was immediately escalated and assigned within TheHive Project case management system, where it received the designation "INC-2024-0892: Suspicious VPN Access - Potential Credential Compromise."

5.2 Detection Phase: Following the Digital Breadcrumbs

The detection phase commenced with a comprehensive analysis of the VPN authentication logs aggregated within OpenSearch. The initial investigation revealed that the user account "finance_user_01" had successfully authenticated to the corporate VPN

from IP address 198.51.100.73, originating from a geographic location inconsistent with the legitimate user's known work patterns.

The investigation then expanded to examine the user's recent email activity through analysis of email gateway logs integrated with the OpenSearch platform. This examination revealed that the compromised user had received a sophisticated phishing email approximately 48 hours prior to the suspicious VPN access. The phishing email, originating from the spoofed sender address "secure-alert@it-support-finncorp.com," contained the subject line "Urgent Security Alert: Action Required for Your Account" and included a malicious URL directing to a credential harvesting site.

5.3 Analysis Phase: Correlating Evidence Across Tools

The analysis phase involved the systematic correlation of artifacts across multiple investigative tools to reconstruct the complete attack timeline. Velociraptor, the endpoint detection and response platform, was deployed to conduct remote forensic analysis of the compromised user's workstation. The browser history artifacts retrieved through Velociraptor confirmed that the user had indeed visited the malicious URL embedded in the phishing email, specifically accessing the fake authentication portal hosted at "hxxp://fake-office365-login.com/auth?user=finance_user_01."

NetworkMiner was utilized to analyze packet capture data from the time period surrounding the suspected credential theft. This analysis revealed DNS resolution requests for the malicious domain, confirming network-level evidence of the user's interaction with the attacker's infrastructure. The correlation of endpoint artifacts with network traffic provided a comprehensive view of the initial compromise vector.

The investigation further expanded to examine the attacker's post-compromise activities. File server access logs, centralized within OpenSearch, revealed that the compromised VPN session had been used to access sensitive financial documents located in the "\FS01\Finance_Reports_Sensitive" network share. The temporal correlation between the VPN authentication and the file access activities provided compelling evidence of unauthorized data access.

Through the integration of TheHive case management capabilities with the various analytical tools, investigators were able to systematically document each artifact and its relationship to the overall attack chain. This comprehensive methodology reflects the exemplary practices delineated by Chaudhry and Rittenhouse [50], who demonstrated that an effective response to phishing incidents is contingent upon establishing connections between initial vectors, lateral movements, and ultimate repercussions.

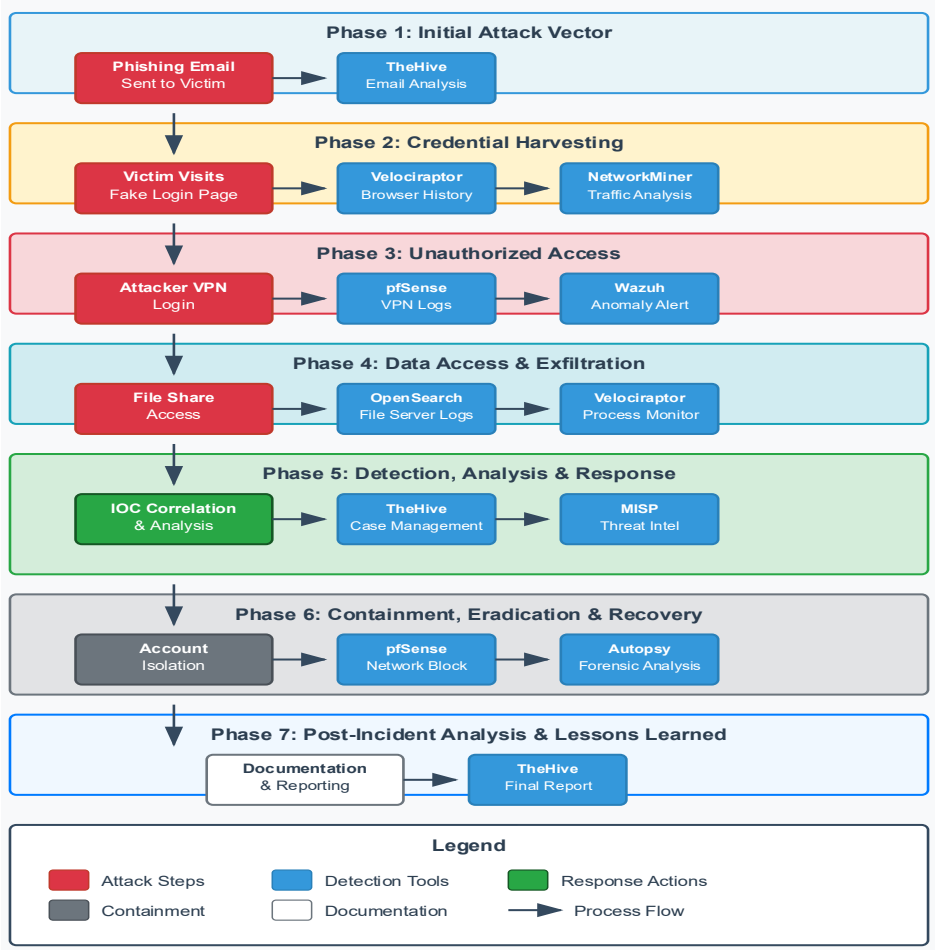

Fig. 2. Phishing Attack Path and Detection Tools Mapping.

The workflow diagram illustrated in Figure 2 provides a visual representation of the attack progression and the corresponding detection tools deployed at each stage. This mapping demonstrates the integrated nature of the response framework, showing how each tool contributed to the overall incident reconstruction.

5.4 Containment and Eradication: Coordinated Response

Upon the validation of the credential breach and illicit data acquisition, prompt containment measures were enacted via a coordinated response that encompassed a multitude of security apparatuses. The pfSense firewall was meticulously configured to obstruct the attacker's originating IP address (198.51.100.73) and to establish supplementary network access protocols to avert any further unauthorized ingress. Concurrently, the compromised user account was deactivated across all authentication platforms, which included VPN, electronic mail, and file server access.

Wazuh's active response capabilities were leveraged to implement automated containment measures, including the deployment of enhanced monitoring rules for the affected user account and related network segments.
The eradication phase focused on eliminating any persistent access mechanisms that the attacker might have established. A comprehensive audit of the compromised user's access permissions was conducted, and all active sessions associated with the account were terminated. The investigation revealed no evidence of malware installation or persistence mechanisms beyond the credential theft, indicating that the attack had been contained before significant system compromise occurred.

5.5 Recovery and Lessons Learned

The recovery phase encompassed the methodical reinstatement of the compromised user's access while concurrently instituting augmented security protocols. The user's workstation was subjected to thorough forensic imaging utilizing Autopsy and The Sleuth Kit to ascertain that no residual compromise artifacts were overlooked. Memory analysis employing the Volatility Framework validated the absence of malicious processes or injected code on the endpoint.
The analysis of lessons learned unveiled several critical insights that were assimilated into enhancements of the organization's security posture. The incident underscored the efficacy of the integrated open-source toolchain in delivering comprehensive visibility across email, network, and endpoint environments. Nevertheless, it also delineated prospects for improvement, encompassing the adoption of more sophisticated email filtering criteria and the initiation of additional user awareness training centered on phishing identification.
The post-incident review process, executed in alignment with established IR frameworks, culminated in revisions to the organization's IR playbooks and the integration of supplementary automated alerting protocols within the Wazuh SIEM platform. These enhancements exemplify the ongoing improvement cycle that is essential to robust IR capabilities.

5.6 Summary analysis of Tool Integration and Incident Timeline

The comprehensive analysis presented in Table 4 demonstrates the systematic utilization of the open-source toolchain throughout the incident lifecycle. Each tool contributed specific capabilities that, when integrated, provided a complete picture of the attack and enabled effective response actions.

Table 4. Analysis of a Phishing-Initiated Credential Compromise Case Study

IR Phase	Tool Utilized	Specific Artifact / Evidence	Investigative Value	Integration Point
Detection	Wazuh SIEM	VPN authentication anomalies	Initial alert generation	Automated log correlation
	OpenSearch	Aggregated VPN access logs	Timeline establishment	Central log repository

	MISP	Threat intel on source IP	Risk assessment enhancement	IOC enrichment
Analysis	TheHive	Email header analysis	Attack vector identification	Case management integration
	Velociraptor	Browser history artifacts	User interaction confirmation	Remote forensic collection
	Network-Miner	DNS resolution logs	Network-level evidence	PCAP analysis correlation
	OpenSearch	File server access patterns	Data access confirmation	Multi-source log correlation
Containment	pfSense	IP blocking implementation	Network access control	Firewall rule automation
	Wazuh	Active response triggers	Automated containment	Real-time response integration
Eradication	TheHive	Account audit documentation	Comprehensive remediation	Case tracking continuity
Recovery	Autopsy	Workstation forensic imaging	System integrity verification	Forensic evidence preservation
	Volatility	Memory analysis results	Malware absence confirmation	Endpoint security validation
Lessons Learned	TheHive	Incident report generation	Knowledge capture	Documentation workflow

The analytical examination of the incident delineated in this case study elucidates how the amalgamation of log analytics, endpoint forensics, and network surveillance facilitates a comprehensive and precise reconstruction of an attack lifecycle. Commencing with the identification of the initial phishing email via TheHive and email gateway scrutiny, the inquiry meticulously traced the assailant's VPN access and subsequent data exfiltration endeavors utilizing instruments such as Velociraptor and Wazuh. Of paramount importance, the revelation of the attacker's infrastructure—including the nefarious login server and VPN ingress IP—and the identification of anomalous process execution enabled prompt containment and response, exemplifying the proactive defense strategy advocated by Atif et al. [51], who underscored the criticality of correlating endpoint, network, and identity data for expeditious threat mitigation.

To provide a clear, chronological overview of the incident response process, Table 5 synthesizes the key events, detection methods, and corresponding response actions into a detailed timeline. This timeline illustrates the practical application of the integrated toolchain in real-time, mapping each stage of the attack—from the initial email delivery to the final system restoration—to the specific tool used and the immediate action taken by the response team. This granular view highlights the framework's effectiveness in achieving a rapid and coordinated response, which is crucial for reducing the mean time to detect (MTTD) and mean time to respond (MTTR).

Table 5. Incident Timeline and Response Actions

Time	Event	Detection Method	Tool Used	Response Action	Status
09:15	Phishing email delivered	Email gateway logs	TheHive alert	Email quarantined	Ongoing
09:23	Employee clicks malicious link	Proxy logs correlation	OpenSearch query	User notified	Ongoing
09:28	Credentials entered on fake site	DNS query analysis	Wazuh alert	Account flagged	Investigating
10:45	Suspicious VPN login detected	Authentication logs	pfSense + Wazuh	VPN session terminated	Contained
10:52	Internal network reconnaissance	Network traffic analysis	Suricata alerts	Network segmentation activated	Contained
11:15	File server access attempt	File server logs	OpenSearch correlation	File server isolated	Contained
11:30	Data exfiltration detected	Process monitoring	Velociraptor hunt	Network blocked	Eradicated
12:00	Forensic collection initiated	Memory/disk imaging	Volatility + Autopsy	Evidence preserved	Recovery
14:30	Systems restored	Clean backup restoration	Automated deployment	Services online	Recovered

The synergistic integration of these open-source tools not only enabled comprehensive incident detection and analysis but also facilitated rapid response and recovery actions. The case study demonstrates the practical efficacy of the proposed framework in reducing MTTD and MTTR, while providing detailed forensic evidence for post-incident analysis and improvement activities.

6 Conclusion and Future Directions

This manuscript delineates a methodical and pragmatic framework for cybersecurity IR, anchored in widely acknowledged standards such as NIST SP 800-61r3 and the SANS PICERL model, and bolstered by a meticulously curated collection of open-source tools. By judiciously integrating the distinct functionalities of solutions such as Wazuh, OpenSearch, TheHive, MISP, Velociraptor, Volatility, and Autopsy/SIFT, the proposed framework empowers organizations to cultivate an efficient, transparent, and highly adaptable IR process. This methodology not only mitigates costs and minimizes vendor lock-in but also enhances flexibility, facilitating customization in accordance with organizational requirements. The case study concerning a phishing-initiated credential compromise unequivocally illustrated the practical applicability and operational significance of the toolchain, exemplifying how such an integrated framework can proficiently detect, investigate, and remediate incidents.

This case study validates the three primary contributions outlined in this paper, (1) The synthesized IR framework enabled systematic investigation from detection through recovery, (2) The curated open-source toolchain provided comprehensive coverage at

lower cost than commercial alternatives, and (3) Organizations with limited resources can implement this approach with proper training and documentation

In anticipation of future developments, the escalating complexity of cyber threats mandates a transition towards structured, repeatable, and quantifiable IR practices, transcending ad hoc and reactive methodologies. The framework articulated in this investigation presents a scalable and reproducible model for attaining expedited detection, comprehensive forensic analysis, streamlined case management, and coordinated response actions—all of which collectively contribute to diminishing MTTD and MTTR, while fortifying overall organizational resilience. Nevertheless, the study also recognizes its limitations, including the controlled nature of the case study and the requisite advanced expertise to adeptly manage these tools. Subsequent research endeavors should explore the integration of AI/ML for automation, the enhancement of tool interoperability, the examination of human factors in IR, the development of shared open-source playbooks, the safeguarding of IR tools themselves, and the execution of rigorous empirical assessments to benchmark the performance and cost-effectiveness of open-source IR frameworks against their commercial counterparts.

References

1. Mijwil, M.M., Unogwu, O.J., Filali, Y., Bala, I., Al-Shahwani, H.: Exploring the Top Five Evolving Threats in Cybersecurity: An In-Depth Overview. Modern J. Cybersecurity 3(1), 1-14 (2023). doi: 10.58496/mjcs/2023/010.
2. Sharma, A., Gupta, B.B., Singh, A.K., Saraswat, V.K.: Advanced Persistent Threats (APT): evolution, anatomy, attribution and countermeasures. J. Ambient Intell. Humaniz. Comput. 1-27 (2023). doi: 10.1007/s12652-023-04603-y.
3. Cukier, M.: Study: Hackers attack every 39 seconds. A. James Clark School of Engineering, University of Maryland (2007).
4. IBM Security: Cost of a Data Breach Report 2024. IBM Corp., Armonk, NY (2024). https://www.ibm.com/reports/data-breach, last accessed 2025/07/04.
5. Nelson, S., Rekhi, M., Souppaya, K., Scarfone, K.: Incident Response Recommendations and Considerations for Cybersecurity Risk Management: A CSF 2.0 Community Profile. NIST Special Publication (SP) 800-61 Rev. 3 (2025). doi: 10.6028/NIST.SP.800-61r3.
6. Staves, A., Anderson, T., Balderstone, H., Green, B., Gouglidis, A., Hutchison, D.: A cyber incident response and recovery framework to support operators of industrial control systems. Int. J. Crit. Infrastruct. Prot. 37, 100505 (2022). doi: 10.1016/j.ijcip.2021.100505.
7. Jorrigala, V.: Business continuity and disaster recovery plan for information security. SANS Institute (2017).
8. Thompson, E.C.: Cybersecurity incident response: How to contain, eradicate, and recover from incidents. Apress, Berkeley, CA (2018).
9. SentinelOne: Cyber Incident Response Guide: Best Practices, Tools & Strategies. https://www.sentinelone.com/cybersecurity-101/services/what-is-an-incident-response/, last accessed 2025/05/30.
10. SANS Institute: An Incident Handling Process for Small and Medium Businesses. SANS Institute (2007). https://www.giac.org/paper/gcih/1902/incident-handling-process-small-medium-businesses/111641, last accessed 2025/07/04.
11. Kral, P.: Incident Handler's Handbook. SANS Institute (2012). https://www.sans.org/white-papers/33901/, last accessed 2025/07/04.

12. Farok, N.A., Zolkipli, M.F.: Incident Response Planning and Procedures. BIJ 7(2), 69-76 (2024).
13. Moeller, B., Lucas, J.: The effective incident response team. Addison-Wesley Professional, Boston, MA (2004).
14. Nour, B., Pourzandi, M., Debbabi, M.: A survey on threat hunting in enterprise networks. IEEE Commun. Surv. & Tutor. 25(4), 2299–2324 (2023).
15. Iyer, K.I.: Proactive Threat Hunting: Leveraging AI for Early Detection of Advanced Persistent Threats. Eur. J. Adv. Eng. Technol. 11(2), 69–76 (2024).
16. Gong, S., Lee, C.: Cyber threat intelligence framework for incident response in an energy cloud platform. Electronics 10(3), 239 (2021).
17. Ofoegbu, K.D.O.: Real-Time Cybersecurity threat detection using machine learning and big data analytics: A comprehensive approach. Comput. Sci. & IT Res. J. 4(3) (2024).
18. Sindiramutty, S.R.: Autonomous threat hunting: A future paradigm for AI-driven threat intelligence. arXiv preprint arXiv:2401.00286 (2023).
19. Katiyar, N., Tripathi, M.S., Kumar, M.P., Verma, M.S., Sahu, A.K., Saxena, S.: AI and Cyber-Security: Enhancing threat detection and response with machine learning. Educ. Adm. Theory Pract. 30(4), 6273–6282 (2024).
20. Brewer, R.: Cyber threats: reducing the time to detection and response. Netw. Secur. 2015(5), 5–8 (2015).
21. Manda, J.K.: Cybersecurity Automation in Telecom: Implementing Automation Tools and Technologies to Enhance Cybersecurity Incident Response and Threat Detection in Telecom Operations. Adv. Comput. Sci. 4(1) (2021).
22. Nguyen, M.D., Mallouli, W., Cavalli, A.R., Montes de Oca, E.: AI4SOAR: A Security Intelligence Tool for Automated Incident Response. In: Proceedings of the 19th International Conference on Availability, Reliability and Security, pp. 1–8. ACM, New York, NY (2024).
23. Chaganti, K.: Adversarial Attacks on AI-driven Cybersecurity Systems: A Taxonomy and Defense Strategies. Authorea Preprints (2023).
24. Tiwari, S., Sresth, V., Srivastava, A.: The Role of Explainable AI in Cybersecurity: Addressing Transparency Challenges in Autonomous Defense Systems. Int. J. Innov. Res. Sci. Eng. Technol. 9, 718–733 (2020).
25. Bezas, K., Filippidou, F.: Comparative analysis of open source security information & event management systems (siems). Indones. J. Comput. Sci. 12(2), 443–468 (2023).
26. IT Pro Today: Observability 2025: Open Source Use Rising, Complexity Challenges Grow. https://www.itprotoday.com/it-operations/observability-in-2025-open-source-use-rising-as-complexity-challenges-grow, last accessed 2025/07/04.
27. Wazuh: Wazuh - Open Source XDR. Open Source SIEM. https://wazuh.com/, last accessed 2025/07/04.
28. Groenewegen, A., Janssen, J.S.: TheHive Project: The maturity of an open-source Security Incident Response platform. HAN University of Applied Sciences (2021).
29. Manzoor, J., Waleed, A., Jamali, A.F., Masood, A.: Cybersecurity on a budget: Evaluating security and performance of open-source SIEM solutions for SMEs. Plos one 19(3), e0301183 (2024).
30. SANS Institute: SIFT Workstation. https://www.sans.org/tools/sift-workstation/, last accessed 2025/07/04.
31. Schlette, D., Caselli, M., Pernul, G.: A comparative study on cyber threat intelligence: The security incident response perspective. IEEE Commun. Surv. & Tutor. 23(4), 2525–2556 (2021).
32. Johansen, G.: Digital Forensics and Incident Response: Incident response tools and techniques for effective cyber threat response. 2nd edn. Packt Publishing, Birmingham (2022).

33. Linskens, A.: The scale of open source: Growth, challenges, and key insights. Sonatype Blog. https://www.sonatype.com/blog/the-scale-of-open-source-growth-challenges-and-key-insights, last accessed 2025/07/04.
34. Nobles, C.: Stress, burnout, and security fatigue in cybersecurity: A human factors problem. Holist. J. Bus. Public Adm. 13(1), 49–72 (2022).
35. Bhadouria, A.S.: Study of: impact of malicious attacks and data breach on the growth and performance of the company and few of the world's biggest data breaches. Int. J. Sci. Res. Publ. 10(10), 1–11 (2022).
36. Vogel, R.: Closing the cybersecurity skills gap. Salus J. 4(2), 32–46 (2016).
37. Payne, C.: On the security of open source software. Inf. Syst. J. 12(1), 61–78 (2002).
38. Rantos, K., Spyros, A., Papanikolaou, A., Kritsas, A., Ilioudis, C., Katos, V.: Interoperability challenges in the cybersecurity information sharing ecosystem. Computers 9(1), 18 (2020).
39. Ullah, F., Babar, M.A.: On the scalability of big data cyber security analytics systems. J. Netw. Comput. Appl. 198, 103294 (2022).
40. Herzog, P.: Open-source security testing methodology manual. Institute for Security and Open Methodologies (ISECOM) (2003).
41. Basta, A., Basta, N., Anwar, W., Essar, M.I.: Open-source Security Operations Center (SOC): A Complete Guide to Establishing, Managing, and Maintaining a Modern SOC. John Wiley & Sons, Hoboken, NJ (2024).
42. Bridges, R.A., et al.: Testing SOAR tools in use. Comput. & Secur. 129, 103201 (2023).
43. Gurabi, M.: Requirements for Playbook-Assisted Cyber Incident Response, Reporting and Automation. Digit. Threats Res. Pract. 5(3), 1–11 (2024).
44. Nair, S.S., Lakshmikanthan, G.: Open Source Security: Managing Risk in the Wake of Log4j Vulnerability. Int. J. Emerg. Trends Comput. Sci. Inf. Technol. 2(4), 33–45 (2021).
45. Park, S.H., et al.: Performance evaluation of open-source endpoint detection and response combining google rapid response and osquery for threat detection. IEEE Access 10, 20259–20269 (2022).
46. Pereira, V.R.: Cyber-attack detection and response using open-source tools. University of Tartu (2023).
47. Fabro, M.: Control systems cyber security: Defense-in-depth strategies. Idaho National Lab.(INL) (2007).
48. Johansen, G.: Digital forensics and incident response. Packt Publishing, Birmingham (2017).
49. Aung, E.S., Zan, C.T., Yamana, H.: A survey of URL-based phishing detection. In: DEIM Forum, pp. G2-3 (2019).
50. Chaudhry, J.A., Rittenhouse, R.G.: Phishing: Classification and countermeasures. In: 7th International Conference on Multimedia, Computer Graphics and Broadcasting (MulGraB), pp. 28–31. IEEE (2015).
51. Ahmad, A., Maynard, S.B., Shanks, G.: A case analysis of information systems and security incident responses. Int. J. Inf. Manag. 35(6), 717–723 (2015).

A Comprehensive Review of Passive Vibration Control Systems for Offshore Wind Turbines

Maziar Fahimi Farzam[1][0000-0001-9635-8186] and Aniseh Ziamehr[2][0009-0005-1082-9597]

and Gebrail Bekdaş[3][0000-0002-7327-9810]

[1, 2] Department of Civil Engineering, Maragheh University, Maragheh, Iran
[3]Department of Civil Engineering, Istanbul University-Cerrahpaşa,Istanbul,Türkiye
M.farzam@maragheh.ac.ir

Abstract
Offshore wind turbines (OWTs) are constantly exposed to environmental loads such as wind, waves, and currents, which can cause structural vibrations, reduce operational efficiency, and raise safety concerns. To enhance dynamic performance and reliability, various vibration control strategies have been proposed. Among these, passive control systems are preferred due to their simplicity, low cost, high reliability in harsh offshore conditions, and independence from external energy sources and complex electronics. Compared to active and semi-active systems, passive devices require minimal maintenance and offer robust performance in inaccessible marine environments. Although several review studies in the mid-2010s addressed passive control in marine structures such as platforms, no comprehensive review focusing specifically on passive control for wind turbines has been published. This paper aims to fill this gap by reviewing recent advancements in passive control for offshore wind turbines. It examines the latest developments and innovations in this field, providing valuable insights for researchers and practical guidance for engineers in selecting optimal passive vibration control strategies for offshore wind turbines.

Keywords: Passive Vibration Control, Offshore Wind Turbines, Offshore Renewable Energy Structures.

1 Introduction

Wind energy dates back to the 7th century AD in Iran and Mesopotamia, where windmills served agricultural and industrial needs. Advances have transformed early vertical-axis designs into modern horizontal-axis turbines, now widely used onshore and offshore at large scale [1].

Wind turbines are an essential renewable energy source that helps decrease reliance on fossil fuels. According to the Global Wind Energy Council (GWEC), global installed capacity reached 117 gigawatts in 2023, marking a 50% increase over the previous year [2]. Among these, offshore wind energy has gained increasing attention due to access to stronger winds, the possibility of large-scale development, and lower environmental impacts; although its initial investment costs are high [3]. Fig 1 shows the global growth trend of installed wind turbine capacity over time.

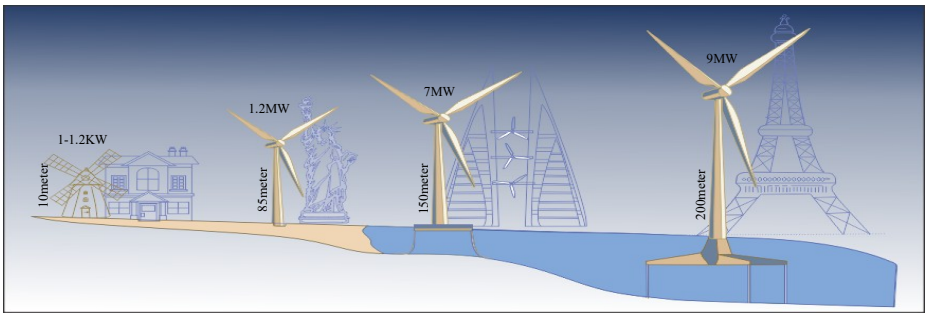

Fig. 1. Growth trend of wind turbine tower height and blade length.

Offshore wind turbines are vulnerable to environmental loads due to their tall height, structural flexibility, and top-heavy mass distribution. These combined forces can cause severe vibrations, fatigue damage, and potentially catastrophic failures. Incidents at projects like Sneddon Law and Dogger Bank underscore the importance of maintaining their dynamic stability [4].

In this regard, Vibration control is a critical challenge in offshore wind turbine design and operation. Passive structural control methods, such as tuned mass dampers (TMD), tuned liquid dampers (TLD/TLCD), and viscous or friction dampers, improve dynamic stability by dissipating vibrational energy without external power. Semi-active systems allow low-energy adjustment of stiffness or damping, while active controls offer high performance but are limited in practice due to complexity and cost [5].

This review comprehensively examines passive vibration control methods for offshore wind turbines, evaluating their performance, benefits, and limitations under environmental loads, and suggests future research directions.

2 Types of Passive Control Methods

Passive damping systems, valued for their simplicity, effectiveness, and reliability, are widely applied in offshore wind turbines. This section provides a comprehensive review of their types, installation, design approaches, and key numerical and experimental findings, with particular emphasis on the growing use of tuned mass dampers (TMDs) and tuned liquid column dampers (TLCDs) in offshore projects. Fig 2 shows the classification of passive vibration control systems in offshore wind turbines.

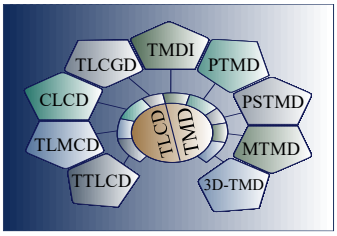

Fig. 2. Passive control systems in offshore wind turbines

2.1 Tuned Mass Dampers (TMDs)

With the growth of offshore wind energy, managing dynamic loads from wind, waves, currents, and earthquakes has become a key design challenge. These loads can increase fatigue, reduce component lifespan, and cause structural failure. Among mitigation strategies, tuned mass dampers (TMDs) offer a simple, cost-effective, and reliable solution to enhance the dynamic performance and safety of offshore wind turbines (OWTs). This article presents a comprehensive review of TMD applications across various platform types, including monopile, barge, spar, TLP, jacket, semi-submersible, and bucket foundations.

Barge-type platforms. Barge platforms, which are widely used due to their simple geometry and high flexibility, have attracted significant attention in research on the effectiveness of TMDs. In the context of an analytical study, a dynamic model of a barge-type floating wind turbine equipped with a TMD in the fore-aft direction was developed, and its performance under combined loading was evaluated using the Levenberg–Marquardt and genetic optimization algorithms. The results showed that the TMD, with an optimal mass ratio of 1.8%, reduced the displacement standard deviation by up to 60% [6]. Another study proposed a passive inerter-based network operating in parallel with the TMD, optimized using the H_2 criterion. This configuration improved control performance without increasing the stroke length of the TMD [7]. To provide a more comprehensive understanding of the inverter configurations in the proposed systems, a schematic illustrating various inverter arrangements alongside the TMD components is included in Fig 3.

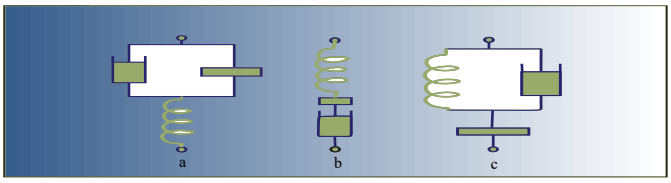

Fig 3. Schematic of inerter configurations combined with TMD components

Within prior research on improving TMDs using inerters, a recent offshore wind turbine study showed that adding an inerter reduced tower fatigue loads by up to 12%, but only in configurations with performance constraints—emphasizing the need for practical implementation and optimized damping performance [8], According to one study, the use of bi-directional suspended mass dampers (TMDX and TMDY) was investigated, with their parameters optimized using a genetic algorithm. This resulted in a 36.7% reduction in structural fatigue and an 11% improvement in overall performance compared to unidirectional dampers [9]. After reviewing bi-directional dampers, the performance of another configuration was compared, showing that omni-directional dampers reduced roll deviation by up to 45% and blade fatigue loads by up to 25% under misaligned wind-wave conditions, offering a notable advantage over the two-axis type [10].

To overcome the limited frequency coverage of single TMDs, MTMD systems have been proposed. Numerical studies using a 6-DOF model and AFSA optimization show that installing MTMDs on both nacelle and platform can reduce tower displacements by up to 75% and platform pitch/roll by 83%, offering a technically and economically optimal solution [11]. Figure 4 illustrates the effect of the AFSA-based optimization on reducing vibrations at the tower top and platform.

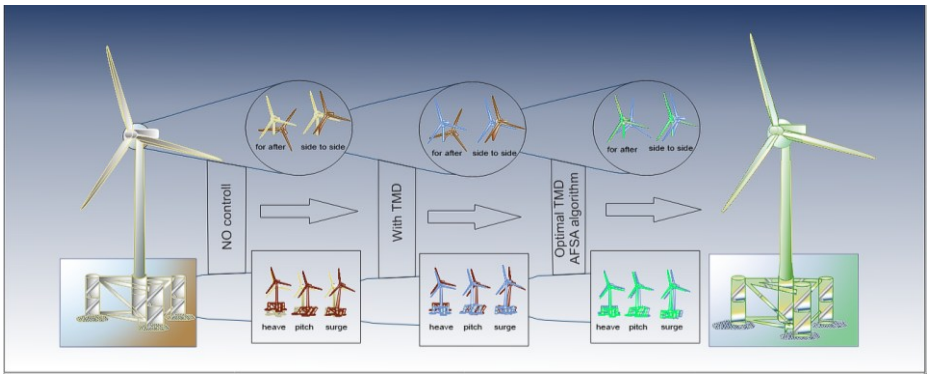

Fig. 4. MTMD vibration reduction with AFSA optimization

Monopile platforms. Monopile platforms have been studied using various TMD types. Recent work on 3D-PTMDs for controlling fore-aft and side-side vibrations in the tower and nacelle showed 10–12% reductions in RMS and peak displacements, outperforming two separate linear dampers in vibration and seismic control [12]. Due to the frequency limitations of single tuned mass dampers (TMDs), multiple tuned mass dampers (MTMDs) have been introduced to increase bandwidth and improve the stability of offshore wind turbines. In a numerical analysis on a monopile-based turbine, the MTMD parameters were optimized using the H_2 method and genetic algorithm. The results showed that under combined wind and wave loading, MTMDs reduced the tower top displacement by up to 80.54% compared to single TMDs[13]. Following previous research on multiple tuned mass dampers (MTMDs), optimization and performance evaluation of two MTMDs with variable mass distribution were conducted on the monopile tower of an offshore wind turbine. The results showed that this system, with a total mass ratio of 5%, was able to reduce the RMS displacement of the tower top by approximately 42% under parked conditions [14]. In line with specialized analyses of MTMDs for vibration reduction in offshore wind turbines, a numerical investigation using 3D finite element analysis evaluated MTMD performance under combined wind, wave, and earthquake loads. Tuning the MTMD to the first two natural frequencies led to vibration reductions of up to 58% for wind-wave and 55% for combined excitations, enhancing structural stability [15].

Spar-type platforms. A scientific study proposed a hybrid method combining a 3D pendulum TMD in the nacelle and two linear impact dampers on the spar-type floating platform to mitigate 3D vibrations. Using an Euler-Lagrange-based model and optimized loading, results showed 32% reduction in tower displacement, 18% in roll, and

50% in pitch. The impact mechanism limits damper stroke and enables compact installation [16]. An innovative approach using a bilinear tuned mass damper (Bilinear TMD) with nonlinear stiffness and damping has reduced vibrations of a spar-type floating wind turbine by up to 25%, and its performance ratio has increased up to 13 times compared to linear models. This method optimized the parameters using a genetic algorithm and fmincon, modeling the damper's motion limit at ±4 meters and tuning the frequency to the floating platform. The use of multiple lightweight units and consideration of nonlinear effects have been proposed for further improvement [17].

Other offshore platforms. Other specialized offshore platforms have also been investigated. In the scope of related studies, specialized platforms have also been examined. A TLP-type floating wind turbine with a nacelle-mounted TMD showed up to 20% reduction in nacelle acceleration at above-rated wind speeds. Numerical optimization using a fully coupled aero-hydro-servo-elastic model revealed that increasing TMD mass and stiffness lowered structural loads but increased platform motion, confirming passive TMDs as a cost-effective solution for vibration and stress mitigation [18]. The semi-submersible platform, due to its stability and cost-efficiency, suits offshore turbines in moderate depths. Using a genetic algorithm, nacelle and platform TMDs were optimized showing the nacelle damper targets higher tower modes, while the platform damper controls torsional motion. Combined in an MTMD setup, they reduced tower base bending loads by up to 26%. The system is robust to dynamic changes but less effective in harsh sea states[19]. Figure 5 shows the TMD locations on the semi-submersible platform.

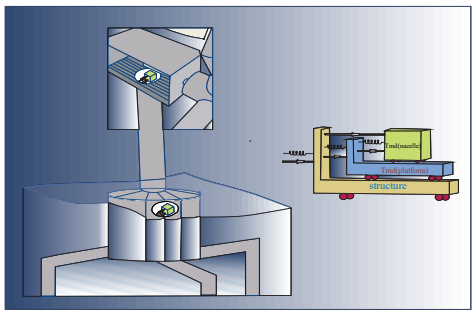

Fig. 5. TMD locations on the semi-submersible turbine.

In continuation of previous efforts, the nonlinear TMDI on a semi-submersible platform effectively reduces heave vibrations with a broader frequency range than linear TMDs. Optimizing mass–matching ratio and damping enhances energy harvesting, while pitch control remains effective depending on wave–design alignment [20]. Finally, a bucket-type foundation equipped with a C-shaped Particle Damper TMD (PD-TMD), modeled using FEM–DEM, achieved up to 45% reduction in relative displacement under strong wind loading and up to 12% reduction under random combined load scenarios, demonstrating its effectiveness for compact-space installations [21].

2.2 Tuned Liquid Column Dampers (TLCDs)

Tuned liquid column dampers (TLCDs) and their derivatives, as passive systems, have gained increasing attention as effective, low-cost solutions for vibration control in offshore wind turbines (OWTs). Their simple mechanism, energy-free operation, and adaptability to diverse wind and wave loads make them especially suitable for enhancing OWT dynamic performance.

Researchers introduced a tuned liquid multi-column damper (TLMCD) to reduce torsional motion of a semi-submersible platform. Experiments and simulations showed the TLMCD cut the pitch angle by up to 67% and maintained over 56% damping within ±5% frequency variation, driven by dynamic pressure differences between liquid columns [22]. To illustrate the installation location and mode of operation, Fig 6 shows the tuned liquid multi-column damper (TLMCD) inside the semi-submersible platform.

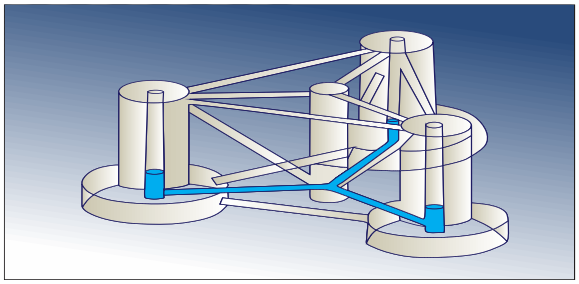

Fig. 6. TLMCD inside semi-submersible platform

In related studies, the performance of Tuned Liquid Column Dampers (TTLCD) was evaluated through scaled Real-Time Hybrid Simulation (RTHS) tests on monopile wind turbines. A model with the highest horizontal-to-vertical length ratio showed a 19% improvement in damping in the side-to-side direction under strong wind, but the increased liquid sloshing amplitude highlighted the need for spatial considerations in the design [23]. In the conducted investigations, the parameters of the TLCD installed on a barge platform were identified using a Lagrangian model and the Levenberg–Marquardt algorithm. The TLCD was able to reduce the tower top displacement by up to 42% and fatigue loads at the tower base and blade root by 10% and 11%, respectively. However, increasing the damper mass requires replacing elastic elements to maintain platform stability [24]. In recent studies, the compliant liquid damper-inerter (CLDI) was proposed for monopile turbines under combined environmental loads. Genetic algorithm-based optimization led to up to 70% and 65% reductions in RMS displacement and acceleration in the FA and SS directions, respectively, with strong seismic vibration suppression across a broad frequency range.[25]. Advanced evaluations compared the performance of TMD, TLCD, and combined TLCD-TMD systems on jacket foundations. TLCD reduced vibration by up to 93% in the parked condition. Optimizing the mass and geometry of the liquid and gas columns is key to improving damping under dynamic loads. The combined TLCD-TMD system offers more stable performance by integrating both approaches [26]. Fig 7 shows the TLCD-TMD installed on a jacket platform nacelle.

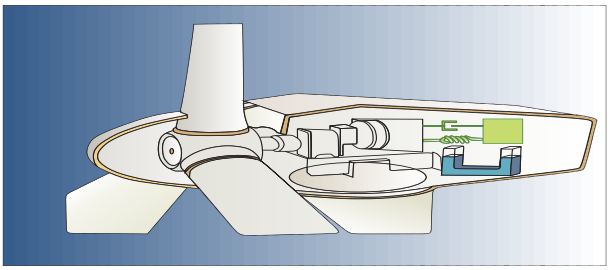

Fig. 7. Combined TLCD-TMD system on jacket platform nacelle

These studies highlight the significant potential of liquid-based damping systems for controlling vibrations in offshore wind turbines under complex loading. Effective performance relies on precise geometric tuning, mass and frequency optimization, and addressing practical constraints.

3 Conclusion

A comprehensive review of passive control systems in offshore wind turbines highlights growing research on Tuned Mass Dampers (TMDs) and Tuned Liquid Column Dampers (TLCDs) for mitigating dynamic loads from wind, waves, and earthquakes. TMDs demonstrate significant vibration and fatigue reduction on barge, monopile, and floating platforms, though studies on Tension Leg Platforms (TLPs) remain limited. TLCDs and their variants effectively address frequency-specific excitations, particularly reducing pitch and fatigue in parked conditions. Hybrid TLCD-TMD systems offer broader control bandwidth. Key challenges include limited experimental validation, nonlinear modeling deficiencies, and insufficient long-term performance data. Future research should prioritize hybrid and semi-active controls, advanced optimization techniques, and enhanced integration with turbine operations.

4 References

[1] H. Allamehzadeh, "Wind energy history, technology and control," in *2016 IEEE Conference on Technologies for Sustainability (SusTech)*, 2016: IEEE, pp. 119-126.

[2] "Global Wind Energy Council (GWEC). Global Wind Report 2024; GWEC: Brussels, Belgium, 2024. Available online: https://gwec.net/global-wind-report-2024/ (accessed on 15 Feb 2025) ".

[3] " WindEurope, 2023. Wind energy in Europe: 2023 Statistics and the outlook for 2024- 2030. WindEurope [WWW Document], URL."

[4] T. M. Naqash and M. M. Alam, "A State-of-the-Art Review of Wind Turbine Blades: Principles, Flow-induced Vibrations, Failure, Maintenance, and Vibration Mitigation," 2025.

[5] H. Zuo, K. Bi, and H. Hao, "A state-of-the-art review on the vibration mitigation of wind turbines," *Renewable and Sustainable Energy Reviews,* vol. 121, p. 109710,2020.

[6] E.-M. He, Y.-Q. Hu, and Y. Zhang, "Optimization design of tuned mass damper for vibration suppression of a barge-type offshore floating wind turbine," *Proceedings of the Institution of Mechanical Engineers, Part M: Journal of Engineering for the Maritime Environment,* vol. 231, no. 1, pp. 302-315, 2016

[7] Y. Hu, J. Wang, M. Z. Q. Chen, Z. Li, and Y. Sun, "Load mitigation for a barge-type floating offshore wind turbine via inerter-based passive structural control," *Engineering Structures,* vol. 177, pp. 198-209, 2018

[8] D. Villoslada, M. Santos, and M. Tomás-Rodríguez, "Inerter-based passive structural control for barge floating offshore wind turbines," *IFAC-PapersOnLine,* vol. 53, no. 2, pp. 12358-12363, 2020.

[9] R. El Hamoud, P. Alkhoury, M. Aït-Ahmed, A.-H. Soubra, F. Schoefs, and R. Dib, "Vibration and Fatigue Mitigation of a 5 MW Barge-Type Floating Offshore Wind Turbine Under Misaligned Wind and Wave Loadings," in *International Conference on Offshore Mechanics and Arctic Engineering*, 2024, vol. 87851: American Society of Mechanical Engineers, p. V007T09A059.

[10] T. Melo, L. Almeida, and J. Lazo, "Improving Floating Wind Turbine Stability with Evolutionary Computation for TMD Optimization," presented at the Proceedings of the 14th International Conference on Pattern Recognition Applications and Methods, 2025.

[11] X. Jin, S. Xie, J. He, Y. Lin, Y. Wang, and N. Wang, "Optimization of tuned mass damper parameters for floating wind turbines by using the artificial fish swarm algorithm," *Ocean Engineering,* vol. 167, pp. 130-141, 2018

[12] C. Sun and V. Jahangiri, "Bi-directional vibration control of offshore wind turbines using a 3D pendulum tuned mass damper," *Mechanical Systems and Signal Processing,* vol. 105, pp. 338-360, 2018

[13] S. R. Patro, S. Panda, G. V. Ramana, and A. Banerjee, "Optimal multiple tuned mass dampers for monopile supported offshore wind turbines using Genetic Algorithm," *Ocean Engineering,* vol. 298, 2024

[14] D. McNamara, A. Pandit, and A. Malekjafarian, "Optimized design of multiple tuned mass dampers for vibration control of offshore wind turbines," *Ocean Engineering,* vol. 305, 2024

[15] Y. Lu *et al.*, "Dynamic analysis of MTMD vibration reduction for offshore wind turbine under combined wind-wave-seismic loads," *Structures,* vol. 72, 2025

[16] V. Jahangiri and C. Sun, "Three-dimensional vibration control of offshore floating wind turbines using multiple tuned mass dampers," *Ocean Engineering,* vol. 206, 2020

[17] G. Park, K.-Y. Oh, and W. Nam, "Bilinear tuned mass damper for spar-type floating wind turbines," *Ocean Engineering,* vol. 261, 2022

[18] Y.-P. Wang *et al.*, "Performance of Tuned Mass Dampers for Vibration Reduction in a TLP Floating Wind Turbine," in *ISOPE International Ocean and Polar Engineering Conference*, 2020: ISOPE, pp. ISOPE-I-20

[19] D. Chen, S. Huang, C. Huang, R. Liu, and F. Ouyang, "Passive control of jacket–type offshore wind turbine vibrations by single and multiple tuned mass dampers," *Marine Structures,* vol. 77, 2021

[20] D. Han, W. Wang, X. Li, and X. Su, "Optimization design of multiple tuned mass dampers for semi-submersible floating wind turbine," *Ocean Engineering,* vol. 264, 2022

[21] X. Dong, S. Ren, Y. Jia, and T. Yu, "Parameter optimization and vibration reduction effect of one C-shaped particle damping-tuned mass damper for offshore wind turbine," *Ocean Engineering,* vol. 305, 2024

[22] M.-A. Xue, P. Dou, J. Zheng, P. Lin, and X. Yuan, "Pitch motion reduction of semisubmersible floating offshore wind turbine substructure using a tuned liquid multicolumn damper," *Marine Structures,* vol. 84 , 2022.

[23] H. Ding *et al.*, "On the size effects of toroidal tuned liquid column dampers for mitigating wind-and wave-induced vibrations of monopile wind turbines," *Ocean Engineering,* vol. 273, p. 113988, 2023.

[24] D. Han, X. Li, W. Wang, and X. Su, "Dynamic modeling and vibration control of barge offshore wind turbine using tuned liquid column damper in floating platform," *Ocean Engineering,* vol. 276, p. 114299, 2023.

[25] A. Das and H. Ding, "Compliant liquid dampers-inerter for mitigating wind-, wave-, and earthquake-induced vibrations of monopile offshore wind turbines," *Ocean Engineering,* vol. 301, p. 117486, 2024.

[26] A. Hemmati, E. Oterkus, and M. Khorasanchi, "Vibration suppression of offshore wind turbine foundations using tuned liquid column dampers and tuned mass dampers," *Ocean Engineering,* vol. 172, pp. 286-295, 2019.

AI-Driven Meeting Science for Construction Design Teams: A Conceptual Model for Effective Communication

Hassan A. Abdelsalam [1] [0000-0001-7695-4378], Marzia Bolpagni [2,3] [0000-0003-3548-1484]

Talib E. Butt [1] [0000-0002-3671-4107], Mai Soliman [4] [0000-0002-8350-0654]

[1] Faculty of Engineering and Built Environment, Northumbria University, City Campus, Newcastle upon Tyne. Post Code: NE1 1ST, England, UK.
[2] Mace, 155 Moorgate, London, Post Code: EC2M 6XB, England, UK.
[3] UCL Bartlett School of Sustainable Construction, 1-19 Torrington Place, London, Post Code: WC1E 7HB, England, UK.
[4] Architectural Engineering Department, Faculty of Engineering, City Campus, Alexandria University, Lotfy El-Sied st. off Gamal Abd El-Naser, Alexandria. Post Code: 11432, Egypt.

Abstract. Effective communication and collaboration, particularly during Construction Design Team Meetings (CDTMs) where key decisions are made, are fundamental to the success of construction projects. However, for a given construction project, the efficacy of CDTMs often diminishes due to lack of coordination. In addition to communication and collaboration, other factors which influence the degree of collaboration in CDTMs are data fragmentation, human behaviour and language, diversity in backgrounds and interests of stakeholders, variability in terminologies, ineffective facilitating mechanisms, organisational behaviour, project complexity and scale, and alike. To overcome such challenges, this study aims to frame a conceptual model that integrates the Meeting Science and Artificial Intelligence (AI) to enhance the efficiency and effectiveness of CDTMs. The research follows a qualitative, theory-building approach rooted in interdisciplinary literature synthesis. It draws from domains including construction management, human-computer interaction, and digital innovation. The study entails mapping CDTMs' operational and behavioural challenges against AI-enabled systems, culminating in a conceptual triangulation between AI, Meeting Science, and CDTMs. The aforementioned conceptual model systematises the interplay between these domains while addressing both technical constraints such as data volume and integration and non-technical factors like group dynamics and behavioural implications. As a forward-looking recommendation, the study advocates for further empirical research to operationalise and evaluate the model, ultimately paving the way for the development of applied e-tools that support more responsive, data-driven, and human-centric meeting practices in construction.

Keywords: Meeting Science; AI, CDTMs, Construction, Communication, Industry 4.0.

1 Introduction

The construction industry holds a pivotal role in the global economy, contributing approximately 6% to global GDP and continuing to grow. However, despite its economic weight and technological advancements, the industry remains characterised by chronic inefficiencies, particularly during the construction implementation phase, which is often the most rigid, high-risk, and cost-intensive period of a project [1, 2]. A central strategy aimed at mitigating these inefficiencies has been the improvement of the Production, Planning, and Control Function (PCF), a managerial mechanism responsible for regulating workflows, material logistics, and operational synchronisation [3, 4]. Traditionally conceptualised through either a contract-based business lens or a transformation-based production view, the PCF has evolved to incorporate principles of flow and value generation [5, 6]. Yet, these frameworks often neglect the intricate relational dynamics within teams and between process components, particularly the critical but underexplored interdependencies between meetings, decision-making bodies, and communication structures [7, 8]. This systemic blind spot limits the potential for holistic performance improvement and contributes to persistent downstream variability and inefficiency [9, 10].

Effective communication and collaboration, particularly during where design intentions are coordinated and key decisions are made, are fundamental to the success of construction projects. However, for any given project, the efficacy of these meetings often diminishes due to persistent coordination failures and socio-technical complexity. A range of factors impinge on collaborative performance within CDTMs, including fragmented data, disciplinary silos, divergent stakeholder interests, behavioural variability, terminological differences, and inadequate facilitation mechanisms. These challenges are further amplified by increasing project scale and complexity, making timely and informed decision-making more difficult to achieve. Despite their centrality to project success, CDTMs are often limited by the lack of structured frameworks that address both the behavioural and procedural components of collaboration. There remains a pressing need to develop conceptual tools that help teams navigate not only technical data integration but also the subtle social interactions that shape participation, influence, and alignment during design coordination.

This study aims to develop a conceptual model that enhances the structure and effectiveness of by integrating insights from Meeting Science and. Adopting a qualitative, theory-building approach, the research synthesises interdisciplinary literature across construction management, organisational psychology, human-computer interaction, and digital innovation. The study maps the operational and behavioural challenges of CDTMs against the affordances of AI-enabled systems, constructing a theoretical triangulation that connects AI, Meeting Science, and CDTMs. The resulting model systematises the interplay between technological capacities and human behaviours in meeting contexts, addressing both technical constraints such as information fragmentation and non-technical concerns like group dynamics, behavioural uncertainty, and communication inefficiencies. It contributes a foundational framework to inform future research and industry practice, with the long-term vision of enabling more responsive, data-informed, and human-centred meeting environments within construction projects

[11, 12]. Further empirical validation is recommended to operationalise and refine this model toward the development of practical tools that support adaptive, inclusive, and intelligent meeting facilitation.

This study investigates three distinct yet interrelated domains; Meeting Science, Construction Design Teams, and AI each examined independently to identify key theories, concepts, and frameworks relevant to the construction sector. Once the foundational constructs of each domain were established through a comprehensive review of interdisciplinary literature, an integrative process was undertaken to explore their intersections within the context of the built environment. The convergence of these domains is conceptually mapped through a triangular model that visualises the relationships between core entities, including their inputs, outputs, and interdependencies. This integration, developed through qualitative synthesis and mind mapping, forms the conceptual model proposed in this research. As a theory-building study, the methodology is qualitative and deductive in nature, relying on existing literature and expert insights to derive a model that conceptualises how AI-enhanced meeting practices can address coordination challenges in.

2 Meeting Science

In recent decades, a growing body of interdisciplinary scholarship has recognised meetings not simply as routine organisational practices, but as complex, consequential events central to decision making, coordination, and communication in knowledge intensive environments. This has given rise to Meeting Science, an emerging field that systematically investigates the design, conduct, and impact of workplace meetings (Allen [13-15]. Grounded in organisational psychology, communication studies, and management science, Meeting Science seeks to understand how meetings influence outcomes such as team cohesion, decision quality, innovation, and performance. Scholars in this domain explore a wide range of variables, including meeting structure, facilitation techniques, behavioural norms, participant roles, and socioemotional dynamics [16, 17]. While meetings are ubiquitous across all industries, their effectiveness is often compromised by poor preparation, unclear objectives, disengagement, and imbalanced participation. Consequently, Meeting Science aims to transform these often-maligned encounters into purposeful, inclusive, and productive forums by applying empirical insights to real world settings.

What distinguishes Meeting Science from broader organisational theory is its specific focus on the micro level behaviours and structures that shape meeting processes and outcomes. Research within this field demonstrates that the perceived value of meetings is not solely determined by their content or duration, but rather by how they are facilitated, how participants interact, and whether outcomes are aligned with team expectations and organisational goals [18]. Variables such as punctuality, agenda clarity, psychological safety, and the equitable distribution of speaking time have been empirically linked to improved engagement and satisfaction [16, 19]. Furthermore, recent developments have introduced new analytical tools such as interaction coding, behavioural mapping, and digital tracking that allow researchers to explore verbal and nonverbal

cues in high resolution detail. As workplace collaboration becomes increasingly virtual and hybrid, Meeting Science has evolved to include studies of how digital environments shape meeting dynamics, from participation inequality to cognitive overload. This adaptability positions Meeting Science as a powerful framework not only for understanding meetings as sociotechnical events but also for reimagining their design in alignment with technological advances and shifting workplace cultures. In the context of construction, where interdisciplinary coordination is essential and meetings often serve as the primary decision-making arena, the application of Meeting Science offers untapped potential for enhancing collaboration, reducing conflict, and improving project outcomes.

The COVID-19 pandemic, while now largely subsided, has had a lasting impact on how meetings are conducted across industries. Historically, meetings were predominantly held face-to-face, even as earlier technologies such as telephony and videoconferencing provided alternatives for geographically dispersed teams. However, the pandemic catalysed a rapid and widespread transition to virtual and hybrid meeting formats, reshaping behavioural norms and technological expectations surrounding workplace collaboration. In the construction sector, where professionals often manage multiple geographically distant projects, this shift has proven particularly significant. The widespread adoption of digital platforms for coordination has not only normalised remote engagement but also created new opportunities for the integration of AI into meeting environments. As meetings increasingly occur in structured digital settings, the feasibility and relevance of AI-enabled systems for supporting real-time facilitation, behavioural analysis, and decision-making have become more apparent. The pandemic thus served as a powerful accelerant, both in digitalising meeting practices and in paving the way for the practical adoption of AI within collaborative workflows.

3 Construction Design Teams (CDTs)

In the contemporary construction industry, Construction Design Teams (CDTs) are essential to the collaborative processes that underpin project success. These interdisciplinary groups bring together architects, engineers, contractors, and other stakeholders to align design intent, resolve technical issues, and make coordinated decisions. However, despite their central role, CDTs frequently encounter inefficiencies stemming from fragmented communication, ambiguous expectations, and coordination breakdowns, issues exacerbated by increasing project scale and stakeholder diversity [11, 17, 20]. These challenges are not merely procedural but are rooted in the behavioural dynamics of team interactions, where varied communication styles and professional perspectives often lead to misalignment [9, 21].

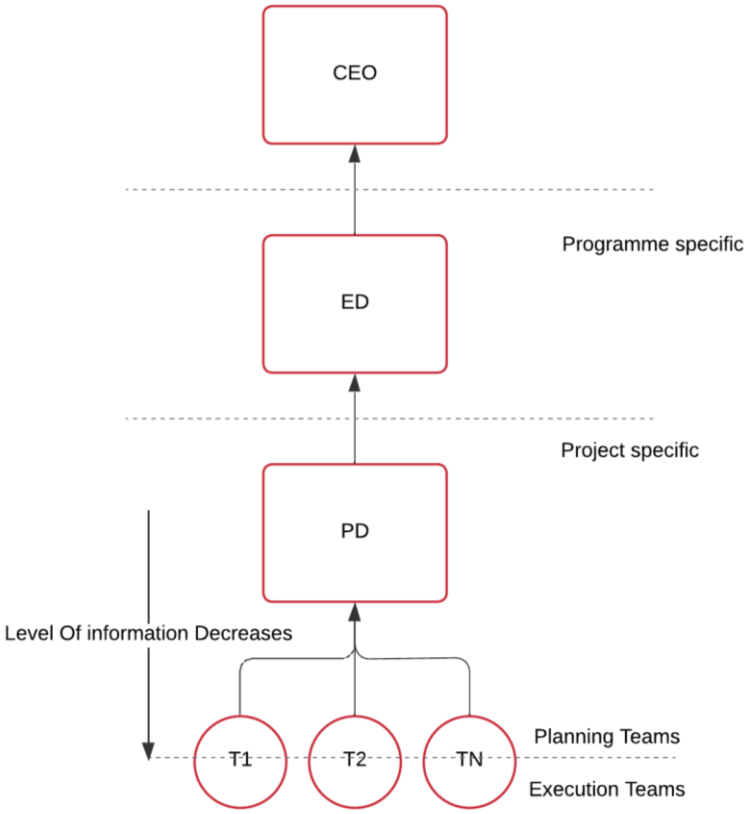

Fig. 1. Construction Design Teams Hierarchy

Recent literature emphasises the need to view CDTs not only as technical taskforces but also as complex social systems. Effective collaboration depends as much on trust, psychological safety, and behavioural cohesion as it does on technical expertise [22, 23] The rise of contractor-led procurement has further shifted responsibility for design management onto main contractors, requiring enhanced interpersonal awareness and coordination skills [24]. Yet, there remains a research gap in understanding the behavioural and non-verbal dynamics that influence design coordination. A more holistic approach is needed one that acknowledges CDTs as both decision-making bodies and arenas of social negotiation where identities, power, and collaborative norms are constantly shaped and reshaped [25, 26].

4 Artificial Intelligence (AI)

AI has rapidly evolved from a theoretical concept into a transformative force reshaping industries such as healthcare, finance, manufacturing, and increasingly, construction.

Defined broadly, AI refers to computer systems capable of performing tasks typically requiring human intelligence, such as learning, reasoning, perception, language processing, and decision-making [27]. In the construction sector, AI has gained traction not only as a tool for automation but also as a strategic enabler across project planning, design, execution, and operation. By leveraging vast and diverse data sets, AI supports predictive modelling, optimisation of construction workflows, and advanced analytics. Applications now include machine learning for risk assessment, computer vision for safety and progress monitoring, natural language processing (NLP) for document management, and generative design [28, 29].

However, despite significant advancements in AI applications for construction operations, its targeted integration into CDTMs remains underexplored in academic literature and industry practice. CDTMs are critical forums for interdisciplinary collaboration, yet they are often hindered by coordination failures, fragmented data, and behavioural inefficiencies. The novelty of this study lies in positioning AI not merely as a tool for process automation but as a proactive facilitator of real-time, human-centric decision-making environments within CDTMs.

This conceptual model addresses an evident gap by integrating AI features with behavioural insights from Meeting Science to systematise both technical and interpersonal elements of design coordination. AI functionalities such as voice recognition, real-time content retrieval, sentiment analysis, and participation tracking offer timely interventions that can improve inclusivity, reduce delays, and reinforce structured decision-making. The need for such a model is underscored by the growing complexity of construction projects and the shift toward hybrid and digital collaboration environments following the COVID-19 pandemic. These conditions present both a challenge and an opportunity to rethink how CDTMs are facilitated.

By focusing on the behavioural dimensions of meetings rather than only on their outputs, this study demonstrates how AI can operate as an intelligent intermediary. The proposed model offers an innovative pathway toward responsive, data-informed, and socially aware coordination processes, representing a novel and necessary evolution in construction meeting facilitation.

5 Integration between Meeting Science, CDTs, and AI

The intersection of Meeting Science, CDTMs, and AI presents a promising avenue for addressing persistent coordination challenges in construction projects. This triangulated model recognises that effective coordination in CDTMs hinges not only on the availability of technical information but also on the behavioural conditions that facilitate or hinder knowledge exchange. Each domain, while distinct, contributes unique insights and capabilities to the shared goal of enhancing collaboration, decision-making, and project outcomes. Meeting Science provides a behavioural and procedural lens to understand and optimise human interactions during meetings. Construction Design Teams embody the multidisciplinary expertise and complex stakeholder dynamics essential to project delivery. Meanwhile, AI offers innovative tools to augment human cognition and streamline meeting processes through data-driven, real-time support. By

integrating these three fields into a unified conceptual model, it becomes possible to reconceptualise CDTMs as dynamic, intelligent systems that adapt to evolving project demands and foster more effective engagement among participants. The proposed conceptual model delineates a structured integration of Meeting Science, Construction Design Teams, and AI to advance the effectiveness and efficiency of CDTMs. Rather than viewing CDTMs as isolated procedural events, the model conceptualises them as emergent sociotechnical systems resulting from the convergence of behavioural, organisational, and computational domains. Through this triangulated framework, CDTMs are redefined as intelligent, adaptive environments where structured human collaboration is supported by data-driven, real-time digital augmentation, aimed at improving decision-making, engagement, and design coordination in construction projects (See Fig. 3)

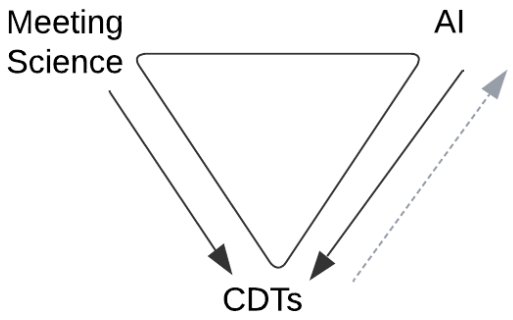

Fig. 2. Integration Triangulation

5.1 Model Dimensions

The first dimension

The first dimension of the model draws from Meeting Science, which offers empirically grounded insights into the behavioural and procedural dynamics that shape meeting quality and outcomes. This includes six critical dimensions: openness and participation, power dynamics and hierarchy, decision-making norms, agenda structure and punctuality, socioemotional climate, and interaction equity (See Fig. 3). These dimensions serve as both analytical variables and design criteria, informing how meeting processes can be structured and monitored for improvement. By elucidating the micro-level behaviours and contextual conditions that influence collaboration, Meeting Science provides a theoretical foundation for translating human interaction patterns into actionable data for AI-supported facilitation.

The second dimension

The second dimension encompasses the Construction Design Teams, which are subdivided into design teams (e.g. architects, structural engineers, MEP engineers, and design managers) and construction teams (e.g. main contractors, cost managers, quantity surveyors, and site engineers). These stakeholders constitute the primary agents within CDTMs, responsible for real-time knowledge exchange, problem-solving, and coordination of design intent and constructability. Their interactions, decisions, and communication behaviours represent the core operational processes within CDTMs. Additional stakeholders, such as client representatives, regulatory authorities, and external consultants, remain essential to the project ecosystem but typically contribute indirectly to the AI system, shaping the meeting's context or influencing outcomes outside of real-time engagement.

The third dimension

The third dimension introduces the AI system as a socio-technical enabler that enhances both the procedural and behavioural dimensions of meetings. The AI system operates across three interrelated temporal phases:

Pre-meeting Phase:

In the preparatory stage, AI contributes to agenda formulation, ensuring alignment between meeting objectives and stakeholder priorities. It facilitates information consolidation, drawing from document repositories, BIM environments, previous meeting records, and stakeholder input to assemble relevant materials. It also supports participant briefing and role clarification, reducing ambiguity and enhancing readiness. This preparatory support addresses common barriers such as fragmented information and unclear expectations, thereby establishing a structured and goal-oriented foundation for the meeting.

In-meeting Phase:

During the meeting, the AI system enables real-time interaction support through mechanisms such as voice recognition, natural language processing, and semantic command identification. When stakeholders reference specific design elements or decisions, the AI system automatically retrieves and displays corresponding BIM components, documents, or prior discussion points, thereby minimising time lost on manual navigation. Concurrently, the system performs behavioural analytics, tracking engagement, participation equity, conversational balance, and emotional tone. These insights inform facilitators in adjusting the meeting flow, addressing dominance or silence, and maintaining inclusive dialogue. The integration of AI in this phase effectively operationalises Meeting Science principles within live interaction contexts.

Post-meeting Phase:

Following the meeting, the AI system facilitates automated documentation, including summarisation of decisions, task assignments, unresolved issues, and traceable references to relevant files or communications. It supports task distribution and monitoring, ensuring follow-up actions are recorded and disseminated. Additionally, it produces

behavioural feedback reports, offering insights into participation patterns, punctuality, and decision quality over time. These reflective analytics inform continuous improvement cycles and foster a learning-oriented team culture.

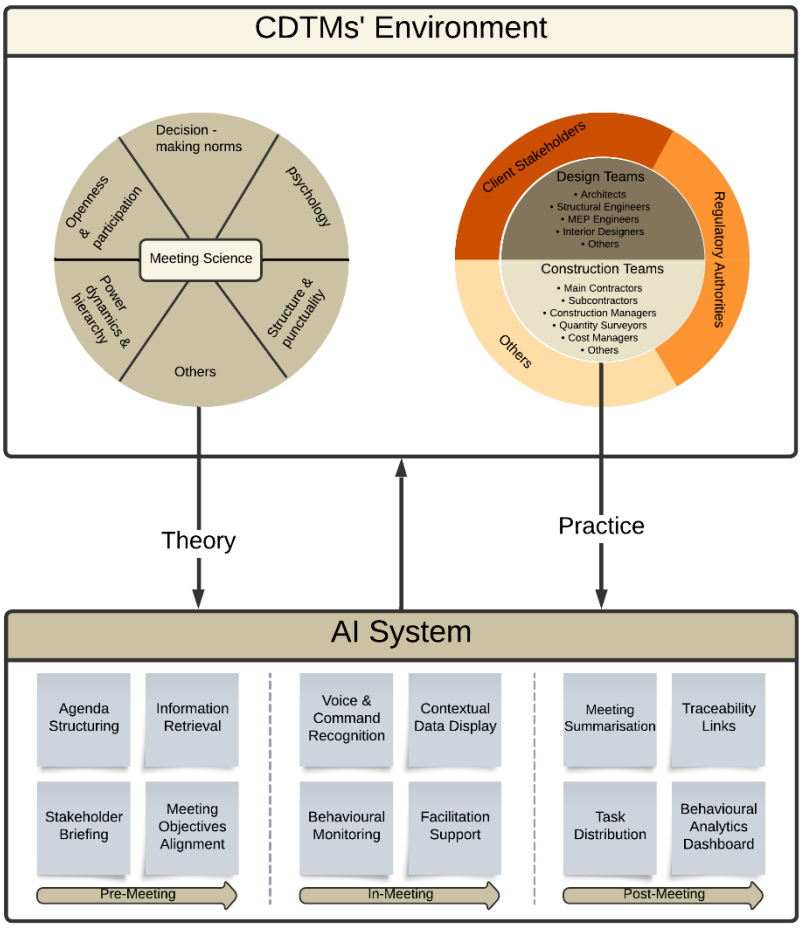

Fig. 3. The Conceptual Model of the Integration between Meeting Science, CDTs, and AI

6 Conclusion Remarks

This study has proposed a novel conceptual framework that integrates insights from Meeting Science and AI to enhance the structure, effectiveness, and behavioural dynamics of CDTMs. By triangulating these three domains, the research presents a multidimensional understanding of the socio-technical complexity that characterises design

coordination in contemporary construction projects. The model positions CDTMs not simply as managerial procedures but as dynamic environments where technical decision-making and human behavioural intersect. It further establishes AI as a mediator that can respond to both structured information and nuanced interpersonal cues, enabling adaptive, inclusive, and data-informed meeting practices. Meeting Science informs this integration by offering a theoretical lens to understand micro-level interactions, while AI provides the analytical and computational tools needed to capture, interpret, and enhance them in real time. Together, these perspectives offer a comprehensive platform to rethink how meetings are conducted, evaluated, and improved within the construction domain.

Despite the conceptual depth of this model, several limitations must be acknowledged. First, the framework remains theoretical and has not yet been empirically validated in live construction settings. The behavioural complexities of CDTMs, particularly their non-verbal, spatial, and emotional dynamics, are difficult to simulate or generalise without rich observational data. Additionally, the effective deployment of AI in meeting contexts faces technical and ethical challenges, including data privacy, bias in algorithmic interpretation, and the potential over-reliance on automation at the expense of human judgement. There is also a risk of over-formalising inherently informal and socially negotiated spaces, which may inadvertently reduce spontaneity and creativity. Moreover, the variation in organisational cultures, project delivery models, and digital maturity across the construction industry may affect the generalisability of the model's applicability and effectiveness.

Future research should focus on operationalising the model through prototyping and testing in both simulated and real-world CDTMs. Empirical studies are needed to evaluate how AI-enabled meeting facilitation influences participation equity, decision quality, and behavioural dynamics across different project types and team configurations. Mixed-methods research combining observational analytics, qualitative interviews, and system performance data will be essential in validating the theoretical assumptions of the model. Furthermore, interdisciplinary collaboration with behavioural scientists, computer scientists, and construction practitioners is crucial to refine AI tools that are ethically sound, contextually aware, and user centric. Ultimately, the framework sets the foundation for a new generation of responsive, intelligent, and human-aware meeting systems, capable of supporting the construction sector's transition toward more collaborative, resilient, and performance-driven project environments.

References

[1] S.B. Prakash, R. Kirkham, A. Nanda, S. Coleman, Exploring the complexity of highways infrastructure programmes in the United Kingdom through systems thinking, Project Leadership and Society 4 (2023) PP. 100081, https://doi.org/10.1016/j.plas.2023.100081.

[2] C. Kock, S. Paavola, H. Buhl, Construction Management and Economics 37 (6) (2019) PP. 309.

[3] J. Burbidge, It's a time of participation, The Journal for Quality and Participation 16 (7) (1993) PP. 30.

[4] G. Ballard, G. Howell, What kind of production is construction, 1998, pp. 13-15.

[5] J.W.M. Bertrand, J. Wingaard, The structuring of production control systems, International Journal of Operations & Production Management 6 (2) (1986) PP. 5-20.

[6] I.D. Tommelein, D.R. Riley, G.A. Howell, Parade game: Impact of work flow variability on trade performance, Journal of Construction Engineering and Management 125 (5) (1999) PP. 304-310.

[7] P.S. Chinowsky, A. Member, E.M. Rojas, A. Member, Virtual teams: Guide to successful implementation, (2003).

[8] Rafael Sacks, Charles Eastman, Ghang Lee , P. Teicholz, BIM handbook : a guide to building information modeling for owners, managers, designers, engineers and contractors, 2018, ISBN: 9781119287537.

[9] O. Zegarra, L.F. Alarcón, Coordination of teams, meetings, and managerial processes in construction projects: using a lean and complex adaptive mechanism, Production Planning and Control 30 (9) (2019) PP. 736-763, 10.1080/09537287.2019.1578905.

[10] U. Lindemann, M. Maurer, T. Braun, Structural complexity management: an approach for the field of product design, Springer Science & Business Media, 2008, ISBN: 3540878890.

[11] A. Celoza, D.P. De Oliveira, F. Leite, Role of BIM Contract Practices in Stakeholder BIM Implementation on AEC Projects, Journal of Legal Affairs and Dispute Resolution in Engineering and Construction 15 (2) (2023), 10.1061/JLADAH.LADR-916.

[12] J. Heisler, Videoconference Site Facilitator's Guide, (1993).

[13] J.A. Allen, N. Lehmann-Willenbrock, S.G. Rogelberg, The Meeting Itself, in: J.A. Allen, N. Lehmann-Willenbrock, S.G. Rogelberg (Eds.), The Cambridge Handbook of Meeting Science, Cambridge University Press, Cambridge, 2015, pp. 245-614, ISBN: 9781107067189, https://doi.org/10.1017/CBO9781107589735.

[14] B.A. Balasubramanian, S.M. Chase, P.A. Nutting, D.J. Cohen, P.A.O. Strickland, J.C. Crosson, W.L. Miller, B.F. Crabtree, U.S. Team, Using Learning Teams for Reflective Adaptation (ULTRA): insights from a team-based change management strategy in primary care., Annals of family medicine (2010), 10.1370/afm.1159.

[15] S. Banerjee, C. Rose, A.I. Rudnicky, The Necessity of a Meeting Recording and Playback System, and the Benefit of Topic–Level Annotations to Meeting Browsing, (2005).

[16] D.J. Leach, S.G. Rogelberg, P.B. Warr, J.L. Burnfield, Perceived Meeting Effectiveness: The Role of Design Characteristics, Journal of Business and Psychology 24 (1) (2009) PP. 65-76, 10.1007/s10869-009-9092-6.

[17] J.A. Allen, N. Lehmann-Willenbrock, The key features of workplace meetings: Conceptualizing the why, how, and what of meetings at work, Organizational Psychology Review (2022) PP. 20413866221129231, 10.1177/20413866221129231.

[18] J.A. Allen, N. Lehmann-Willenbrock, S.G. Rogelberg, Introduction, in: J.A. Allen, N. Lehmann-Willenbrock, S.G. Rogelberg (Eds.), The Cambridge Handbook of Meeting Science, Cambridge University Press, Cambridge, 2015, pp. 1-46, ISBN: 9781107067189, https://doi.org/10.1017/CBO9781107589735.

[19] N. Lehmann-Willenbrock, J.A. Allen, How fun are your meetings? Investigating the relationship between humor patterns in team interactions and team performance., The Journal of applied psychology (2014), 10.1037/a0038083.

[20] H. Ponton, A. Osborne, N. Thompson, D. Greenwood, The power of humour to unite and divide: a case study of design coordination meetings in construction, Construction Management and Economics 38 (1) (2020) PP. 32-54, 10.1080/01446193.2019.1656339.

[21] C.A. Gorse, S. Emmitt, Construction Management and Economics 25 (11) (2007) PP. 1197.

[22] H.F. Ponton, Social interactions in construction design team meetings, Northumbria University, 2021 Available at: http://nrl.northumbria.ac.uk/policies.html (Accessed.

[23] J.J. Gross, R. Thompson, Emotion Regulation: Conceptual Foundations, Handbook of Emotion Regulation, 2007, pp. 3-27.

[24] M. Alaqad, K. Gidado, P. Piroozfar, M. Alkhadim, A. Dorgham, Efficacy of value management system in building projects: a UK perspective, 2020, pp. 146-155.

[25] M.S. Cidik, D. Boyd, Construction Management and Economics null (null) (2019) PP. null.

[26] S. Mehrbod, S. Staub-French, N. Mahyar, M. Tory, Characterizing interactions with BIM tools and artifacts in building design coordination meetings, Automation in Construction 98 (2019) PP. 195-213, https://doi.org/10.1016/j.autcon.2018.10.025.

[27] S. Russell, P. Norvig, F. Popineau, L. Miclet, C. Cadet, Intelligence artificielle: une approche moderne (4e édition), Pearson France, 2021

[28] T. Bock, T. Linner, Advanced Construction and Building Technology, Robot-Oriented Design, 2015, pp. 1-17, ISBN: 9781139924146, 10.1017/cbo9781139924146.002.

[29] A. Ghosh, S. Nundy, S. Ghosh, T.K. Mallick, Study of COVID-19 pandemic in London (UK) from urban context, Cities 106 (2020) PP. 102928.

Prediction of Shear Strength of Reinforced Concrete Beam-Column Joints

Yaren Aydın[1], Gebrail Bekdaş[1], Sinan Melih Nigdeli[1] and Ümit Işıkdağ[2]

[1]Department of Civil Engineering, Istanbul University-Cerrahpaşa,
34320 Avcılar/Istanbul/Turkey
yaren.aydin@iuc.edu.tr, bekdas@iuc.edu.tr, melihnig@iuc.edu.tr
[2] Department of Architecture, Mimar Sinan Fine Arts University, 34427 Istanbul, Turkey
umit.isikdag@msgsu.edu.tr

Abstract. In this study, a machine learning-based approach was developed to predict the shear strength of beam-column joints. A comprehensive dataset including column height, beam length, beam and column width, beam and column depth, and vertical reinforcement ratio was used. This study aimed to predict the shear strength of beam-column connections using data obtained from a total of 203 different reinforced concrete beam-column connection tests reported in the literature in another study. Linear Regression method was applied in the estimation process, and the performance of the model was evaluated using statistical metrics such as R^2 score, Root Mean Square Error (RMSE), Mean Absolute Error (MAE), Mean Absolute Percent Error (MAPE) and Variance Explained Score.. The findings showed that the linear regression model can predict the shear strength of beam-column joints with high accuracy. The findings were also supported by graphical analysis, thus increasing the reliability of the results. The main contribution of the study is to demonstrate that machine learning methods can be used as a reliable estimation tool in structural engineering.

Keywords: Beam-Column Joints, Shear, Linear Regression

1 Introduction

Although the structure is expected to exhibit ductile behavior under seismic loads, in frame systems, it is not sufficient for individual elements to meet the necessary conditions to guarantee this behavior. In such structures, high shear forces develop in the beam-column connection regions as a result of seismic effects, and these regions are subjected to intense stresses. Serious damage that may occur in the joint region causes a sudden decrease in the rigidity of the structure. The primary function of the beam-column joint is to transfer the stresses at the beam ends to the column. A strong column-weak beam approach is generally used to achieve this transfer. The goal is to ensure that the beams deform before the columns collapse to prevent damage to the structure under horizontal loads.

Various capacity approaches and simplified formulas have been developed in the literature to determine the shear strength of reinforced concrete elements [1], [2]. With the increase in experimental studies and parameters, it has become possible to adapt

and calibrate these models for general use. In traditional methods, calibration is usually performed based on the average values of experimental data. In contrast, machine learning (ML) methods can capture these interactions more flexibly by learning from large and multidimensional data sets, offering accuracy potential beyond traditional models.

Machine learning methods are also widely used to estimate the shear strength of reinforced concrete members. This section will review existing literature on machine learning-based studies applied to estimate the shear strength of reinforced concrete members such as columns and beams. Jeon et al. [3] proposed probabilistic beam-column joint shear strength models using conventional multiple Linear Regression, multivariate adaptive regression splines (MARS), and symbolic regression (SR) methods. Analysis results showed that the MARS approach was the most accurate estimation method, and the derived model achieved higher accuracy compared to existing relationships. Mangalathu and Jeon [4] used machine learning to predict the failure modes and shear strengths of beam-column connections using 536 experimental tests. They used Linear, Stepwise, Ridge, Lasso, Elastic Net, and Random Forest models, and Lasso regression showed the best efficiency in classification and prediction. Almasabha [5] used XGBoost, LightGBM, and Artificial Neural Network (ANN) models to predict the shear strength of short connections. The results showed that the LightGBM and XGBoost models provided higher accuracy compared to the AISC code and ANN, with LightGBM in particular performing the best. Furthermore, the overstrength ratio predicted by LightGBM was superior compared to the Gene Expression and Finite Element models. Liu et al. [6] proposed Support Vector Regression (SVR) and Random Forest Regression (RFR) models for the prediction of shear transfer strength (STS) of concrete joints using 512 test data, with customized training procedures and a novel weighted feature selection method. The results show that the SVR and RFR models are more accurate and stable than the mechanics-based models. To estimate the shear strength of ultra-high-performance fiber-reinforced concrete (UHPFRC) beams, Ni and Duan [7] generated a dataset of 200 UHPFRC beam samples and analyzed the influence factors using the random forest (RF) method. Artificial Neural Networks (ANN), Support Vector Regression (SVR), and XGBoost models were then applied to estimate the shear strength. The results showed that the longitudinal reinforcement area was the most influential parameter. Among the models, SVR achieved the highest accuracy (R^2=0.9016). Zhang et al. [8] developed a random forest (RF) model to predict the shear strength of RC beams. RF hyperparameters were optimized using a modified insect antenna search algorithm using Levy flight and inertial weighting. The model was trained on stirrup and non-stirrup beam datasets with 194 and 1849 samples, respectively, and the model showed high accuracy with correlations of 0.9367 and 0.9424. Abuodeh et al. [9] used resilient back-propagating neural network (RBPNN) to study the behavior of shear-strengthened CC beams with edge-bonded and U-wrapped FRP laminates. The results showed that with the selected parameters, the prediction accuracy of RBPNN (r^2=0.885; RMSE=8.1 kN) increased compared to the original model (r^2=0.668; RMSE=16.6 kN). The model also outperformed existing standard predictions (ACI 440.R-17, fib14, CNR-DT200).

In this study, it was aimed to predict the shear strength of beam-column joints using experimental data obtained from 203 different reinforced concrete beam-column joint test results reported in the literature.

2 Methodology

2.1 Dataset

The dataset used in this study was taken from the dataset [10], which is compiled from 203 reinforced concrete beam-column connection tests reported in the literature. The data set used in this study includes independent variables such as beam and column geometry, reinforcement ratios and concrete strength, as well as the experimentally measured target variable of shear strength (V_{exp}). In the dataset, H_c is the Height of column, L is the Length of the beam, b_b is the Beam width, b_c is the Column width, h_c is the Column depth, h_b is the Beam depth, ρ_{sv} is the Vertical reinforcement ratio.

Basic statistical analyses were performed on the dataset. This dataset is used as input data for Linear Regression to predict the shear strength of beam-column connections. Basic statistics are summarized in Table 1, and the data distribution is visualized in Fig. 1.

Table 1. Linear Regression results.

Statistics	H_c (mm)	L (mm)	h_c (mm)	b_c (mm)	h_b (mm)	b_b (mm)	f_{cm} (MPa)	ρ_{sv} (MPa)	V_{exp} (kN)
count	203	203	203	203	203	203	203	203	203
mean	2341.748	1304.418	290.906	264.157	362.802	233.384	41.091	1.458	419.220
std	744.990	577.015	94.073	100.846	117.077	89.210	16.389	1.798	353.734
min	1400	600	150	100	150	100	14.41	0	23.72
max	4100	3048	500	500	610	500	93.8	7.59	2095.35

From Table 1, it can be seen that the independent variables are numerical, with height of column ranging from 1400–4100 mm and beam lengths ranging from 600–3048 mm. Fig. 1 shows boxplots for the input and output variables.

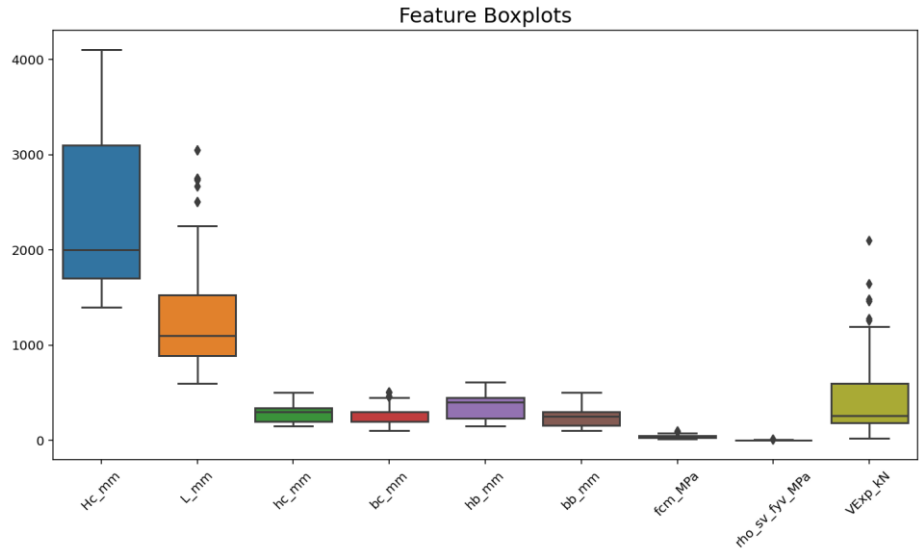

Fig. 1. Boxplots for the input and output variables.

2.2 Linear Regression

In this study, machine learning (ML) was used. ML is a field of artificial intelligence (AI) that allows computers to perform specific tasks by gaining experience with data, without being directly programmed. Algorithms in this field can create models from data and perform tasks such as pattern recognition, prediction, classification, and decision-making. In this study, Linear Regression was used to predict the shear strength of beam-column joints. Machine learning methods are divided into four main categories: Supervised Learning, Unsupervised Learning, Semi-Supervised Learning and Reinforcement Learning.

Linear Regression is a method that models the desired output using various input variables. This method typically reveals the relationship between the input variables and the predicted value. Using Linear Regression analysis, the relationship between a dependent variable and one or more independent variables can be examined. In a linear model, the dependent variable is expressed as directly proportional to the value of the independent variable. In simple Linear Regression, there is only one independent variable. The dependent variable (y) is the variable that is explained or predicted in the regression model and is assumed to have a functional relationship with the independent variable. The independent variable (x) is the variable that is thought to have an impact on the dependent variable and is used to predict the value of the dependent variable [11].

$$y = \alpha + \beta x + \varepsilon \tag{1}$$

In Equation 1, y is the dependent variable, x is the independent variable, α is the constant term, β is the slope of the regression line, and ε is the error term or residual value.

2.3 Performance Metrics

The metrics used to evaluate the performance of machine learning models vary depending on the task type, such as regression, classification, or object detection. In regression tasks, these metrics are used to evaluate the model's accuracy in predicting continuous values, its errors, and its generalization capacity. The study used several performance metrics used in regression tasks: R^2 Score, Root Mean Square Error (RMSE), Mean Absolute Error (MAE), Mean Absolute Percentage Error (MAPE) and Explained Variance Score.

2.4 K-Fold Cross Validation

K-fold cross validation is used to increase the generalizability of the Model. To examine whether the model's optimal performance was due to a single random data split, we applied 10-fold cross-validation. In this method, the dataset was divided into 10 equal parts, with a different part used as the validation set in each iteration, while the remaining nine parts were combined for training. In this study, machine learning applications were developed using the Python programming language. Data processing and analysis were effectively performed using the Scikit-learn [12] and Pandas libraries.

3 Results

Table 1 summarizes the predictive performance of the Linear Regression model. Table 1 includes the average R^2 score, RMSE, MAE, MAPE, and explained variance scores of the Linear Regression model.

Table 2. Linear Regression model performance metrics

Model	Average MAE
Average R^2 Score	0.8375
Average RMSE	130.6470
Average MAE	98.1251
Average MAPE	0.4214
Average Explained Variance Score	0.8407

As can be seen in Table 1, the model exhibits a high R2 score (0.8375) and explained variance (0.8407). Furthermore, the MAPE value reveals that the percentage prediction error is low. Overall, Table 1 shows that the Linear Regression model exhibits good

predictive performance on the data set. Fig. 2 shows different evaluation graphs of the Linear Regression model.

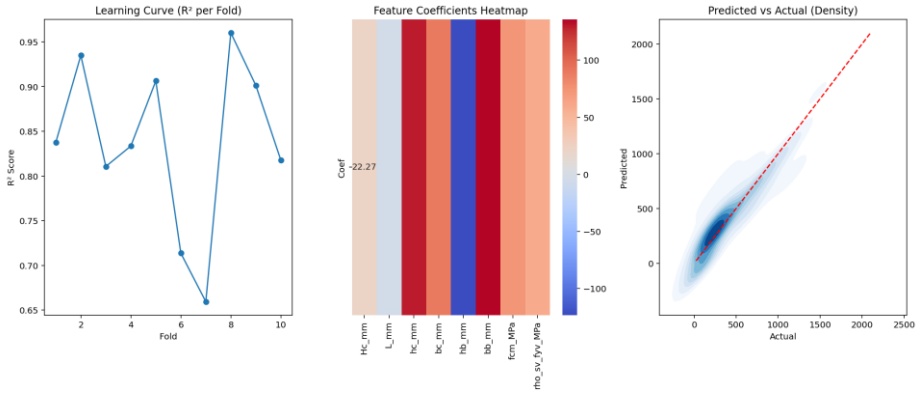

Fig. 2. Evaluation graphs of the Linear Regression model.

The first graph shows the R^2 scores obtained in 10-fold cross-validation. The scores range from 0.67 to 0.96, indicating that the model is unstable in some data segments and may have high variance. The second graph presents a heat map of the coefficients of the features in the model. This shows how the model is affected by each feature. Some variables ("L (mm)") have a positive effect, while others have a negative effect. The third graph compares the predicted values with the actual values. The predictions are generally accurate, particularly concentrated at low values. Fig. 3 shows Error and residual analysis graphs of the Linear Regression model.

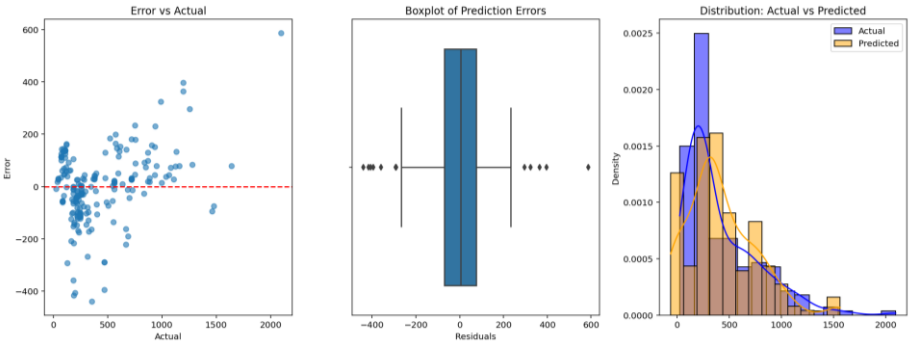

Fig. 3. Error and residual analysis graphs of the Linear Regression model.

The first graph, "Error vs Actual," shows the relationship between the model's predicted values and the actual values. Since the vast majority of predictions are close to the ideal red dashed line, it can be said that the model is generally accurate in its predictions. The second graph, "Boxplot of Prediction Errors" shows how the model's

errors vary with the actual values. The third graph, "Distribution of Actual vs Predicted values" summarizes the overall distribution of the model's prediction errors.

4 Conclusions

In this study, a linear regression-based modeling approach was used to predict the shear strength of beam-column joints, and evaluations were conducted on a comprehensive dataset. The dataset considered numerous parameters that directly affect shear behavior, including column height, beam length, beam width, column width, column depth, beam depth, and vertical reinforcement ratio. The model's performance was extensively tested using statistical metrics such as R^2 score, Root Mean Square Error (RMSE), Mean Absolute Error (MAE), Mean Absolute Percent Error (MAPE) and Variance Explained Score. The analyses demonstrated that the linear regression model was able to predict the shear strength of beam-column joints with a high level of accuracy. Furthermore, the graphical support of the findings visually demonstrated the model's success.

These results demonstrate the significant potential of artificial intelligence and machine learning-based approaches in engineering, particularly in predicting structural behavior.

Future works aim to compare different machine learning algorithms and test them on larger data sets.

References

[1] M. J. N. Priestley, R. Verma, and Y. Xiao, "Seismic Shear Strength of Reinforced Concrete Columns," *Journal of Structural Engineering*, vol. 120, no. 8, pp. 2310–2329, Aug. 1994, doi: 10.1061/(ASCE)0733-9445(1994)120:8(2310).

[2] Applied Technology Council, "Improved Seismic Design Criteria for California Bridges: Provisional Recommendations," 1996.

[3] J. Jeon, A. Shafieezadeh, and R. DesRoches, "Statistical models for shear strength of RC beam-column joints using machine-learning techniques," *Earthq Eng Struct Dyn*, vol. 43, no. 14, pp. 2075–2095, Nov. 2014, doi: 10.1002/eqe.2437.

[4] S. Mangalathu and J.-S. Jeon, "Classification of failure mode and prediction of shear strength for reinforced concrete beam-column joints using machine learning techniques," *Eng Struct*, vol. 160, pp. 85–94, Apr. 2018, doi: 10.1016/j.engstruct.2018.01.008.

[5] G. Almasabha, O. Alshboul, A. Shehadeh, and A. S. Almuflih, "Machine Learning Algorithm for Shear Strength Prediction of Short Links for Steel Buildings," *Buildings*, vol. 12, no. 6, p. 775, Jun. 2022, doi: 10.3390/buildings12060775.

[6] T. Liu, Z. Wang, J. Zeng, and J. Wang, "Machine-learning-based models to predict shear transfer strength of concrete joints," *Eng Struct*, vol. 249, p. 113253, Dec. 2021, doi: 10.1016/j.engstruct.2021.113253.

[7] X. Ni and K. Duan, "Machine Learning-Based Models for Shear Strength Prediction of UHPFRC Beams," *Mathematics*, vol. 10, no. 16, p. 2918, Aug. 2022, doi: 10.3390/math10162918.

[8] J. Zhang, Y. Sun, G. Li, Y. Wang, J. Sun, and J. Li, "Machine-learning-assisted shear strength prediction of reinforced concrete beams with and without stirrups," *Eng Comput*, vol. 38, no. 2, pp. 1293–1307, Apr. 2022, doi: 10.1007/s00366-020-01076-x.

[9] O. R. Abuodeh, J. A. Abdalla, and R. A. Hawileh, "Prediction of shear strength and behavior of RC beams strengthened with externally bonded FRP sheets using machine learning techniques," *Compos Struct*, vol. 234, p. 111698, Feb. 2020, doi: 10.1016/j.compstruct.2019.111698.

[10] T. H. Fitwi, "Dataset of Exterior Reinforced Concrete Beam-Column Joint Experiments," 2025.

[11] G. James, D. Witten, T. Hastie, R. Tibshirani, and J. Taylor, "Linear Regression," 2023, pp. 69–134. doi: 10.1007/978-3-031-38747-0_3.

[12] scikit-learn, "scikit-learn." Accessed: Jun. 02, 2025. [Online]. Available: https://scikit-learn.org/stable/

A Photo to 3d Workflow for Generation of LOD3 Digital Building Representations

Handan Aş Çemrek[1[0009-0007-7369-8576]], Ümit Işıkdağ[2[0000-0002-2660-0106]],

Gebrail Bekdaş[3[0000-0002-7327-9810]], Sinan Melih Niğdeli[4[0000-0002-9517-7313]]

[1,2] Mimar Sinan Fine Arts University, Istanbul, 34427, Türkiye
[3,4] Istanbul University, Cerrahpasa, Istanbul, 34098, Türkiye

[1] 20242109002@ogr.msgsu.edu.tr; [2] umit.isikdag@msgsu.edu.tr
[3] bekdas@iuc.edu.tr; [4] melihnig@iuc.edu.tr

Abstract. This study proposes a novel method for generating three-dimensional (3D) models from a single building photograph. The proposed approach integrates state-of-the-art artificial intelligence models, namely Google's Gemini Flash 2.5 and Tencent's Hunyuan 3D 2.1, to produce rapid and automated digital representations of architectural structures. In the first step, the Gemini Flash 2.5 image editing model is employed to isolate the building within the photograph and re-render it under daylight conditions from an approximately isometric perspective. In the second step, the processed image is provided as input to the Hunyuan 3D 2.1 model, which specializes in image-to-3D conversion, to generate the building's digital 3D model in formats such as .glb or .obj. As a case study, experiments were conducted with 16 building photographs selected from Early Republican and Ottoman architecture. The results demonstrate that the proposed approach offers a practical solution for the digital documentation of cultural heritage and for academic research in architecture. The study highlights the potential of creating 3D digital twins of architectural objects from a single image and presents an innovative method to produce digital architectural representations.

Keywords: Single-image 3D reconstruction, Gemini Flash 2.5, Hunyuan3D 2.1, AI-based modeling, LOD3 digital building representations, Cultural heritage documentation, Architectural digital twin, PBR textured mesh, Image-to-3D generation, Diffusion model.

1 Introduction

Digital technologies are playing an increasingly important role in the documentation and preservation of architectural heritage. Three-dimensional recording of historic buildings provides significant value for academic research, virtual experiences, and education. Traditionally, photogrammetry and laser scanning have been used to obtain 3D models by combining multiple photographs or sensor data. Photogrammetry can deliver highly accurate results, but it is time-consuming and requires extensive data collection. Recently, AI-assisted approaches have enabled 3D model generation from a single photograph. Generative Adversarial Networks (GANs) and diffusion-based models have shown notable progress in reconstructing shapes from limited input, while Neural Radiance Fields (NeRFs) can infer geometry and novel views even from one image (Münster et al., 2024).

Major technology companies have also advanced single-image 3D modeling. In late 2024, **Google DeepMind** released **Gemini Flash 2.5**, a lightweight variant of the Gemini family optimized for fast and cost-effective inference (Saadat et al., 2025). Known as **"Nano Banana,"** it was made accessible via **OpenRouter**, allowing developers to test its image-processing capabilities (AINews, 2025). Although it does not directly generate 3D meshes, Gemini Flash 2.5 can support single-view 3D modeling by synthesizing new perspectives or filling missing parts.

Tencent has similarly introduced successive models for 3D content creation. Hunyuan3D 2.0, launched in early 2024, focused on text-to-3D and image-to-3D generation (Tencent Hunyuan3D Team, 2025). Its successor, Hunyuan3D 2.1, released in 2025 as a fully open-source framework, was specifically designed for high-fidelity single-image 3D generation (Reddit, 2025). The system integrates Hunyuan3D-DiT, a diffusion-based shape generator, with Hunyuan3D-Paint, a texture-generation module. This two-stage process merges geometry and **PBR textures** consistently, producing outputs at near-cinematic quality (Hunyuan3D et al., 2025).

Hunyuan3D has been benchmarked against large-scale models such as **Michelangelo** (Zhao et al., 2023), **Craftsman 1.5** (Li et al., 2024), and **Trellis** (Xiang et al., 2024). Reports highlight its superiority in preserving geometric detail, maintaining multi-view consistency, and generalizing to open-world objects. Compared with newer methods like **TripoSG** (Li et al., 2025) and **Direct3D-S2** (Wu et al., 2025), Hunyuan3D 2.1 better retains complex surface details and texture–photo consistency, and was preferred in human evaluations (Hunyuan3D et al., 2025).

In cultural heritage applications, **image-to-3D generation** has attracted increasing attention. Montas-Laracuente et al. (2025), for example, proposed a photo-based workflow for Romanesque–Mudéjar churches, using Gaussian Splatting to reconstruct triangular mesh surfaces more efficiently than traditional **LiDAR**-based methods. Their results showed that faster and consistent reconstructions suitable for **HBIM** integration could be achieved (Montas-Laracuente et al., 2025).

Such studies illustrate AI's potential as a tool for digital heritage and architectural modeling. Single-image 3D modeling has advanced through diffusion models, NeRFs, GANs, and open-source frameworks, forming a knowledge base of academic and industrial value.

This study proposes a workflow for generating a 3D model from a single architectural photograph using two recent **AI tools**. The first is **Gemini 2.5 Flash Image**, developed by Google DeepMind **(also known as "Nano Banana").** Gemini Flash 2.5 is an image generation and editing model that enables targeted manipulations through natural language prompts—for example, removing objects, recoloring regions, or altering poses (Google Developers Blog, 2025). In our case, it was used to convert building photographs into isometric views and isolate the structures from their backgrounds. With the prompt **"Make image daytime and isometric (building only),"** the model re-rendered the buildings as daylight, isometric-like views, and could even reconstruct hidden details such as wall surfaces or cables (weixin_47221050, 2025).

The second tool is Hunyuan3D 2.1, an open-source framework by Tencent for text-to-3D and image-to-3D generation (echo3D, 2025). Based on diffusion-driven architecture, Hunyuan3D creates detailed 3D meshes with PBR textures from a single image (Hunyuan3D, 2025). Its two-stage process first generates the geometric mesh (Hunyuan3D-DiT), then applies textures and material maps via multi-view diffusion (Team Hunyuan3D et al., 2025; Tencent Hunyuan3D Team, 2025). Thus, a single photo can yield a realistic, textured 3D asset (echo3D, 2025).

The aim of this research is to generate digital 3D models of Turkish architectural heritage **by combining Gemini Flash 2.5 and Hunyuan3D 2.1** in a single workflow. The method was tested on 16 photographs of Early Republican and Late Ottoman civil architecture, enabling evaluation across different architectural styles and conditions. The findings show that the approach provides a practical solution for digital heritage documentation and academic research.

2 Method

The proposed method consists of four main steps.

2.1 Step 1 – Image selection

A suitable photograph of the target building is selected. Ideally, the image should depict the structure from a diagonal façade view, approximating an isometric perspective, and taken under daylight conditions. If the available image is a nighttime shot or deviates significantly from isometric perspective, these issues can be partially corrected in the next step using Gemini Flash 2.5.

2.2 Step 2 – Image preprocessing with Gemini Flash 2.5.

The selected building photograph is provided as input to the Google Gemini 2.5 Flash Image model. After uploading the photograph to the model's interface, the text prompt **"make image daytime and isometric (building only)"** is applied. As a result, the model isolates the building from its background and reconstructs it against a neutral backdrop. Additionally, the façade is adjusted with slight perspective corrections, producing an isometric-like appearance as if captured from a bird's-eye angle.

In some cases, missing or ambiguous details (e.g., side walls) were also completed by the model. (weixin_47221050, 2025).

As the input dataset, sixteen architectural landmarks from Türkiye, representing both modern and Early Republican period buildings, were selected and **provided to the Gemini model.** The dataset includes Ankara Palas, TBMM Museum, Ankara Republic Museum, Gazi Education Institute, Aynalıkavak Pavilion, Baruthane, Baruthane Tower, Bruno Taut Villa, Doğan Apartment, Florya Atatürk Marine Mansion, Frej Apartment, Arif Paşa Apartment, Narmanlı Han, Pera Palas, Safranbolu House, and the İkinci Evkaf Apartment.

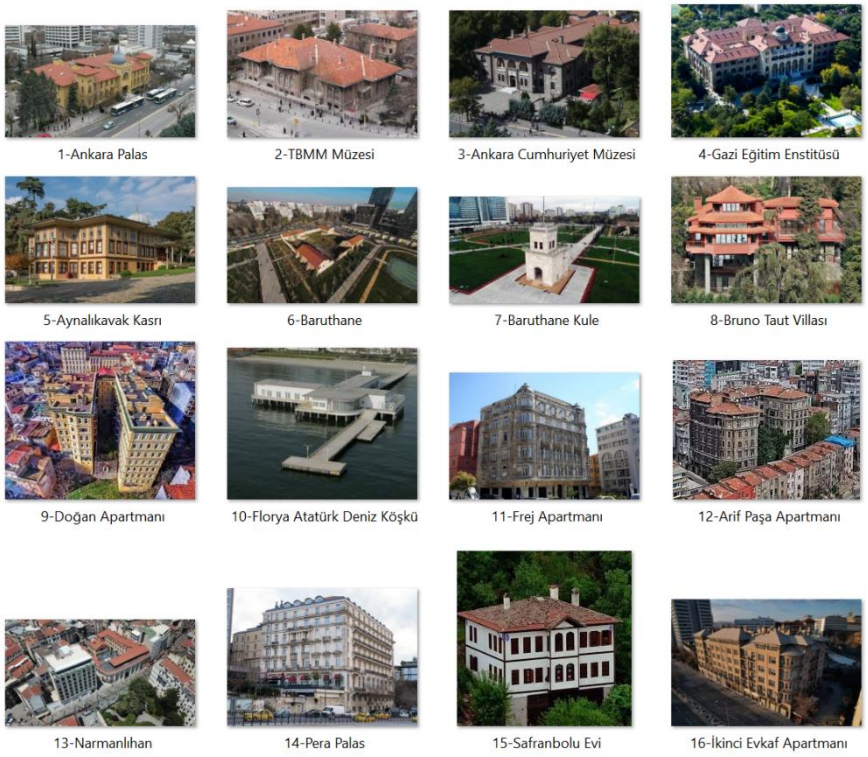

Fig. 1. Input dataset of selected Turkish architectural landmarks provided to Gemini.

After processing with the Gemini Flash 2.5 model, the resulting isometric daylight building image (output) successfully isolated the structure from the original background, converted the lighting conditions to daytime, and reconstructed the building in an approximately isometric perspective. Remarkably, the model also completed side wall details and certain architectural elements that were not visible in the original image.

2.3 Step 3 – 3D reconstruction with Hunyuan3D 2.1. The third step

Involves transferring the isometric, isolated building image to the Hunyuan3D 2.1 model. In its image-to-3D operating mode, when a single façade image is provided as input, the model generates a 3D object based on the 2D representation (Hunyuan3D, 2025). In our workflow, the output processed with Gemini was uploaded directly into the Hunyuan3D interface. The generation process unfolds in two substages: first, the three-dimensional form of the building (polygonal mesh) is estimated and constructed; second, realistic textures are applied onto the geometry. Since **Hunyuan3D 2.1** employs **physically based rendering (PBR)** material models for shading, the produced 3D model acquires realistic material properties (e.g., metallic surfaces, reflections, or rough details (echo3D, 2025).

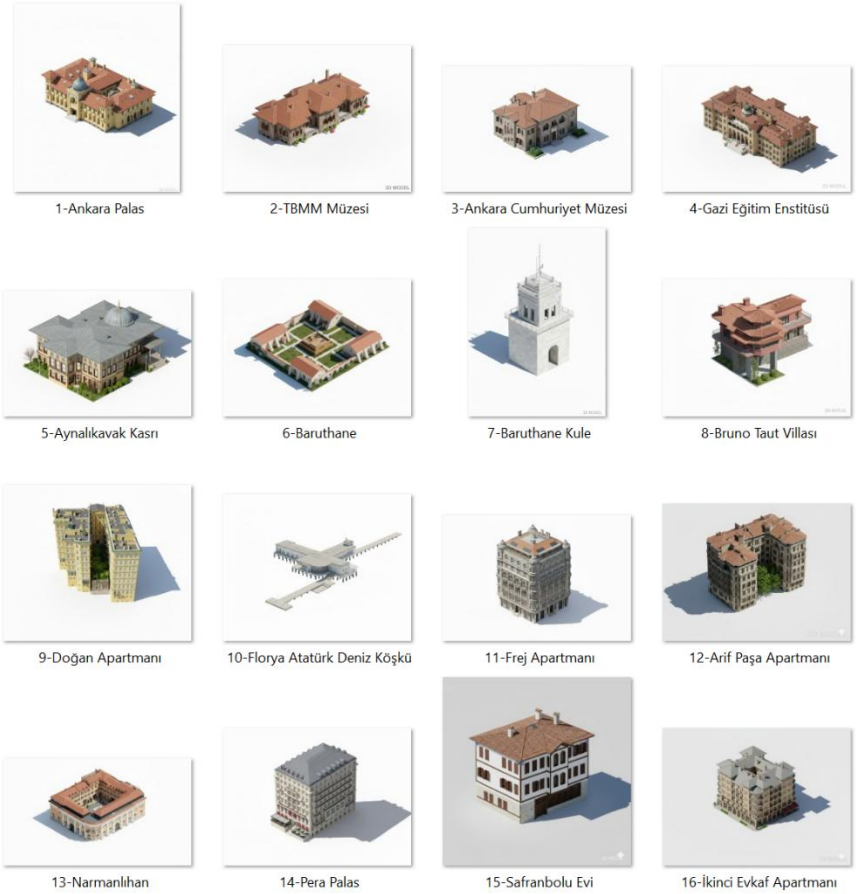

Fig. 2. Output images generated by Gemini. The models were produced based on the real building photographs provided as input **(see Figure 1)**.

Specifically, image completion processes with Gemini Flash were applied sequentially prior to the Hunyuan model: in other words, photographs with **missing parts were first completed using Gemini,** and these **"enriched images"** were then provided to **Hunyuan3D to generate the final 3D models**.

Fig. 3. Three-step visualization of the modeling process using the Safranbolu House example: (left) original building photograph, (center) 3D model output generated by Gemini Flash 2.5, (right) 3D model output generated by Hunyuan3D 2.1.

Fig. 4. Three-step process illustrated with the İkinci Evkaf Apartment example: (left) original building photograph, (center) 3D model output generated by Gemini Flash 2.5, (right) 3D model output generated by Hunyuan3D 2.1.

2.4 Step 4 – Model evaluation

The generated 3D model files are examined and evaluated. In this study, each produced model was opened and visualized using software such as Autodesk Revit, ArcGIS Pro, and CloudCompare. As a BIM (Building Information Modeling)-based tool, Revit was employed to verify the architectural scale and dimensional consistency of the models. In ArcGIS Pro, the models were tested in a geospatial environment, enabling experiments such as georeferencing and placement within an urban model. CloudCompare, an open-source software for analyzing point cloud and mesh datasets, was used to inspect technical characteristics of the models, including mesh topology, vertex count, and the accuracy of texture mapping.

The Hunyuan3D 2.1 model produced an integrated 3D asset output for each of the 16 buildings included in the study. By default, the outputs were generated in glTF (.glb) format, comprising both triangular mesh geometry and PBR-based texture maps (Albedo, Metallic, Roughness, Normal). The resulting file sizes generally ranged between ~4–5 MB, varying depending on the geometric complexity of the buildings.

The generated **.glb files** were first opened and examined in **CloudCompare.** It was observed that both the geometry and the texture maps were processed as expected. In addition, since the **.glb** format is an industry standard, the files could also be seamlessly opened in widely used software such as **Blender, Autodesk 3ds Max, and Unity**. This highlights their direct usability across different platforms.

As output examples, Figures 1 and 2 present the dataset of 16 buildings used in the study. Subsequently, Figures 3 and 4 illustrate the modeling process in detail for two selected examples. These visualizations show that key architectural elements—such as arches, columns, and wooden details—were largely reproduced accurately; however, the models are not exact replicas of the original buildings, as certain parts not visible in the photographs were inferred and generated by the AI models. Furthermore, some models were compared against existing drawings or measurements to evaluate their consistency with real-world dimensions. Repeating this workflow across all selected buildings resulted in a set of case studies demonstrating the application of the proposed method.

3 Results

The outputs of the proposed method demonstrate that, for each of the historic buildings examined, the general form and characteristic features of the structures were successfully captured. **In Early Republican examples** (e.g., a government office building from the 1920s), the façade composition, window arrangements, and overall roof geometry were accurately represented in the 3D models**. In Ottoman-era residential architecture** (e.g., a 19th-century mansion), characteristic elements such as wooden projections and bay windows could also be observed in the models. This is particularly noteworthy **for a model operating from a single image**, as it suggests that the **AI**, trained on a large dataset, appears to have **"learned"** the stylistic properties of architectural typologies

From an architectural accuracy perspective, the method was found to be particularly effective in **capturing the main mass and proportions** of the buildings, while certain variations **occurred in finer details.** For instance, in a model of an Early Republican building, window frames appeared as simplified geometries rather than their original profiles, while in an Ottoman mansion, wooden ornaments were represented in a more generalized manner. Nevertheless, overall observations indicate that both models **(Gemini Flash and Hunyuan3D)** produced stylistically consistent results: when modeling a modernist reinforced concrete structure, the generated 3D asset reflected its modernist character, whereas in the case of a traditional Ottoman house, distinctive features such as pitched roofs and lattice windows were accurately reproduced in the generated 3D model.

From a performance and efficiency perspective, the proposed approach provides a significant advantage compared to traditional methods. **The Gemini Flash 2.5** model, operating through a cloud-based service, processed a single image within a few seconds, whereas the **Hunyuan3D 2.1** model generated a 3D model from a single image in approximately 1–2 minutes via its online interface. Consequently, the method

proves particularly effective for rapid prototyping or in scenarios where many buildings need to be modeled.

4 Discussion

The findings indicate that the proposed method is a promising tool for generating digital architectural representations. Its main advantage lies in creating 3D models from extremely limited data (a single photograph). This is particularly valuable in cases where only a few visual records exist or where the original buildings no longer survive. For instance, reconstructing a demolished structure from its sole remaining photograph becomes feasible through such AI-based approaches. This represents an important step in digitally reviving cultural heritage and transmitting it to future generations (Münster et al., 2024).

Nevertheless, the method presents limitations that require careful consideration. Since the generated model is ultimately an **AI "prediction,"** it should not be regarded as an exact replica of the real structure. Especially in unseen areas or fine details, the model extrapolates information from its training data. Therefore, such outputs should be considered AI-assisted visualizations rather than precise digital documents of heritage. In academic or conservation projects, they should serve as preliminary visualizations or conceptual references, not exact construction plans.

Another issue is optimization and integration. Meshes produced by Hunyuan3D may cause performance issues in real-time applications due to high polygon counts. However, the open-source nature of the model allows for improvements such as decimation, retopology, or texture refinement, enabling lighter and more versatile outputs.

The fundamental differences between classical photogrammetry and the method presented in this study are also worth discussing. Since photogrammetry relies on real-world data, it is superior in terms of geometric accuracy and scale; however, it requires a large number of photographs and considerable manual effort. By contrast, the single-image modeling approach offers an alternative in cases of data scarcity. When only a single view of a building is available in historical photographic archives, this method can provide a viable three-dimensional representation. In the future, hybrid approaches may prove useful: for instance, when multiple historical photographs are available, the Hunyuan3D model could **generate** more consistent results **with multi-view input**, or **AI-generated models** could be **combined with laser-scanned** point clouds to **fill in missing parts**.

From a cultural and educational perspective, the method has strong potential for making architectural heritage more accessible. The produced 3D models can be integrated into web viewers or VR/AR applications, allowing interactive presentations for museum visitors, students, or the public. These models may also support urban planning or tourism promotion. It is important, however, to communicate the limitations of AI-based models clearly to users, emphasizing that they provide approximations rather than exact replicas.

5 Conclusion

This study presented a method for generating 3D digital models of architectural structures from photographs **using two AI-based models.** The **Gemini Flash 2.5** model, with its advanced 2D image editing capabilities, was employed to isolate building photographs and adapt them to an isometric perspective; subsequently, the **Hunyuan3D 2.1** model automatically generated the three-dimensional geometry and surface textures of the buildings from these processed images. Experiments conducted on selected examples from Turkish architectural heritage demonstrated that the method produced generally consistent results across different styles and periods. The ability to obtain a **3D model from a single photograph** opens new opportunities in the field of digital cultural heritage. These include the revitalization of historical monuments with limited visual documentation, the reinterpretation of archival photographs, and their use as visualization tools in architectural history research.

Nevertheless, the output of the method must be approached with caution in terms of accuracy. The AI-generated models represent generalized outcomes of their training datasets and cannot fully substitute for the real objects. Therefore, in contexts requiring scientific or technical precision, these models should not be used as definitive references but rather as supportive visual aids.

In the future, accuracy and scope could be enhanced by integrating multiple images, or by training AI models to specialize in particular architectural details (e.g., the features of a specific historical period). Similar approaches could also be extended to large-scale 3D city models or interior architecture.

In conclusion, the sequential use of **Gemini Flash 2.5** and **Hunyuan3D 2.1** provides an innovative workflow for producing digital architectural representations, offering value not only for academic research but also for the digital preservation of cultural heritage.

6 References

1. AINews. (2025, May 20). Google I/O: new Gemini native voice, Flash, DeepThink, AI Mode (DeepSearch+Mariner+Astra). News.Smol.ai https://news.smol.ai/issues/25-05-20-google-io/
2. Echo3D. (2025, August 14). A guide to creating and sharing 3D models with Hunyuan-3D-2.1 and echo3D [Blog post]. Medium. https://medium.com/echo3d/a-guide-to-creating-and-sharing-3d-models-with-hunyuan-3d-2-1-and-echo3d-da99f677b740
3. Google Developers Blog. (2025, August 26). Introducing Gemini 2.5 Flash Image, our state-of-the-art image model. Google. https://developers.googleblog.com/en/introducing-gemini-2-5-flash-image/#:~:text=Gemini%202,up%20with%20a%20simple%20prompt
4. Hunyuan3D. (2025). Advanced 3D asset generation with AI. https://hunyuan-3d.com/
5. Hunyuan3D, T., Yang, S., Yang, M., Feng, Y., Huang, X., Zhang, S., ... & Guo, C. (2025). Hunyuan3D 2.1: From Images to High-Fidelity 3D Assets with Production-Ready PBR Material. arXiv preprint arXiv:2506.15442.

6. Li, Y., Zou, Z. X., Liu, Z., Wang, D., Liang, Y., Yu, Z., ... & Cao, Y. P. (2025). Triposg: High-fidelity 3d shape synthesis using large-scale rectified flow models. arXiv preprint arXiv:2502.06608.
7. Montas-Laracuente, N., Delgado Martos, E., Pesqueira-Calvo, C., Intra Sidola, G., Maitín, A., Nogales, A., & García-Tejedor, Á. J. (2025). Automatic 3D Reconstruction: Mesh Extraction Based on Gaussian Splatting from Romanesque–Mudéjar Churches. Applied Sciences, 15(15), 8379.
8. Münster, S., Maiwald, F., di Lenardo, I., Henriksson, J., Isaac, A., Graf, M. M., Beck, C., & Oomen, J. (2024). Artificial Intelligence for Digital Heritage Innovation: Setting up a R&D Agenda for Europe. Heritage, 7(2), 794-816. https://doi.org/10.3390/heritage7020038
9. Reddit. (2025). Hunyuan 3D 2.1 released today - Model, HF Demo, Github links on X. r/StableDiffusion. https://www.reddit.com/r/StableDiffusion/comments/1laq8he/hunyuan_3d_21_released_today_model_hf_demo_github/#:~:text=Hunyuan%203D%202,ready%20PBR%203D%20generative%20model
10. Saadat, A., Aziz, S., Mahmud, S., Mahi, A. I. M., & Ahmed, S. (2025). VisionTrap: Unanswerable Questions On Visual Data. *arXiv preprint arXiv:2507.17262*.
11. Team Hunyuan3D, Yang, S., Yang, M., Feng, Y., Huang, X., Zhang, S., … Guo, C. (2025). Hunyuan3D 2.1: From images to high-fidelity 3D assets with production-ready PBR material [Preprint]. ArXiv.https://ar5iv.labs.arxiv.org/html/2506.15442#:~:text=To%20bridge%20this%20gap%2C%20we,consistent%20textures
12. Tencent-Hunyuan. (2025). *Hunyuan3D-2: High-Resolution 3D Assets Generation with Large Scale Hunyuan3D Diffusion Models. GitHub. https://github.com/Tencent-Hunyuan/Hunyuan3D-2
13. Tencent Hunyuan3D Team. (2025). *Hunyuan3D-2.1: From Images to High-Fidelity 3D Assets with Production-Ready PBR Material. GitHub. https://github.com/Tencent-Hunyuan/Hunyuan3D-2.1
14. Tencent Hunyuan3D Team. (2025). Hunyuan3D 2.0: Scaling Diffusion Models for High Resolution Textured 3D Assets Generation. arXiv preprint arXiv:2501.12202. https://huggingface.co/tencent/Hunyuan3D-2#:~:text=This%20repository%20contains%20the%20models,For
15. Weixin_47221050. (2025, September 8). Guge zhe ci you ying ma le: Nano Banana zhengshi bian shen Gemini-2.5-Flash-Image + mianfei tiyan rukou? [Blog post]. CSDN. https://blog.csdn.net/weixin_47221050/article/details/151116078#:~:text=
16. Wu, S., Lin, Y., Zhang, F., Zeng, Y., Yang, Y., Bao, Y., ... & Yao, Y. (2025). Direct3d-s2: Gigascale 3d generation made easy with spatial sparse attention. arXiv preprint arXiv:2505.17412.
17. Xiang, J., Lv, Z., Xu, S., Deng, Y., Wang, R., Zhang, B., ... & Yang, J. (2025). Structured 3d latents for scalable and versatile 3d generation. In *Proceedings of the Computer Vision and Pattern Recognition Conference* (pp. 21469-21480).
18. Zhao, Z., Liu, W., Chen, X., Zeng, X., Wang, R., Cheng, P., ... & Gao, S. (2023). Michelangelo: Conditional 3d shape generation based on shape-image-text aligned latent representation. *Advances in neural information processing systems*, *36*, 73969-73982.

Prediction of the Seismic Response of Structures with Tuned Liquid Dampers Using Machine Learning

Ayla Ocak[1] , Gebrail Bekdaş[1] , Sinan Melih Nigdeli[1] and Ümit Işıkdağ[2]

[1] Istanbul University - Cerrahpaşa, 34320 İstanbul, Turkey
aylaocak@outlook.com,
bekdas@iuc.edu.tr,melihnig@iuc.edu.tr
[2] Department of Architecture, Mimar Sinan Fine Arts University
umit.isikdag@msgsu.edu.tr

Abstract. Tuned liquid damper (TLD) systems are simple and economical designs used to reduce the response of structures exposed to various vibrations. These devices dampen vibration by utilizing the oscillation of their own solid mass through the sloshing of the liquid mass they contain. Their design is effective in ensuring structural control. The parameters contained in the structure and control systems have different effects on the structural response. Predicting the behavior of a structure with a control system in response to various vibrations is possible using artificial intelligence methods. This study aims to predict the structural response based on the system characteristics and mass ratio of a TLD to be added to the structure for the control of structures with different periods and natural damping. Models predicting the structure's response to seismic vibrations were developed using machine learning methods. For this purpose, the seismic response of the structure was recorded using combinations of structures and dampers with different characteristics under a far-fault earthquake. The results obtained were converted into a dataset and models were produced using ensemble algorithms for use in machine learning. The performance metrics of the models were compared to determine the best algorithm. The final prediction model created explained the variance in the data with an R2 score exceeding 99% level and showed high prediction performance with a mean deviation error of less than 5% from the actual value.

Keywords: Tuned Liquid Damper (TLD), Structural Control, Machine Learning.

1 İntroduction

Tuned liquid damper systems are liquid mass dampers within the passive control system group. Their basic operating mechanism involves the damper tank and the liquid mass remaining stationary within the tank acting as a solid mass, damping energy by utilizing the motion of the liquid sloshing within the damper tank. As with other passive devices, they reduce structural response by converting the energy of vibrations

transmitted to the structure into mechanical energy without requiring an external energy source. In control systems using TLDs, the damping capacity of the TLD depends on the period and damping ratio of the damper, as well as the dimensions of the damper tank and the structural mass ratio. Studies have shown that the ratio between the liquid height and the effective liquid length at the base [1] affects damper performance. Furthermore, it has been observed that the ratio between the structural mass ratio, which is generally recommended to be between 1-5% [2-5], does not produce a significant performance difference for the structural types studied when a ratio of 20% or more is taken [6]. Among the results obtained is that changes in the structure's natural damping rate and period make a difference in the effectiveness of TLDs in vibration control [6]. Based on all the information, it is understood that the structure's damping and period, the mass ratio determined for the TLD, and the TLD properties are effective features in controlling the structure's vibration. TLDs are devices that can be added to the structure during construction or later. Adding a TLD appropriate to the structural properties can have different consequences on the structural response. TLDs offer a wide range of design alternatives due to the parameters they contain. This diversity of design options increases the number of analyses required to predict structural response in vibration control. Today, various artificial intelligence applications make it possible to train a machine and predict structural behavior by generating data from a limited number of analyses. Machine learning is a prominent sub-branch of artificial intelligence that refers to the processes of training a machine and providing it with inference capabilities. This method has been used to generate and successfully apply predictive models for many control system problems, such as damper parameters, structural behavior, damping force, and fatigue in damper design [7-10].

In this study, machine learning models were developed to predict the response of a structure equipped with a tuned liquid damper under a selected FEMA far-fault earthquake [11]. For this purpose, various TLD designs were taken for various structural properties with different natural damping periods and structure mass ratios ranging from 1% to 20%, randomly selected within predefined limits, and the structural response under the FEMA far fault earthquake was recorded. The resulting combinations of structure-TLD properties and structural behavior were converted into a dataset, and structural response prediction models were generated using machine learning algorithms. The performances of the developed models were compared, and the artificial intelligence model that produced the highest accuracy and lowest error was determined.

2 Methodology

2.1 Design of tuned liquid dampers

Tuned liquid damper (TLD) systems are named and designed based on the base geometry of the damper tank. The circular-based TLD designed in this study is defined as a cylindrical TLD. The liquid within a TLD device is not completely sloshing, and some of the liquid acts as a solid mass and moves with the damper tank. The sloshing liquid (m_s) is calculated based on the total liquid mass (m_{st}), the damper tank base radius (R), and the liquid height (h). The passive tank, which is not sloshing and acts as a solid

mass, moves in a state of freedom. Equation 1 gives the equation for the sloshing liquid (m_s), and Equation 2 gives the equation for the mass of the passive liquid (m_d) moving with the tank.

$$\mathrm{m_s} = \mathrm{m_{st}} \times \mathrm{R} \times \frac{\tanh\left(\frac{1.84\mathrm{h}}{\mathrm{R}}\right)}{2.2\mathrm{h}} \tag{1}$$

$$\mathrm{m_d} = \mathrm{m_{tld}} - \mathrm{m_s} \tag{2}$$

m_{tld} in Equation 2 represents the total mass of the damper, R represents the tank base radius, and h represents the liquid height in the tank.

Damper stiffness (k_d) and liquid stiffness (k_s) are given in Equation 3 and Equation 4, respectively.

$$\mathrm{k_d} = \mathrm{m_d} \times \left(\frac{2\pi}{\mathrm{T_d}}\right)^2 \tag{3}$$

$$\mathrm{k_s} = \mathrm{m_{st}} \times \frac{\mathrm{g}\left\{\tanh\left(\frac{1.84\mathrm{h}}{\mathrm{R}}\right)\right\}^2}{1.19\mathrm{h}} \tag{4}$$

In the equations, g represents the gravitational acceleration, T_d represents the damper period. The damping coefficients for the damper and the sloshing liquid are shown in Equation 5 and Equation 6, respectively..

$$\mathrm{c_d} = 2 \times \zeta_d \times \sqrt{m_d \times k_d} \tag{5}$$

$$\mathrm{c_s} = 2 \times \zeta_s \times \sqrt{m_s \times k_s} \tag{6}$$

The ζ_d given in Equation 5 indicates the TLD damping ratio, and the ζ_s shown in Equation 6 indicates the damping ratio of the sloshing liquid. The TLD damping ratio (ζ_d) calculation is given in Equation 7, and the sloshing liquid (ζ_s) damping ratio calculation is given in Equation 8.

$$\zeta_\mathrm{d} = \frac{c_d}{2m_d\sqrt{\frac{k_d}{m_d}}} \tag{7}$$

$$\zeta_\mathrm{s} = 4.98 v^{1/2} R^{-3/4} g^{-1/4} \left[1 + \frac{0.318}{sinh\left(\frac{1.84h}{R}\right)} \frac{1-\frac{h}{R}}{cosh\left(\frac{1.84h}{R}\right)}\right] \tag{8}$$

The v given in Equation 8 represents the kinematic viscosity of the liquid used in the damper.

In this study, the structure specific properties are shown as unindexed, the properties specific to the movement of the damper tank are shown as "d", and the properties related to the sloshing liquid movement are shown as "s". The mass, stiffness, and damping coefficient matrices to be used in the basic equations of motion of a TLD structure are given in Equations 9, 10, and 11, respectively. The basic equation of motion of the TLD system is shown in Equation 12.

$$[M] = \begin{bmatrix} m & 0 & 0 \\ 0 & m_d & 0 \\ 0 & 0 & m_s \end{bmatrix} \quad (9)$$

$$[K] = \begin{bmatrix} k+k_d & -k_d & 0 \\ -k_d & k_d+k_s & -k_s \\ 0 & -k_s & k_s \end{bmatrix} \quad (10)$$

$$[C] = \begin{bmatrix} c+c_d & -c_d & 0 \\ -c_d & c_d+c_s & -c_s \\ 0 & -c_s & c_s \end{bmatrix} \quad (11)$$

$$[M]\{\ddot{X}\} + [C]\{\dot{X}\} + [K]\{X\} = -[M]1\{\ddot{X}_g\} \quad (12)$$

The m, k, and c equations represent the mass, stiffness, and damping coefficient of the structure, respectively. In Equation 12, $\ddot{X}$ represents the acceleration, $\dot{X}$ represents the velocity, X represents the displacement, and $\ddot{X}_g$ represents the ground acceleration.

2.2 Machine Learning

Machine learning is the training process required to equip a machine with the inference-making ability acquired through human learning. By introducing a set of data, the machine is expected to establish a connection between the attributes in the data and the feature to be predicted. Consequently, the machine is trained to create a prediction model. In machine learning, when the variable to be predicted specifies a class or type, the problem is considered a classification problem, and when it specifies a numerical value, it is considered a regression problem [12, 13]. In this study, prediction models were created for a regression-type problem using the bagging, random forest, xgboost, and catboost algorithms. Brief information about the algorithms is provided below.

Bagging: This is an ensemble algorithm developed by Breiman [14]. With the Bagging regressor, subsets of the data are randomly selected, and the predictions of these sets are combined using voting or mean to determine the final prediction [15].

Random Forest: This is an ensemble algorithm that creates random decision trees and combines the results by mean the predictions of these decision trees. It takes predictions from the randomly generated decision trees to reduce the model's variance and performs bootstrap aggregation [16].

Xgboost: This is an advanced, scalable example of the gradient boosting algorithm [17]. It is an approach where individual models are created, trained, and combined to obtain the best output in an ensemble of learners [18].

Catboost: This is an ensemble algorithm developed for gradient boosting. It is particularly advantageous for optimally handling categorical data and missing values in the data [19]. It searches for a relationship between the attributes in the data and the outputs and categorizes the data according to the inputs.

2.3 Model Metrics

In machine learning methods, the problem is evaluated based on the type of output targeted for prediction. In cases where the prediction output is numerical, regression is

considered, while in cases where it represents a class or group, the problem is considered classification. In regression-type problems, various metrics are used to evaluate a prediction model. The most important of these evaluation metrics is the R-squared (R^2) score. This value represents the ability of the prediction model created for the regression problem to explain the variance in the data. In other words, it is the regression variance ratio. In addition to R^2, various metrics are obtained for model evaluation using parameters such as the mean of the samples in the data and the predicted value. Some of these are mean absolute error (MAE), mean absolute percentage error (MAPE), mean squared error (MSE), and root mean squared error (RMSE). The calculation equations for the R^2 score are given in Equation 13, the MAE in Equation 14, and the MAPE in Equation 15. The MSE and RMSE metrics are shown in Equation 16 and Equation 17, respectively.

$$R^2 = 1 - \frac{\sum_{i=1}^{N}(y_i - \hat{y}_i)^2}{\sum_{i=1}^{N}(y_i - \bar{y}_i)^2} \tag{13}$$

$$MAE = \frac{1}{N}\sum_{i=1}^{N}|\hat{y}_i - y_i| \tag{14}$$

$$MAPE = 100\frac{1}{N}\sum_{i=1}^{N}\left|\frac{y_i - \hat{y}_i}{y_i}\right| \tag{15}$$

$$MSE = \frac{1}{N}\sum_{i=1}^{N}(\hat{y}_i - y_i)^2 \tag{16}$$

$$RMSE = \sqrt{\frac{1}{N}\sum_{i=1}^{N}(\hat{y}_i - y_i)^2} \tag{17}$$

In the equations, the number of observations is shown as N, the observation values are shown as y_i, the predicted observation values are shown as $\hat{y}_i$, and the mean of the observation values is shown as $\bar{y}_i$.

2.4 Model Evaluation

Many methods are used to validate artificial intelligence models. K-fold cross-validation is one such validation method. In this method, the data is divided into k parts, each part is used to test the model, and k-1 parts are used to train the model. An R^2 score is calculated from each of the k-folds, and the mean of all folds is taken to arrive at the final R^2 score for the model. Figure 1 provides a visual summary of the k-fold cross-validation technique.

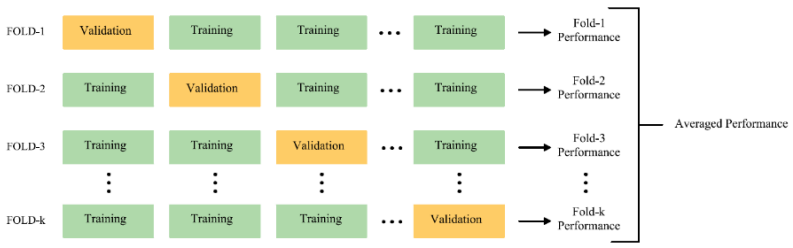

Fig. 1. K-fold cross-validation method.

3 Numerical Example

In this study, a tuned liquid damper (TLD) was placed on a 100-ton single-degree-of-freedom (SDOF) structure. The DUZCE/BOL090 earthquake record, available within the FEMA far fault earthquake records [11], was transmitted to the structure via Matlab Simulink [20], and the structure's behavior was recorded. In this study, limits were defined for the structure, TLD parameters, and the structure mass ratio. 2000 analyses were conducted for designs consisting of features randomly selected within these ranges. Different combinations were tested for the structure's natural damping and period, the TLD tank radius, the liquid height, period, and damping ratio, and the structure-TLD mass ratio. The SDOF structure-TLD system used in the study is shown in Figure 2, and the selected design ranges are shown in Table 1.

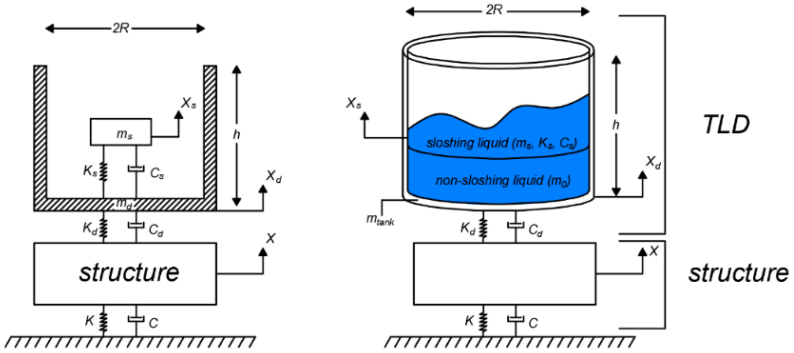

Fig. 2. TLD + structure model.

Table 1. Design limits for structure and TLD.

Variable	Description	Design limit
T	Structure period	0.1-2 s
T_d	TLD period	1-5 s
R	TLD tank radius	0.1-10 m
h	Liquid height in TLD tank	0.1-5 m
ζ	Structure damping ratio	1-10%
ζ_d	TLD damping ratio	1-50%
μ	Mass ratio	1-20%

The structure displacement and total acceleration obtained from the analysis results, along with the structure and TLD properties, were converted into a 2000-row dataset. The correlation matrix showing the relationship between the dependent and independent variables in the data is shown in Figure 3, and the first 10 rows of the data are shown in Table 2. In the table, the structure displacement is denoted by X and the total acceleration by act.

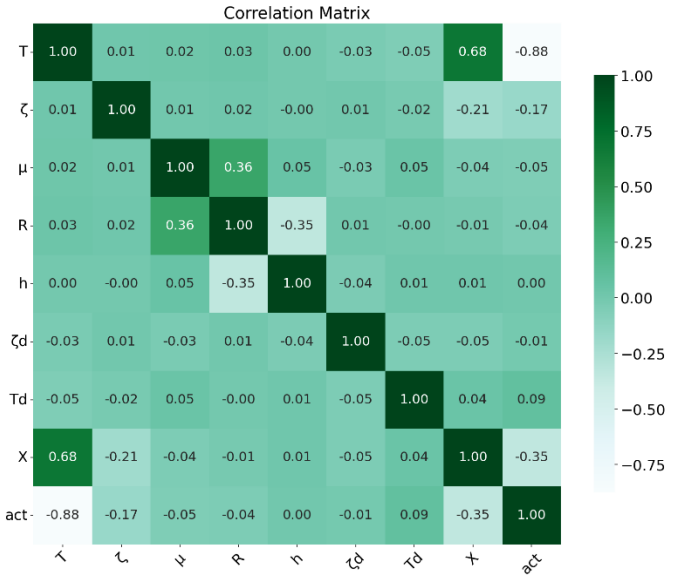

Fig. 3. Correlation matrix.

Table 2. 10 rows of the data set.

T	ζ	μ	R	h	ζ_d	T_d	X	act
0,2299	0,0493	0,0430	0,3584	4,7779	0,2210	1,1538	0,0123	9,1510
1,5486	0,0107	0,1392	0,5825	2,8084	0,2806	4,1276	0,2078	3,4884
0,6221	0,0317	0,0562	0,1119	1,6505	0,4685	1,7251	0,1142	11,6079
1,4293	0,0663	0,1132	1,5637	1,0710	0,2558	1,9538	0,1935	3,8001
1,3773	0,0488	0,1419	1,2496	0,3825	0,2708	3,8824	0,2124	4,4986
1,9616	0,0356	0,1230	1,0060	3,1117	0,1046	3,6334	0,2977	3,1832
0,1209	0,0616	0,1600	0,9944	1,3508	0,2890	4,7544	0,0042	11,5061
1,7313	0,0920	0,1429	0,9910	1,6726	0,2923	1,7575	0,1647	2,2188
1,0717	0,0155	0,1479	1,1876	0,6377	0,4167	1,5650	0,2685	8,7831
0,6128	0,0572	0,1948	0,4261	0,3639	0,1528	1,5986	0,0942	10,5758

Using the generated dataset, bagging, random forest, xgboost, and catboost algorithms, models were created that together predict the structure displacement (X) and total acceleration values (act) shown in Table 2. A 10-fold cross-validation method was applied to the developed models. The evaluation metrics obtained from the models are presented in Table 3. Scatter plots of the structure displacement and total acceleration for the test set of the model with the highest R^2 score are shown in Figure 4.

Table 3. Performance metrics of prediction models developed for structure response.

Algorithm	MAE		MAPE %		MSE		RMSE		R^2	
	Train	Test	Train	Test	Train	Test	Train	Test	Train	Test
Bagging	0.0662	0.1585	1.90	4.63	0.0232	0.1194	0.1521	0.3431	0.9960	0.9787
Random Forest	0.0550	0.1478	1.61	4.35	0.0147	0.1060	0.1213	0.3239	0.9973	0.9813

Xgboost	0.0124	0.1341	0.75	4.67	0.0006	0.0807	0.0237	0.2829	0.9999	0.9854
Catboost	0.0429	0.1077	1.93	4.64	0.0061	0.0569	0.0779	0.2378	0.9992	0.9909

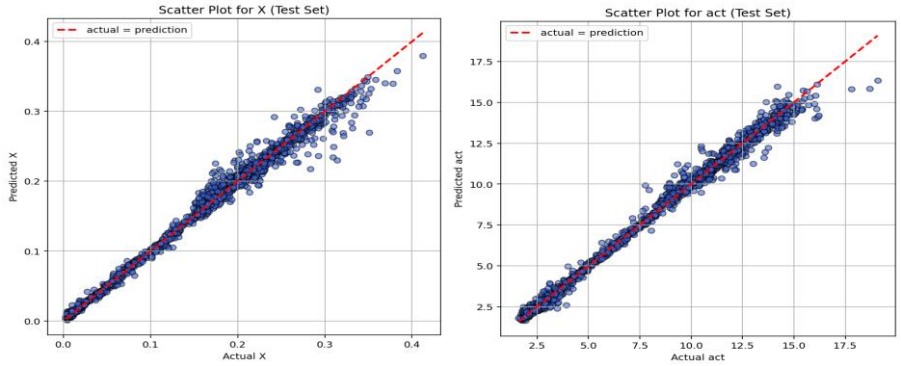

a) b)

Fig. 4. Scatter plots of the test set for the Catboost model: a) for X output, b) for act output.

4 Discussion and Conclusions

In this study, the behavior of a control system designed for different structural and tuned liquid damper properties under an earthquake excitation was recorded, and structural response prediction models were generated using machine learning methods. All developed models demonstrated above 97%. Among the four ensemble algorithms tested (bagging, random forest, xgboost, and catboost), the catboost model achieved the highest R^2 score. The catboost algorithm stands out among the other models by its strength in overfitting, which allows it to establish categorical relationships between the outputs by searching for relationships between data attributes. An R^2 score exceeding 99% was calculated on the test set, resulting in a low mean absolute error of 0.1077 units. The predicted output represents a tolerable error probability of approximately 11 cm for displacement and 0.1077 m/s^2 for total acceleration, with a deviation of 0.1077. According to the mean absolute percentage error value obtained from the Catboost model, the model makes an error of 4.64%. Examining the scatter plots in Figure 4, it is seen that a large portion of the predicted values are on-axis. This indicates that the model's predicted values are the same or very close to the actual values. In light of all the findings, it is understood that the seismic response of structures can be predicted with high accuracy using models developed according to the characteristics of the structure and control system.

References

1. Fujino, Y., Sun, L., Pacheco, B. M., & Chaiseri, P. (1992). Tuned liquid damper (TLD) for suppressing horizontal motion of structures. *Journal of Engineering Mechanics*, *118*(10), 2017-2030.

2. Vickery BJ, Isyumov N, Davenport AG (1983). The role of damping, mass, and acceleration. *J. Wind Eng. Ind. Aerodyn.*, *11*(1-3), 285-294.
3. Sun LM, Fujino Y, Pacheco BM, Chaiseri P (1992). Modeling of tuned liquid damper (TLD). *Journal of Wind Engineering and Industrial Aerodynamics, 43*(1-3), 1883-1894.
4. Rana R and Soong TT (1998). Parametric study and simplified design of tuned mass dampers. *Engineering structures, 20*(3), 193-204.
5. Yu JK, Wakahara T, Reed DA (1999). A non-linear numerical model of the tuned liquid damper. *Earthquake engineering & structural Dynamics, 28*(6), 671-686.
6. Ocak, A., Bekdaş, G., & Nigdeli, S. M. (2023). Mass ratio factor in control performance of optimum tuned liquid dampers. *The Structural Design of Tall and Special Buildings*, *32*(18), e2063.
7. Yucel, M., Bekdaş, G., Nigdeli, S. M., & Sevgen, S. (2019). Estimation of optimum tuned mass damper parameters via machine learning. *Journal of Building Engineering*, *26*, 100847.
8. Farrokhi, F., & Rahimi, S. (2020). Supervised probabilistic failure prediction of tuned mass damper-equipped high steel frames using machine learning methods. *Studia Geotechnica et Mechanica*, *42*(3), 179-190.
9. Bahiuddin, I., Imaduddin, F., Mazlan, S. A., Ariff, M. H., Mohmad, K. B., & Choi, S. B. (2021). Accurate and fast estimation for field-dependent nonlinear damping force of meandering valve-based magnetorheological damper using extreme learning machine method. *Sensors and Actuators A: Physical*, *318*, 112479.
10. Bae, J., Lee, C. H., Park, M., Alemayehu, R. W., Ryu, J., & Ju, Y. K. (2020). Modified low-cycle fatigue estimation using machine learning for radius-cut coke-shaped metallic damper subjected to cyclic loading. *International Journal of Steel Structures*, *20*(6), 1849-1858.
11. FEMA P-695, *Quantification of Building Seismic Performance Factors*, Federal Emergency Management Agency, Washington DC, 2009.
12. Abioye, S. O., Oyedele, L. O., Akanbi, L., Ajayi, A., Delgado, J. M. D., Bilal, M., ... & Ahmed, A. (2021). Artificial intelligence in the construction industry: A review of present status, opportunities, and future challenges. *Journal of Building Engineering*, *44*, 103299.
13. Kotsiantis, S. B., Zaharakis, I., & Pintelas, P. (2007). Supervised machine learning: A review of classification techniques. *Emerging artificial intelligence applications in computer engineering*, *160*(1), 3-24.
14. Breiman, L. (1996). Bagging predictors. *Machine learning*, *24*, 123-140.
15. https://scikit-learn.org/stable/modules/generated/sklearn.ensemble.BaggingRegressor.html#r4d113ba76fc0-1
16. Venkatraman Jagatha, J., Schneider, C., & Sauter, T. (2024). Parsimonious Random-Forest-Based Land-Use Regression Model Using Particulate Matter Sensors in Berlin, Germany. *Sensors*, *24*(13), 4193.
17. Friedman, J. H. (2001). Greedy function approximation: a gradient boosting machine. *Annals of statistics*, 1189-1232.
18. Avanijaa, J. (2021). Prediction of house price using xgboost regression algorithm. *Turkish Journal of Computer and Mathematics Education (TURCOMAT)*, *12*(2), 2151-2155.
19. Tang, J., Cheng, J., & Zhang, M. (2024). Forecasting Airbnb prices through machine learning. *Managerial and Decision Economics*, *45*(1), 148-160.
20. MathWorks Inc., 2019, MATLAB R2019a. Natick, MA, USA.

Advances in Machine Learning for Chronic Liver Disease Detection: A Comprehensive Review

Jyoshna Allenki[1] [0000-0002-5825-0024] andHemant Kumar Soni [2] [0000-0002-8335-6146]

[1,2] Department of Computer Science and Engineering, Amity School of Engineering and Technology, Amity University Madhya Pradesh, Gwalior 474005, India

allenkijyoshna@gmail.com,hemantsoni.gec@gmail.com

Abstract. Chronic Liver Disease has emerged as a major public health issue globally due to the progressive damage to the liver that leads to cirrhosis, liver failure, and even death. To improve patient management, early intervention and diagnosis are essential, as well as the application of Artificial Intelligence (AI) in its detection and management through the use of extensive clinical, genetic, and imaging databases. This review paper discuss the different supervised and unsupervised CLD detection and prediction models using machine learning and focuses on learning decision trees, support vector machines, deep learning, and ensemble models. We assess how well these models performed in classifying different types of CLD, estimating its progression, and formulating personalized treatment strategies. This review looks at how ML models are brought together. It talks about current studies to make better the accuracy and early finding of long-term liver diseases using machine learning methods. The paper ends with recommendations for new research lines that would change the use and boundaries of artificial intelligence in the diagnostics and management of the chronic liver diseases.

Keywords: chronic liver disease, machine learning, deep learning, feature selection, data preprocessing.

Optimum design of SFRC members accounting for serviceability and ultimate limit state constraints

Rad Bazargan and Panagiotis Mergos

Department of Engineering, School of Science and Technology, City St George's University of London
jfjimenez@us.es

Abstract. The need for sustainability in concrete construction industry has become increasingly significant in recent years. Use of material efficient strategies, such as structural optimisation, can be highly beneficial in this regard as they achieve more sustainable concrete structures by reducing their economic and environmental impacts. Additionally, the use of alternative reinforcement in the form of steel fibres can further improve efficiency of concrete structures by improving the mechanical properties of concrete. Increased interest by designers in using Steel Fibre Reinforced Concrete (SFRC) has resulted in the inclusion of this material in modern design regulations, such as the new generation of Eurocode 2.

Previous optimisation studies have compared the structural efficiency of SFRC with Normal Reinforced Concrete (NRC) members. However, they focused solely on the design of these structures for Ultimate Limit State (ULS) constraints without considering the main advantage of SFRC, which is its performance under Serviceability Limit State (SLS) conditions, especially for crack width control. To bridge this gap, this paper designs optimally SFRC and NRC structural members to meet both SLS and ULS design constraints. Useful findings are obtained regarding the effect of different parameters, including member length and ultimate applied load, on the sustainable design of SFRC members. Additionally, interesting conclusions are made with respect to the sustainability of SFRC against NRC structural members in term of embodied carbon, considering different carbon factors for steel fibres and rebars.

Machine Learning-Based Surrogate Models to Control the Dynamic Response of Nonlinear Civil Engineering Structures

Javier Fernando Jiménez-Alonso[1][0000-0002-4592-0375] and Javier Naranjo-Perez[1][0000-0003-2239-7048]

[1] Universidad de Sevilla, Seville, Spain
jfjimenez@us.es

Abstract. Civil engineering structures are prone to vibrate under dynamic loads. To mitigate the vibration levels of these structural systems, vibration absorbers are commonly installed on them. Despite the random nature of the wind or earthquake loads, these vibration absorbers have been usually designed considering a passive behavior. Thus, the stochastic conditions, associated with both the random action and the evolution of the modal properties of civil engineering structures over time, reduce the performance of these control devices, making recommendable to analyze the performance of vibration absorbers designed according to an active constitutive law. However, previous studies about the nonlinear dynamic control of civil engineering structures are limited, due to the complexity of integrating finite-element models, used to simulate the nonlinear behavior of civil engineering structures, with nonlinear control algorithms, used to compute the driving force. To shed some light on this issue, this study presents a comprehensive study of the performance of machine-learning-based surrogate models (physics-informed neural networks) when they are used to simulate the nonlinear behavior of civil engineering structures. Thus, the study delves into the strengths and limitations (computational efficiency, generalization capabilities and accuracy) of this neural network architecture in approximating the response of civil engineering structures together with its potential integration in the real-time nonlinear control applications. Additionally, a case study has been included herein to highlight the performance of this surrogate model when it is implemented to control the dynamic response of a civil engineering structures.

Keywords: Surrogate models, Nonlinear dynamics, Nonlinear control algorithms, Physics-informed neural networks, Civil engineering structures, Random vibrations.

Hybrid CNN-Spiking Neural Network for mammography classification

Abdhine Ben Ali[#1], Fahadi Mugigayi[*2]

[1]Institute of Information Technology, Gazi University, Ankara, Türkiye

[2] Islamic University in Uganda Department of Computer Science

abdhinebenali@gmail.com; mugigayi.fahadi@iuiu.ac.ug

Abstract. Breast cancer remains one of the primary causes of cancer-related women's mortality worldwide, with accurate mammographic analysis being crucial for early detection and treatment planning. Traditional Convolutional Neural Networks (CNNs) have shown promise in mammographic image analysis but face limitations in computational efficiency and temporal pattern recognition. We propose a novel hybrid model combining CNN feature extraction with Spiking Neural Networks (SNNs) for breast cancer mammography classification. We use SpikingJelly, an open-source deep learning framework for SNNs, on Google Colab Pro to implement this approach. We evaluated the model on integrated MIAS, DDSM, and INbreast datasets with 24,576 mammography images with benign and malignant masses.
Our hybrid CNN-SNN model achieved exceptional performance metrics, with 0.997 accuracy, 0,998 precision, a recall of 99.74%, and an AUC-ROC of 1.00. The model shows a higher performance compared to baseline ResNet50, EfficientNet, VGG16, LSTM, and GRU architectures while achieving a 27.6% reduction in computational complexity (FLOPs) compared to EfficientNet-B3. These results demonstrate the first successful integration of CNNs and spiking neural networks in breast cancer mammography classification, improving radiological image analysis accuracy and energy efficiency.

Keywords: Breast Cancer, Mammography, Convolutional Neural Network, Spiking Neural Network.

Machine Learning Approaches for Predicting Drying and Shrinkage Behavior in Fly Ash-Based Concrete: A Critical Review and Future Directions

Farnaz Ahadian, Gebrail Bekdaş and Sinan Melih Nigdeli

1 Depaertment of Civil Engineering, Istanbul University-Cerrahpaşa, Avcılar, 34320 İstanbul, Turkey

Abstract:

Concrete remains the most widely used construction material, but its long-term performance is significantly affected by drying shrinkage and associated cracking. Traditional constitutive and empirical models often struggle to capture the complex nonlinear behavior of concrete, particularly in fly ash-based geopolymer concrete (FA-GPC), which is increasingly recognized as a sustainable alternative to Portland cement-based systems. This review critically examines the potential of machine learning (ML) techniques—such as support vector machines, random forests, gradient boosting, and hybrid ensemble models—for predicting drying and shrinkage behavior in concrete. The paper highlights how ML approaches can overcome the rigidity of classical models by handling high-dimensional, multivariable datasets, thus improving prediction accuracy. Special emphasis is placed on practical applications, including mix design optimization and the influence of curing conditions in FA-GPC. By bridging civil engineering knowledge with artificial intelligence, this study provides a comprehensive framework for advancing predictive modeling, reducing experimental costs, and supporting sustainable construction practices.

Keywords: Fly Ash-Based Geopolymer Concrete, Drying Shrinkage, Mix Design Optimization, Support Vector Machine (SVM), Ensemble Learning

Mechanical Characterization of Pipe Zones Using Hybrid Robotic Sensing and Machine Learning

Tuna Hamza Adıgüzel, Sinan Melih Nigdeli and Gebrail Bekdaş

Department of Civil Engineering, Istanbul University-Cerrahpaşa, Istanbul, Türkiye

Abstract. This study examines the mechanical properties of welded steel pipe regions, specifically the base metal, weld metal, and heat-affected zone (HAZ). The methodology integrates traditional metallurgical analysis with artificial intelligence (AI) and machine learning (ML) techniques. A CatBoostRegressor model was trained using features derived from static material properties and dynamic sensor data collected from accelerometer, gyroscope, and magnetometer measurements. Model evaluation demonstrated strong predictive performance, with a mean squared error (MSE) of 0.90 and an R^2 value of 0.93. Analytical tools such as SHAP value analysis, residual error distribution, and correlation matrices were employed to identify behaviors unique to each region. The findings indicate that weld metal exhibits the highest strength, while the heat-affected zone displays transitional mechanical properties that are highly sensitive to rotational dynamics. This framework is significant for real-time quality control, predictive maintenance, and process optimization in the automotive, aerospace, and construction sectors.

Keywords: Welded Steel Pipe Characterization, Machine Learning, Sensor – Based Predictive Modeling .

Conference Topics:

- Emerging Trends in Artificial Intelligence and Machine Learning
- Advancements in Renewable Energy Technologies
- Nanoengineering and Nanotechnology Applications
- Robotics and Automation in Modern Industry
- Smart Cities and Internet of Things (IoT) Solutions
- Advanced Materials for Future Engineering Applications
- Sustainable Engineering and Green Technologies
- Cybersecurity and Data Protection in Engineering
- Quantum Computing and Its Engineering Applications
- Bioengineering and Biomedical Innovations
- Advanced Computational Techniques in Engineering
- Engineering Education and Innovation
- Additive Manufacturing and 3D Printing
- Data Science and Big Data Analytics in Engineering
- Climate Change and Environmental Engineering
- Space Engineering and Technologies
- Structural Engineering Innovations
- Automotive Engineering and Electric Vehicles
- Telecommunication and Networking Engineering
- Artificial Intelligence for Sustainable Development Goals

Organized by:
Gebrail Bekdaş
Sinan Melih Niğdeli
Ümit Işıkdağ
Ayla Ocak
Yaren Aydın